EUROPEAN COMMISSION

Community Research

RAPHAEL

Contract Number: 516508 (FI6O)

DELIVERABLE (D-FT4.3)
BN past experience
Fuel and irradiation description, PIE results

Author(s): **……G. TOURY**
……

Reporting period: 15/04/2005– 14/04/2007
Date of issue of this report :

Start date of project : **15/04/2005** Duration : **48 Months**

Project co-funded by the European Commission under the Euratom Research and Training Programme on Nuclear Energy within the Sixth Framework Programme (2002-2006)		
Dissemination Level		
PU	Public	
RE	Restricted to the partners of the RAPHAEL project	
CO	Confidential, only for specific distribution list defined on this document	**X**

Distribution list

Person and organisation name and/or group	Comments
OBRY Patrick (CEA)	On SINTER network
LANSIART Sylvie (CEA)	
MICHEL Frédéric (CEA)	
PELLETIER Michel (CEA)	
WERNER Heinz (FZJ)	
NABIELEK Heinz (FZJ)	
OVER Hans Helmut (JRC/IE)	
FUETTERER michael (JRC/IE)	
ABRAM Tim (Nexia Solutions)	
MARTIN David (Nexia Solutions)	
GUILLERMIER Pierre (AREVA NP)	
DANIEL Lucile (AREVA NP)	
SHIHAB Sammy (BN)	
TOURY Grégoire (BN)	
BOGUSH Edgar (AREVA GmbH)	
MANOLATOS Panagiotis (EC)	
CHAUVET Vincent (LGI Consulting)	

ReActor for Process heat, Hydrogen And ELectricity generation (RAPHAEL)		
Sub-project: SP-FT **Work package:** 4	**RAPHAEL document no:** RAPHAEL-0606-D-FT4-3	**Document type:** Deliverable
Issued by: BN **Internal no.:** 0601018/220 0601019/220 0601020/220 0601021/220 0601022/220 0601023/220 0601024/220		**Document status:** final

Document title

BN PAST EXPERIENCE – FUEL AND IRRADIATION DESCRIPTION, PIE RESULTS

Executive summary

This document is constituted from the results of R&D, fabrication and irradiation of coated particles during about twenty years in Belgium. These HTR fuel data can be divided into two parts: the R&D programme associated to the Belgian BR2 reactor, essentially devoted to uranium fuels, and the plutonium coated particle development with high burn-up tests in various reactors. These data are synthesised by particle types (content, fabrication and dimensions), irradiation conditions (burn-up, and fast fluence) and PIE results (as available in the reports).

Revisions

Rev.	Date	Short description	Author	WP Leader	SP Leader	Coordinator
00		First issue	G TOURY BN	P. OBRY CEA	M.PHÉLIP CEA	E. BOGUSH FANP

	Type of document:	Reference No / File - "Rev." - Page
	Technical Note	**0601021/220-"-"- 1**
		Other reference:

Client: EC	Author(s) G. TOURY
Project: Raphael IP – SP Fuel Technology WP-FT4 Performance Modelling	
Subject:	

HTR particles Irradiation Experiment BN database

MT LET Experiment

Rev.	Date	Chrono Filing No.	Status	Initials dactylo.	Author: Initials	Author: Visa 1	Verified by: Initials	Verified by: Visa 2	Approved by: Initials	Approved by: Visa 3	Q.A.: Initials	Q.A.: Visa 4	Issued by: Initials	Issued by: Visa 5	Number of pages
C															
B															
A															
-	17/05/06	0601021	Draft		GTY		SSH						GTY		66

Distribution:

RAPHAEL Project: Mr. OBRY (1 copy +1 CD)

BN: SSH, GTY

BELGONUCLEAIRE N.V.
Avenue Ariane, 4 - 1200 Brussels
TVA: BE 403.126.258
RCB: 271.300
TEL: 32-2774 05 11
FAX: 32-2-774 05 47

LIST of MODIFICATIONS		
DATE	**REVISION**	**OBJECT**
17/05/2006	-	Draft

NOTICE

PERSONNEL IN CONFIDENCE, NOT FOR PUBLICATION

This work is performed under the term and conditions of the Consortium Agreement of the RAPHAEL Project supported by the EC under contract n° 516508 (FI6O)

LIABILITY

This document was prepared by BELGONUCLEAIRE (BN). Neither BN, nor any person acting on behalf of BN:

a) gives any warranty, expressed or implied, with respect to the accuracy, completeness of the information contained in this document, or that the use of any information, apparatus, method or process disclosed in this document may not infringe third party rights, or

b) assumes any liabilities with respect to the use of, or for damage resulting from the use of any information, apparatus, method or process disclosed in this document.

	Type of document:	Reference No / File - "Rev." - Page
	Technical Note	**0601021/220-"-"- 4**
		Other reference:

Abstract:

This experiment was made of two sets of four elements known as the Matrix Tests (MT) and the Low Enrichment Replacement Series (LET). The two series form a combined experiment testing a wide range of matrix varieties over a succession of neutron doses and temperatures in two forms of compacts.

Table of content

List of Tables

List of Figures

1. INTRODUCTION

Two sets of four elements, the Matrix Test (MT) and the Low Enrichment Replacement Series (LET) were irradiated in the DRAGON reactor for four different periods of time.

The two series, containing compacts fabricated by the Dragon Project and BELGONUCLEAIRE, formed a combined experiment, testing a wide range of matrix varieties over a succession of neutron doses and temperatures.

The main purpose of these experiments was to provide information on the behaviour of fuel compacts having materials and dimensions in the range of interest for a future power reactor fuel.

This report details the characteristics, the irradiation histories and the post-irradiation examinations of the BN compacts loaded in these two series.

2. COMPACTS CHARACTERISTICS

The coated particles used in the BELGONUCLEAIRE compacts of the MT and LET series were supplied by the Dragon Project with the exception of the compacts labelled M of the LET series which contain coated particles fabricated by BELGONUCLEAIRE.

The characteristics of the various coated particles types are given in Table 1.

The various compacts were fabricated as follows:

- for the A, B, C and D series, the coated particles were overcoated with a resin bonded natural graphite (L.C.L. -14 % resin) to produce the required volume loading when pressed;
- for the E, F and G series, the coated particles were overcoated with a thin layer of resin bonded natural graphite and consolidated with a liquid resin (P514);
- for the H series, the coated particles were not overcoated, but consolidated with a liquid resin (P514);
- for the M series, the coated particles were overcoated with a resin bonded natural graphite (L.C.L. - 14 % resin) to produce the required volume loadings when pressed.

The characteristics and identification of the compacts are given in Table 2; their mean dimensions are given in Table 3.

3. LOADING PLANS

The LET series consisted of four graphite elements, each one containing eight fuel stringers in teledial geometry.

Each fuel stringer had six levels and each level contained five cylindrical compacts.

The levels were numbered from the core bottom.

The LET loading plan of the BN compacts is given in Table 4.

In addition to the compacts indicated in Table 4, four compacts of the M series were loaded in every fuel stringer of the four fuel elements, two at the upper end of the stringer and two at the lower end.

The total number of BN compacts loaded in the LET series was 160.

The MT series consisted of four graphite centre rod assemblies containing a fuel stack of annular compacts.

Each fuel stack had six levels, each one containing eight annular compacts,

The levels were numbered from the core bottom.

The MT loading plan of the BN compacts is given in Table 5.

The total number of BN compacts loaded in the MT series was 16.

4. IRRADIATION HISTORY

All the elements of the MT and LET series were loaded at the same time, and their irradiation started with the charge IV, core 3 in the Dragon Reactor.

They were unloaded successively as follow:

MT-1 and LET-1	Charge IV, end of core 4.
MT-2 and LET-2	Charge IV, end of core 6.
LET-3	Charge V, end of core 5.
MT-3, MT-4 and LET-4	Charge V, end of core 7.

The Figure 1 shows a bar chart of the irradiation programme together with the maximum burn-up, the peak fast neutron dose and the estimated peak irradiation temperature. The difference between the fuel and the outer graphite sleeve temperatures was about 300°C.

The elements MT4 and LET4 were prematurely unloaded at the end of core 7 (Charge V), because of the termination of the Dragon Project.

5. POST-IRRADIATION EXAMINATION

5.1. First unloading.

5.1.1. LET-1 experiment

Dismantling

All the compacts were slid out of the teledial block, except the compacts of the M series loaded at the top and at the bottom of the fuel stringer, which were shaken free of the block.

Visual examination.

Most of the compacts of the M series were corroded and some had disintegrated.

The compacts loaded in the stringer 4 showed a good aspect, while those of stringers 5 and 7 were damaged.

Measurements.

The outer diameter and length of the undamaged compacts were measured with a dial gauge device, previously calibrated by standards.

The results of the dimensional measurements and the mean irradiation conditions are given in Table 6.

The dimensional changes of the compacts have been plotted versus the fast neutron dose at Figures 17 and 22.

5.1.2. MT-1 experiment

Dismantling.

All the compacts were discharged through the bottom of the tube, although the rod appeared to be slightly bowed.

Visual examination.

A poor surface coating with a slight pitting on the outer surface and chips around the top of bore were observed on compact B55.

A poor surface coating was also observed on compact A55; the compacts A81 and A21 showed a good aspect.

Measurements.

The measurements of the length, of the outer and of the inner diameters of the compacts, were carried out with a dial gauge device calibrated by standards.

The results of the measurements are given in Table 7 and are plotted in Figures 26, 29 and 32 for the mean irradiation temperature of 1200 °C, and in Figure 28,31 and 34 for the mean irradiation temperature of 700°C.

Gamma spectrometry.

The total fission products inventory of the fuel has been measured and computed; the activity of the isotopes obtained by these two methods as well as the deduced burn-up, are compared in the Table 8.

The good agreement between the measurements and the calculations should be noticed.

At Figure 2, the axial burn-up distribution obtained by the Cs137 peak activity (662 keV) measurements and the calculations, is compared with the total gamma profile above 250 keV; the similar shape of the two curves emphasises the good behaviour of the coated particles used in these compacts.

The total isotope content of the empty graphite tube gives an image of the coated particle release and of the matrix retention; these values are given in Table 9.

The total gamma profile of the empty tube gives the positions of the activity peaks and indicates the contributing compacts.

This gamma profile is compared respectively with the fractional release of various isotopes : Cs134 and Cs137, Ba140 and Zr95, Ag110, in Figures 3, 4 and 5.

As appears in Figure 5, the activity of this profile is given mainly by the Ag110 release of the compacts loaded at the mid-core level; these compacts were operating at temperatures ranging between 1200 and 1300°C.

The relatively high activity measured at the bottom of the tube is due to the condensation of volatile fission products.

5.2. Second unloading

5.2.1. LET-2 experiment

Dismantling.

All the compacts were discharged without any difficulties with the master-sleeve manipulator as it is shown in Figure 6.

Visual examination.

The compacts were visually examined (Figure 7) and were all found to be intact and in good condition.

Figure 8. Shows the compacts M40 and M11 loaded at the bottom of the fuel stringer 8, and Figure 9, the compacts H25 and E45 coming from the stringer 7, level 5; the aspect of the surface of compact H25 should be noticed; this damage is probably due to the fabrication process.

Measurements.

The outer diameter and the length of the teledial compacts were measured with a specially designed jig.

The results of these measurements and the mean irradiation conditions are given in Table 10.

The results are plotted in Figures 17 and 22 for the mean irradiation temperature of 1200°C, in Figures 18 and 23 for the mean irradiation temperature of 1000°C and in Figures 20 and 25 for the mean irradiation temperature of 700°C.

Gamma spectrometry.

The measured and computed values of the total fission product activities together with the deduced burn-up, are compared in Table 11.

Both sets of values are in good agreement.

The total gamma profile above 250 keV of the fuel stringer 7, is shown in Figure 10; it reveals the good behaviour of the coated particles.

The isotope contents of the graphite tubes without fuel are given in Table 12.

The total gamma profile of the channel 7 without fuel shows a large peak at approximately 105 cm from the channel bottom. It is probably due to Co60 coming from the thermocouple sheath material and not to the fission products; this is confirmed by the Figures 11, 12 and 13, which give the axial distribution of Cs134, Cs137, Ba140 and Zr95.

The relativity high Ag release detected at the level of the E45 and H25 compacts, seems to indicate that the fission product retention is significantly influenced by the matrix density.

5.2.2. MT-2 experiment.

Dismantling.

All the compacts came out without difficulties.

Visual examination.

The compacts were found in excellent conditions.

The compact A41 showed dark spots on its internal surface.

The compacts B25 and A41 are shown in Figure 14, together with DRAGON compacts of the level 5; the compacts A15 and A25 are shown in Figure 15, together with the DRAGON compacts of the level 1.

Dimensional measurements.

The length, the outer and the inner diameters of the compacts were measured with the same gauge devices as used for the MT-1 experiment.

The results of the measurements and the mean irradiation temperatures are given in Table 13. They are plotted versus the fast neutron dose and for the mean irradiation temperature of 1200, 800 and 700°C in Figures 26 to 34.

5.3. Third unloading

5.3.1. LET-3 experiment

Dismantling.

All the fuel compacts were discharged without any difficulties through the top end of the teledial block by pushing them with a Teflon rod from the bottom end.

Visual examination.

The fuel compacts were generally in excellent conditions.

All the compacts of the M series loaded at the top and at the bottom end of the fuel stringers had a good aspect.

Within the fuel stringers, the compacts H31 and E61 showed crumbled ends, the compact D45 had a piece of matrix edged off at the top end and the compacts C11, D55 and C51 had a good aspect.

Dimensional measurements.

The outer diameter and length of the compacts were measured with the specially designed jig already used for LET-2.

The results of the measurements are presented in Table 14 and plotted versus the fast neutron dose and for the mean irradiation temperature of 1300°C, 1000°C and 800°C in the Figures 16, 18, 19, 21, 23 and 24.

5.4. Fourth unloading.

5.4.1. MT-3 experiment.

Dismantling.

The compacts A61 and A11, loaded at the core bottom, were removed easily from the tube, while the compacts A35 and A51, irradiated in the hottest zone, offered more resistance to the removal.

Visual examination.

A fairly smooth shiny surface with a lifting of the matrix surface in a few places has been noticed on the compact A35. Some coated particles are lost.

Some rough patches on otherwise smooth external surface and cracks on the inner surface edges were observed on the compact A51.

The compact A61 had a shiny smooth surface with sharp edges.

During handling, the compact edge has been chipped when it has been dropped on the edge of a metallic tray.

The compact A11 shows also a shiny smooth surface. The coated particles appear to be very close to the matrix surface.

Dimensional measurements.

The length, the inner and the outer diameters of the compacts have been measured.

The results, together with the corresponding irradiation conditions, are given in Table 15. They are plotted versus the neutron dose and for three-irradiation temperature (1200°C, 800°C and 700°C) in the Figures 26 to 34.

5.4.2. LET-4 and MT-4 experiment.

These two experiments, which were foreseen for a peak fast neutron dose of $4.9x10^{21}n.cm^{-2}$ DNE, were unloaded prematurely, after having reached a peak fast neutron dose of $2.9x10^{21}n.cm^{-2}$ DNE only, because of the termination of the Dragon Project.

No post-irradiation examinations have been carried out on the compacts of these experiments.

6. DISCUSSION OF THE RESULTS

6.1. Cylindrical compact behaviour

The information obtained by the irradiation of these compacts did not give the possibility to deduce a parametric function in order to fit the measurement results; the following remarks can, nevertheless, be made :

(a) All the compacts of the E and H series have shown crumbling ends after irradiation and present a relatively high Ag release. The consolidation process used to manufacture these low density compacts does not, therefore, seem adequate.

(b) The diameter changes measured on the compacts of the C and D series and irradiated at temperatures ranging between 1170 and 1300°C, indicate a shrinkage ranging from 0.8 to 1.6 % for fast neutron doses from $0.8x10^{21}$ to $2.8x10^{21}n.cm^{-2}$ DNE (Figures 16-17)

(c) The length changes of the compacts irradiated at temperature between 1170 and 1300°C give:

- for the compacts of the C series, no length increase up to $1.5x10^{21}$ n.cm^{-2} DNE and a mean length increase of 0.4 % at $2.7x10^{21}n.cm^{-2}$ DNE;
- for the compacts of the D series, no length increase up to $0.8x10^{21}$ $n.cm^{-2}$ DNE and a mean length increases of 0.25 and 0.68 % at 1.53 and $2.78x10^{21}$ $n.cm^{-2}$ DNE respectively (Figures 21-22).

(d) The diameter changes measured on the compacts of the M series, indicate:

- an average shrinkage of 1.2 % for a fast dose of 1.0×10^{21} n.cm^{-2} DNE and a temperature of 1000°C (Figure 18);

- an average shrinkage of 1.4 % for a fast dose of 2.1×10^{21} n.cm^{-2} DNE and a temperature of 800°C (Figure 19).

(e) No length changes were noticed on the compacts of the M series up to a fast dose of 1.0×10^{21} n.cm^{-2} DNE at 1000°C (Figure 23) and up to 2.1×10^{21} n.cm^{-2} DNE at 800°C (Figure 24).

6.2. Annular compact behaviour

The results of the measurements of these compacts lead to the following conclusions concerning their general behaviour:

(a) Outer diameter changes:

- at 1200°C and for the compacts of the A and B series, the maximum shrinkage seems to be reached at 1.0×10^{21} n.cm^{-2} DNE with a value of 1.3 %; this shrinkage is reduced to 1.0 % at 2.1×10^{21} n.cm^{-2} DNE (Figure 26);

- at 700-800°C and for the compacts of the A series, the shrinkage levels at 0.5 % for doses from 0.5 to 2.1×10^{21} n.cm^{-2} DNE (Figures 27 and 28).

(b) Inner diameter changes:

- at 1200°C and for compacts of the A and B series, a maximum shrinkage of about 1.0 % is reached at 0.4×10^{21} n.cm^{-2} DNE , this dimensional change is completely compensated at about 1.5×10^{21} n.cm^{-2} DNE ; it is followed by a diameter increase reaching 0.5 % at 2.2×10^{21} n.cm^{-2} DNE (Figure 29);

- at 700 - 800°C and for the compacts of the A series, a maximum shrinkage of 0.5 % is reached at 0.3×10^{21} n.cm^{-2} DNE; this dimensional change is completely compensated at about 2.0% at 2.0×10^{21} n.cm^{-2} DNE (Figures 30-31).

(c) Length changes:

- at 1200°C, the compacts of the A series show a maximum shortening of 1.4 % at 0.5×10^{21} n.cm^{-2} DNE ; it is reduced to 0.2 % at about 2.2×10^{21} n.cm^{-2} DNE; the compacts of the B series seem to have their turn around point at about 2.0 % for a dose of 1.0×10^{21} n.cm^{-2} DNE (Figure 32);

- at 700 - 800°C, the compacts of the A series have an average maximum shortening of 1.2 % at about 1.0×10^{21} n.cm^{-2} DNE ; it is reduced to 0.6 % at 2.1×10^{21} n.cm^{-2} DNE (Figures 33-34).

6.3. Volume changes of the compacts

The volume changes of the annular and cylindrical compacts were deduced from the dimensional measurements.

These results were plotted versus the fast neutron dose, for the mean irradiation temperatures of 1200, 1000, 800 and 700°C at Figures 35 to 38 respectively.

The annular compacts show a higher volume change than the cylindrical compacts as it can be seen in Figures 35, 37 and 38.

This fact can be explained as follow:

- The dimensional changes, deduced from the measurements performed on the compacts, consist in permanent strains.
- These permanent strains are given, in this case, by the combined effect of the densification, the swelling and the irradiation creep.

The comparison of the characteristics of the cylindrical and of the annular compacts shows that:

(a) the enrichment and the HML of the cylindrical compacts are higher (Tables 1 and 2);

(b) the diameter of the cylindrical compacts is equal to 1.7 times the annular compact thickness (Table 3).

From this comparison, it results that, for a given peak fuel temperature, the thermal gradient, and therefore the stress build-up, is higher in the cylindrical compact than in the annular compact. The irradiation creep strains induced in the cylindrical compacts and the resultant volume increase are, therefore, more important and counterbalance to a greater extent the compact densification.

The difference in behaviour of the two compacts types, due to the combined effect of irradiation induced densification, swelling and creep, is more pronounced at 1200°C (Figure 35) than at 800 and 700°C (Figures 37-38). This difference is probably due to the higher stress build-up resulting from the higher thermal gradient and to the higher creep coefficient.

Later in life, around 2.5×10^{21} $n.cm^{-2}$ DNE, when the stresses in the cylindrical compacts are sufficiently relaxed by creep, the volume changes of both compact types seem to evolve in a similar way (Figure 35).

Manufacturer	Variant	Fuel type	Porosity	Enrichment	Kernel diam.	Individual layer thickness					Total coating thickness	Overall diam.
						Buffer	Total inner PyC	SiC	Outer HD PyC			
-	-	-	(%)	% U5	(µm)	(µm)	(µm)	(µm)	(µm)		(µm)	(µm)
DP	A	UO_2	23.20	6.053	771	35	91	35	32		157	1091
DP	B	UO_2	20.6	3051	781	30	90	35	30		155	1110
DP	C	UO_2	21.20	6.11	766	33	105	49	38		191	1149
BN	GI3/1/2 F	UO_2	11.7	3.025	770	41	96	39	37		172	1133

Table 1: Coated Particles Characteristics

Irradiation Experiment	Compact Series	Coated Particle Variant	Mean HML	Mean Volume Loading	Fabrication Process	Matrix density
-	-	-	g.U/cm³	%	-	g/cm³
MT series	A	B	0.89	34.5	Compaction	1.60
	B	B	0.84	32.3	Compaction	1.25
LET series	C	A	0.94	35.2	Compaction	1.70
	D	A	0.945	35.3	Compaction	1.50
	E	A	1.04	39.0	Consolidation	1.20
	F	A	1.19	44.0	Consolidation	1.00
	G	A	1.09	40.0	Consolidation	1.20
	H	C	1.30	56.0	Consolidation	0.80
	M*	G13/1/2F	0.923	35.0	Compaction	1.56

* These compacts were placed at the top and at the bottom of the fuel stringers.

Table 2: Characteristics and identification of the compacts

Experiment Series	Compacts series	Diameter		Length
		Inner	Outer	
-	-	mm	mm	mm
MT	A	39.81	25.86	33.26
	B	39.71	25.80	33.11
LET	C	11.88		24.87
	D	11.87		24.81
	E	11.53		23.95
	F	11.52		23.15
	G	11.44		23.20
	H	11.83		22.38
	M	11.87		24.85

Remarks :

(1) The compacts for the MT experiments have an annular shape, while the compacts for the LET experiments are cylindrical.
(2) Only mean values are given in this table.

Table 3: Mean dimensions of the compacts

Element number	Stringer number	Level number	Compact identification	Level number	Compact identification
1	4	1	E35 E21	5	C71 D51
	5	1	E55 E11	5	C55 D21
	7			5	H15 E41
2	4			5	C31 D41
	5			5	C25 D31
	7			5	H25 E45
3	4			5	C11 D55
	5			5	H31 E61
	7			5	C51 D45
4	4	1	E15 E25	5	C65 D15
	5	1	E71 E65	5	H11 E51
	7			5	C15 D11

Table 4: Loading plan of the BN compacts in the LET carriers

Assembly number	Level number	Compact identification	Level number	Compact identification
1	1	A55 A21	5	B55 A81
2	1	A15 A25	5	B25 A41
3	1	A61 A11	5	A35 A51
4	1	A65 A75	5	B35 A71

Table 5: Loading plan of the BN compacts in the MT assemblies

Fuel Stringer	Compact position	Compact number	Diameter change	Length change	Fast dose	Average temperature
-	cm	-	%	%	10^{20}n cm^{-2} DNE	°C
1	TOP	M23	damaged	damaged	2.8	999
	TOP	M36	▲	▲	2.8	999
	BOTTOM	M33			5.6	720
	BOTTOM	M53			5.6	720
2	TOP	M30			2.8	999
	TOP	M43			2.8	999
	BOTTOM	M34			5.6	720
	BOTTOM	M12			5.6	720
3	TOP	M56			2.8	999
	TOP	M59			2.8	999
	BOTTOM	M32			5.6	720
	BOTTOM	M27			5.6	720
4	TOP	M37	▼	▼	2.8	999
	TOP	M60	damaged	damaged	2.8	999
	107.5	C71	1.34	+ 0.02	8.0	1239
	107.5	D51	- 1.18	+ 0.02	8.0	1239
	7.5	E35	+ 3.31	+ 5.20	7.0	809
	7.5	E21	+ 2.42	+ 5.20	7.0	809
	BOTTOM	M58	damaged	damaged	5.6	720
	BOTTOM	M01	damaged	damaged	5.6	720
5	TOP	M45	damaged	damaged	2.8	999
	TOP	M47	▲	▲	2.8	999
	112.5	C55			7.6	1224
	112.5	D21			7.6	1224
	12.5	E55			8.0	874
	12.5	E11			8.0	874
	BOTTOM	M35			5.6	720
	BOTTOM	M51			5.6	720
6	TOP	M61			2.8	999
	TOP	M22			2.8	999
	BOTTOM	M02			5.6	720
	BOTTOM	M57			5.6	720
7	TOP	M10			2.8	999
	TOP	M24			2.8	999
	107.5	H15			8.0	1239
	107.5	E41			8.0	1239
	BOTTOM	M49			5.6	720
	BOTTOM	M50			5.6	720
8	TOP	M38	▼	▼	2.8	999
	TOP	M55			2.8	999
	BOTTOM	M13			5.6	720
	BOTTOM	M20	damaged	damaged	5.6	720

Table 6: LET-1 Results of the measurements and irradiation conditions

Compact position	**Compact number**	**Outer diameter change**	**Inner diameter change**	**Length change**	**Fast dose**	**Average temperature**
cm	-	%	%	%	10^{20}n cm^{-2} DNE	°C
111.89	B55	- 1.00	- 1.04	- 1.49	5.3	1215
108.55	A81	- 0.75	- 0.92	- 1.40	5.5	1225
5.01	A55	- 0.55	- 0.42	- 0.72	5.4	711
1.67	A21	- 0.65	- 0.35	- 0.87	5.2	681

Table 7: MT-1 Results of the measurements and irradiation conditions

All values refer to shutdown date June 16, 1972	**Activity measured in total γ - scan Ci**	**Calculated activity Ci**
Sr89		$1.55x10^{+03}$
Sr90		$2.8x10^{+01}$
Zr95	$2.36x10^{+03}$	$2.44x10^{+03}$
Ru103	$2.21x10^{+03}$	$2.08x10^{+03}$
Ru106 - Rh106	$2.15x10^{+02}$	$2.71x10^{+02}$
Am11Om		$2.62x10^{-01}$
Ag111		$8.68x10^{+01}$
I131		$1.93x10^{+03}$
Xe133		$3.95x10^{+03}$
Cs134	$1.45x10^{+01}$	$1.43x10^{+01}$
Cs137	$3.76x10^{+01}$	$3.71x10^{+01}$
Ba140 - La140	$3.54x10^{+03}$	$3.3x10^{+03}$
Ce141		$2.99x10^{+03}$
Ce144 - Pr144	$1.01x10^{+03}$	$8.60x10^{+02}$
Pa233		
Burn-up (% FIFA)	34.1	33.0
(Mean) (% FIMA)		1.2

Table 8: MT-1 Total fission product inventory

Fission products			**Activation products**	
Isotope	Measured activity Ci	Fractional release	Isotope	Measured activity Ci
Zr95	1.5×10^{-03}	8.6×10^{-07}	Sc46	
Ru103	1.3×10^{-03}	8.6×10^{-07}	Cr51	3.2×10^{-02}
Ru106 - Rh106	2.0×10^{-03}	1.0×10^{-05}	Mn54	1.6×10^{-03}
Ag110m	7.2×10^{-03}	3.9×10^{-02}	Co60	3.8×10^{-03}
I131	7.0×10^{-03}	5.0×10^{-06}	Ta182	6.6×10^{-03}
Cs134	5.4×10^{-04}	5.1×10^{-05}	Fe59	7.0×10^{-04}
Cs137	7.2×10^{-04}	2.6×10^{-05}		
Ce144 - Pr144	1.6×10^{-03}	2.5×10^{-06}		
Ba140 - La140	1.7×10^{-03}	6.9×10^{-07}		
Pa233				

Table 9: MT-1 Total isotope content of the graphite tube without fuel (All values referred to shut-down date, June 16, 1972)

Fuel Stringer	Compact position	Compact number	Diameter change	Length change	Fast dose	Average temperature
-	cm	-	%	%	10^{20}n cm^{-2} DNE	°C
1	TOP	M87	- 0.84	- 0.04	8.6	960
	TOP	M64	- 1.01	0.00	8.6	960
	BOTTOM	M92	- 0.84	- 0.24	13.6	693
	BOTTOM	M17	- 1.01	+ 0.28	13.6	693
2	TOP	M14	N.M.	N.M.	8.6	960
	TOP	M15	- 1.43	- 0.04	8.6	960
	BOTTOM	M66	- 1.01	- 0.12	13.6	693
	BOTTOM	M62	N.M.	N.M.	13.6	693
3	TOP	M05	- 0.93	0.00	8.6	960
	TOP	M74	- 0.84	- 0.12	8.6	960
	BOTTOM	M84	- 1.26	- 0.04	13.6	693
	BOTTOM	M63	- 1.43	- 0.12	13.6	693
4	TOP	M124	- 0.84	- 0.04	8.6	960
	TOP	M39	- 0.84	- 0.12	8.6	960
	108.8	C31	- 0.84	- 0.12	15.2	1180
	106.3	D41	- 0.84	+ 0.32	15.6	1189
	BOTTOM	M07	- 1.10	+ 0.12	13.6	693
	BOTTOM	M26	- 1.01	+ 0.08	13.6	693
5	TOP	M03	- 1.26	- 0.16	8.6	960
	TOP	M08	- 1.01	N.M.	8.6	960
	113.8	C25	- 1.43	+ 0.08	14.8	1168
	111.3	D31	- 1.43	+ 0.20	15.0	1178
	BOTTOM	M18	N.M.	N.M.	13.6	693
	BOTTOM	M16	N.M.	N.M.	13.6	693
6	TOP	M32	- 0.76	+ 0.08	8.6	960
	TOP	M94	- 1.01	- 0.20	8.6	960
	BOTTOM	M28	- 1.01	+ 0.08	13.6	693
	BOTTOM	M19	- 0.93	- 0.04	13.6	693
7	TOP	M79	- 0.84	- 0.16	8.6	960
	TOP	M09	- 1.01	- 0.12	8.6	960
	108.8	H25	- 1.49	damaged	15.2	1180
	106.3	E45	- 1.64	damaged	15.6	1189
	BOTTOM	M96	- 0.76	- 0.00	13.6	693
	BOTTOM	M42	- 0.76	+ 0.08	13.6	693
8	TOP	M25	- 0.84	- 0.00	8.6	960
	TOP	M103	- 1.18	- 0.16	8.6	960
	BOTTOM	M40	N.M.	N.M.	13.6	693
	BOTTOM	M11	- 1.10	- 0.97	13.6	693

Table 10: LET–2 Results of the measurements and irradiation conditions

All values refer to shut-down date September 14, 1973	**Activity measured in total γ - scan Ci**	**Calculated activity Ci**
Kr85		$2.25 \times 10^{+01}$
Sr89		$1.83 \times 10^{+03}$
Sr90		$8.76 \times 10^{+01}$
Zr95	$2.14 \times 10^{+03}$	$2.97 \times 10^{+03}$
Ru103	$2.58 \times 10^{+03}$	$3.12 \times 10^{+03}$
Ru106 - Rh106	$5.05 \times 10^{+02}$	$6.49 \times 10^{+02}$
Ag110m		$1.11 \times 10^{+00}$
Ag111		$1.69 \times 10^{+02}$
I131	$2.25 \times 10^{+03}$	$3.48 \times 10^{+03}$
Xe133		$6.96 \times 10^{+03}$
Cs134	$9.10 \times 10^{+01}$	$6.93 \times 10^{+01}$
Cs137	$1.20 \times 10^{+02}$	$1.20 \times 10^{+02}$
Ba140 - La140	$5.14 \times 10^{+03}$	$5.78 \times 10^{+03}$
Ce141		
Ce144 - Pr144	$1.51 \times 10^{+03}$	$1.55 \times 10^{+03}$
Pa233		
Mean burn-up (% FIFA)	47.8	46.9
(% FIMA)		2.77

Table 11: LET-2 Total fission product inventory

Fission products			**Activation products**	
Isotope	Measured activity Ci	Fractional release	Isotope	Measured activity Ci
Zr95	1.0×10^{-02}	3.4×10^{-06}	Sc46	
Ru103	1.2×10^{-02}	3.8×10^{-06}	Cr51	1.3×10^{-01}
Ru106 - Rh106			Mn54	1.4×10^{-03}
Ag110m	5.4×10^{-03}	4.9×10^{-03}	Co60	2.4×10^{-02}
I131			Ta182	4.8×10^{-03}
Cs134	1.6×10^{-03}	2.3×10^{-05}	Fe59	2.7×10^{-03}
Cs137	3.6×10^{-03}	3.0×10^{-05}		
Ce144 - Pr144				
Bal140 - La140	3.5×10^{-02}	6.0×10^{-06}		

Table 12: LET-2 Channel 7 Total isotope content of the graphite tubes without fuel (All values referred to shut-down date, September 14, 1973)

Compact position	**Compact number**	**Outer diameter change**	**Inner diameter change**	**Length change**	**Fast dose**	**Average temperature**
cm	-	%	%	%	10^{20}n cm^{-2} DNE	°C
111.89	B25	- 1.18	- 0.23	-1.80	9.0	1220
108.55	A41	- 1.35	- 0.42	-1.14	9.4	1228
5.01	A15	- 0.48	+0.19	-0.99	8.5	751
1.67	A25	- 0.70	- 0.04	-1.34	7.8	721

Table 13: MT-2 Results of the measurements and irradiation conditions

Fuel stringer	Compact position	Compact number	Diameter change	Length change	Fast dose	Average temperature
-	cm	-	%	%	10^{20}n cm^{-2} DNE	°C
1	TOP	M69	- 1.01	+0.28	10.4	1078
	TOP	M118	- 1.26	- 0.04	10.4	1078
	BOTTOM	M120	- 1.26	0.00	21.0	818
	BOTTOM	M109	- 1.52	- 1.15	21.0	818
2	TOP	M110	- 1.43	- 0.32	10.4	1078
	TOP	M122	- 1.43	+0.04	10.4	1078
	BOTTOM	M83	- 1.43	+0.04	21.0	818
	BOTTOM	M81	- 1.18	- 0.04	21.0	818
3	TOP	M100	- 1.26	- 0.16	10.4	1078
	TOP	M88	- 1.35	- 0.08	10.4	1078
	BOTTOM	M106	- 1.52	- 0.32	21.0	818
	BOTTOM	M77	- 1.60	- 0.16	21.0	818
4	TOP	M67	- 1.26	- 0.04	10.4	1078
	TOP	M91	- 1.26	- 0.32	10.4	1078
	108.8	C11	- 1.51	+0.32	26.8	1295
	106.3	D55	- 1.43	+0.81	27.8	1304
	BOTTOM	M144	- 1.43	+0.40	21.0	818
	BOTTOM	M95	- 1.35	+0.04	21.0	818
5	TOP	M117	- 1.10	+0.08	10.4	1078
	TOP	M86	- 1.35	+0.04	10.4	1078
	113.8	H31	- 1.52	damaged	25.4	1283
	111.3	E61	+ 0.69	damaged	26.2	1293
	BOTTOM	M112	- 1.01	+0.24	21.0	818
	BOTTOM	M90	- 1.43	- 0.28	21.0	818
6	TOP	M73	- 1.68	+0.16	10.4	1078
	TOP	M116	- 1.43	+0.04	10.4	1078
	BOTTOM	M75	- 1.52	- 0.20	21.0	818
	BOTTOM	M99	- 1.35	- 0.08	21.0	818
7	TOP	M126	- 1.26	- 0.16	10.4	1078
	TOP	M113	- 1.26	- 0.24	10.4	1078
	108.8	C51	- 1.43	+0.48	26.8	1295
	106.3	D45	- 1.60	+0.56	27.8	1304
	BOTTOM	M115	- 1.26	- 0.00	21.0	818
	BOTTOM	M76	- 1.52	- 0.24	21.0	818
8	TOP	M78	- 1.26	- 0.04	10.4	1078
	TOP	M107	- 1.35	+0.12	10.4	1078
	BOTTOM	M101	- 1.43	- 0.20	21.0	818
	BOTTOM	M98	- 1.68	- 0.28	21.0	818

Table 14: LET-3 Results of the measurements and irradiation conditions

Compact position	**Compact number**	**Outer Diameter change**	**Inner Diameter change**	**Length change**	**Fast dose**	**Average temperature**
cm	-	%	%	%	10^{20}n cm^{-2} DNE	°C
119.89	A35	- 1.00	+0.54	- 0.24	22.0	1200
108.55	A51	- 0.88	+0.54	- 0.24	22.6	1200
5.01	A61	- 0.53	+1.98	- 0.72	21.4	800
1.67	A11	- 0.55	+2.13	- 0.54	20.5	700

Remark: Fast neutron doses and temperatures are estimated from predicted peak values.

Table 15: MT-3 Results of the measurements and irradiation conditions

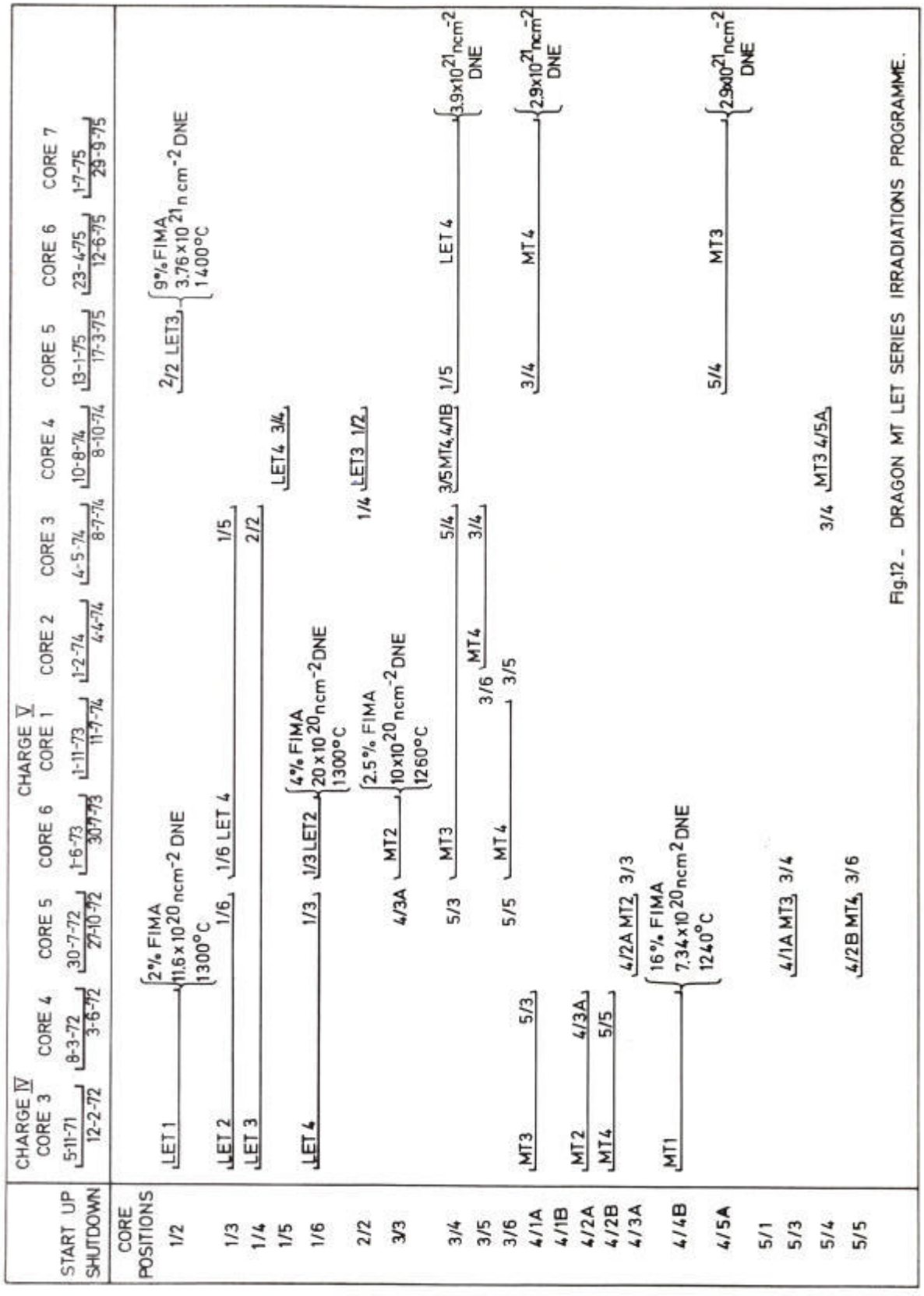

Fig.12 - DRAGON MT LET SERIES IRRADIATIONS PROGRAMME.

Figure 1: MT-LT experiment – Irradiation program

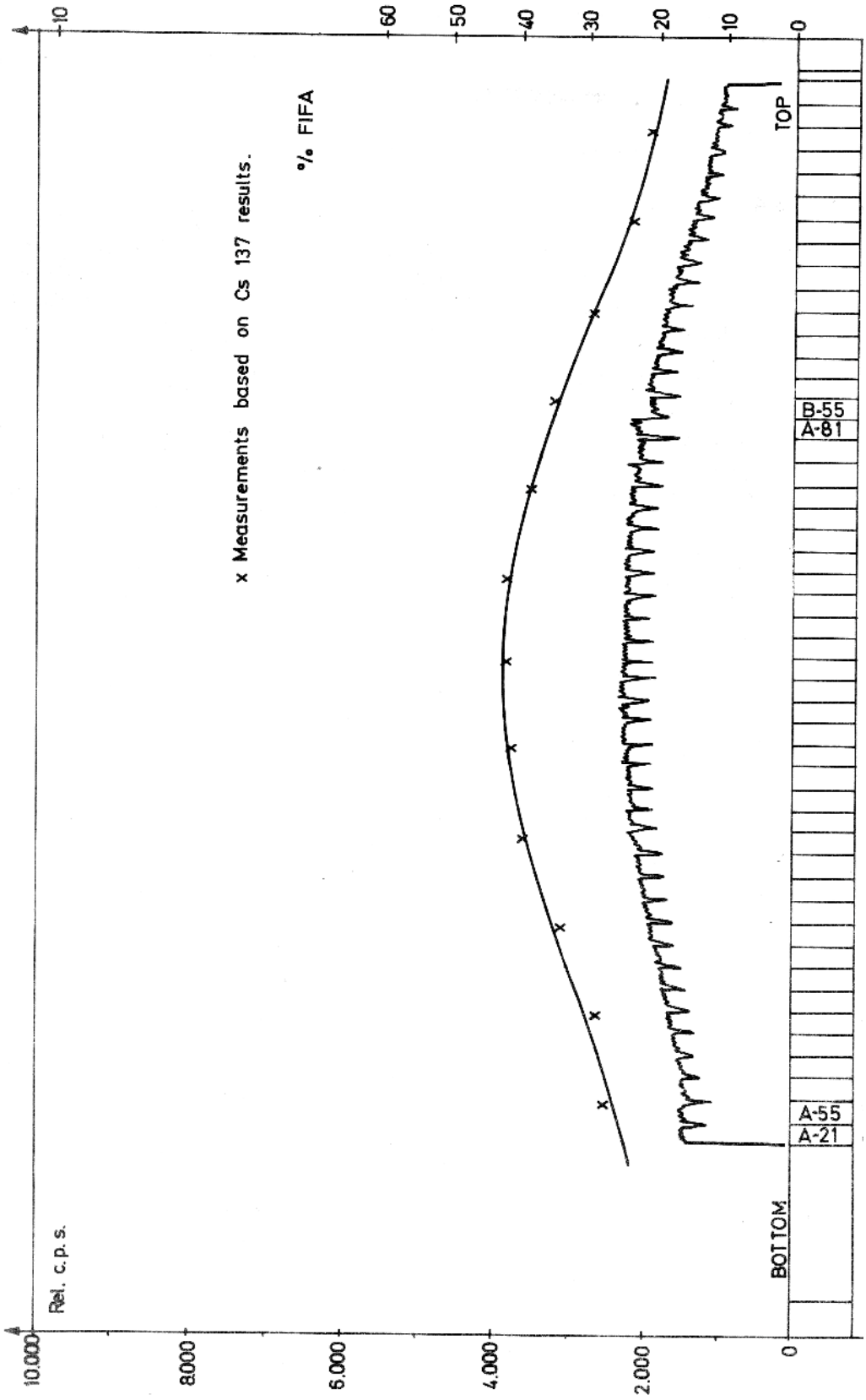

Figure 2: Total gamma profile above 250 keV for fuel element MT1 and axial burn-up

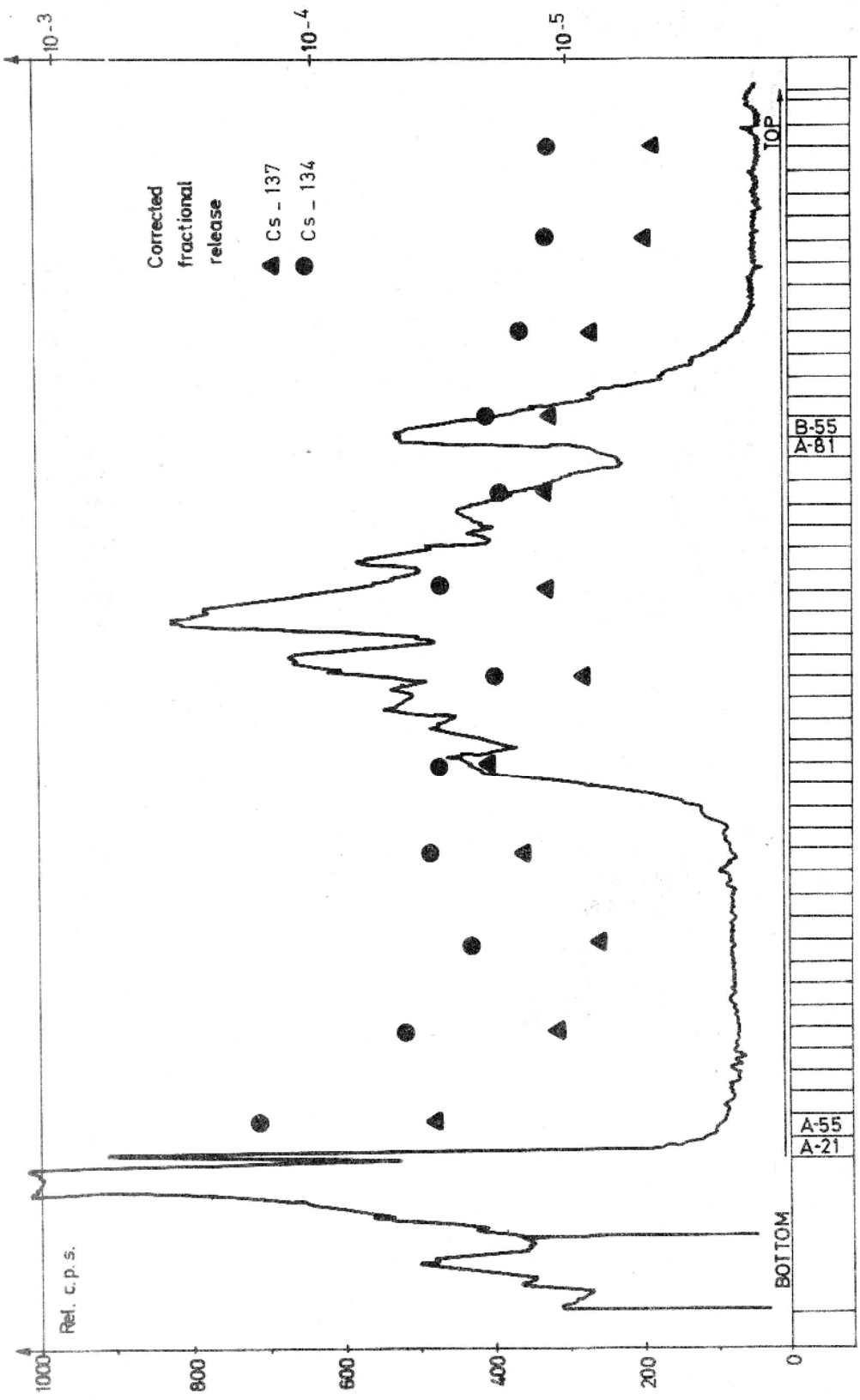

Figure 3: Total gamma profile above 250 keV for the empty fuel element MT1 and fractional release of Cs137 and Cs134

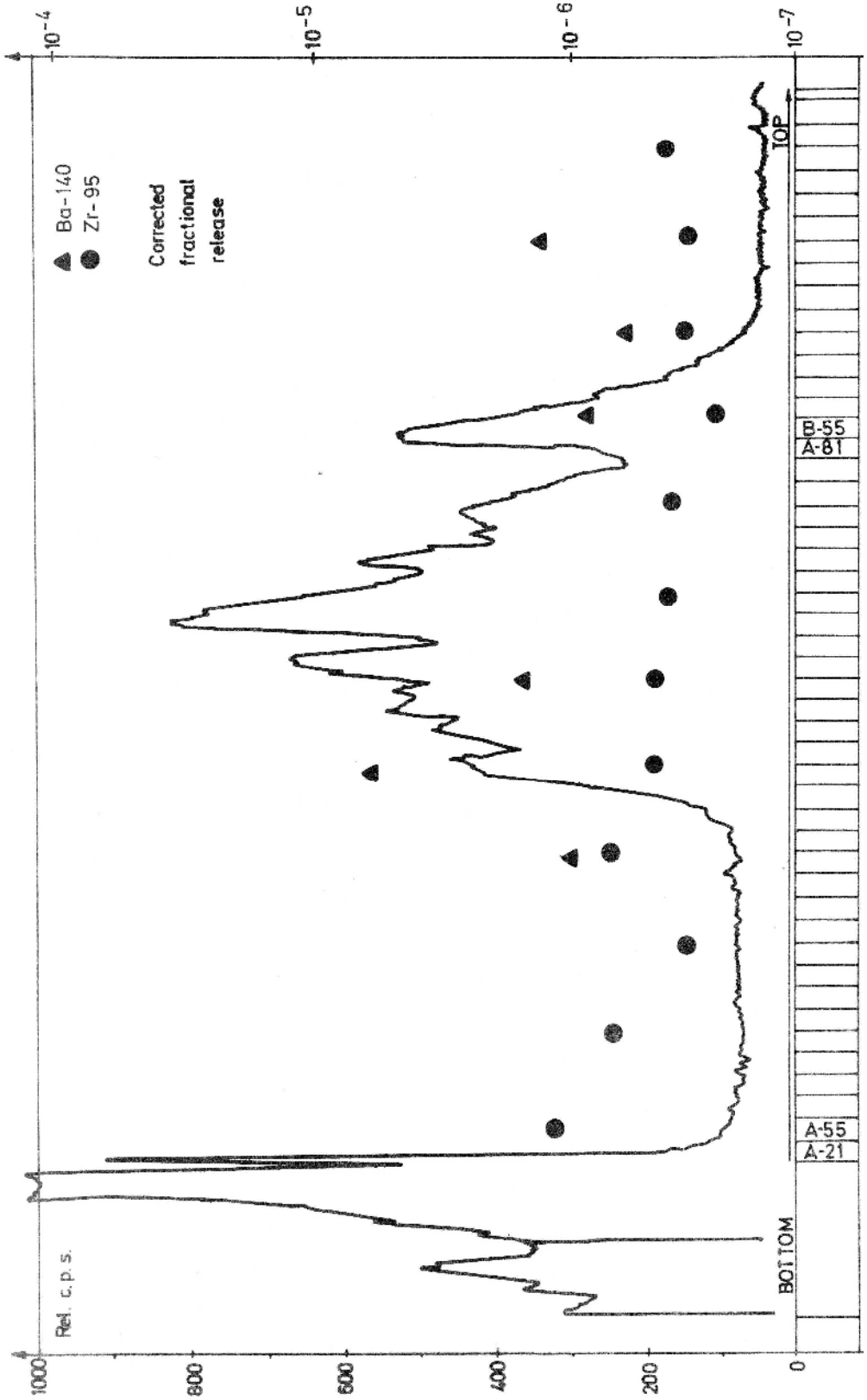

Figure 4: Total gamma profile above 250 keV for the empty fuel element MT1 and fractional release of Zr95 and Ba140

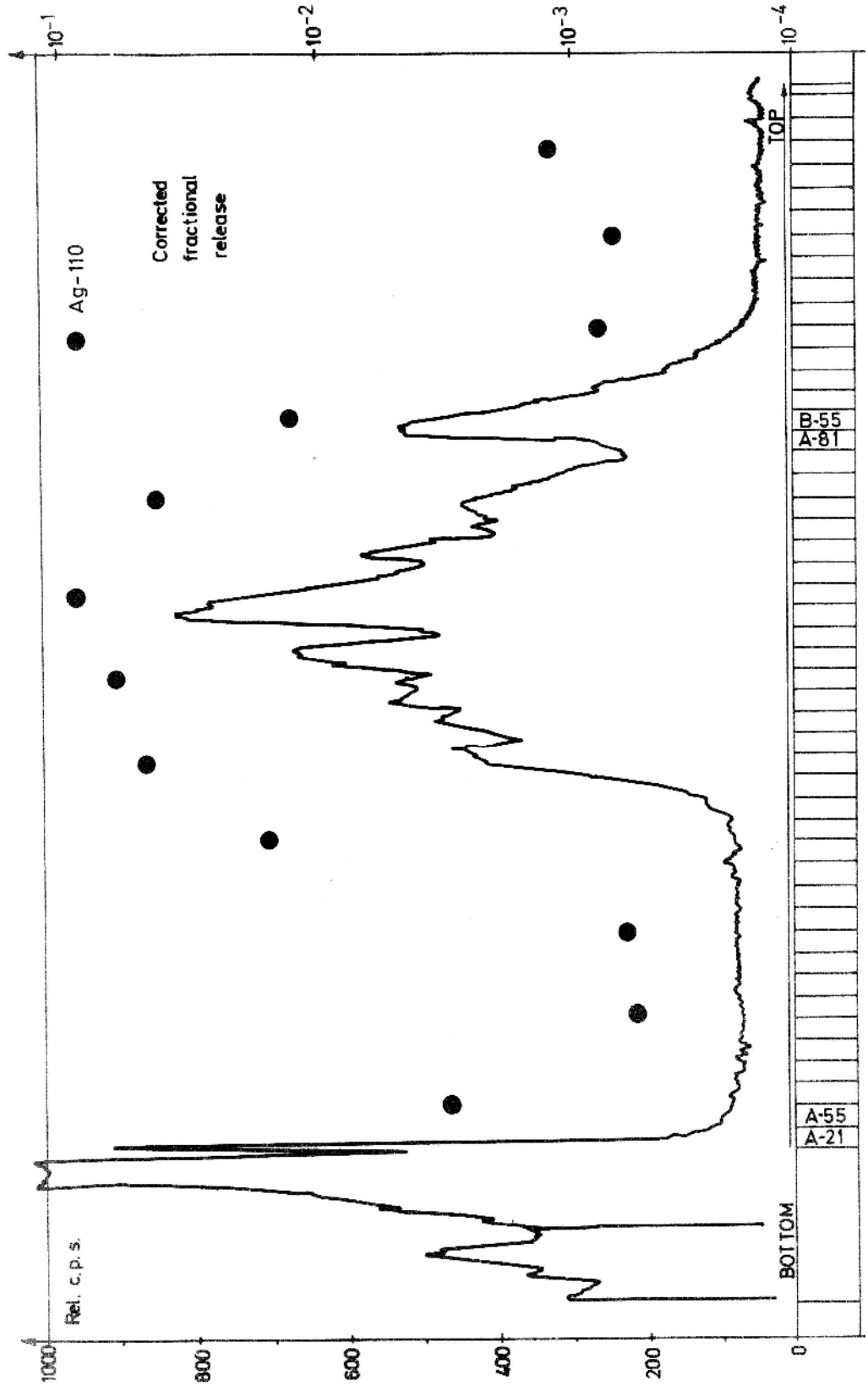

Figure 5: Total gamma profile above 250 keV for the empty fuel element MT1 and fractional release of Ag110m

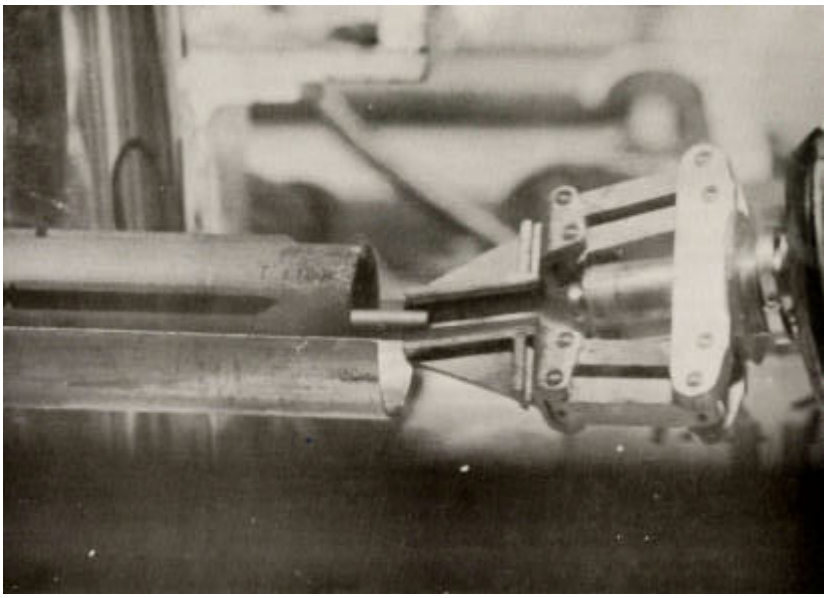

Figure 6: Compact discharged with master-sleeve manipulator

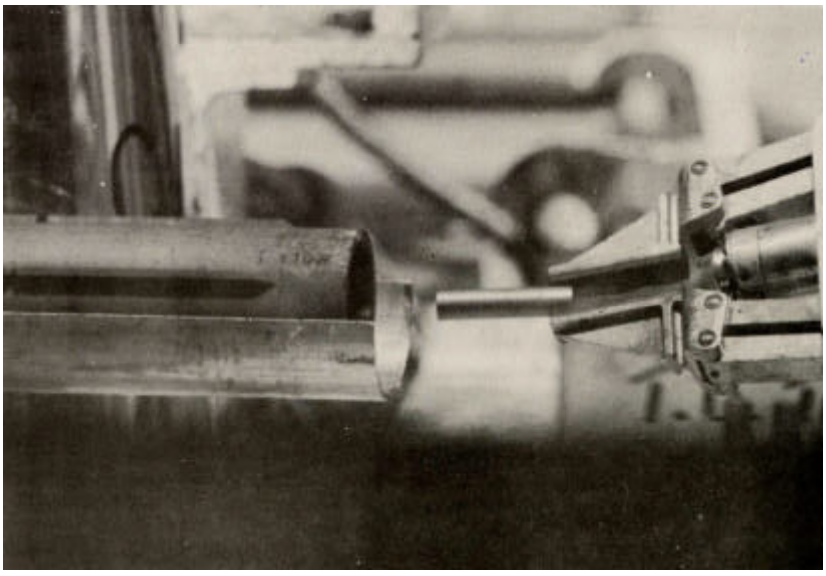

Figure 7: Visual examination of compacts

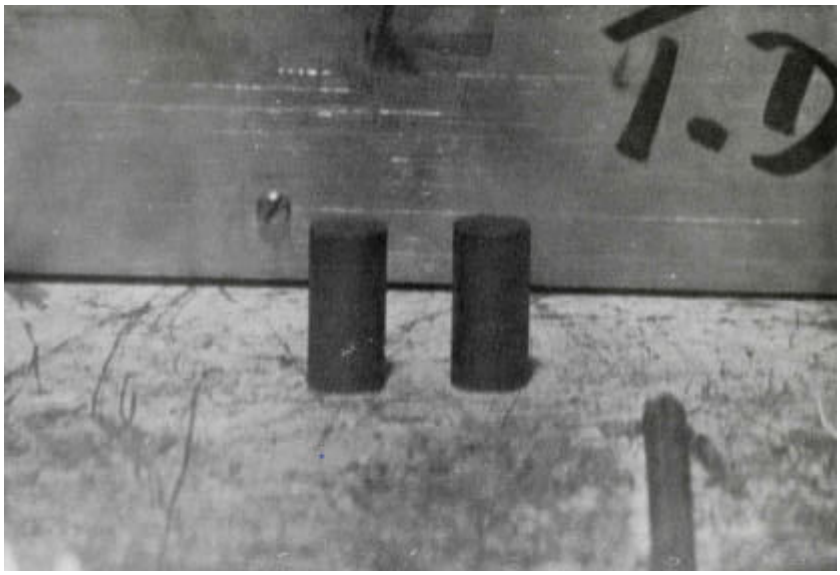

Figure 8: Compacts M40 and M11

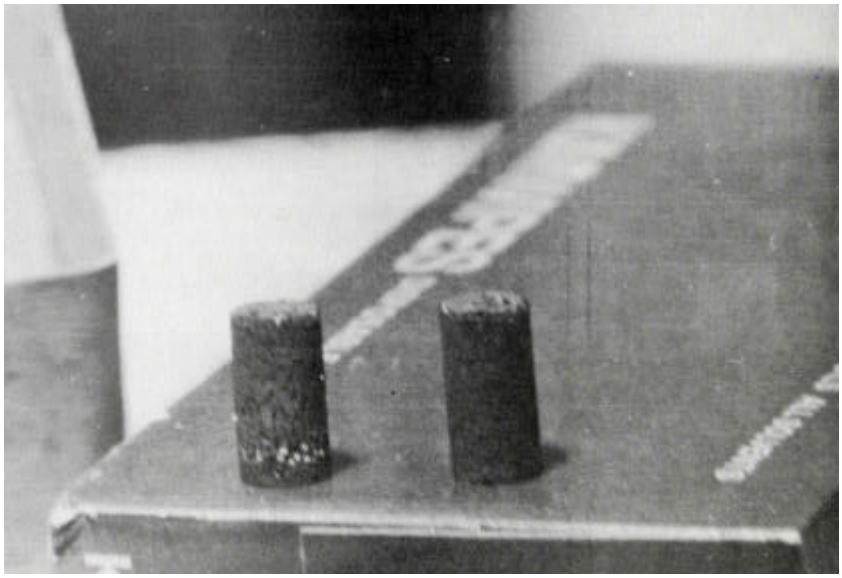

Figure 9: Compacts H25 and E45

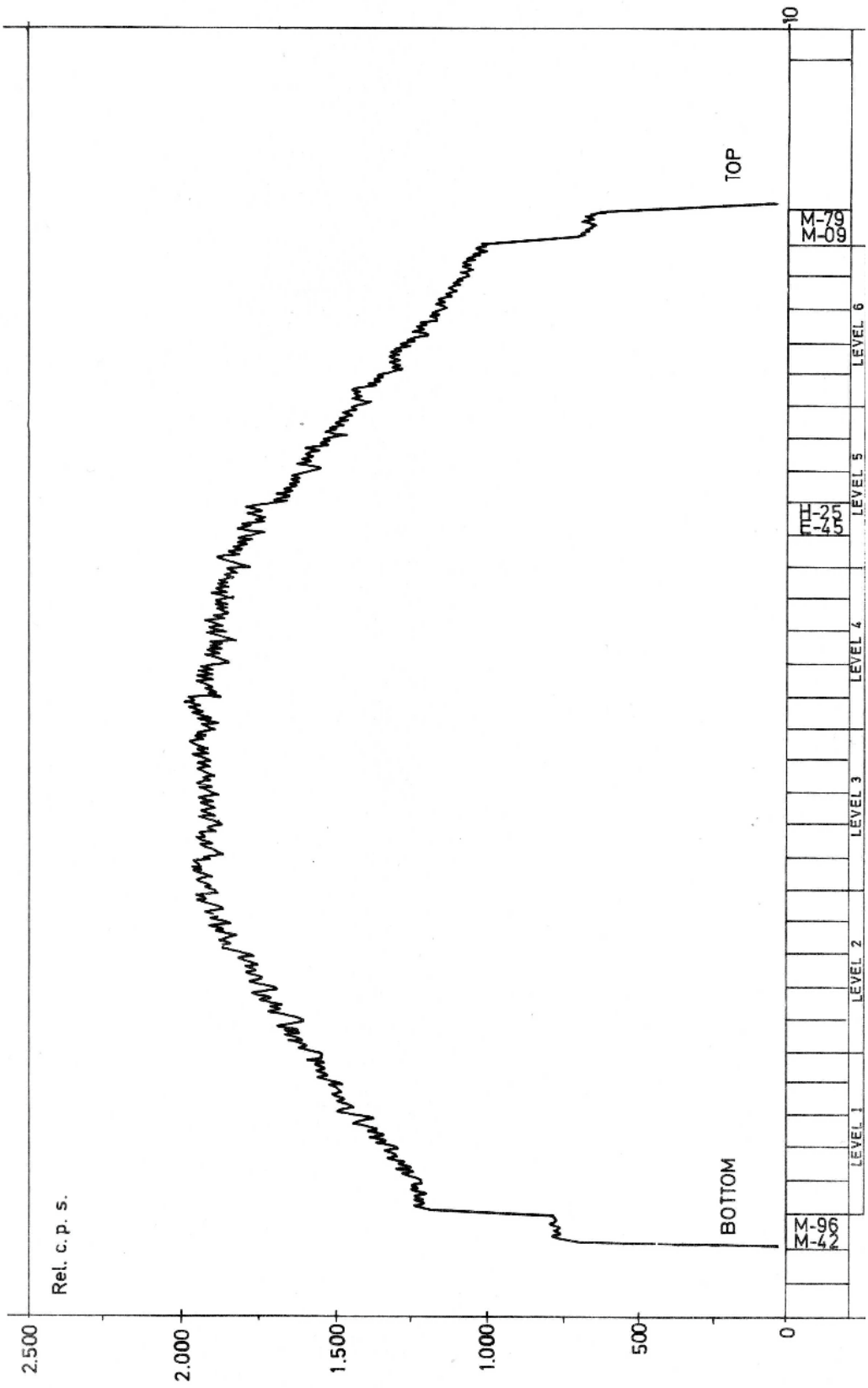

Figure 10: Total gamma profile above 250keV for fuel stringer 7 – LET2

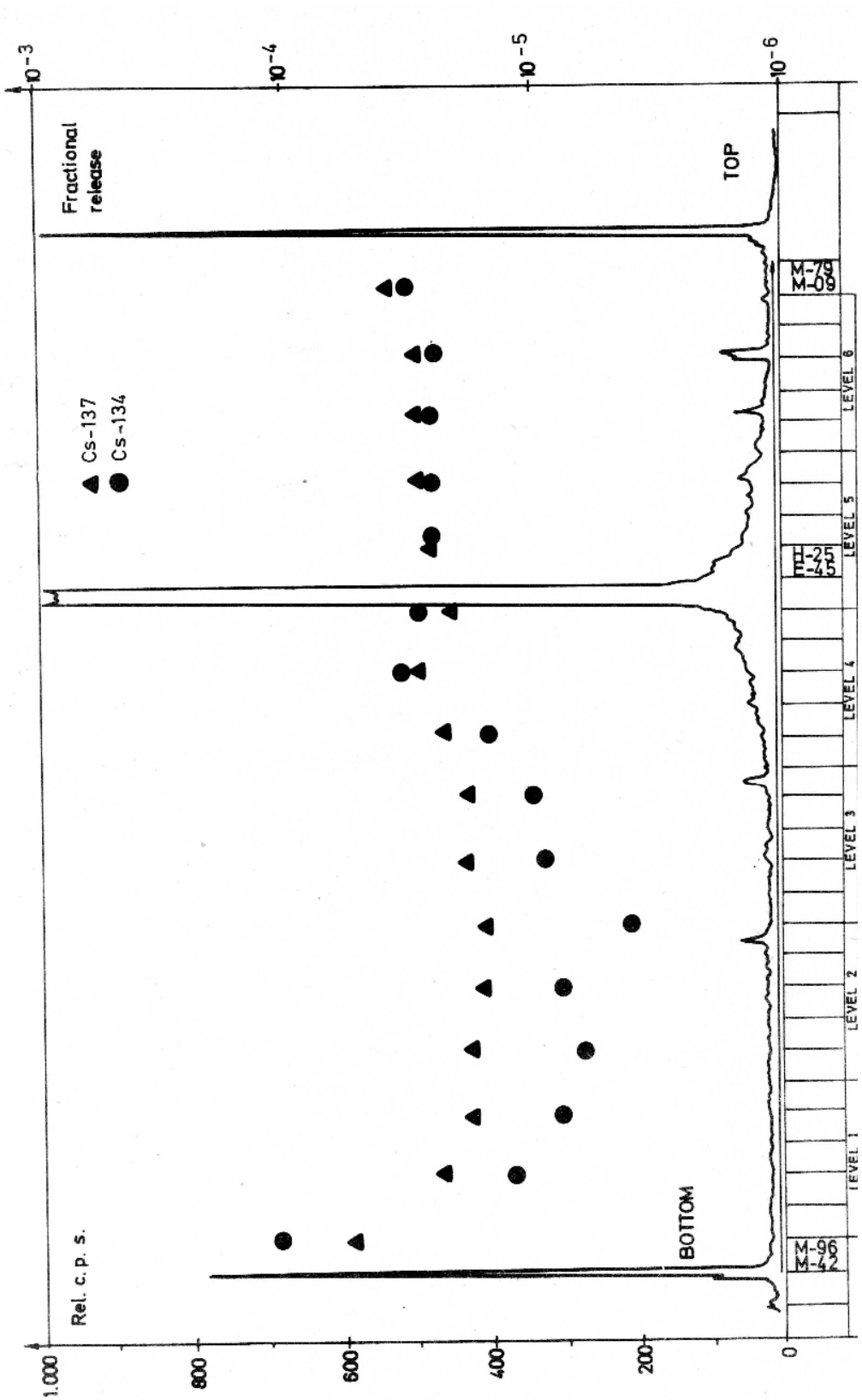

Figure 11: Total gamma profile above 250keV for the empty channel 7 and fractional release of Cs134 and Cs137

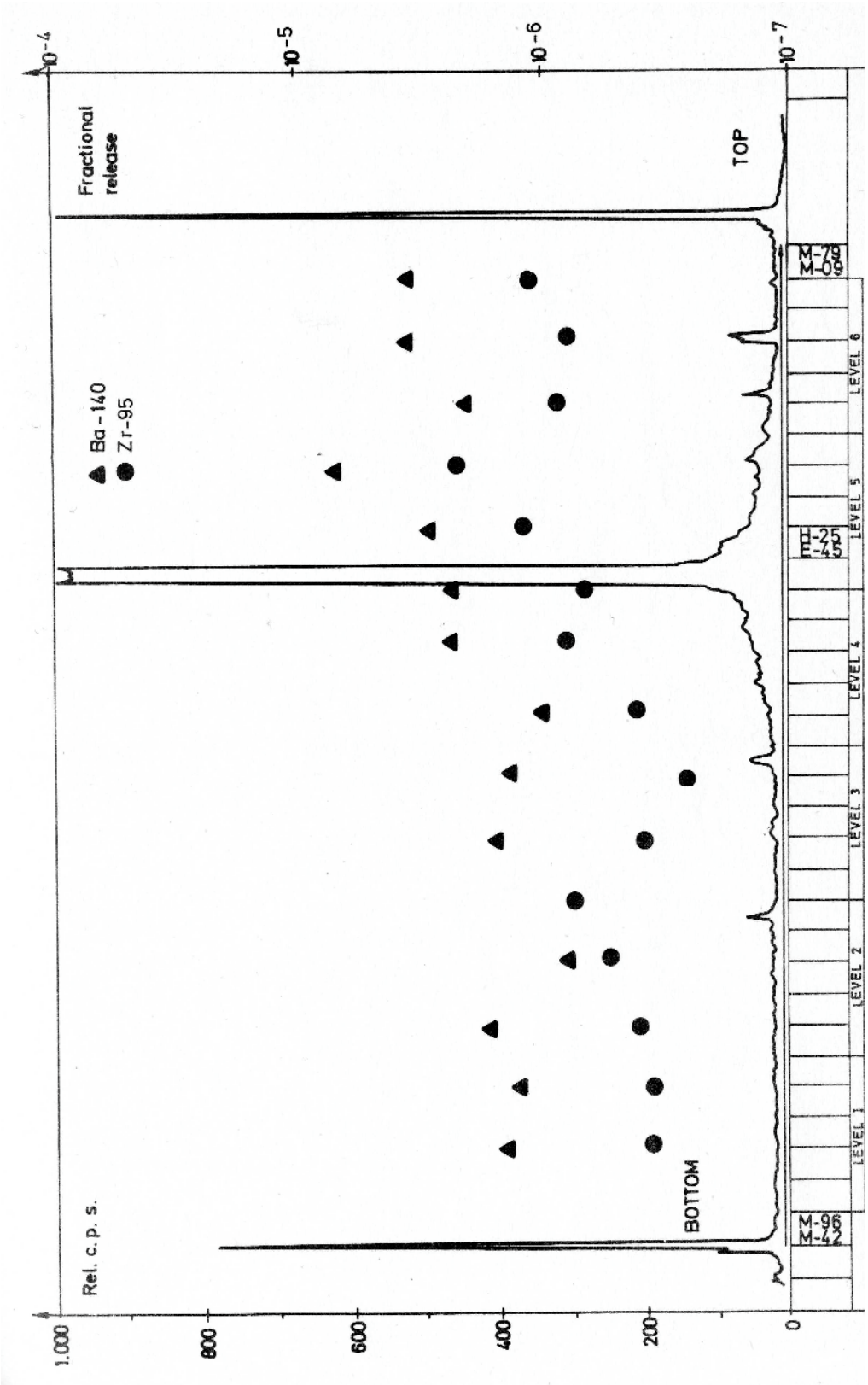

Figure 12: Total gamma profile above 250keV for the empty channel 7 and fractional release of Zr95 and Ba140

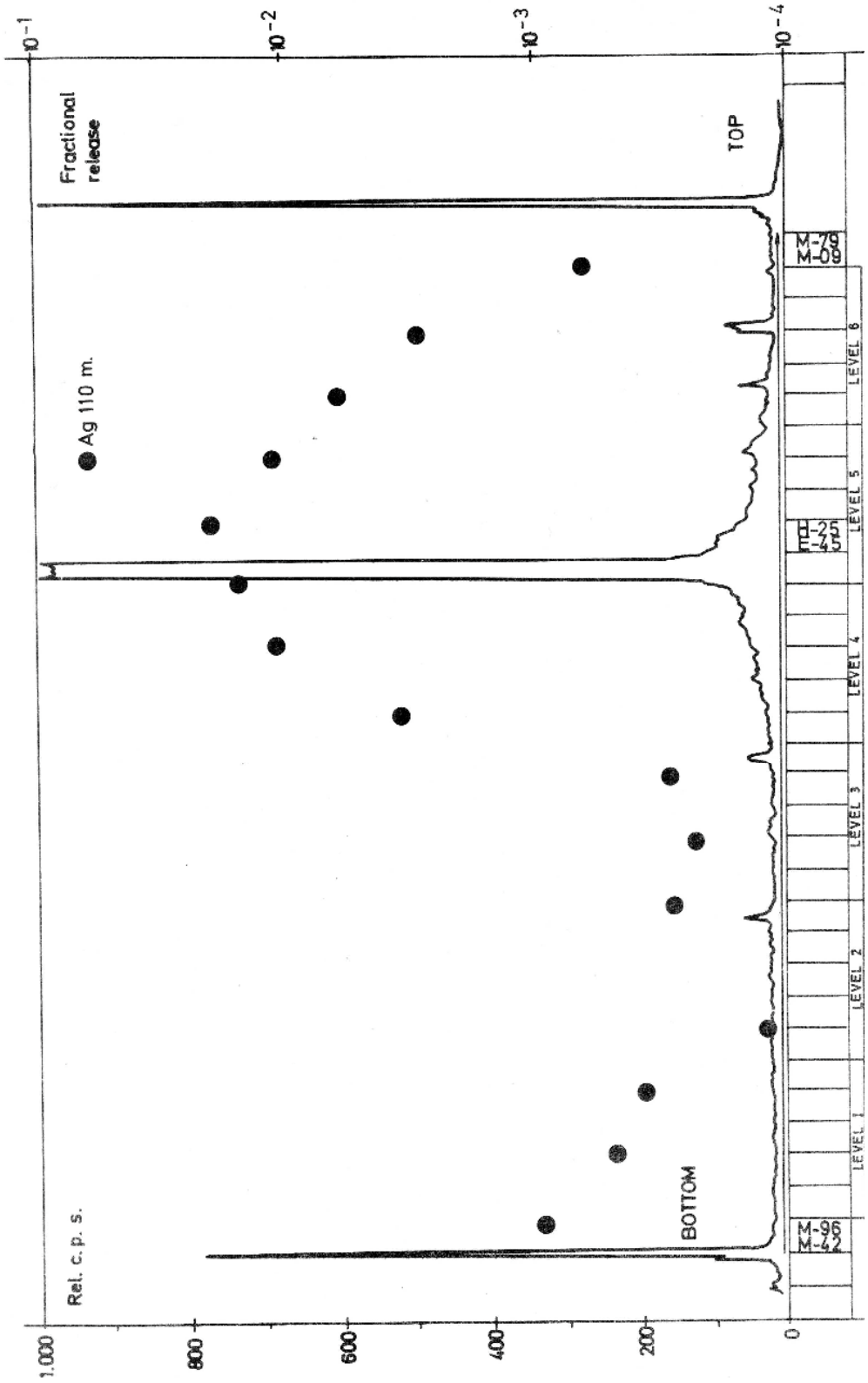

Figure 13: Total gamma profile above 250keV for the empty channel 7 and fractional release of Ag110m

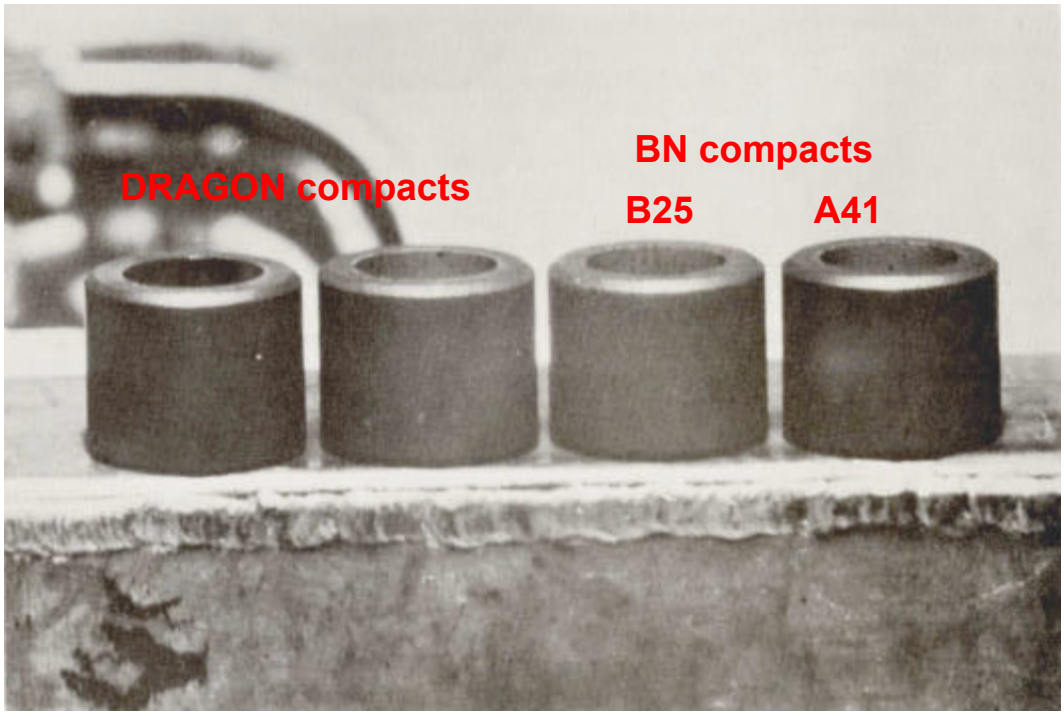

Figure 14: BN and DP compacts of the level 5 – MT-2 experiment

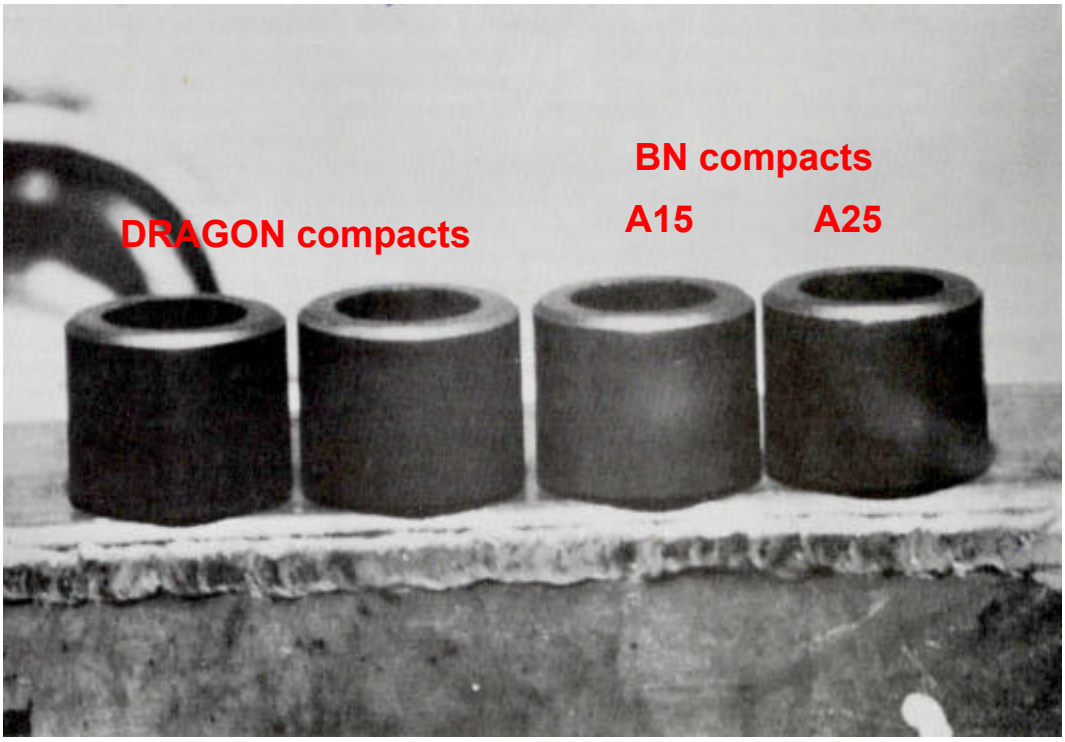

Figure 15: BN and DP compacts of the level 1 – MT-2 experiment

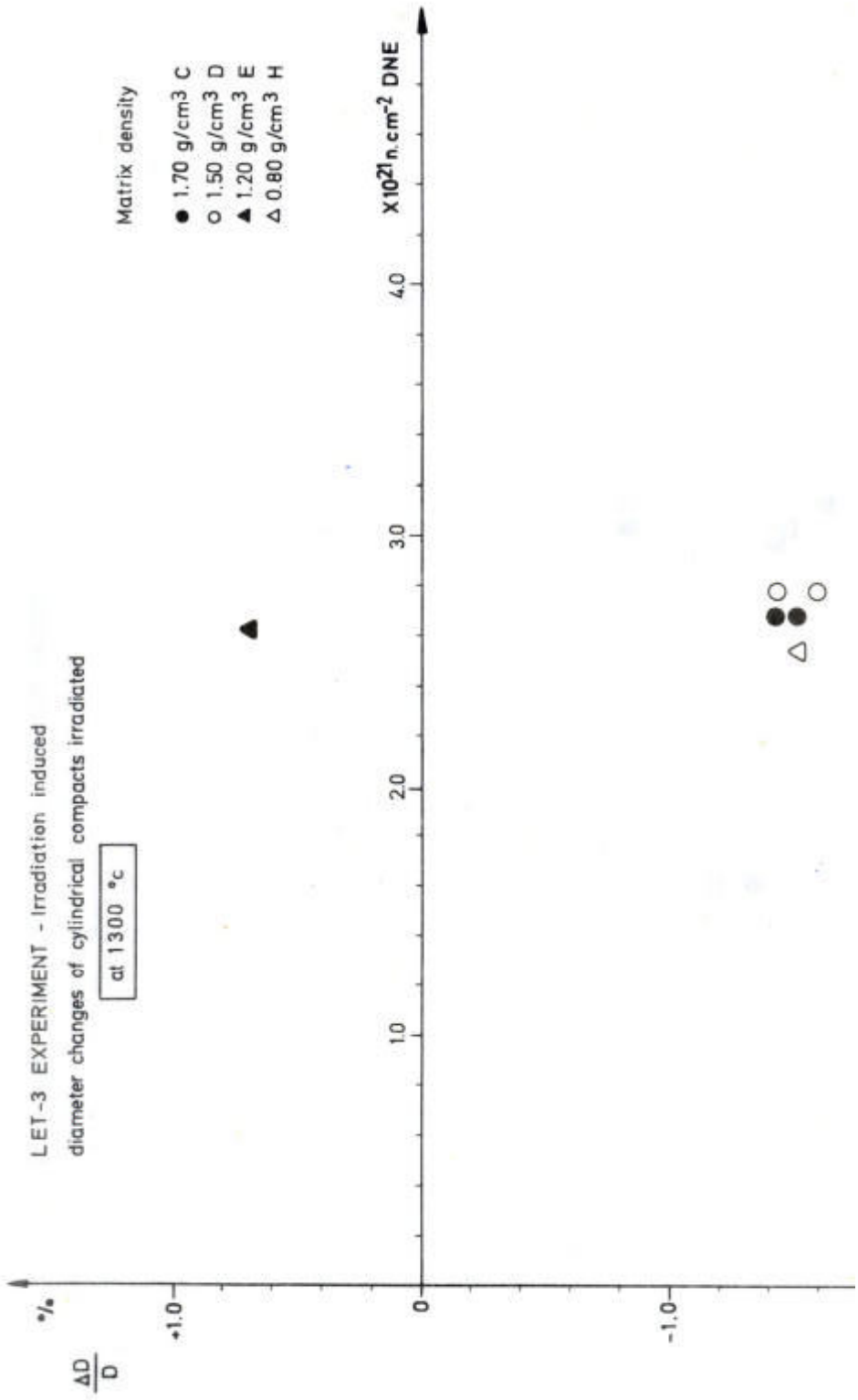

Figure 16: LET-3 irradiation induced diameter change of cylindrical compacts irradiated at 1300°C

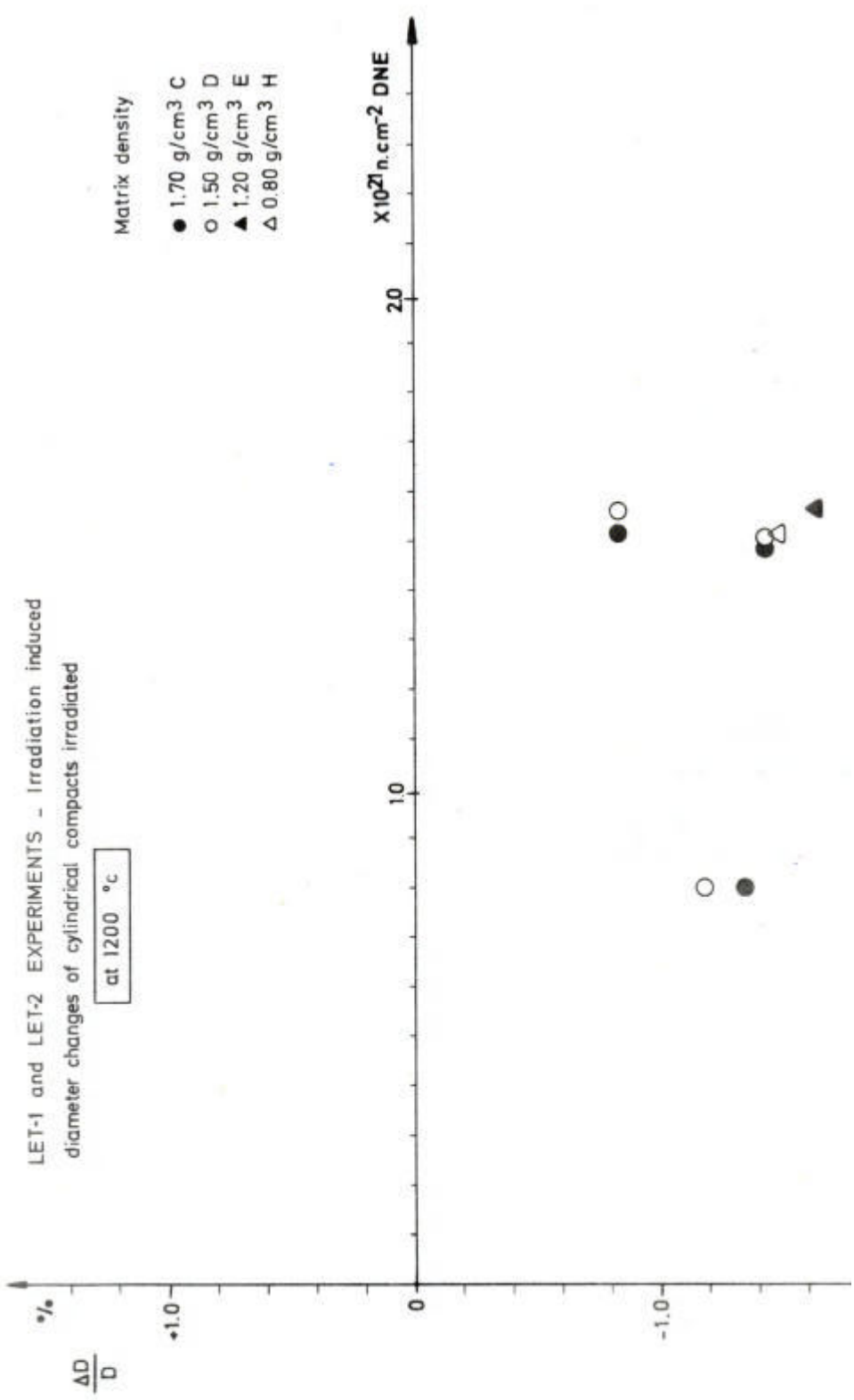

Figure 17: LET-1 and LET-2 Irradiation induced diameter change of cylindrical compacts irradiated at 1200°C

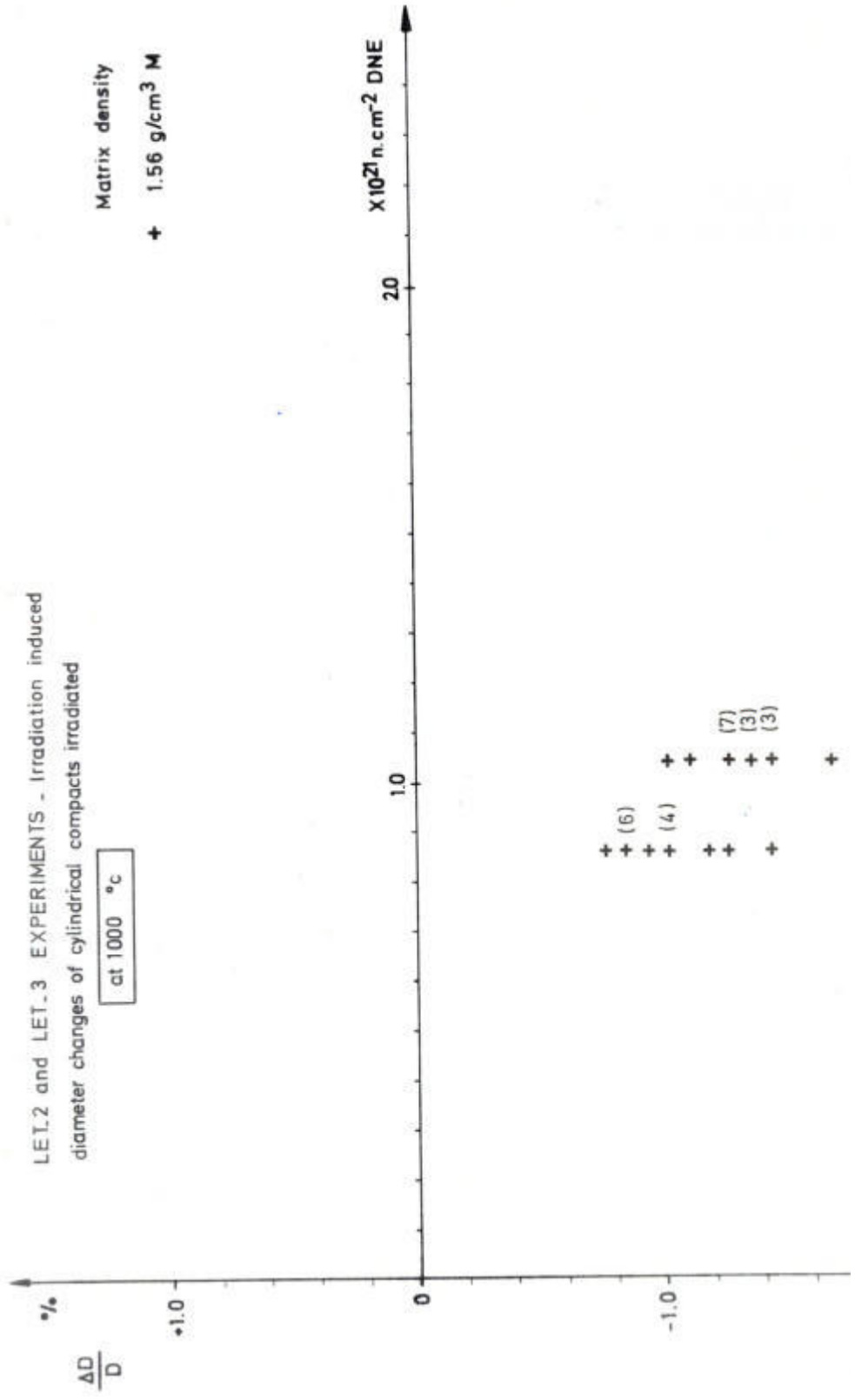

Figure 18: LET-2 and LET-3 Irradiation induced diameter change of cylindrical compacts irradiated at 1000°C

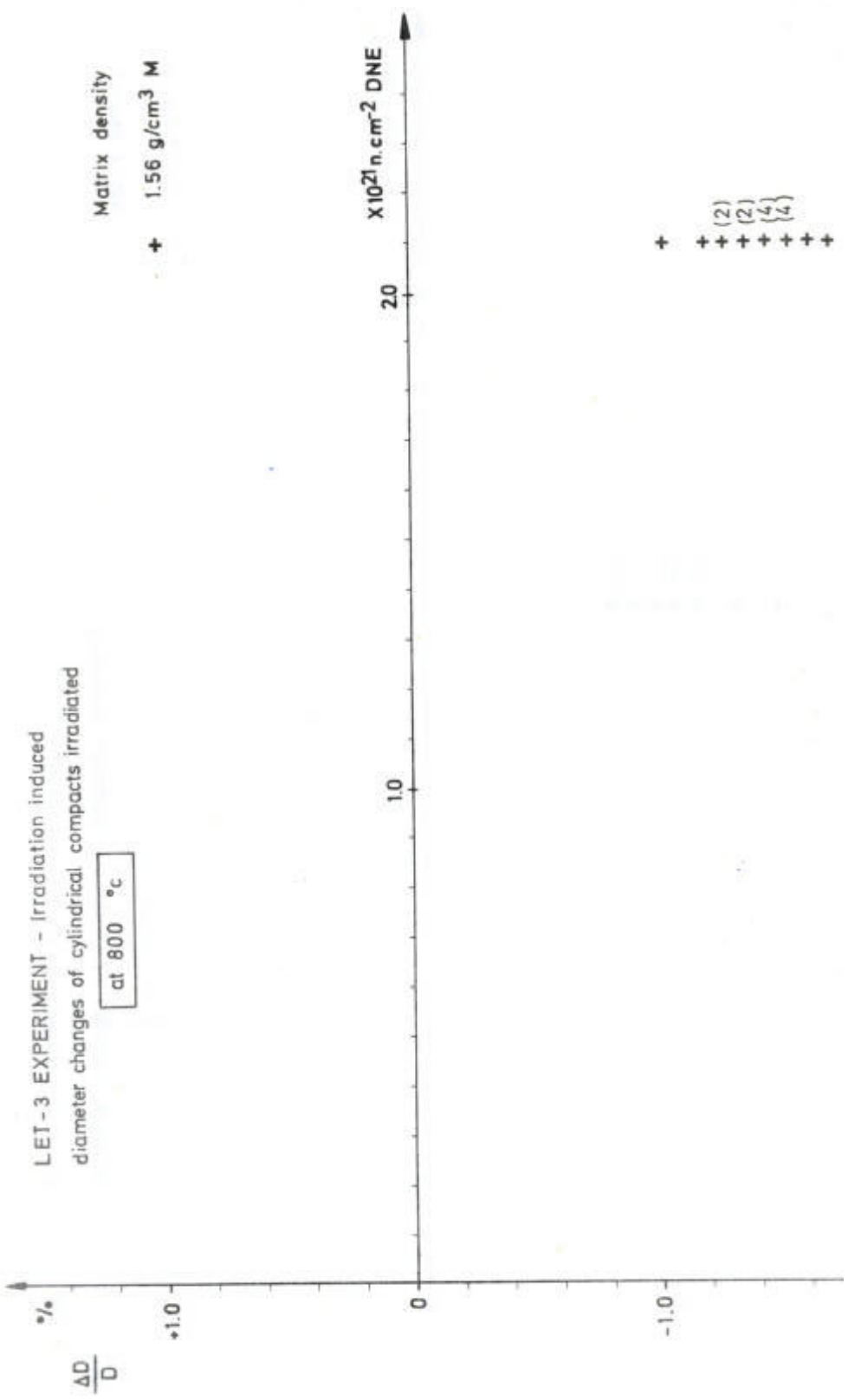

Figure 19: LET-3 Irradiation induced diameter change of cylindrical compacts irradiated at 800°C

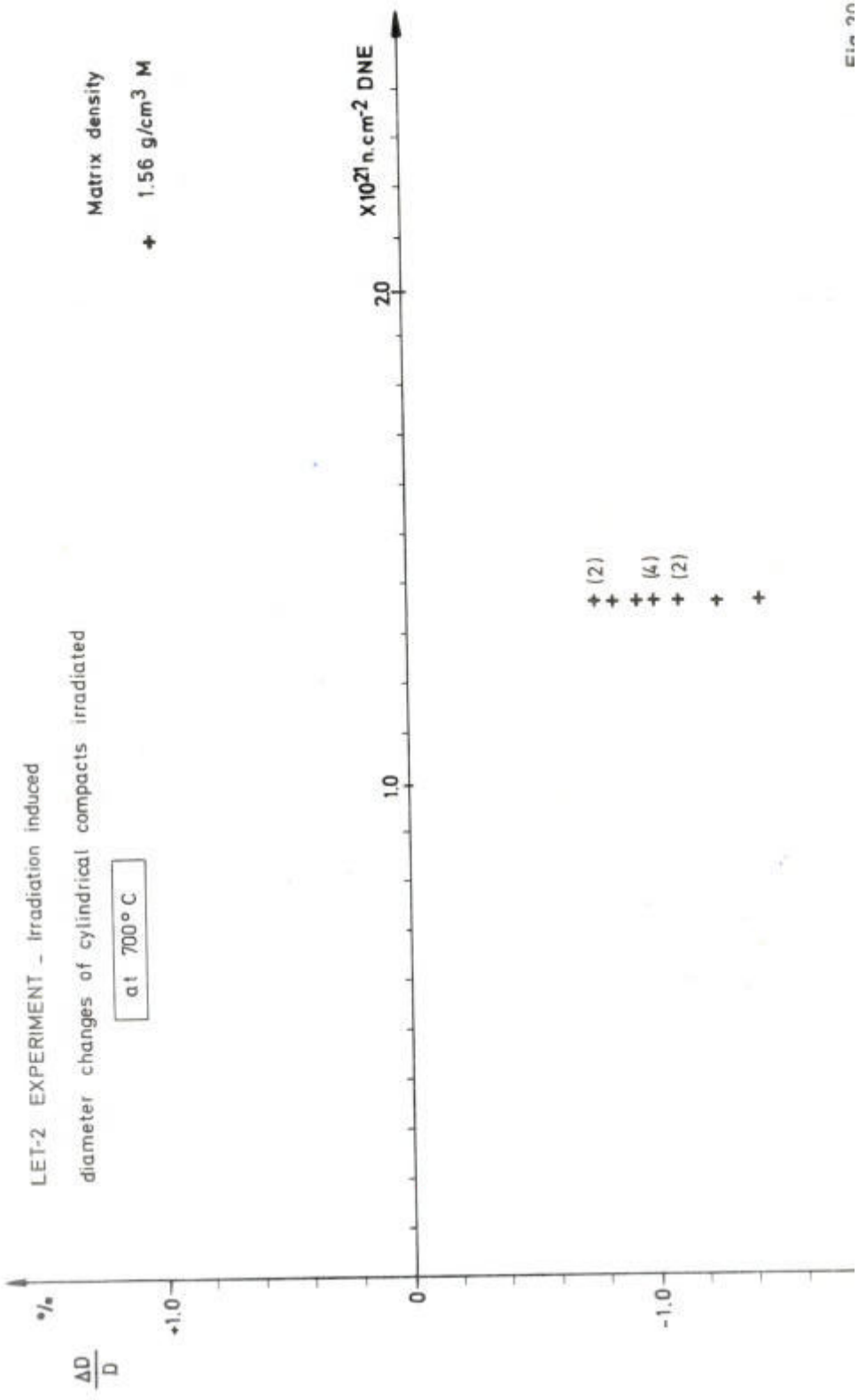

Figure 20: LET-2 Irradiation induced diameter change of cylindrical compacts irradiated at 700°C

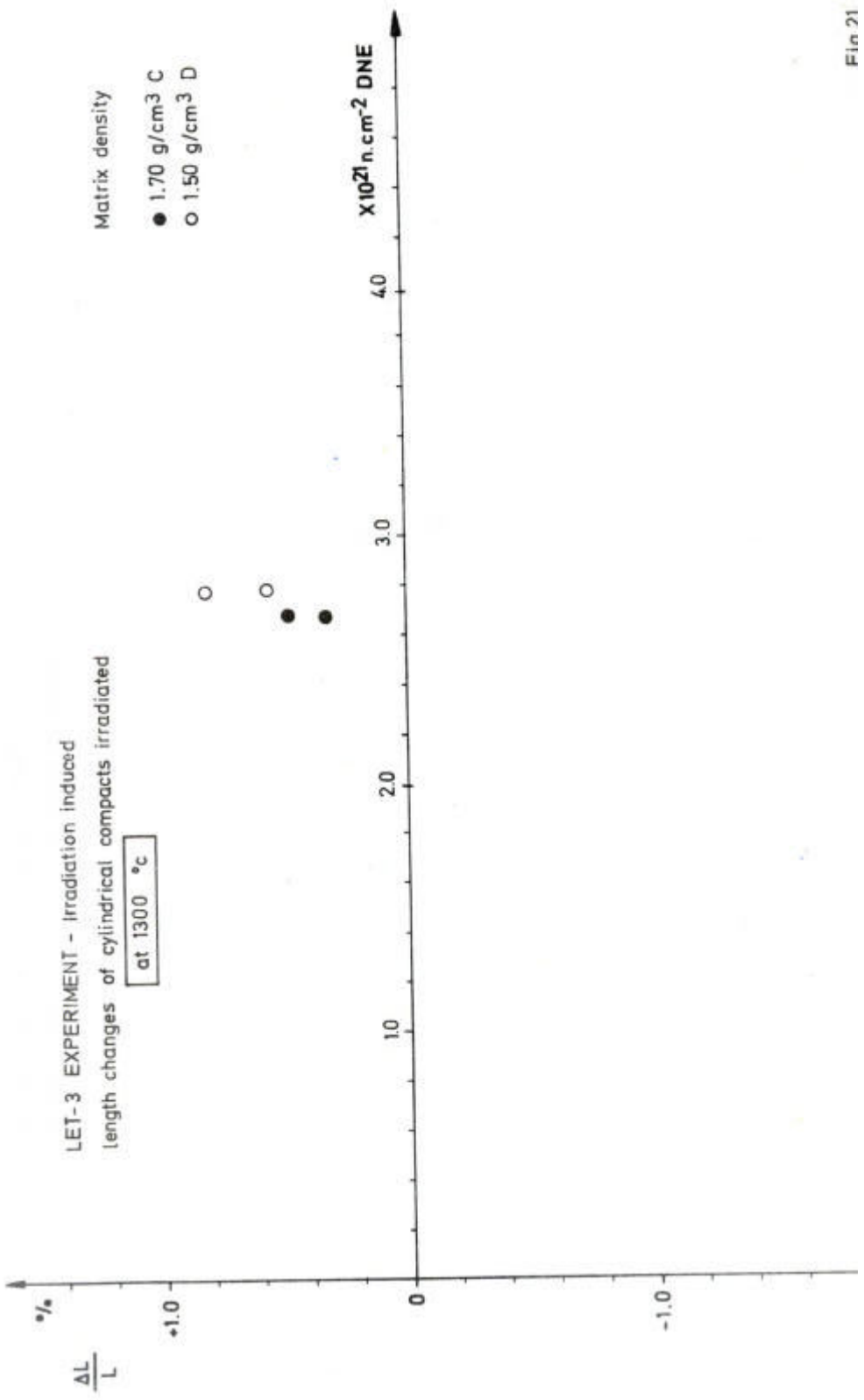

Figure 21: LET-3 Irradiation induced length changes of cylindrical compacts irradiated at 1300°C

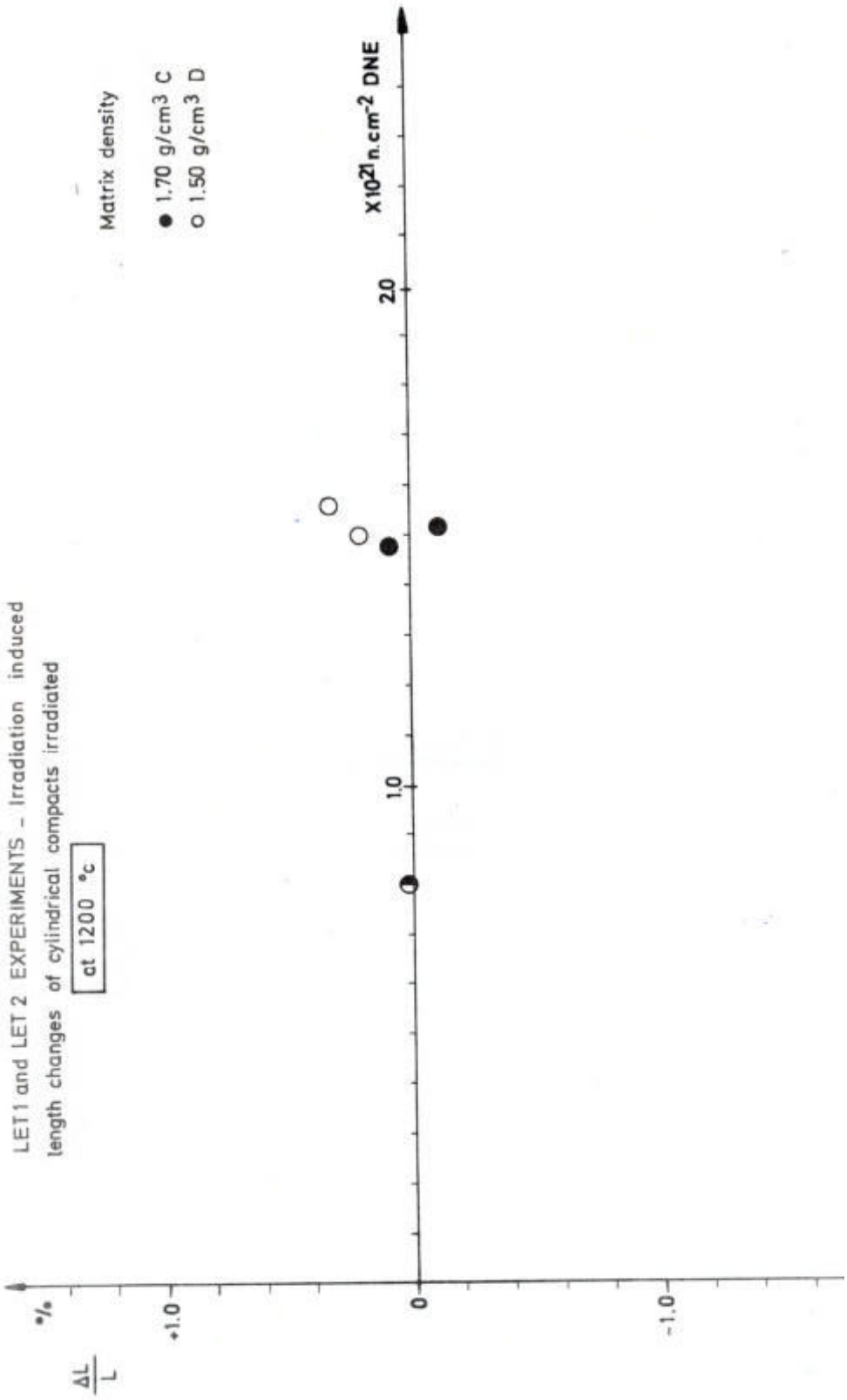

Figure 22: LET-1 and LET-2 Irradiation induced length changes of cylindrical compacts irradiated at 1200°C

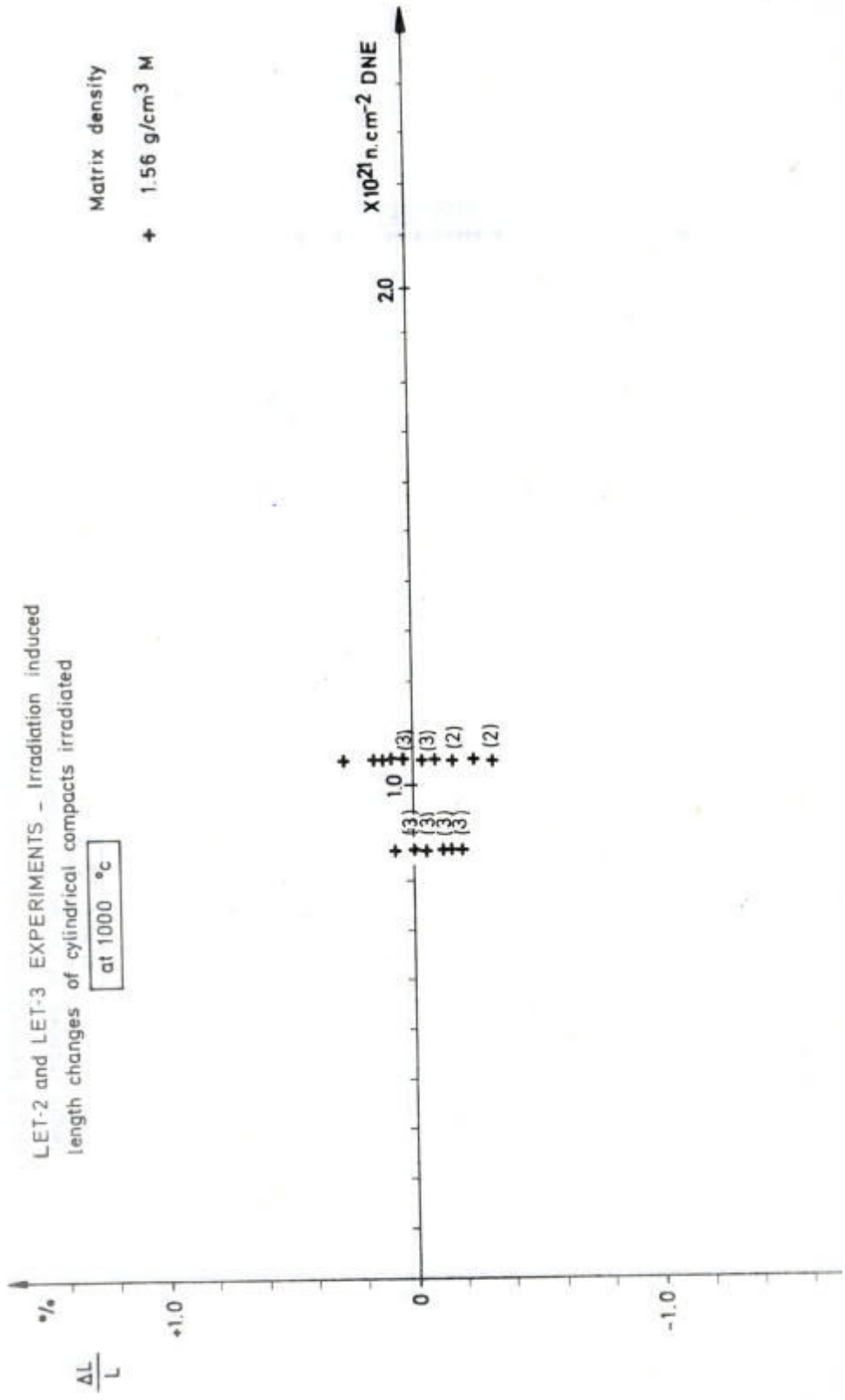

Figure 23: LET-2 and LET-3 Irradiation induced length changes of cylindrical compacts irradiated at 1000°C

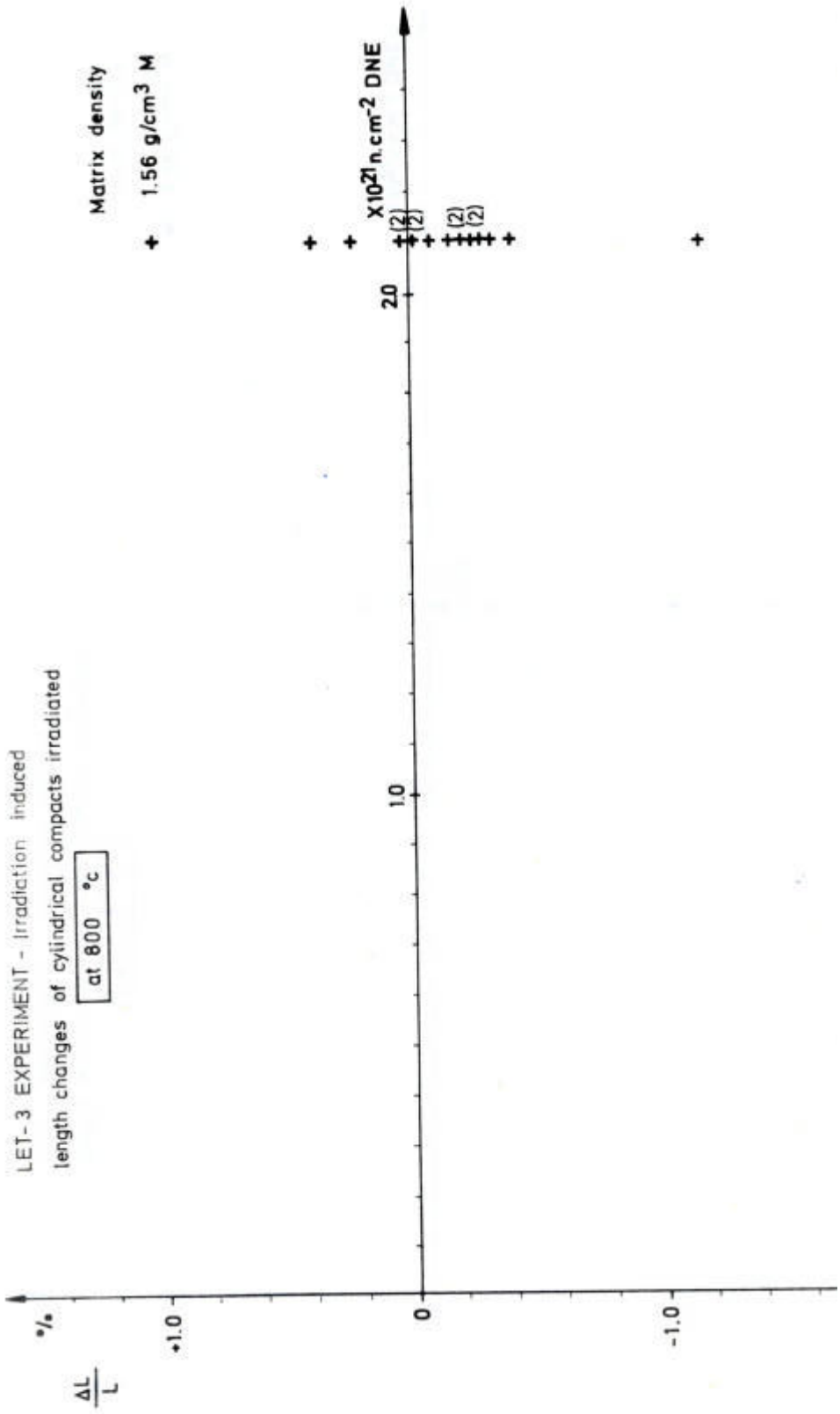

Figure 24: LET-3 Irradiation induced length changes of cylindrical compacts irradiated at 800°C

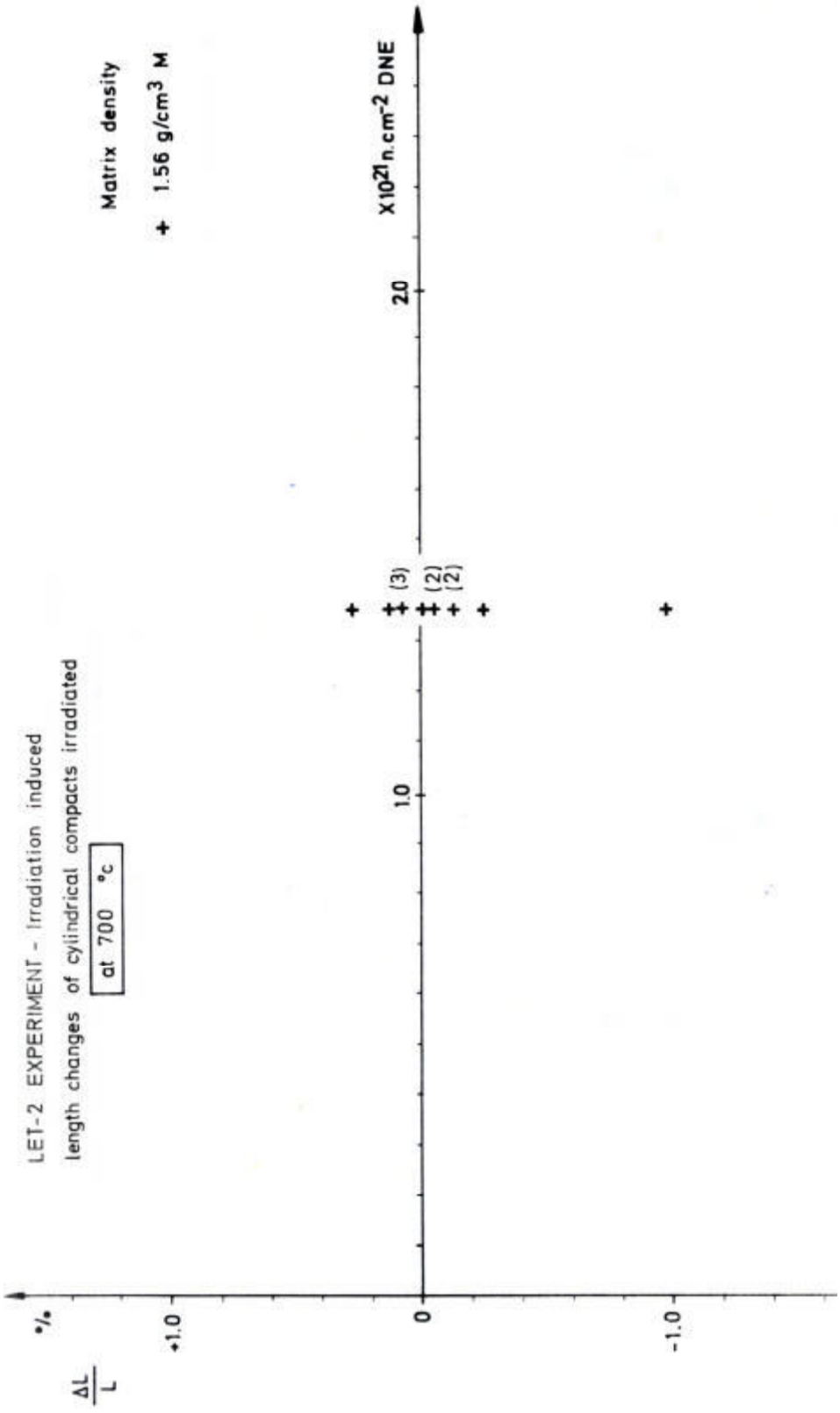

Figure 25: LET-2 Irradiation induced length changes of cylindrical compacts irradiated at 700°C

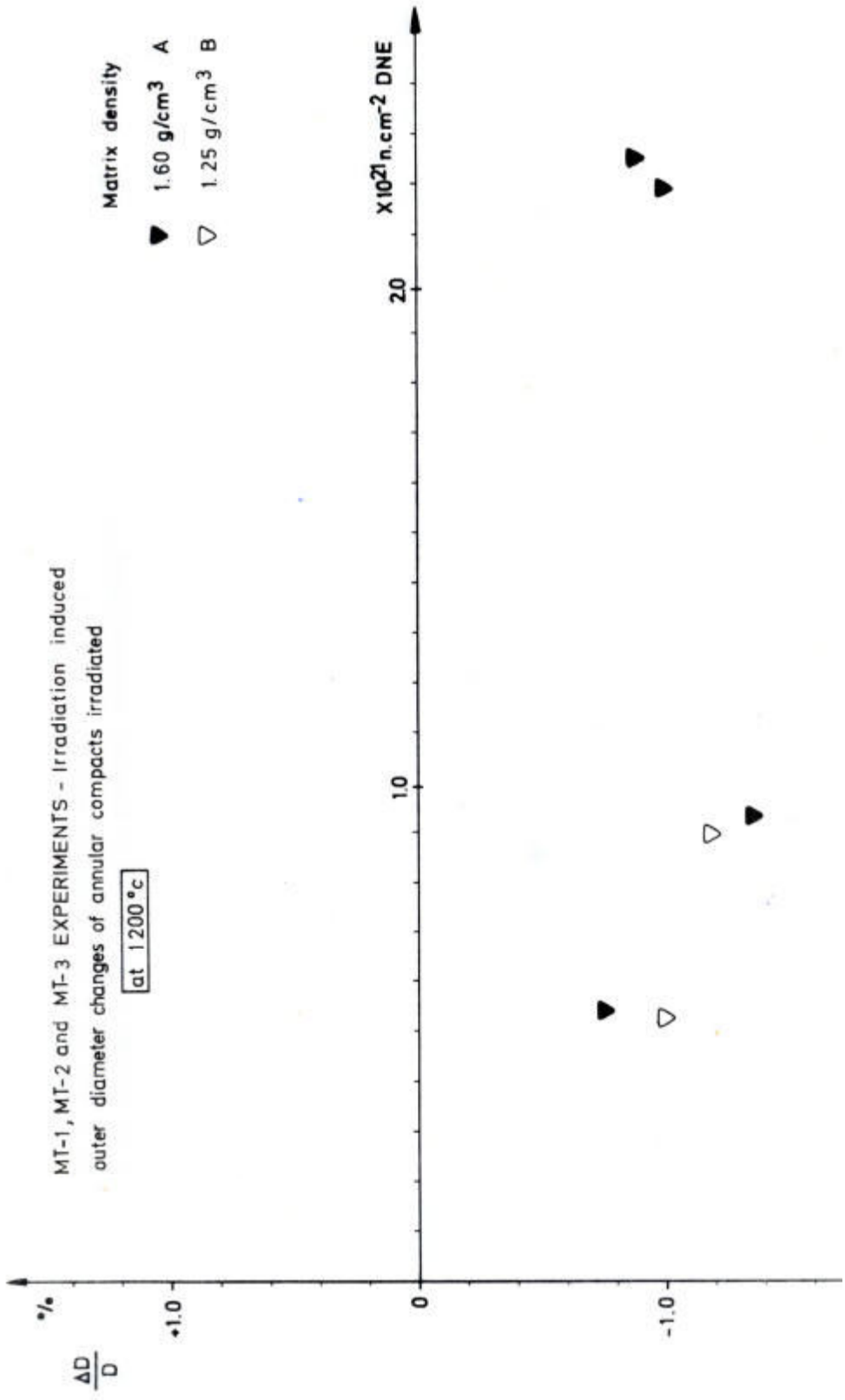

Figure 26: MT-1, MT-2 and MT-3 Irradiation induced outer diameter changes of annular compacts irradiated at 1200°C

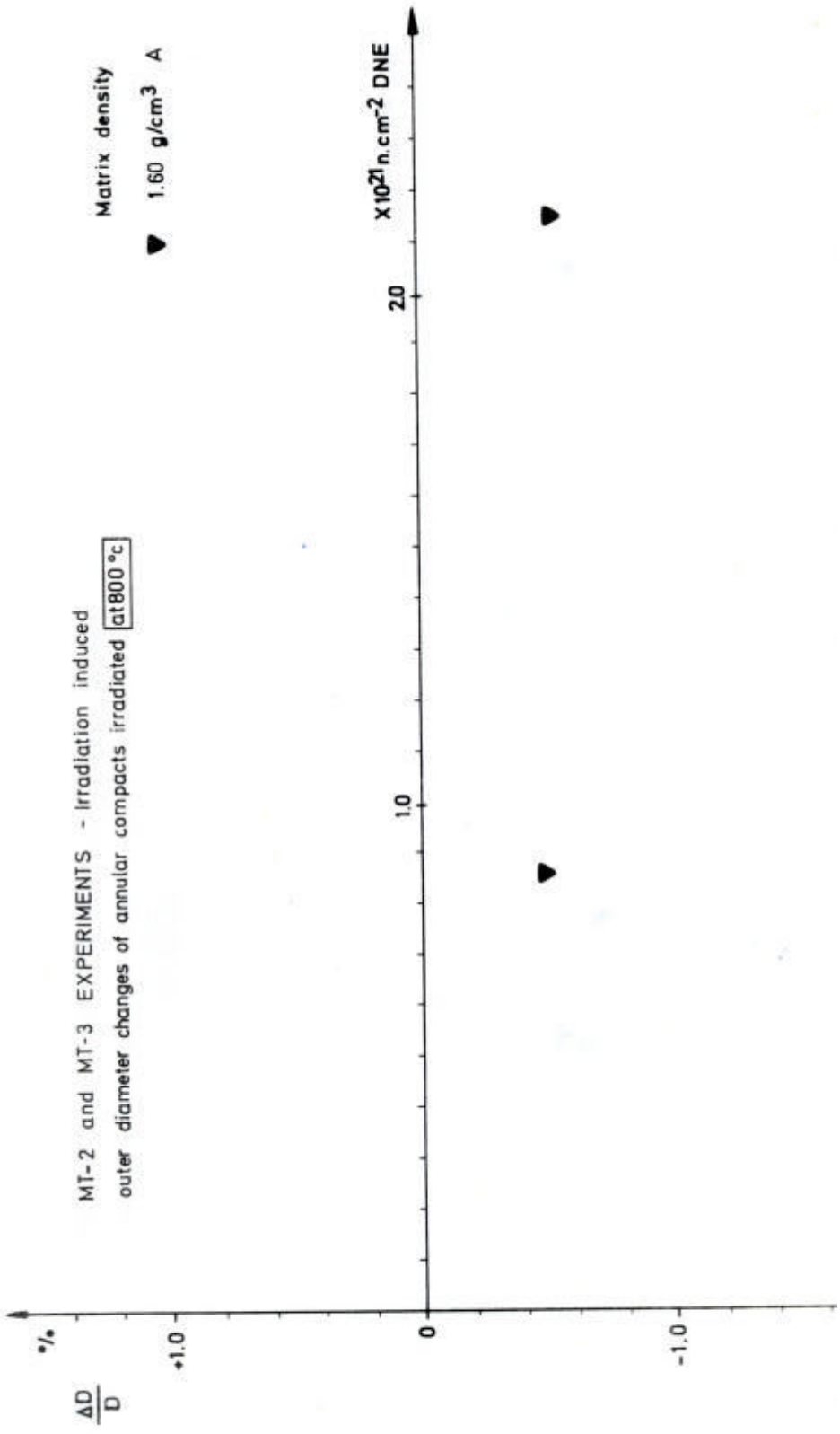

Figure 27: MT-2 and MT-3 Irradiation induced outer diameter changes of annular compacts irradiated at 800°C

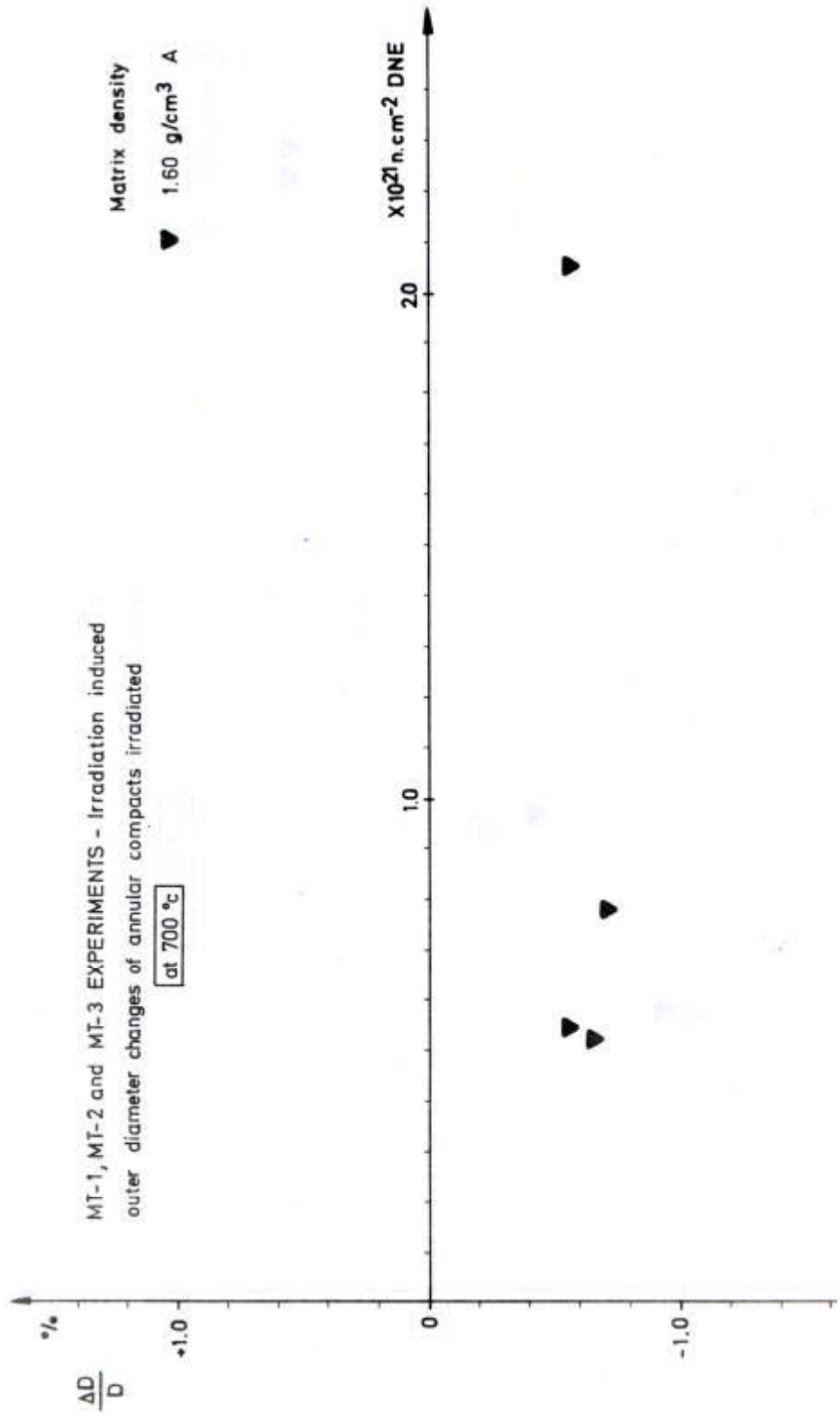

Figure 28: MT-1, MT-2 and MT-3 Irradiation induced outer diameter changes of annular compacts irradiated at 700°C

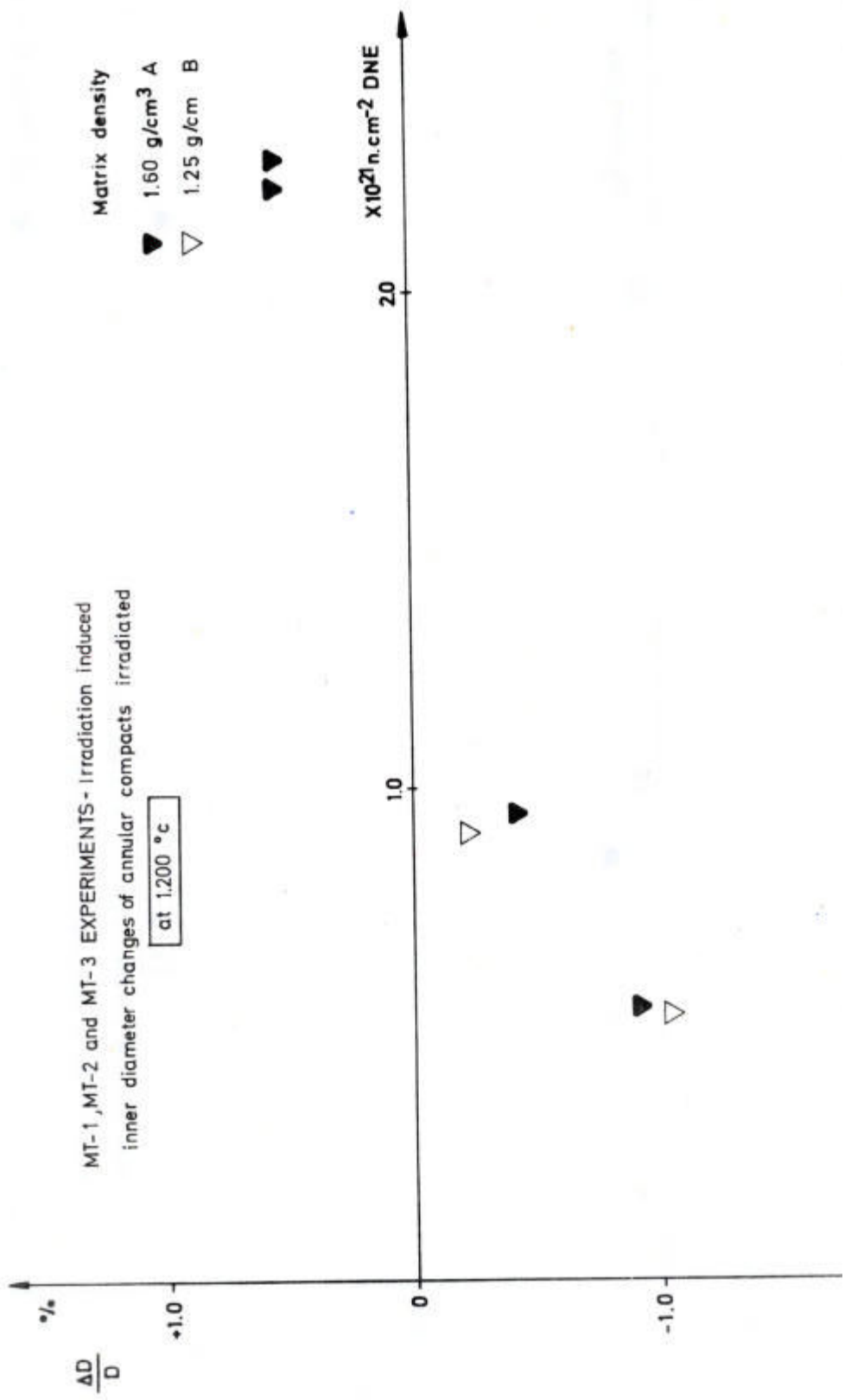

Figure 29: MT-1, MT-2 and MT-3 Irradiation induced inner diameter changes of annular compacts irradiated at 1200°C

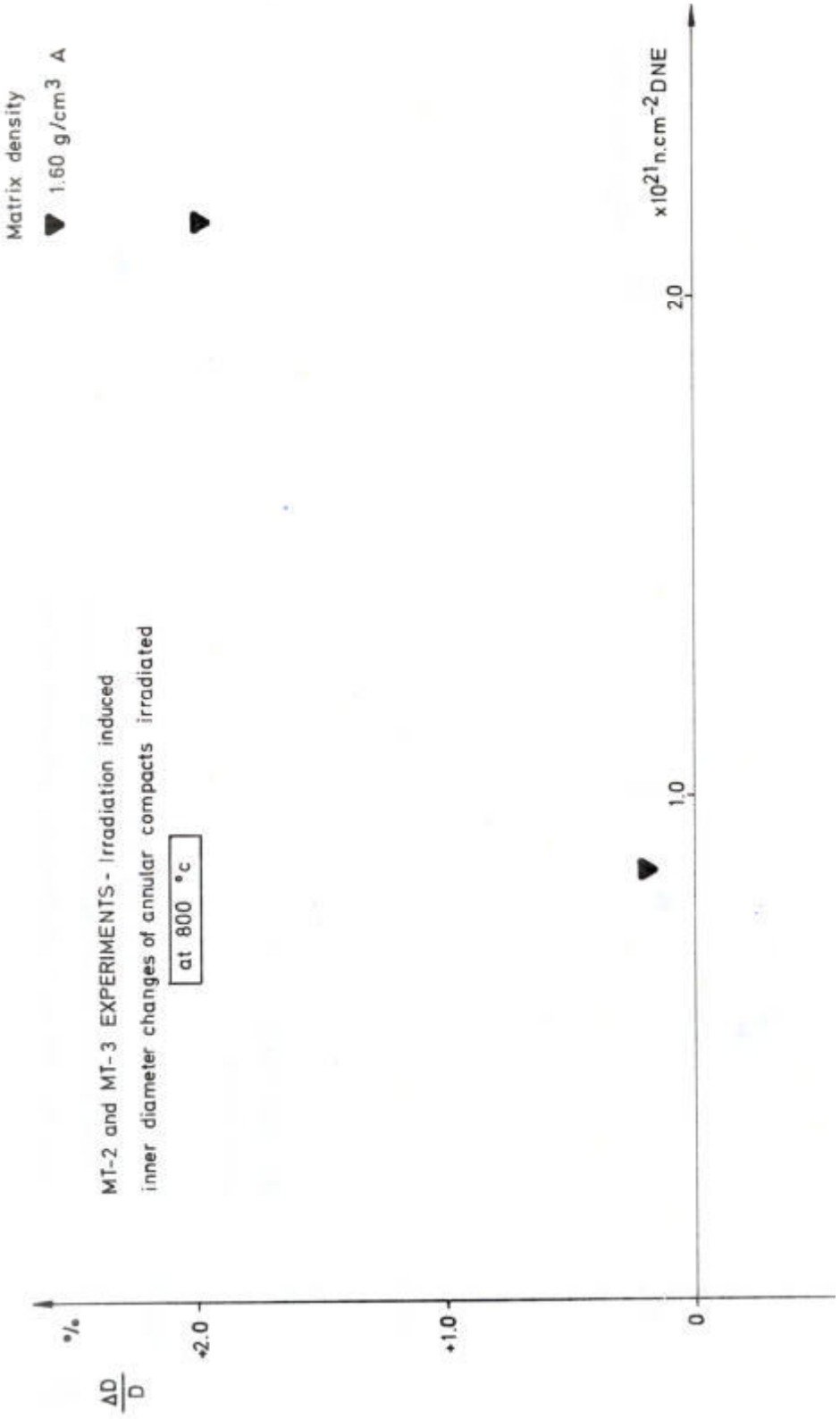

Figure 30: MT-2 and MT-3 Irradiation induced inner diameter changes of annular compacts irradiated at 800°C

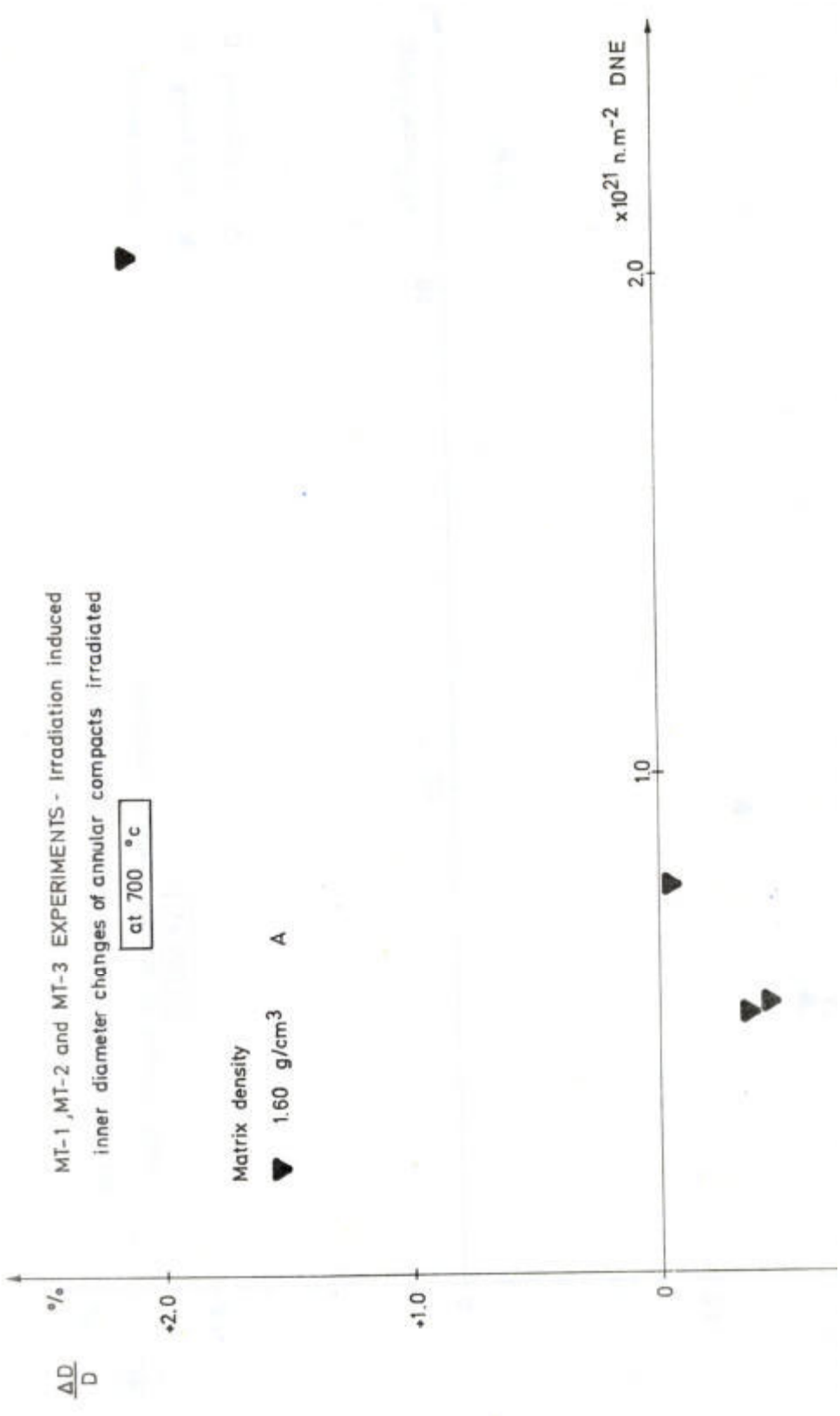

Figure 31: MT-1, MT-2 and MT-3 Irradiation induced inner diameter changes of annular compacts irradiated at 700°C

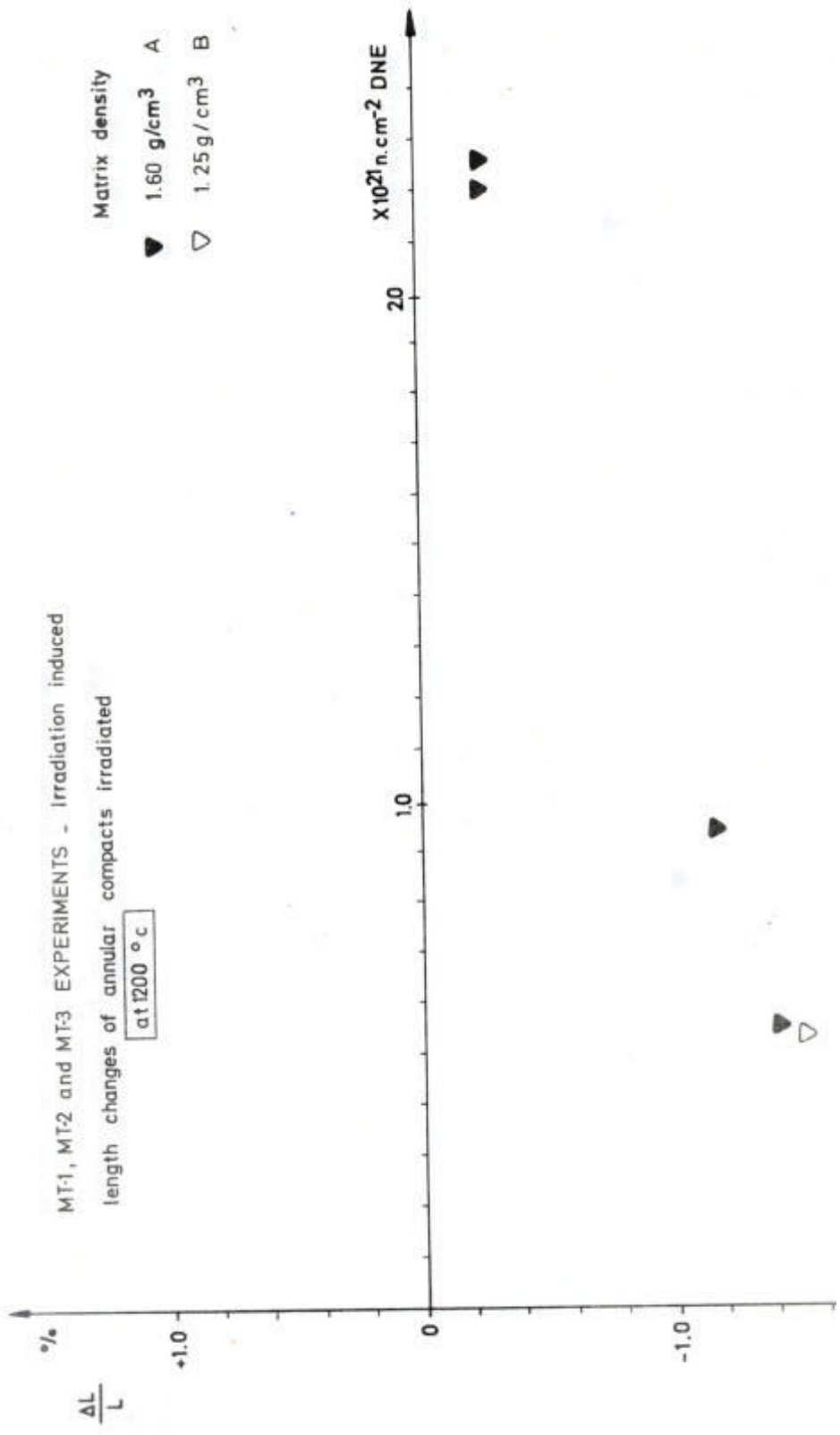

Figure 32: MT-1, MT-2 and MT-3 Irradiation induced length changes of annular compacts irradiated at 1200°C

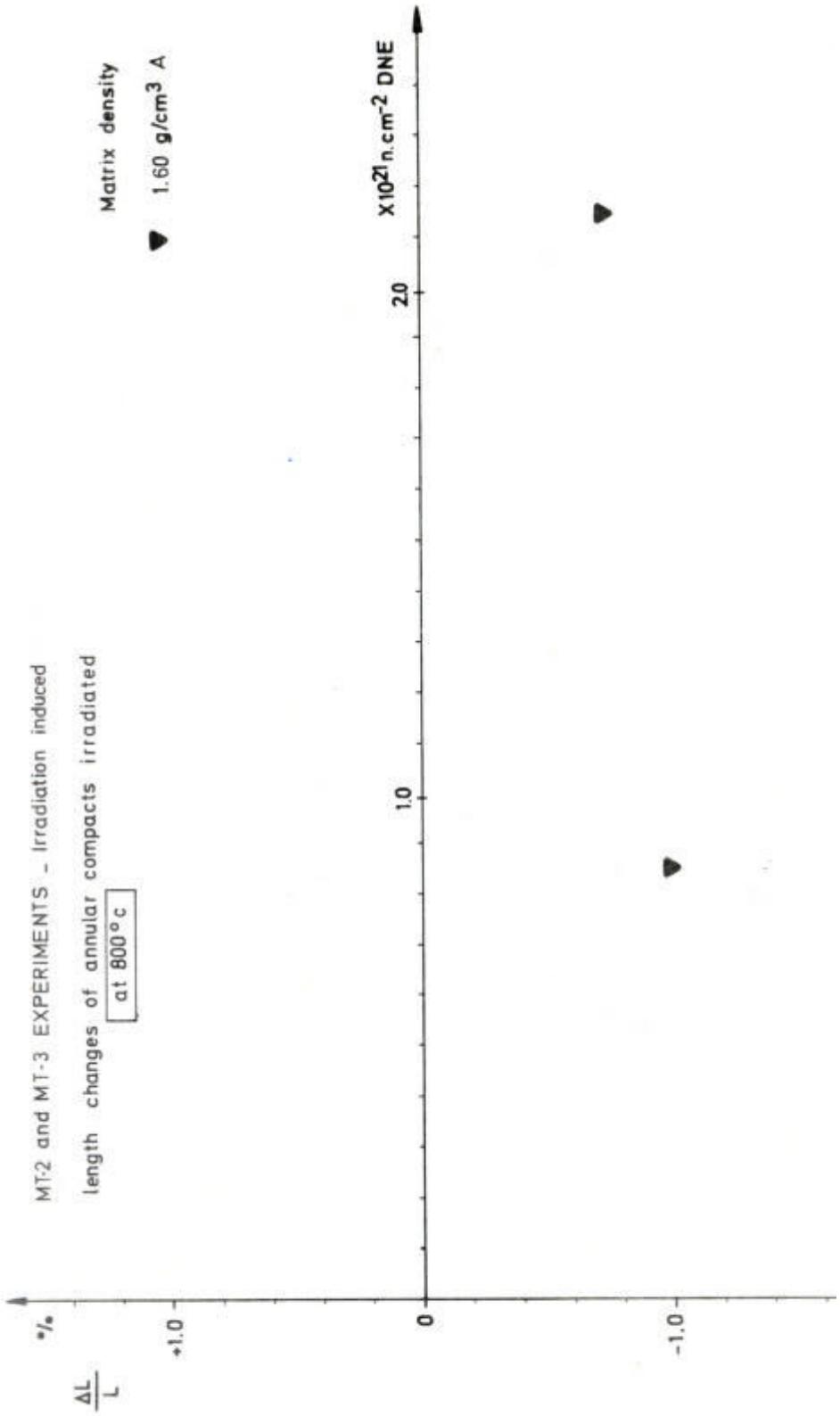

Figure 33: MT-2 and MT-3 Irradiation induced length changes of annular compacts irradiated at 800°C

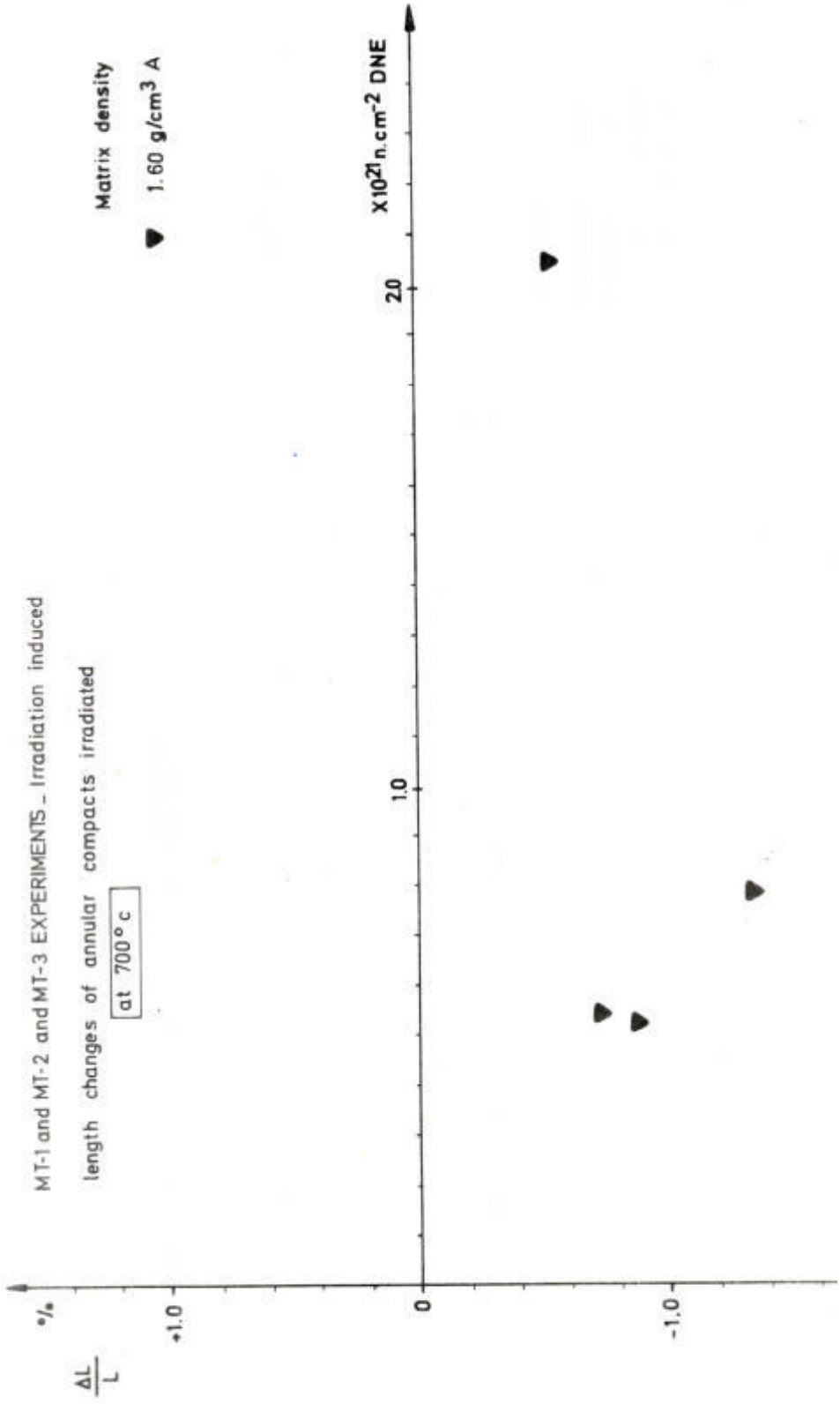

Figure 34: MT-1 and MT-2 and MT-3 Irradiation induced length changes of annular compacts irradiated at 700°C

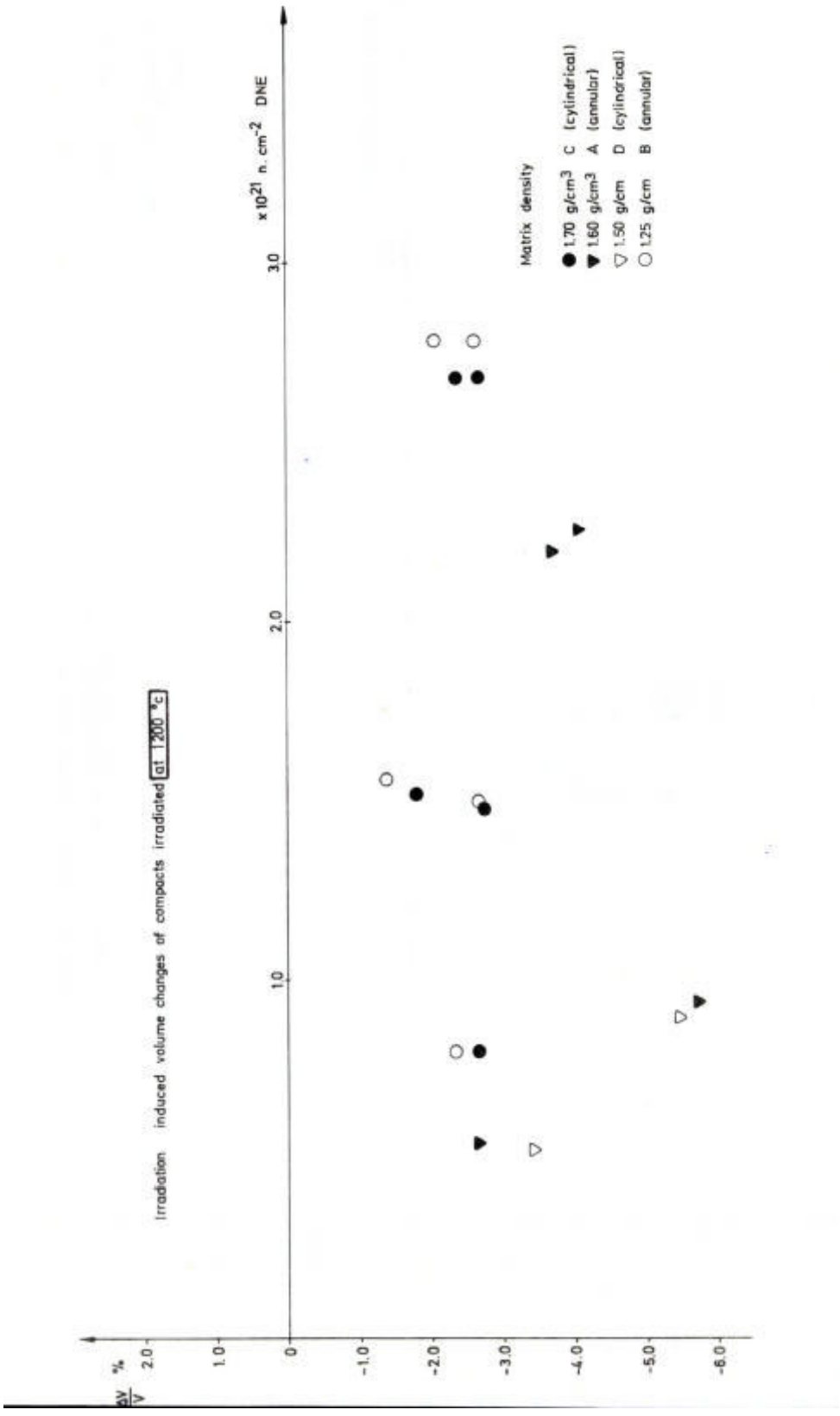

Figure 35: Irradiation induced volume changes of compacts irradiated at 1200°C

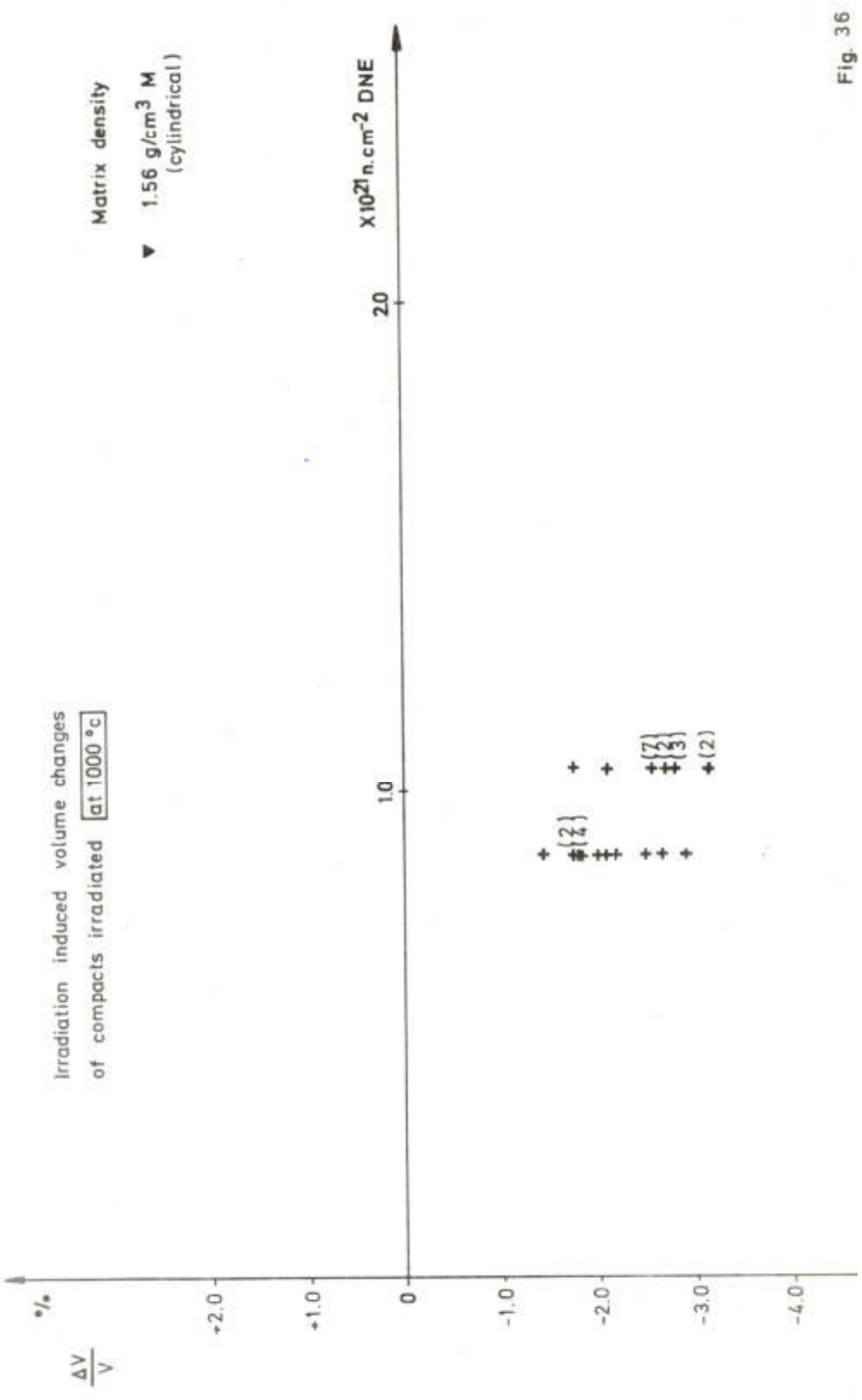

Figure 36: Irradiation induced volume changes of compacts irradiated at 1000°C

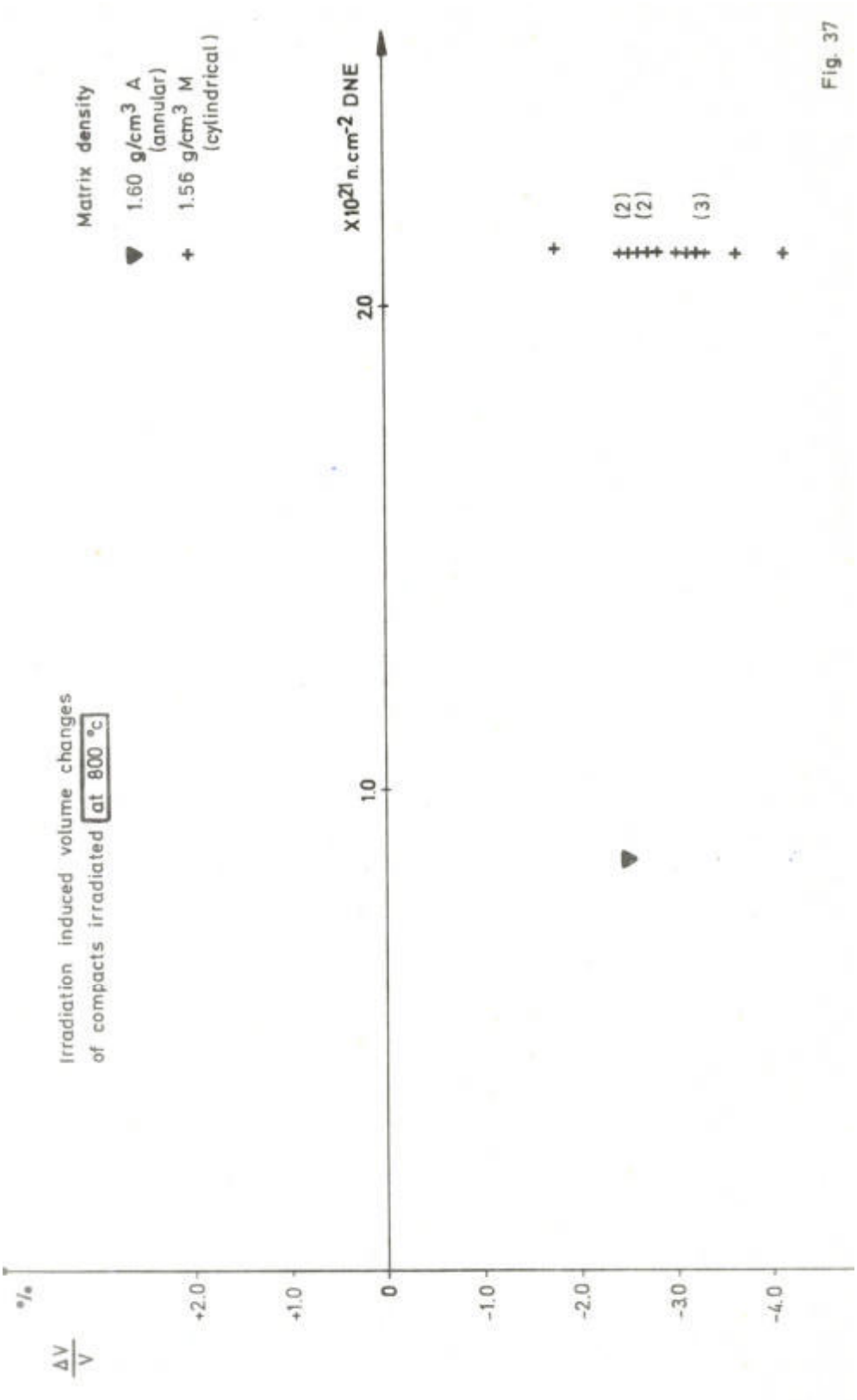

Figure 37: Irradiation induced volume changes of compacts irradiated at 800°C

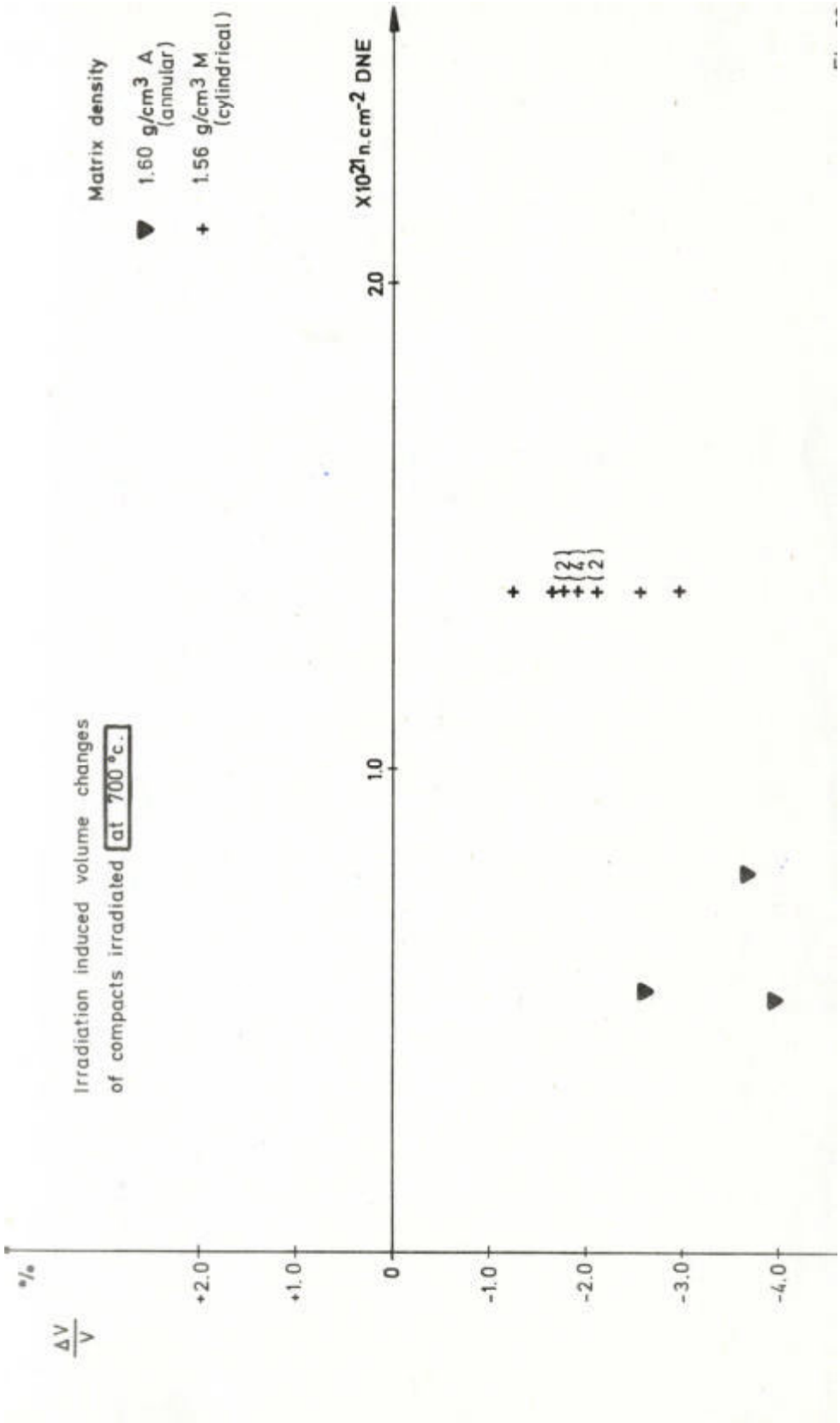

Figure 38: Irradiation induced volume changes of compacts irradiated at 700°C

	Type of document:	Reference No / File - "Rev." - Page
	Technical Note	**0601024/220-"-" - 1**
		Other reference:

Client: EC	Author(s) G. TOURY
Project: Raphael IP – SP Fuel Technology WP-FT4 Performance Modelling	
Subject:	

HTR particles Irradiation Experiment BN database

BR3/2bis Experiment

Rev.	Date	Chrono Filing No.	Status	Initials dactylo.	Author: Initials	Author: Visa 1	Verified by: Initials	Verified by: Visa 2	Approved by: Initials	Approved by: Visa 3	Q.A.: Initials	Q.A.: Visa 4	Issued by: Initials	Issued by: Visa 5	Number of pages
C															
B															
A															
-	17/05/2006	0601024	Draft		GTY		SSH						GTY		28

Distribution:

RAPHAEL Project: Mr. OBRY (1 copy +1 CD)

BN: SSH, GTY

	Type of document:	Reference No / File - "Rev." - Page
	Technical Note	**0601024/220-“-“ - 2**
		Other reference:

BELGONUCLEAIRE N.V.
Avenue Ariane, 4 - 1200 Brussels
TVA: BE 403.126.258
RCB: 271.300
TEL: 32-2774 05 11
FAX: 32-2-774 05 47

LIST of MODIFICATIONS

DATE	REVISION	OBJECT

15/05/2006	-	Draft

NOTICE

PERSONNEL IN CONFIDENCE, NOT FOR PUBLICATION

This work is performed under the term and conditions of the Consortium Agreement of the RAPHAEL Project supported by the EC under contract n° 516508 (FI6O)

LIABILITY

This document was prepared by BELGONUCLEAIRE (BN). Neither BN, nor any person acting on behalf of BN:

a) gives any warranty, expressed or implied, with respect to the accuracy, completeness of the information contained in this document, or that the use of any information, apparatus, method or process disclosed in this document may not infringe third party rights, or

b) assumes any liabilities with respect to the use of, or for damage resulting from the use of any information, apparatus, method or process disclosed in this document.

Abstract

The purpose of this experiment was the study of the behaviour under irradiation in the BR3 reactor, core 2bis, of matrix materials with and without particles, up to a dose of 10^{21} n.cm^{-2} DNE in the temperature range 300-1200°C.

Table of content

List of Tables

List of Figures

1. INTRODUCTION

The following samples were irradiated in the BR3 core 2bis, moderator channel 80:

- matrixes without fuel,
- compacts with depleted particles,
- compacts with blending of U-depleted particles and 12%U enriched particles, leading to an average enrichments of 5.7% and 8.5%,
- compacts with 12%U enriched particles.

The objective of the experiment was to study the behaviour of matrix materials with and without particles, up to a dose of 10^{21} EDN and in the temperature range 300-1200°C.

2. FUEL SPECIFICATIONS

The specifications of the enriched and depleted particles are given in Table1.

The specifications of the compacts with and without particles are presented in Tables 2 to 6.

Samples with enriched particles were surrounded by a graphite ring, to obtain the expected central temperature.

The U235 linear density has been verified by gamma scanning for all the samples.

3. IRRADIATION HISTORY

The irradiation started in core BR3/2bis in July 1969 and ended in December 1970. The core load diagram is given in Figure 1 and the sample loading position is presented in Table 7.

No temperature measurement in the channel 80 has been carried during irradiation.

During the dismantlement of the experimental device, the thermal monitors were damaged; the irradiation temperatures have then been estimated from the fission cross section and thermal flux in the channel 80, according to the following relation:

$$P = e\left[(\sigma_f^1\theta^1 + \sigma_f^2\theta^2)N_{235} + \sigma_f^1\theta^1 N_{238}\right]F$$

with

P	power density (W/cm3)
e	released energy by fission (J)
σ_f^1	Fission cross section of fast group (cm^2)
σ_f^2	Fission cross section of thermal group (cm^2)

θ^1 Neutronic flux of fast group (/cm^2.s)

θ^2 Neutronic flux of thermal group (/cm^2.s)

F Axial form factor

N_{235} Number of U^{235} atoms per volume unit (-/cm^3)

N_{238} Number of U^{238} atoms per volume unit (-/cm^3)

The axial distribution of the thermal flux is given in Figure 2.

The maximal fuel temperature has been determined from these data, assuming 0.15 W/cm°C for the compact thermal conductibility and 0.01W/cm°C for the carbon thermal conductibility.

Results are presented in Table 8.

4. POST-IRRADIATION EXAMINATIONS

The experiment was unloaded at the beginning of 1971. Difficulties during the dismantling of the experiment led to the destruction of some samples (in particular 2/1 and 7/2). Only one temperature monitor has been recovered undamaged. Some compacts were still intact (Figure 3), whereas others presented damaged end faces (Figure 4).

4.1. Diameter shrinkage

The diameter measurements have shown a shrinkage between 0.3% and 0.8% for the matrix samples, and 0.4 to 1% for the compacts with depleted fuel particles.

4.2. Ceramographic examinations:

Sample 7/1 (12%U enrichment)

This sample was intact after irradiation. The matrix presented no cracks but was relatively porous and heterogeneous (Figure 5). Of the 14 particles that were observed, three showed important radial cracks in the coating, certainly resulting from the fabrication, as suggested by the penetration of the matrix material inside the cracks (Figure 6). A few tangential cracks were also noticeable inside and between the layers.

Sample 4/2 (8.5% average enrichment)

The matrix behaviour was similar to that of sample 7/1.

All the observed particles were intact (Figure 7); however, some metallic inclusions were observed in the internal PyC layer.

Sample 2/9 (depleted U)

The interface between the external PyC layer and the matrix was more distinct, which results of the vibration instead compaction process used.

The matrix appeared denser than those of compacted samples, 19 over 52 observed particles showed radial and tangential cracks in the coating (Figure 8).

Sample 4/1 (8.5%U average enrichment)

The matrix aspect is similar as for the samples 7/1 and 4/2.

3 over 13 particles were broken.

Sample 2/13 (depleted U)

15 over 27 particles were damaged.

The ceramographic observations have shown:

- A good behaviour of the matrix materials
- The number of particles with cracks along the coating layers is relatively high; but most of the cracks resulted from the fabrication process;
- No amoeba effect was observed;
- Damages seemed to be independent to the dose and temperature level.

4.3. Burn-up determination

The burn-up has been determined for three samples:

Sample 2/8 (depleted U): 7000 MWd/t_{ox} (Nd)

Sample 8/2 (5.7% average enrichment): 12800 MWd/t_{ox} (137Cs)

Sample 4/3 (8.5% average enrichment): 48000 MWd/t_{ox} (137Cs)

The burnup of the 12% enriched particles from the sample 4/3 was estimated to be 66000MWd/t_{ox}.

4.4. Gas measurement

A quantity of 0.237 ml STP/g UO_2 of residual Xe was measured in the sample 8/1 (5.6% average enrichment). This value was compared to 0.31 ml STP/g UO2 produced for a burn-up of 14000 MWd/tHM (23.5% FGR).

4.5. Dosimetry

The axial distribution of the fast neutron dose is given in Figure 9.

A maximum about $8x10^{20}$ $n.cm^{-2}$ DNE (Dido Nickel Equivalent) has been received by the sample 3/22.

5. CONCLUSION

The interpretation of the results has been rather difficult because of the samples damage during dismantling, the particle breakage during fabrication and the uncertainty on the temperatures. One should mention that this fuel fabrication has been carried out in 1969.

Anyway, the irradiation in core BR3/2bis has shown a satisfactory behaviour of matrix materials and particles with different U enrichments.

No amoeba effect was noticed but some interaction between particles and the matrix was observed.

Parameter \ Batch N°		**TM/3/8/2Fo (12% enriched particle)**	**TM/3/7/11/F (depleted particles)**
Kernel :	diameter (mm)	854	851
	% theoretical density(%)	88,7	90,6
	stoechiometry	< 2,005	< 2,005
Buffer layer :	Thickness(μm)	30	30
	Density (g/cc)	1,05	1,5
Transition layer:			
	Thickness(μm)	40	40
Internal PyC layer :			
	Thickness(μm)	30	30
	Density (g/cc)	1,75	1,75
	Anisotropy	1,6	1,6
	Deposit Temperature(°C)	1700 → 2050	1700 → 2050
Sic layer :	Thickness(μm)	40	40
	Density (g/cc)	3,19	3,19
	Deposit Temperature(°C)	1650	1650
External PyC layer :			
	Thickness(μm)	40	40
	Density (g/cc)	1,8	1,8
	Anisotropy	1,5	1,5
	Deposit Temperature(°C)	1800 → 2050	1800 → 2050

Table 1 : Coated particles specifications

Sample number	Matrix Composition	Carbon content (%)	Compaction pressure (kg/cm²)	Diameter (mm)	Height (mm)
3/1	Th + G	5	40	13,5	9,7
3/2	Th + G	5	40	13,5	9,6
3/3	Th + G	5	40	13,5	9,8
3/4	Th + G	5	40	13,5	9,4
3/5	Th + G	5	40	13,5	9,9
3/6	P514 + G	5	40	13,5	10,2
3/7	P514 + G	5	40	13,5	10,5
3/8	P514 + G	5	40	13,5	10,4
3/9	P514 + G	5	40	13,5	10,2
3/10	P514 + G	5	40	13,5	42
3/11	Th + G	5	80	13,5	10,2
3/12	Th + G	5	80	13,5	10,4
3/13	Th + G	5	80	13,5	10,2
3/14	Th + G	5	80	13,5	11
3/15	Th + G	5	80	13,5	10,6
3/16	Th + G	5	140	13,5	9,8
3/17	Th + G	5	140	13,5	10,6
3/18	Th + G	5	140	13,5	10,4
3/19	TH + P514 + G	5	40	13,5	10,5
3/20	TH + P514 + G	5	40	13,5	10,6
3/21*	P514 + G	5	40	13,5	20
3/22*	P514 + G	5	40	13,5	35

Th : "thor resin bonded graphite" with 14% resin and 86% graphite.
P514 :phenolic resin with micronised natural graphite
G : for graphite
***** : sample for length adjustment – have not been loaded

Table 2 : Characteristics of matrix samples without fuel

Sample number	Matrix composition	Heavy metal loading (g/cc)	FBOC[(1)] (μm)	MOC[(2)] (μm)	Graphite powder	Compaction pressure (kg/cm²)	Diameter (mm)	Height (mm)
2/1	Th	1	-	300	-	40	13,5	37,8
2/2	Th	0,6	-	300	-	40	13,5	20
2/3	Th	1	60	240	-	40	13,5	(3)
2/4	Th	1,5	60	240	-	40	13,5	(3)
2/5	P514	1	-	300		40	13,5	(3)
2/6	P514	1,5	60	240		40	13,5	(3)
2/7	P514	1,5	60	-	saldo	vibrated	13,5	(3)
2/8	Th	1	-	300		40	13,5	29,8
2/9	Th	1	-	300	saldo	vibrated	13,5	29,7
2/10	Th	1,5	-	300	saldo	vibrated	13,5	40,9
2/11	Th	1,8	-	(250)	-	40	13,5	37
2/12	Th	1,8	-	(250)	-	40	13,5	47,8
2/13	Th	1	-	250	-	40	13,5	40,8
2/14	Th	1	-	250	-	40	13,5	43,1
2/R1	Th	1	-	250	-	40	13,5	45

[(1)]: FBOC fluidised bed overcoating.

[(2)]: MOC mechanical overcoating.

[(3)]: Unloaded compacts

Table 3 : Characteristics of compacts with depleted particles

Sample number	Matrix composition	Heavy metal loading (g/cc)	FBOC (μm)	MOC (μm)	Compaction pressure (kg/cm^2)	Diameter (mm)	Height (mm)
8/1	Th + G	1,5	60	240	40	10	38,8
8/2	Th + G	1;5	60	240	80	10	38,9

Remark: The mean enrichment was obtained by blending 45 % of 12% enriched particles with 55% of depleted particles.

Table 4 : Characteristics of compacts with an average enrichment of 5.7%U

Sample number	Matrix composition	Heavy metal loading (g/cc)	FBOC (μm)	MOC (μm)	Compaction pressure (kg/cm^2)	Diameter (mm)	Height (mm)
4/1	Th + G	1	60	240	40	10	37,7
4/2	Th + G	1	60	240	40	10	37,1
4/3	Th + G	1	60	240	40	10	37,4
4/4	P514	1	60	240	40	10	36,4

Remark: The mean enrichment was obtained by blending 70 % of 12% enriched particles with 30% of depleted particles.

Table 5 : Characteristics of compacts with an average enrichment of 8.5%U

Sample number	Matrix composition	Heavy metal loading (g/cc)	FBOC (μm)	MOC (μm)	Compaction pressure (kg/cm^2)	Diameter (mm)	Height (mm)
7/1	Th	1	60	240	40	10	33,5
7/2	Th	1	60	graphite powder	40	10	35
7/3	1514	1	60	240	0	10	(1)
7/4	1514	1	60	graphite powder	40	10	37
9/1	Th + G	1	60	325	80	10	20
9/2	Th + G	1	60	325	80	10	(1)

(1) Unloaded compacts

Table 6 : Characteristics of compacts with an average enrichment of 12%U

Sample N°	Height	Rod position
3/10	42.0	Top
2/13	40.0	
2/14	43.1	
2R1	45.0	
3/16	9.8	
3/20	10.6	
2/13	40.8	
2/12	47.8	
3/13	10.2	
3/19	10.5	
2/11	37.0	
2/8	39.8	
3/17	10.6	
3/18	10.4	
4/1	37.7	
4/4	36.4	
3/4	9.4	
3/8	10.4	
8/1	38.8	CENTER
8/2	38.9	
3/22	35.0	
3/3	9.8	
3/11	10.2	
2/2	20.0	
2/1	37.8	
3/5	9.9	
3/15	10.6	
2/9	29.7	
2/10	40.9	
3/6	10.2	
3/7	10.5	
4/2	37.1	
4/3	37.4	
3/2	9.6	
3/14	11.0	
7/2	35.0	
3/21	20.0	
9/1	20.0	
3/9	10.2	
3/12	10.4	
7/4	37.0	
7/1	33.5	
3/1	9.7	BOTTOM

Table 7: Samples loading diagram

Sample number	Enrichment % U^5	H.M.L. g.U/cm^3	Linear power (W/cm)	Max. fuel temperature (°C)
7/1	12	1,0	65	617
7/4	12	1,0	65	617
9/1	12	0,6	48	520
7/2	12	1,0	118	910
4/3	8,5	1,0	103	830
4/2	8,5	1,0	114	895
2/10	0,4	1,5	21,6	273
2/9	0,4	1,0	14,2	265
2/1	0,4	1,0	14,7	266
2/2	0,4	0,6	9	259
8/2	5,7	1,6	156	1130
8/1	5,7	1,6	167	1195
4/4	8,5	1,0	148	1090
4/1	8,5	1,0	136	1020
2/8	0,4	1,0	11	262
2/11	0,4	1,5	14,7	266
2/12	0,4	1,5	12,2	263
2/13	0,4	1,0	6,1	257
2/R1	0,4	1,0	5,5	256
2/14	0,4	1,0	5	255

Table 8 : Thermal characteristics of the samples in the channel 80

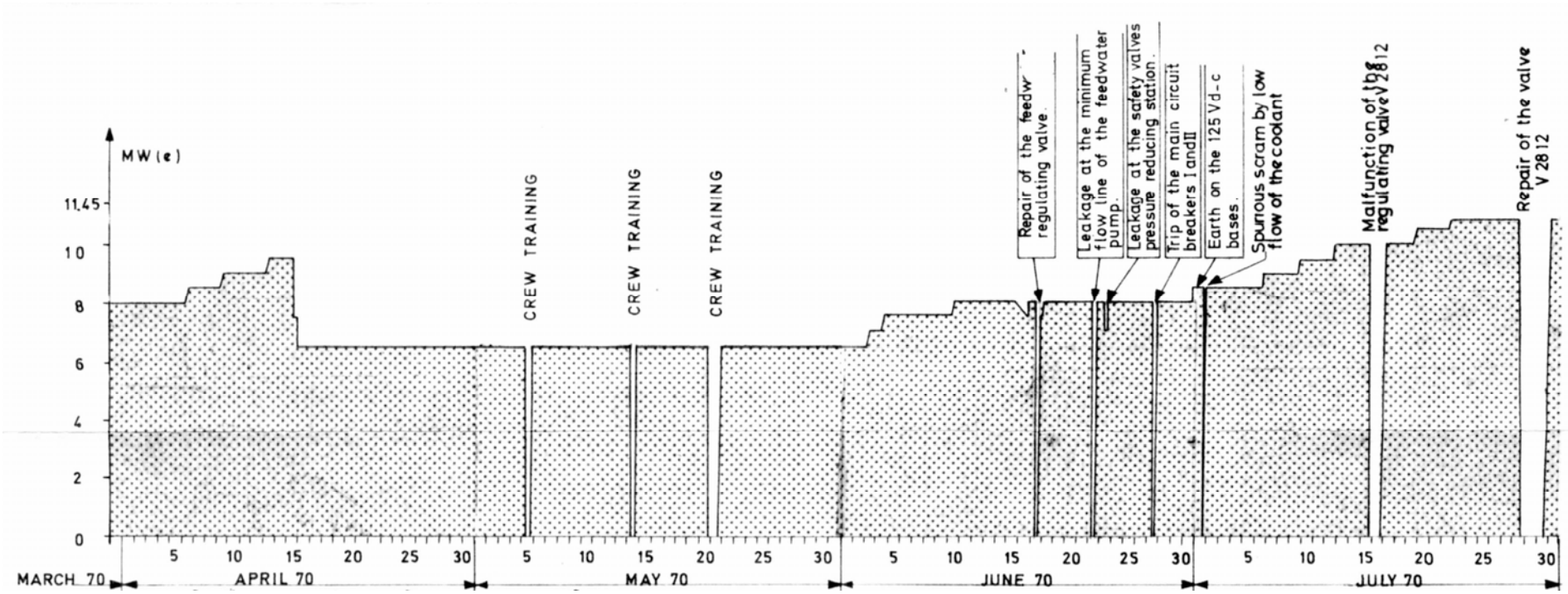

Figure 1: Load diagram of core BR3/2bis (continued)

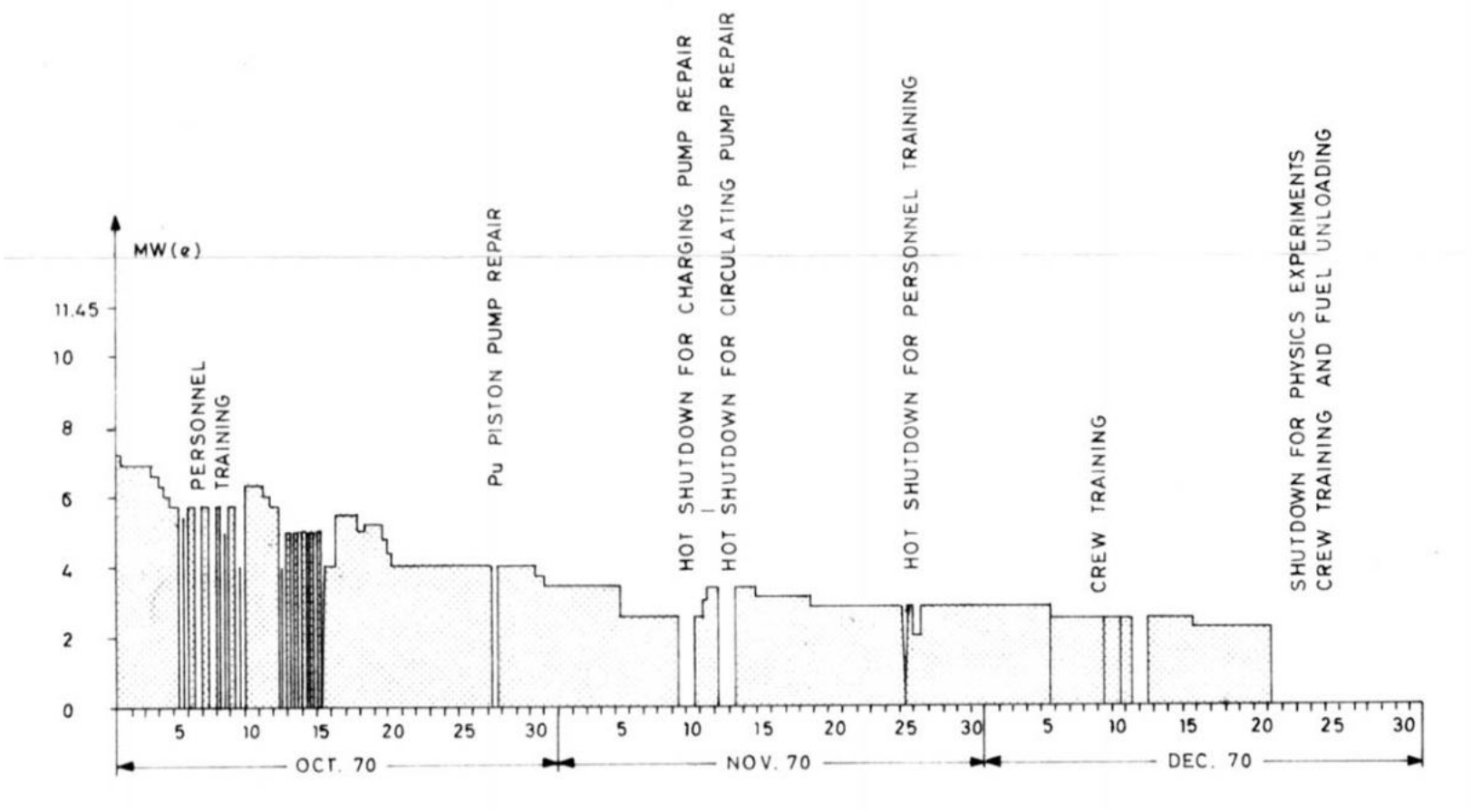

Figure 1: Load diagram of core BR3/2bis (continued)

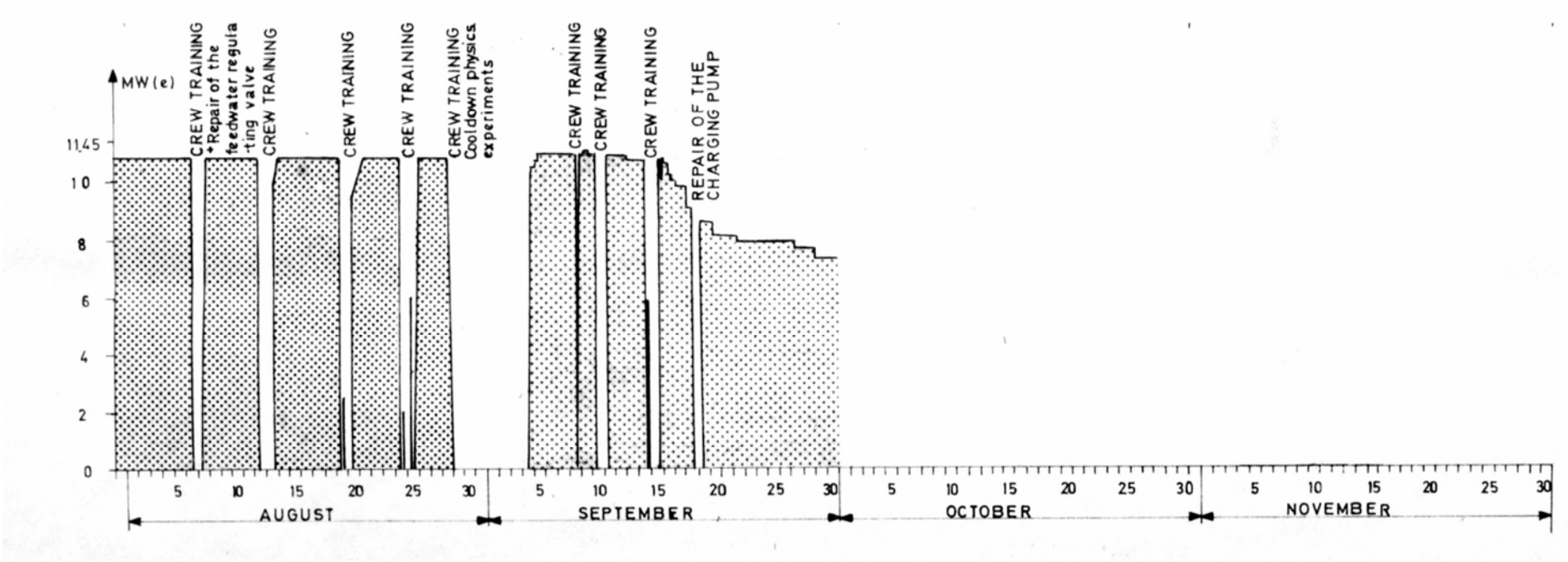

Figure 1: Load diagram of core BR3/2bis (continued)

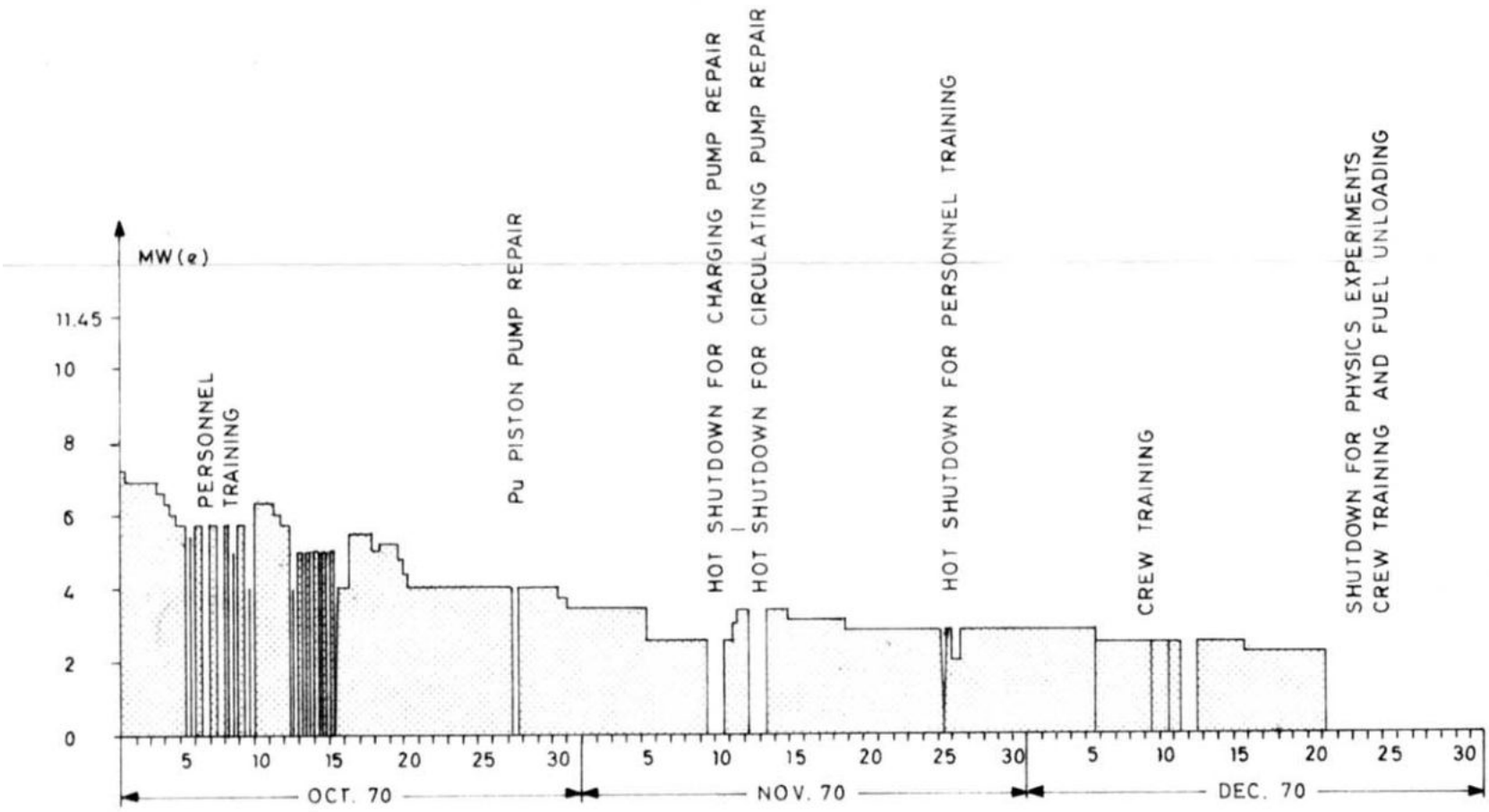
MW(e)
11.45
10
8
6
4
2
0
PERSONNEL TRAINING
Pu PISTON PUMP REPAIR
HOT SHUTDOWN FOR CHARGING PUMP REPAIR
HOT SHUTDOWN FOR CIRCULATING PUMP REPAIR
HOT SHUTDOWN FOR PERSONNEL TRAINING
CREW TRAINING
SHUTDOWN FOR PHYSICS EXPERIMENTS
CREW TRAINING AND FUEL UNLOADING
5 10 15 20 25 30
OCT. 70
5 10 15 20 25 30
NOV. 70
5 10 15 20 25 30
DEC. 70

Figure1: Load dia e BR3/2bis (continued)

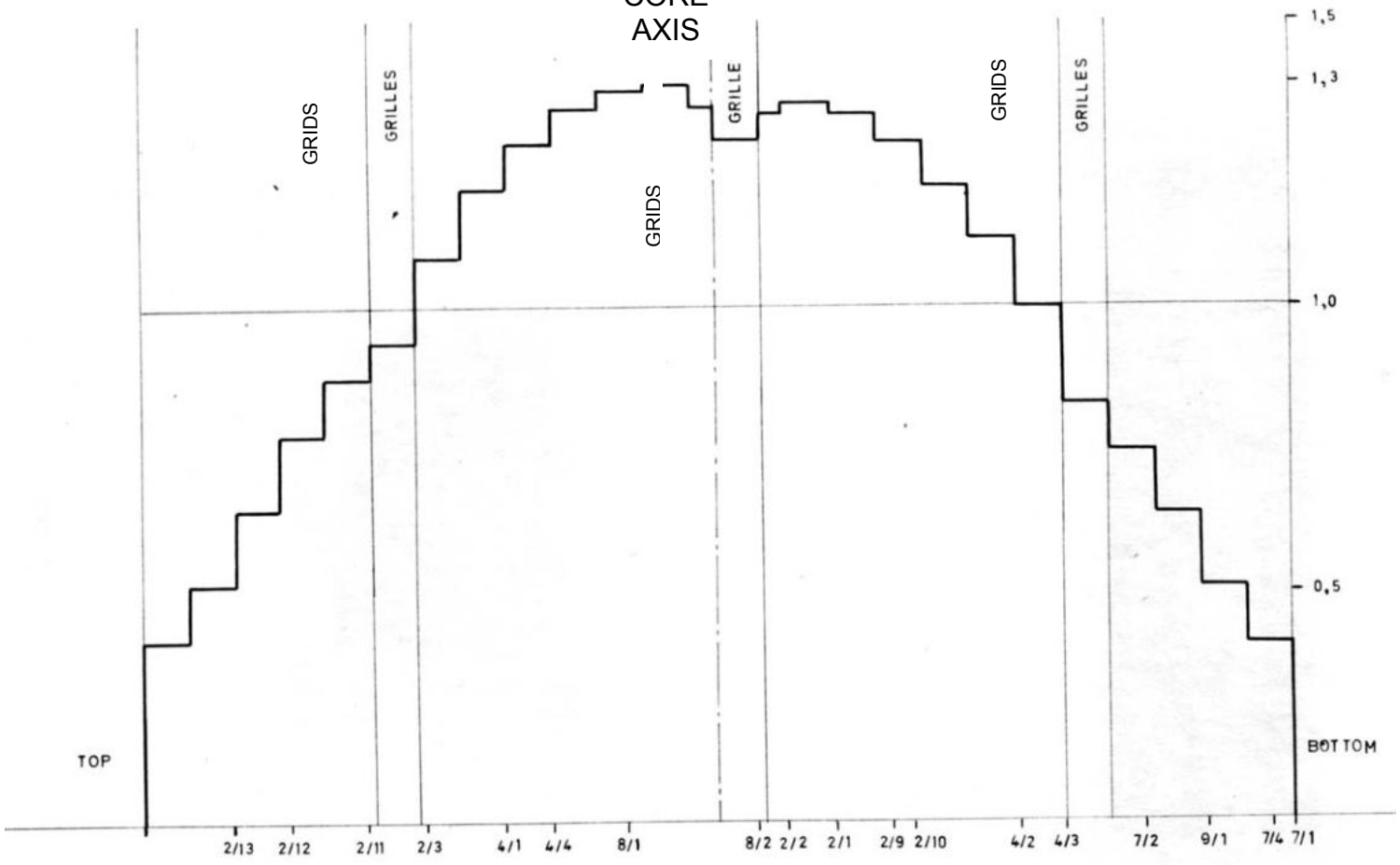

Figure 2: Normalised distribution of the thermal flux in channel 80

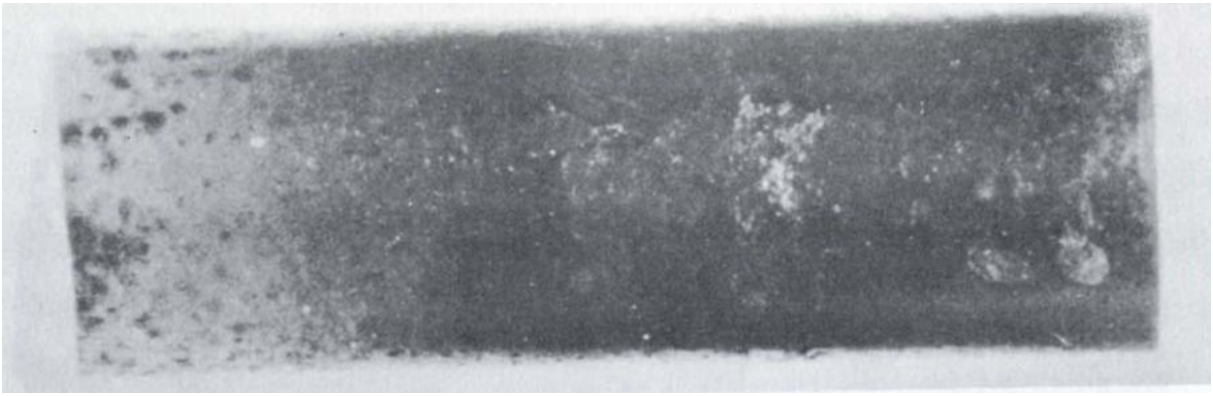

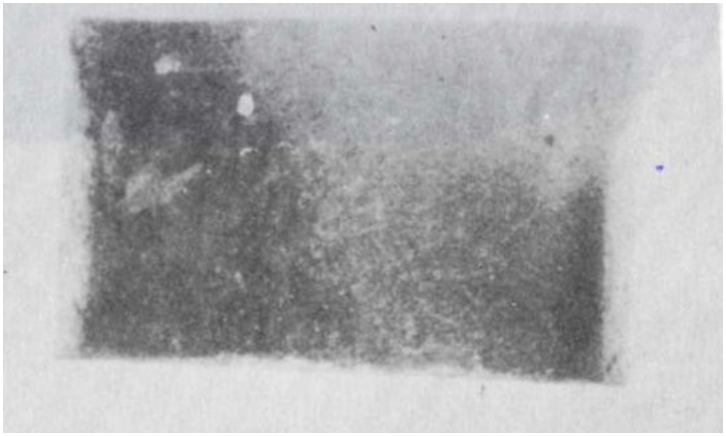

Figure 3: samples 2/14 and 3/16 after irradiation

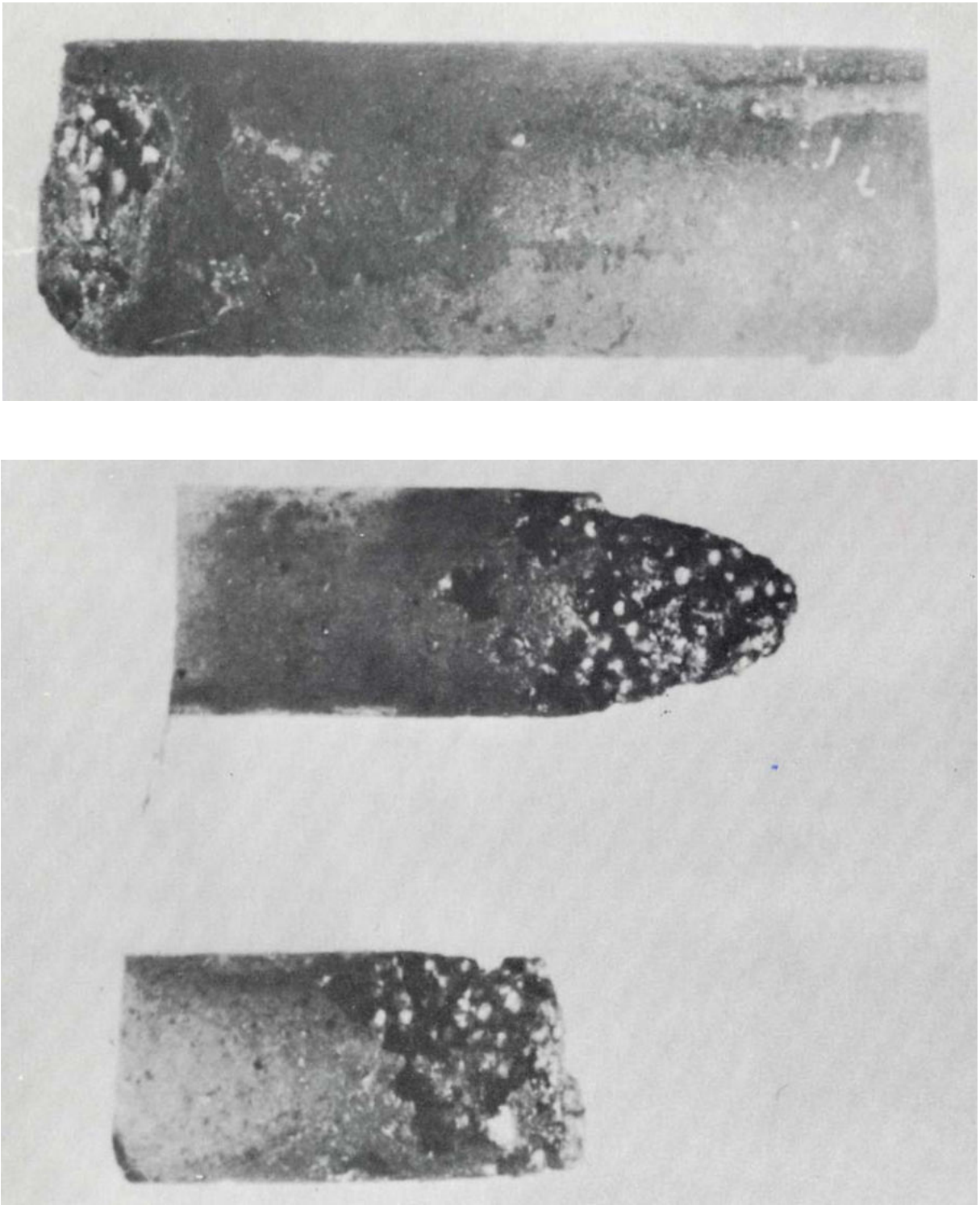

Figure 4: Samples 4/1 and 8/1 after irradiation

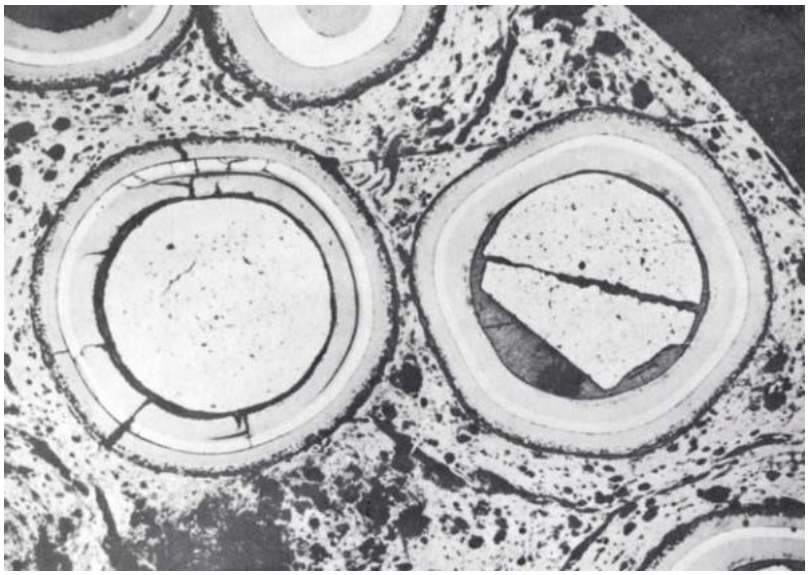

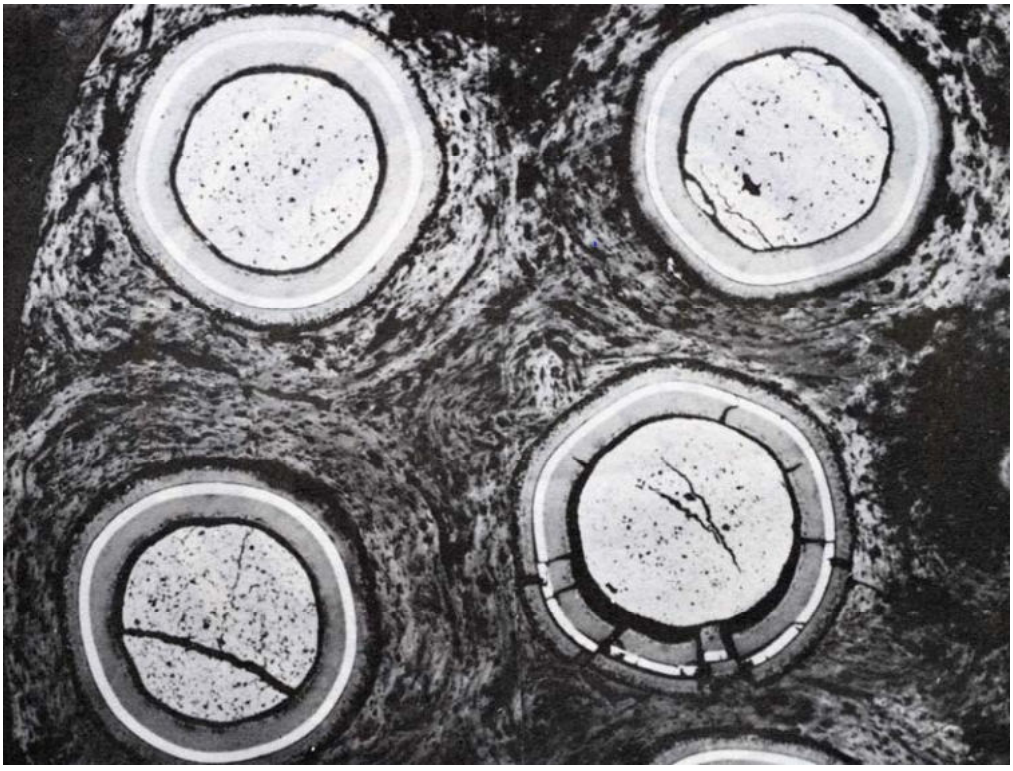

Figure 5: Metallographic cross sections of sample 7/1

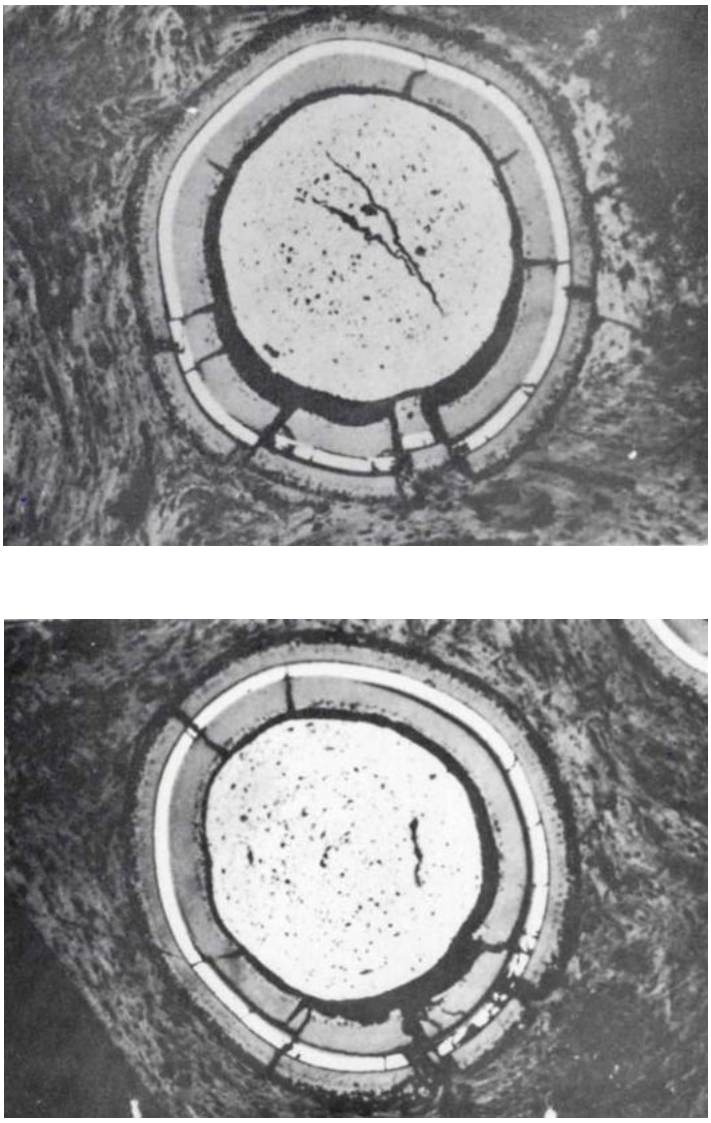

Figure 6: Sample 7/1- damaged particles during fabrication process

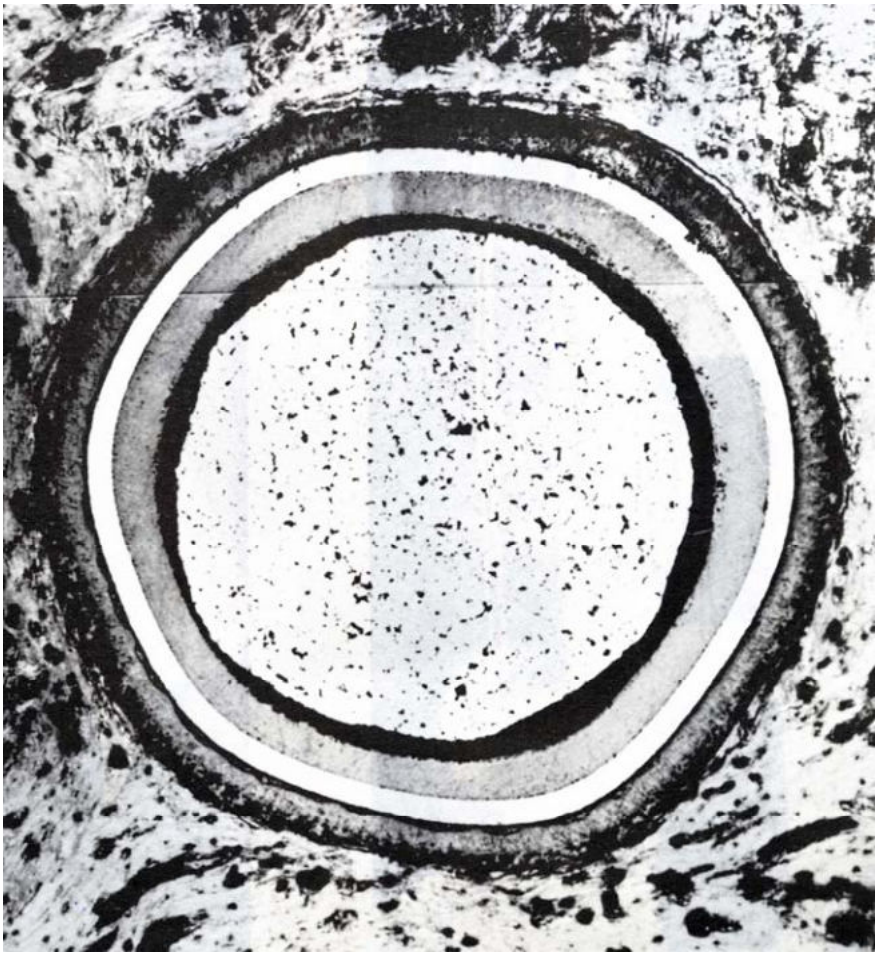

Figure 7: Particle in sample 4/2

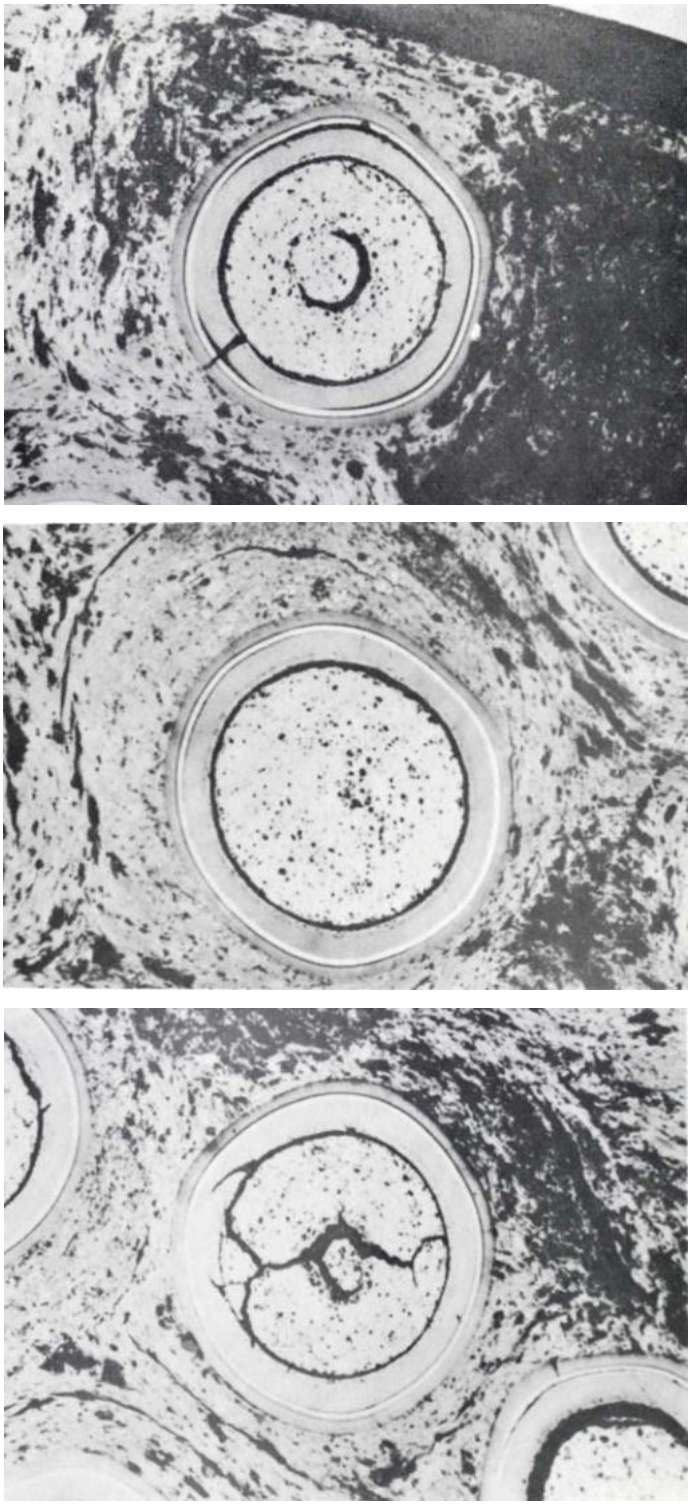

Figure 8: Particles in sample 2/9

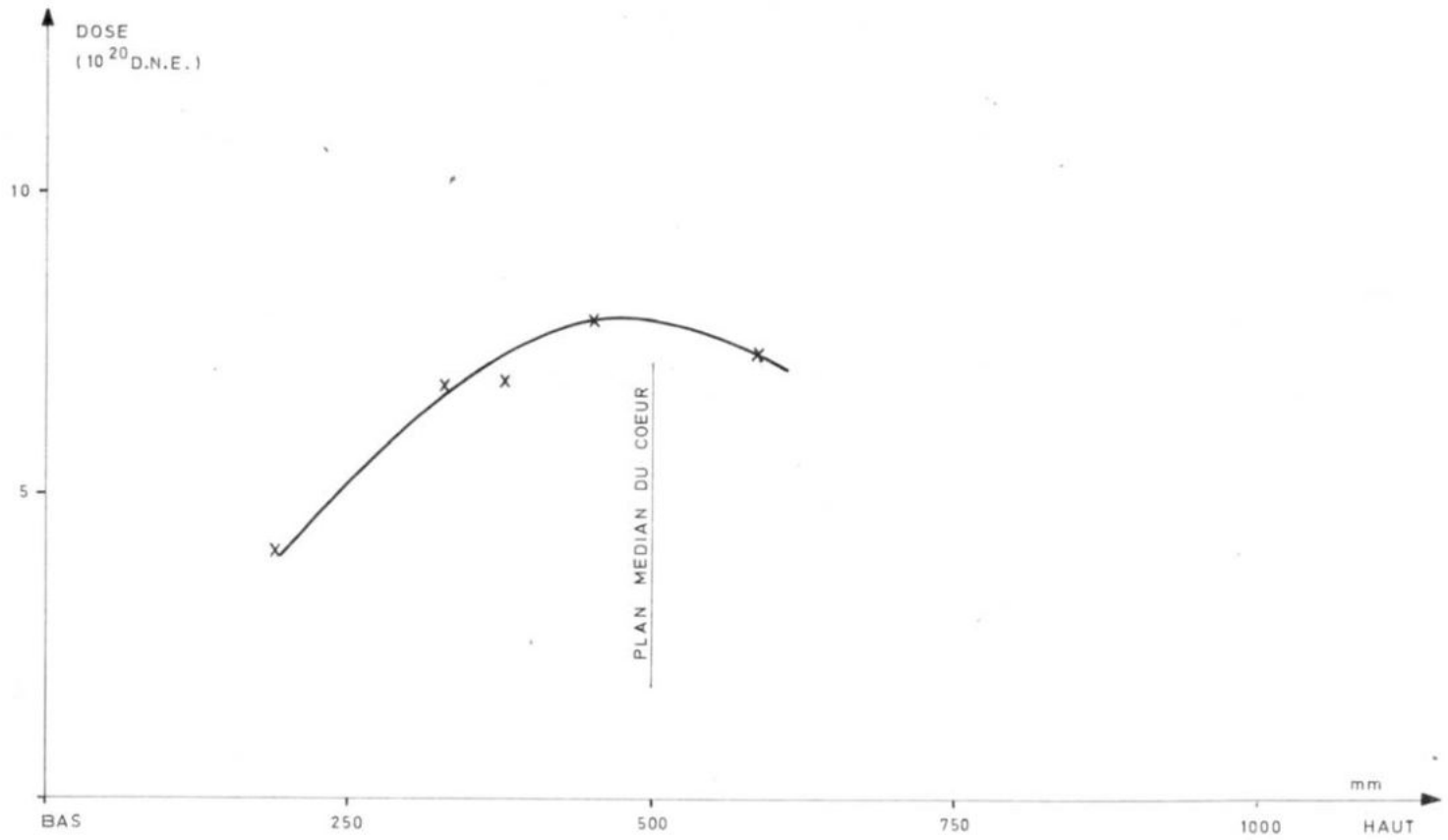

Figure 9: Axial distribution dose (DNE) in channel 80 of core BR3/2bis

	Type of document:	Reference No / File - "Rev." - Page
	Technical Note	**0601023/220-"-" - 1**
		Other reference:

Client: EC	Author(s) G. TOURY
Project: Raphael IP – SP Fuel Technology WP-FT4 Performance Modelling	
Subject:	

HTR particles Irradiation Experiment BN database

DR-S Experiment

Rev.	Date	Chrono Filing No.	Status	Initials dactylo.	Author: Initials	Author: Visa 1	Verified by: Initials	Verified by: Visa 2	Approved by: Initials	Approved by: Visa 3	Q.A.: Initials	Q.A.: Visa 4	Issued by: Initials	Issued by: Visa 5	Number of pages
C															
B															
A															
-	17/05/06	0601023	Draft		GTY		SSH						GTY		56

Distribution:

RAPHAEL Project: Mr. OBRY (1 copy +1 CD)

BN: SSH, GTY

BELGONUCLEAIRE N.V.
Avenue Ariane, 4 - 1200 Brussels
TVA: BE 403.126.258
RCB: 271.300
TEL: 32-2774 05 11
FAX: 32-2-774 05 47

LIST of MODIFICATIONS		
DATE	**REVISION**	**OBJECT**
17/05/2006	-	Draft

NOTICE

PERSONNEL IN CONFIDENCE, NOT FOR PUBLICATION

This work is performed under the term and conditions of the Consortium Agreement of the RAPHAEL Project supported by the EC under contract n° 516508 (FI6O)

LIABILITY

This document was prepared by BELGONUCLEAIRE (BN). Neither BN, nor any person acting on behalf of BN:

a) gives any warranty, expressed or implied, with respect to the accuracy, completeness of the information contained in this document, or that the use of any information, apparatus, method or process disclosed in this document may not infringe third party rights, or

b) assumes any liabilities with respect to the use of, or for damage resulting from the use of any information, apparatus, method or process disclosed in this document.

Abstract

This report presents irradiation results of two experiments DR-S2 and DR-S5 both loaded in the DRAGON reactor at the beginning of the 70's. The specific fuel pin design was "Tubular Interacting", characterised by annular fuel compacts supported on a graphite centre tube. The coated particles were U235 enriched and embedded in graphite matrix. For the DR-S2 experiment, fuel compacts have the particularity to have a fuel free layer of graphite bonded to the inner and outer surface.

The irradiation results that are presented concern essentially the irradiation effect on the dimensional change and physical properties of HTR compacts.

Table of content

List of Tables

List of Figures

1. INTRODUCTION

The Dragon Project has examined several fuel pin concepts in its irradiation programme. Amongst these is the "tubular interacting" (TI) design in which the fuel compacts were annular and supported on a graphite centre tube, and were free to shrink in this tube. The pin was then cooled both internally and externally. The mechanically integrity of the compact was important in this design, to avoid any fission products release into the coolant, as a result of the compact failure.

The DR-S2 and DR-S5 are two of the experiments that were loaded in the DRAGON reactor to study the irradiation and temperature induced effects on the mechanical integrity of TI rods.

For each experiment, the fuel was U235 enriched coated particles diluted in graphite matrix. The DR-S2 fuel compact was typical, with a central fuelled zone embedded in an unfuelled zone, both forming a coherent body of the same matrix material (graphite) as the centre and outer tube.

The results that are presented in this report are essentially relative to the irradiation effect on the dimensional parameters and physical properties of the fuel compacts.

2. DR-S EXPERIMENTS DESCRIPTION

The DR-S2 and DR-S5 experiments have been irradiated in the DRAGON reactor under the sponsor of HRB and KFA, and respectively HOBEG and NUKEM as particle kernels manufacturers.

The experiments were loaded in carrier block Dragon type D16/10 for the DR-S5 and block type D21 for the DR-S2, each block containing seven channels (Figure 1). The central channel (68 mm bore) could provide three axial ribs for alignment of the test elements. The other six surrounding channels which were 50 mm bore contained highly enriched driver fuel which could be removed when depleted and replaced.

Each fuel pin consisted of graphite outer and inner tubes, screwed end cap and a stack of fuel compact (Figures 2-3).

In the DR-S2 experiment, the central channel contained one single pin with 27 annular compacts of 60 mm diameter and 60 mm height loaded as a stack of 1620 mm length. The bottom end part of the fuel stack was spring loaded in order to accommodate any differential expansion. In DR-S2, the inner and outer surface of the fuel compacts consisted of unfuelled matrix material of about 4 mm thickness (Figure 4). The experiment was loaded with two types of fuel, 6.6% enriched U235 and $(Th,U)O_2$. Both type of compact were made with electrographite based matrix.

Moreover, the coatings of fuel particles had no SiC layer.

Only results relative to U fuel compacts are presented in this document.

In the DR-S5 experiment, the central channel contained the tubular interacting Nukem experiment consisting of three TI fuel pins, each carrying 12 annular compacts of 50 mm outer diameter and 42.5 mm length. The U enrichment of the coated particles was 9.5%U235. Two electrographite matrixes have been used. Compact stacks are showed in Figure 5.

The characteristics of the fuel pins are presented in Table 1, and their loading plan in Table 2.

3. FUEL CHARACTERISTICS

The fuel characteristics (kernels, coated particles and compacts) are gathered in Table 3.

The specifications of the particles coating are detailed in Table 4. Only particles from DR-S5 experiment had SiC layer.

Cross sections of the particles are visualised in Figures 6-10.

Cross sections of compacts are visualised in Figures 11-12. In DR-S2 compact, isolated kernels are visible.

X-ray radiographs of whole compact are shown in Figure 14-15.

Figure 16 presents a view of DR-S5 compact before the pin loading.

Some physical properties of the fresh fuel compacts DR-S2 and DR-S5 are presented respectively in Tables 5 and 6.

The as-fabricated metrology of the compacts is given in Table 7.

4. IRRADIATION HISTORY

4.1. DR-S2 experiment

The DR-S2 experiment was loaded in DRAGON reactor during the charge IV in cores 3 and 4 (280 EFPD). The irradiation history is presented in Figures 17 and 18.

In Figures 19 and 20 are given the axial temperature and power profiles (start and end of each core).

A maximum fuel temperature of 1250°C was reached at the end of the core 4. The estimated burn-up was about 2%FIMA.

4.2. DR-S5 experiment

The irradiation of the DR-S5 experiment started on 8/03/1972 in core 4 charge IV of the DRAGON reactor and had to be terminated when the grapple head of its carrier was damaged. The experiment was withdrawn at the end of core 5 on 27/10/1972. The element was irradiated in core position 5/2 for 189 days at 21 MW reactor power for a total of 3774 MWd's.

The estimated fast neutron dose was approximately 5.6×10^{20} $n.cm^{-2}$ DNE and the estimated peak burn-up about 2.6% FIMA.

The estimated maximum fuel temperature was approximately 1300°C and the maximum graphite surface temperature about 1050°C.

5. POST IRRADIATION EXAMINATIONS

5.1. PIE on DR-S2

5.1.1. Visual examination

After unloading of the pin, all the compacts appeared intact, only some local rub marks caused by T/C's were visible, as well as some apparent surface corrosion at inner channel between position 5 and 19.
Figures 22 to 23 exhibit a selection of photographs taken by periscope.

5.1.2. Compact weighing change

Mass variation measured on each compact before end after irradiation are gathered in Table 8. It should be said that initial weight figures referred to the manufacturers certificate prior to drilling of thermocouples holes. Weight losses due to drilling were very small however and with about 20mg/hole negligible uncountable for the weight losses observed. Only where the deep touchmarks from the T/C's were present in compacts position 9-14, additional weight losses could have reached 200mg. It was learnt from surface examination under compact in position 9 that the loss was mainly due to corrosion that was found more pronounced on the inner wall of the specimens (Figure 23).

5.1.3. Compact dimensional change

Measurements of outer and inner diameter and length have been performed on the DR-S2 compacts after irradiation. These values are gathered with as-fabricated values in the Table 9. The shrinkage is directly related to the temperature/position of the compact, the maxima are observed between positions 9 and 14.

5.1.4. Burn-up determination

Burn-up has been determined by quantitative analyse of the Cs^{137} inventory (by gamma spectrometry) in comparison to the initial heavy metal contents. Individual measurement was made at the center of several compacts. Burn-up results are given in Table 10. 1.94%FIMA was determined as the average burn-up, with a peak burn-up of 2.39% FIMA at the position 19.

5.1.5. Post-irradiation annealing measurements of Fission Gas Release

The compacts 8 and 21 were annealed in helium at 1000°C; the release rates of Xe^{133} and Kr^{85} were measured, although the Kr^{85} release was below the detection limit. The amount of Xe133 (A_{SD} Curies) present at the shutdown in all the 22 compacts has been calculated by the IRREL code. The average value of X^{133} (N_{Xe133} atoms/sec) for each compact at the time of the annealing test was then calculated as follow:

$$N_{Xe^{133}} = \frac{A_{SD}(Xe^{133})}{22} \exp(-\ln 2 \frac{t}{T_{1/2}}) x 3.7.10^{10}$$

where t = cooling time (days) since shutdown

$T_{1/2}$= half life of Xe^{133} = 5.27 days

By assuming that the axial profile along the fuel stack of the Xe^{133} ($T_{1/2}$=5.27) was very similar to the measured profile of the Ba^{140} ($T_{1/2}$=12.8), the mean value of A_{SD} or N_{Xe133} has been adjusted to take account of the axial variation of Xe^{133} production.

Results of the annealing test are given in Table 11.

5.1.6. Compression test

To analyse the mechanical behaviour of the compacts, two devices were utilised. the first device had been installed to break spherical fuel elements at a fixed but rather high rate of movement of the upper platen thus rendering quick results of still good accuracy. This device was used to check the behaviour under axial load (up to 4t). The second device was a material test machine allowing various operations; in this case a 1t bending accessory was used in connection with an auxiliary tool to line up the test specimen. Here the speed of platens could be controlled and was kept low. Deflection was deduced from 2 dial gauge readings.

Table 12 gives the results of the diametrical compression performed on irradiated and fresh compacts of DR-S2 experiment.

The results show that for the irradiation condition of the DR-S2 experiment, the mechanical properties of the compacts have not changed very much as results obtained after irradiation still fall into the scatter of pre-testing results. When low values were met, the compacts had undergone a pre-testing radially up to about 2/3 or rather

3/4 of fracture load as was requested, and any structural changes on microscale with this pre-treatment can then be excluded.

A number of photographs display the type of fracture as observed on fresh and irradiated compacts under radial compression or hydraulic burst (Figures 24-26). Whenever particles became released from their matrix compound, they remained intact with their overcoating as seen in Figure 27. This was confirmed by ceramographic examination of small pieces obtained after mechanical testing: no damage was found other than a rather obscure crack in one of the particles (Figure 28).

5.2. PIE on DR-S5

5.2.1. Visual examination

The three fuelled pins of the centre channel of DR-S5 experiment have been discharged after irradiation. The pin surface appeared clean with very slight pitting corrosion; some thermocouple "burn" marks were visible (Figure 30).

Visual examination of the compacts is presented in Figures 31 and 32. Several compacts were found cracked.

5.2.2. Compact dimensional measurement

The dimensional measurements on the compacts have been carried out. The outer diameter and length of the compacts have been measured each in two positions, the outer diameter 90°, the length 180° displaced. The measurements were made with a dial gauge device, which was calibrated against a standard. The results are recorded in Table 13, and plotted in Figure 33 in terms of percentage of shrinkage.

Experiment	**DR-S2**	**DR-S5**		
		DR-S5/4	DR-S5/5	DR-S5/6
Compacts				
Number of compacts / pin	27	12	12	12
Outer diameter (mm)	60.0 ±0.1	50.125 ±0.025	50.125 ±0.025	50.125 ±0.025
Inner diameter (mm)	20.0 ±0.3	35.95 ±0.05	35.95 ±0.05	35.95 ±0.05
Height (mm)	60.0 ±0.15	42.5 ±0.1	42.5 ±0.1	42.5 ±0.1
Fuel free zone thickness				
radial (mm)	5.0 ±1.0	-	-	-
axial (mm)	4.0 ±1.0	-	-	-
Pin				
Channel diameter (mm)	68	68	68	68
Stack length (mm)	1620	549.4	549.2	549.8
Fuel length (mm)	1404	509.8	510.0	509.2
Fuel weight (g)	8184	1209.6	1210.5	1209.8

Table 1: Fuel pin characteristics

DR-S2 experiment				DR-S5 experiment				
Position	Core height (cm)	Compact number	Fuel	Pin n°	Core height (cm)	Compact number	Matrix type*	Fuel
1 (Top)	162	2081	UO_2	PIN DR-S5/6	160.3	2213	1/1	UO_2
2		2088			156.0	2220	1/1	
3	150.0	2113			151.8	2221	1/1	
4		2105			147.5	2223	1/1	
5		2103			143.3	2225	1/1	
6		2116			139.0	2229	1/1	
7		2114			134.8	2261	2/1	
8	120.0	2112			130.5	2269	2/1	
9		2104			126.3	2270	2/1	
10		2097			122.0	2271	2/1	
11		2089			117.8	2273	2/1	
12		2093			113.5	2275	2/1	
13	90.0	2095		PIN DR-S5/5	105.4	2195	1/1	UO_2
14		2108			101.1	2196	1/1	
15		2079			96.9	2198	1/1	
16		2085			92.4	2207	1/1	
17		2086			88.4	2209	1/1	
18	60.0	2110			84.1	2210	1/1	
19		2087			79.9	2243	2/1	
20		2090			75.6	2251	2/1	
21		2091			71.4	2254	2/1	
22		2092			67.1	2255	2/1	
23	30.0	2340	$(Th,U)O_2$		62.9	2257	2/1	
24		2341			58.6	2258	2/1	
25		2342		PIN DR-S5/4	50.4	2231	1/1	UO_2
26		2344			46.2	2232	1/1	
27	6.0	2345			41.9	2187	1/1	
(Bottom)					37.7	2189	1/1	
					33.4	2190	1/1	
					29.2	2194	1/1	
					24.9	2263	2/1	
					20.7	2264	2/1	
					16.4	2265	2/1	
					12.2	2268	2/1	
					7.9	2280	2/1	
					3.7	2283	2/1	

* matrix types are defined in Table 3

Table 2: Fuel pin loading plan

		DR-S2	DR-S5
KERNELS	Chemical form	UO_2	UO_2
	Enrichment (% U235)	6.59 ±0.02	9.49 ±0.05
	Fabrication route	Liquid	Liquid
	Sieved size (µm)	500-630	500-630
	Mean diameter (µm)	600	616
	Density (g/cm3)	10.5-10.7	10.3
	O/U	2.00	2.00
	Manufacturer	HOBEG	NUKEM
COATED PARTICLES	Sieve fraction (µm)	800-1000	800-1000
	Mean particle size	-	964
	Geometrical density (g/cm^3)	4.17	4.32
	U content (%)	60.00	55.29
	Impurities (ppm		
	B	< 0.08	< 0.08
	Cd	< 0.07	< 0.07
	Dy	0.02	0.06
	Eu	< 0.02	< 0.02
	Gd	0.08	0.10
	Sm	< 0.04	< 0.04
COMPACTS	Coated particle volume loading	~37%	~33%
	Heavy metal density (g/cm^3)	0.92	0.8
	HM loading (g) U235	3.98	3.03
	U238	56.32	28.96
	Nb of particles per unit of fuelled volume (cm^{-3})	~850	~700
	Nb of particles per experiment	$1.4x10^6$	$1x10^6$
	Matrix type*	2/1	1/1 - 2/1
	Matrix density after heat treatment (g/cm^3)	1.70	1.60
	Failed particles fraction	$\leq 5x10^{-4}$	$\leq 3x10^{-4}$
	Impurity elements (boron equivalent)	< 3ppm	< 3ppm

* Type 1/1 matrix on a natural-electrographite base, ratio 4:1 (Nukem A3 matrix) + 12%phenolic resin + 1.3% hardener

Type 2/1: matrix on electrographite base (Nukem-KRB matrix using an artificial needle coke) + 12% phenolic resin

Table 3: DR-S fuel characteristics

Experi - ment	Layer n°	Type	Deposition			Layer density (g/cm^3)	Nominal thickness (µm)	Anisotropy BAF*	Number of measured particles
			source	T (°C)	Rate (µm/h)				
DR-S2	1	Porous PyC	C_2H_2	1450	~550	< 1.1	76 ±15.4		72
	2	HDI PyC	C_3H_6	1350	~250	1.95 ±0.05	92 ±13.6	1.07	
DR-S5	1	Porous PyC	C_2H_2		~550		104 ±13.7	1.09	72
	2	Inner HDI PyC	C_3H_6		~220				
	3	SiC	CH_3SiCl_3		~30	3.19	34 ±2.4		
	4	Outer HDI PyC	C_3H_6		~240	1.92–1.95	36 ±3.9	1.00	

* Bacon’s Anisotropy Factor deduced from thickness/anisotropy curve

Table 4: Coating layer characteristics

	Unit	Measured on complete compact		Measured on fuelled zone		Measured on fuel free zone
		Axial*	Radial**	Axial	Radial	Axial
Density	g/cm^3					1.69-1.69-1.69 x=1.69
Thermal conductivity 20°C	cal/°C.cm.s					0.14-0.13-0.13 x=0.13
Thermal conductivity 1000°C	cal/°C.cm.s		0.09		0.10	
Thermal expansion $x10^6$ 20-500°C	1/°C			2.23***	1.85***	4.172-4.361-4.726
Bending strength	kp/cm^2					171.1-155.9-142.7 x=156.6
Elastic modulus (dyn) $x10^{-4}$	kp/cm^2					3.8-3.8-3.8 x=3.8
Electrical resistivity $x10^3$	Ω.cm					2.70-2.76-2.75 x=2.74
Ultimate compressive strength	kp/cm^2	211				
Ultimate compressive load	Kp		1115			
Tensile strength	kp/cm^2					67.2-77.6-75.1 x=73.3

* axial = ⊥ pressing condition ** radial = // pressing condition *** from compact of slightly different composition

Table 5: DR-S2 compacts physical properties (as fabricated)

	Unit	Matrix Type 1/1		Matrix Type 2/1	
		Axial	Radial	Axial	Radial
Thermal expansion x10^6 20–500°C	1/°C	2.781-2.406-2.732	2.594-2.337-2.498	2.358-2.740-2.260	1.902-1.871-2.418
Anisotropy factor	⊥ / II	1.06		1.21	
Electrical resistivity x10^3	Ω.cm	3.3-3.6-2.9-3.8 x=3.4		4.0-4.0-3.6-6.0 x=3.9	
Axial compressive strength	kp/cm^2	139.5 - 134.9 x=137.2		209.0 - 175.0 x=192.0	
Radial rupture load	kp		26.0 - 31.5 x=28.75		43.3 - 51.5 x=47.4
Compact N°		2193	2197	2278	2285
Compact density	g/cm^3	2.504	2.506	2.514	2.506
Matrix density	g/cm^3	1.598	1.599	1.610	1.604
Volume loading	%	33.26	33.35	33.36	33.20
Bursting Test					
Young Modulus* x10^3	MN/m^2	9.80-7.52-+	10.70-7.87-6.90	8.49-6.61-6.08	10.75-7.66-7.18
Surface strain at failure	%	0.052	0.078	0.084	0.082
Ultimate Tensile strength	MN/m^2	4.79	5.66	6.53	7.09

* three successive loading cycles on each compact +: failure

Table 6: DR-S5 compacts physical properties (as fabricated)

Pos.	Compact N°	Outer diameter (mm)				Inner Diameter (mm)				Length (mm)			Weight (g)
		1	2	3	Mean	1	2	3	Mean	1	2	Mean	
1	2081	59.96	59.96	59.96	59.96	20.04	20.03	20.02	20.03	59.96	59.96	59.96	312.0
2	2088	59.97	59.97	59.98	59.97	20.04	20.03	20.03	20.03	59.87	59.98	59.93	310.2
3	2113	59.96	59.96	59.95	59.96	20.02	20.02	20.02	20.02	59.91	59.94	59.93	311.5
4	2105	59.93	59.94	59.94	59.94	20.02	20.03	20.02	20.02	59.92	59.86	59.89	309.4
5	2103	59.97	59.96	59.97	59.97	20.02	20.02	20.01	20.02	59.98	59.98	59.98	311.3
6	2116	59.96	59.95	59.95	59.95	20.02	20.02	20.03	20.02	59.94	59.93	59.94	312.6
7	2114	59.95	59.95	59.96	59.95	20.02	20.02	20.03	20.02	59.94	59.94	59.94	311.6
8	2112	59.95	59.94	59.94	59.94	20.06	20.03	20.03	20.04	59.98	59.97	59.98	312.1
9	2104	59.98	59.98	59.98	59.98	20.02	20.02	20.03	20.02	59.99	59.97	59.98	311.4
10	2097	59.98	59.98	59.98	59.98	20.01	20.03	20.03	20.02	59.98	59.96	59.97	313.8
11	2089	59.96	59.97	59.97	59.97	20.02	20.02	20.02	20.02	59.89	59.91	59.90	311.3
12	2093	59.97	59.97	59.97	59.97	20.02	20.02	20.02	20.02	59.97	59.97	59.97	313.4
13	2095	59.98	59.99	59.99	59.99	20.02	20.03	20.03	20.03	60.00	59.95	59.98	313.6
14	2108	59.95	59.97	59.97	59.96	20.07	20.03	20.02	20.04	59.94	59.94	59.94	313.5
15	2079	59.95	59.95	59.95	59.95	20.02	20.03	20.03	20.03	60.06	60.05	60.06	308.3
16	2085	59.95	59.96	59.97	59.96	20.05	20.03	20.03	20.04	60.00	59.87	59.94	307.8
17	2086	59.97	59.97	59.97	59.97	20.02	20.03	20.03	20.03	59.97	59.97	59.97	310.1
18	2110	59.94	59.94	59.94	59.94	20.03	20.02	20.02	20.02	59.89	59.91	59.90	312.7
19	2087	59.96	59.97	59.97	59.97	20.03	20.02	20.02	20.02	59.95	59.98	59.97	311.6
20	2090	59.98	59.97	59.97	59.97	20.02	20.02	20.03	20.02	59.99	59.92	59.96	312.5
21	2091	59.90	59.90	59.92	59.91	20.02	20.02	20.03	20.02	59.94	60.00	59.97	313.2
22	2092	59.97	59.95	59.97	59.96	20.02	20.03	20.02	20.02	59.89	59.97	59.93	312.4

Table 7: DR-S2 compacts as-fabricated measurements

Position	Compact N°	Weight in (g)		Δ	loss %
		before	after		
1	2081	312.0	311.9	0.1	0.030
2	2088	310.2	309.9	0.3	0.097
3	2113	311.5	311.3	0.2	0.064
4	2105	309.4	309.2	0.2	0.065
5	2193	311.3	311.1	0.2	0.064
6	2116	312.6	212.25	0.3	0.096
7	2114	311.6	31.3	0.3	0.096
8	2112	312.1			
9	2104	311.4	310.6	0.8	0.157
10	2097	313.8	312.75	1	0.320
11	2089	311.3	310.2	1.1	0.350
12	2093	313.4	312.55	0.8	0.255
13	2095	313.6	313	0.6	0.190
14	2108	313.5	312.9	0.6	
15	2079	303.3	308	0.3	0.097
16	2085	307.8	307.5	0.3	0.097
17	2086	310.1	309.8	0.3	0.097
18	2110	312.7	312.45	0.2	0.064
19	2087	311.6	311.5	0.1	0.030
20	2090	312.5	312.4	0.1	0.030
21	2091	313.2			
22	2092	312.4	312.4	0.0	

Table 8: DR-S2 compact weight loss after irradiation

Pos.	Compact N°	Outer diameter (mm)			Inner diameter (mm)			Length (mm)		
		$D_{initial}$	$D_{irradiated}$	$\Delta D/D_{init.}$ (%)	$D_{initial}$	$D_{irradiated}$	$\Delta D/D_{init.}$ (%)	$L_{initial}$	$L_{irradiated}$	$\Delta L/L_{init.}$ (%)
1	2081	59.96	D1 = 59,63 D2 = 59,63 D3 = 59,63	-0,550 -0,550 -0,550	20.03	d1 = 19,94 d2 = 19,93 d3 = 19,97	-0,448 -0,498 -0,299	59.56	L1 = 59,63 L2 = 59,43 L3 = 59,49	-0,717 -0,885 -0,784
2	2088	59.97	D1 = 59,60 D2 = 59,56 D3 = 59,63	-0,618 -0,684 -0,568	20.03	d1 = 19,91 d2 = 19,90 d3 = 19,93	-0,598 -0,648 -0,498	59.93	L1 = 59,44 L2 = 59,36 L3 = 59,40	-0,818 -0,952 -0,886
3	2113	59.96	D1 = 59,48 D2 = 59,47 D3 = 59,52	-0,800 -0,817 -0,734	20.02	d1 = 19,88 d2 = 19,88 d3 = 19,90	-0,698 -0,698 -0,598	59.93	L1 = 59,41 L2 = 59,39 L3 = 59,40	-0,868 -0,901 -0,886
4	2105	59.94	D1 = 59,40 D2 = 59,38 D3 = 59,37	-0,901 -0,935 -0,952	20.02	d1 = 19,86 d2 = 19,86 d3 = 19,87	-0,798 -0,798 -0,748	59.89	L1 = 59,29 L2 = 59,22 L3 = 59,19	-1,001 -1,118 -1,169
5	2103	59.97	D1 = 59,38 D2 = 59,37 D3 = 59,44	-0,985 -1,001 -0,884	20.02	d1 = 19,83 d2 = 19,83 d3 = 19,84	-0,947 -0,947 -0,898	59.98	L1 = 59,30 L2 = 59,28 L3 = 59,32	-1,133 -1,168 -1,100
6	2116	59.95	D1 = 59,28 D2 = 59,21 D3 = 59,32	-1,118 -1,234 -1,088	20.02	d1 = 19,82 d2 = 19,82 d3 = 19,83	-0,998 -0,998 -0,948	59.94	L1 = 59,28 L2 = 59,25 L3 = 59,26	-1,101 -1,151 -1,135
7	2114	59.95	D1 = 59,24 D2 = 59,17 D3 = 59,23	-1,183 -1,300 -1,201	20.02	d1 = 19,81 d2 = 19,86 d3 = 19,82	-1,045 -0,798 -0,998	59.94	L1 = 59,19 L2 = 59,28 L3 = 59,25	-1,251 -1,101 -1,151
9	2104	59.98	D1 = 59,21 D2 = 59,10 D3 = 59,21	-1,285 -1,468 -1,285	20.02	d1 = 19,79 d2 = 19,81 d3 = 19,76	-1,148 -1,048 -1,298	59.98	L1 = 59,19 L2 = 59,13 L3 = 59,10	-1,319 -1,419 -1,405
10	2097	59.98	D1 = 59,16 D2 = 59,03 D3 = 59,09	-1,368 -1,587 -1,485	20.02	d1 = 19,79 d2 = 19,86 d3 = 19,79	-1,148 -0,799 -1,148	59.97	L1 = 59,13 L2 = 59,17 L3 = 59,15	-1,402 -1,337 -1,370
11	2089	59.97	D1 = 59,14 D2 = 59,00 D3 = 59,12	-1,388 -1,619 -1,419	20.02	d1 = 19,79 d2 = 19,86 d3 = 19,79	-1,148 -0,799 -1,148	59.9	L1 = 59,03 L2 = 59,08 L3 = 59,12	-1,453 -1,369 -1,303

Table 9: DR-S2 compacts dimensional change

Pos.	Compact N°	Outer diameter (mm)			Inner diameter (mm)			Length (mm)		
		$D_{initial}$	$D_{irradiated}$	$\Delta D/D_{init.}$ (%)	$D_{initial}$	$D_{irradiated}$	$\Delta D/D_{init.}$ (%)	$L_{initial}$	$L_{irradiated}$	$\Delta L/L_{init.}$ (%)
12	2093	59.97	D1 = 59,15 D2 = 59,97 D3 = 59,07	-1,368 -1,667 -1,502	20.02	d1 = 19,77 d2 = 19,80 d3 = 19,76	-1,248 -1,099 -1,298	59.97	L1 = 59,18 L2 = 59,18 L3 = 59,13	-1,318 -1,318 -1,402
13	2095	59.99	D1 = 59,13 D2 = 59,04 D3 = 59,95	-1,435 -1,582 -1,736	20.02	d1 = 19,77 d2 = 19,76 d3 = 19,75	-1,297 -1,347 -1,397	59.98	L1 = 59,19 L2 = 59,14 L3 = 59,18	-1,319 -1,401 -1,333
14	2108	59.96	D1 = 59,16 D2 = 59,04 D3 = 59,12	-1,336 -1,536 -1,401	20.02	d1 = 19,79 d2 = 19,78 d3 = 19,83	-1,246 -1,296 -1,046	59.94	L1 = 59,15 L2 = 59,17 L3 = 59,18	-1,319 -1,287 -1,268
15	2079	59.95	D1 = 59,79 D2 = 59,07 D3 = 59,13	-1,269 -1,470 -1,369	20.02	d1 = 19,82 d2 = 19,78 d3 = 19,80	-1,047 -1,247 -1,147	60.06	L1 = 59,30 L2 = 59,35 L3 = 59,25	-1,263 -1,181 -1,349
16	2085	59.96	D1 = 59,26 D2 = 59,15 D3 = 59,21	-1,168 -1,352 -1,253	20.02	d1 = 19,82 d2 = 19,80 d3 = 19,83	-1,098 -1,196 -1,047	59.94	L1 = 59,11 L2 = 59,25 L3 = 59,26	-1,387 -1,186 -1,136
17	2086	59.97	D1 = 59,31 D2 = 59,20 D3 = 59,19	-1,103 -1,286 -1,302	20.02	d1 = 19,80 d2 = 19,80 d3 = 19,80	-1,146 -1,146 -1,146	59.97	L1 = 59,16 L2 = 59,22 L3 = 59,24	-1,353 -1,253 -1,219
18	2110	59.94	D1 = 59,35 D2 = 59,19 D3 = 59,25	-1,017 -1,252 -1,152	20.02	d1 = 19,83 d2 = 19,82 d3 = 19,82	-0,949 -0,998 -0,998	59.9	L1 = 59,34 L2 = 59,30 L3 = 59,32	-0,936 -1,002 -0,969
19	2087	59.97	D1 = 59,42 D2 = 59,30 D3 = 59,32	-0,918 -1,118 -1,085	20.02	d1 = 19,86 d2 = 19,83 d3 = 19,83	-0,798 -0,949 -0,949	59.97	L1 = 59,28 L2 = 59,33 L3 = 59,32	-1,152 -1,068 -1,085
20	2090	59.97	D1 = 59,44 D2 = 59,35 D3 = 59,44	-0,886 -0,985 -0,885	20.02	d1 = 19,86 d2 = 19,84 d3 = 19,83	-0,799 -0,899 -0,798	59.96	L1 = 59,37 L2 = 59,36 L3 = 59,31	-0,986 -1,003 -1,084
22	2092	59.96	D1 = 59,53 D2 = 59,49 D3 = 59,48	-0,719 -0,803 -0,835	20.02	d1 = 19,89 d2 = 19,87 d3 = 19,87	-0,649 -0,748 -0,746	59.93	L1 = 59,28 L2 = 59,29 L3 = 59,27	-1,087 -1,068 -1,102

Table 9 (continued): DR-S2 compacts dimensional change

Compact N°	Compact position	Activity (dec.sec) $X10^{11}$	Burn-up (%FIMA)
TOP			
2088	2	0.87	1.19
2105	4	1.02	1.39
2103	5	1.12	1.52
2116	6	1.22	1.65
2104	9	1.53	2.07
2089	11	1.69	2.29
2095	13	1.73	2.35
2079	15	1.72	2.33
2086	17	1.62	2.20
2087	19	1.76	2.39
2092	22	1.49	2.02
Bottom			

Table 10: DR-S2 compact individual Burn-up calculation

Compact N°	Anneal . T (°C)	$A_{SD}(Xe^{133})$ (Ci)	$A_{test}(Xe^{133})$ (Ci)	N_{Xe133} (atoms/sec)	Release rate R (atoms/sec	R/N_{Xe133}
8	1000	$3.26x10^{2}$	1.14	$4.23x10^{10}$	$2.15x10^{5}$	$5.1x10^{-6}$
21	1000	$3.48x10^{2}$	2.35	$8.71x10^{10}$	$1.78x10^{5}$	$2.0x10^{-6}$

Table 11: Annealing measurement of Xe^{133} release in irradiated DR-S2 compacts

Compact n°	Pos.	Type of test*	Pres-stressed		Load to fracture (Kp)	E (MN/cm_2)	UTS corrected		S/E ratio (%)
			yes	no			Kp/cm_2	MN/m_2	
2088	2	DC	+		875		132	12.9	
2105	4	DC	+		950		145	14.2	
2114	7	DC	+		1070		166	16.2	
2112	8	DC		+	1001	4276	151	14.8	0.346
2089	11	DC	+		820**		(128)	(12.5)	
2095	13	DC		+	1120		174	17.1	
2085	16	DC	+		1110		172	16.9	
2087	19	DC	+		950	4390	146	14.3	
2091	21	DC		+	1137		171	16.8	0.383
2092	2	DC	+		1125		173	16.9	
2110	FRESH COMPACTS	DC		+	1115	-	167	16.4	-
2100		DC		+	975	3166	147	14.4	0.454
2101		DC		+	1369	4079	206	20.2	0.496
2094		DC		+	1153	3450	174	17.0	0.483
2096		HB		+	-	-	194	19.0	-
2098		HB		+	-	-	171	16.8	-

* DC: DIAMETRICAL COMPRESSION HB: HYDRAULIC BURST

** Compact had been frilled for T/C insertion

Table 12: Mechanical tests on DR-S2 irradiated and unirradiated compacts

DR-S5 pin N°	Core Height (cm)	Compact N°	OUTER DIAMETER			LENGTH		
			Pre-Irradiation (mm)	Post-Irradiation (mm)	Shrinkage (%)	Pre-Irradiation (mm)	Post-Irradiation (mm)	Shrinkage (%)
DR-S5/6	160.3	2213	50.10	49.98	-0.24	42.44	42.29	-0.35
	156.0	2220	50.13	49.98	-0.3	"	42.34	-0.24
	151.8	2221	50.15	49.98	-0.44	"	42.25	-0.45
	147.5	2223	50.13	49.92	-0.42	"	42.22	-0.52
	143.3	2225	50.13	49.85	-0.5	"	42.25	-0.45
	139.0	2229	50.13	49.9	-0.46	"	42.21	-0.54
	134.8	2261*	50.15	49.9	-0.5	"	42.24	-0.47
	130.5	2269*	50.15	49.92	-0.46	"	42.09	-0.82
	126.3	2270	50.15	49.81	-0.58	"	42.27	-0.4
	122.0	2271*	50.15	49.9	-0.5	"	42.15	-0.68
	117.8	2273	50.13	49.79	-0.68	"	42.31	0
	113.5	2275	50.15	49.8	-0.7	"	42.12	-0.75
DR-S5/5	105.4	2195	50.10	49.88	-0.44	42.5	42.21	-0.68
	101.1	2198*	50.10	49.91	-0.38	"	42.14	-0.85
	96.9	2188*	50.13	49.89	-0.48	"	42.18	-0.75
	92.6	2207*	50.13	49.9	-0.46	"	42.23	-0.64
	88.4	2209*	50.13	49.89	-0.48	"	42.15	-0.82
	84.1	2210*	50.13	49.9	-0.46	"	42.23	-0.64
	79.9	2243*	50.15	49.68	-0.94	"	42.08	-0.99
	75.6	2251	50.13	49.69	-0.88	"	42.23	-0.64
	71.4	2254	50.13	49.7	-0.86	"	42.12	-0.89
	67.1	2255	50.15	49.74	-0.82	"	42.11	-0.92
	62.9	2257	NR	49.75		"	42.02	-1.13
	58.6	2258	50.15	49.82	-0.66	"	42.04	-1.08
DR-S5/4	50.4	2231*	50.13	50.01	-0.24	42.48	42.25	-0.54
	46.2	2232*	50.13	50.01	-0.24	"	42.2	-0.66
	41.9	2187*	50.13	49.98	-0.3	"	42.46	-0.05
	37.7	2189*	50.13	50	-0.26	"	42.27	-0.49
	33.4	2190	50.13	49.9	-0.46	"	42.39	-0.21
	29.2	2194*	50.13	50.03	-0.2	"	42.36	-0.28
	24.9	2263	50.13	49.93	-0.4	"	42.32	-0.38
	20.7	2264	50.15	49.92	-0.46	"	42.22	-0.61
	16.4	2265	NR	49.93		"	42.24	-0.56
	12.2	2268	50.15	49.96	-0.38	"	42.23	-0.59
	7.9	2280	NR	49.96		"	42.25	-0.54
	3.7	2283	50.13	49.98	0.3	"	42.43	-0.12

* cracked NR: non recorded

Table 13: DR-S5 compacts dimensional measurement

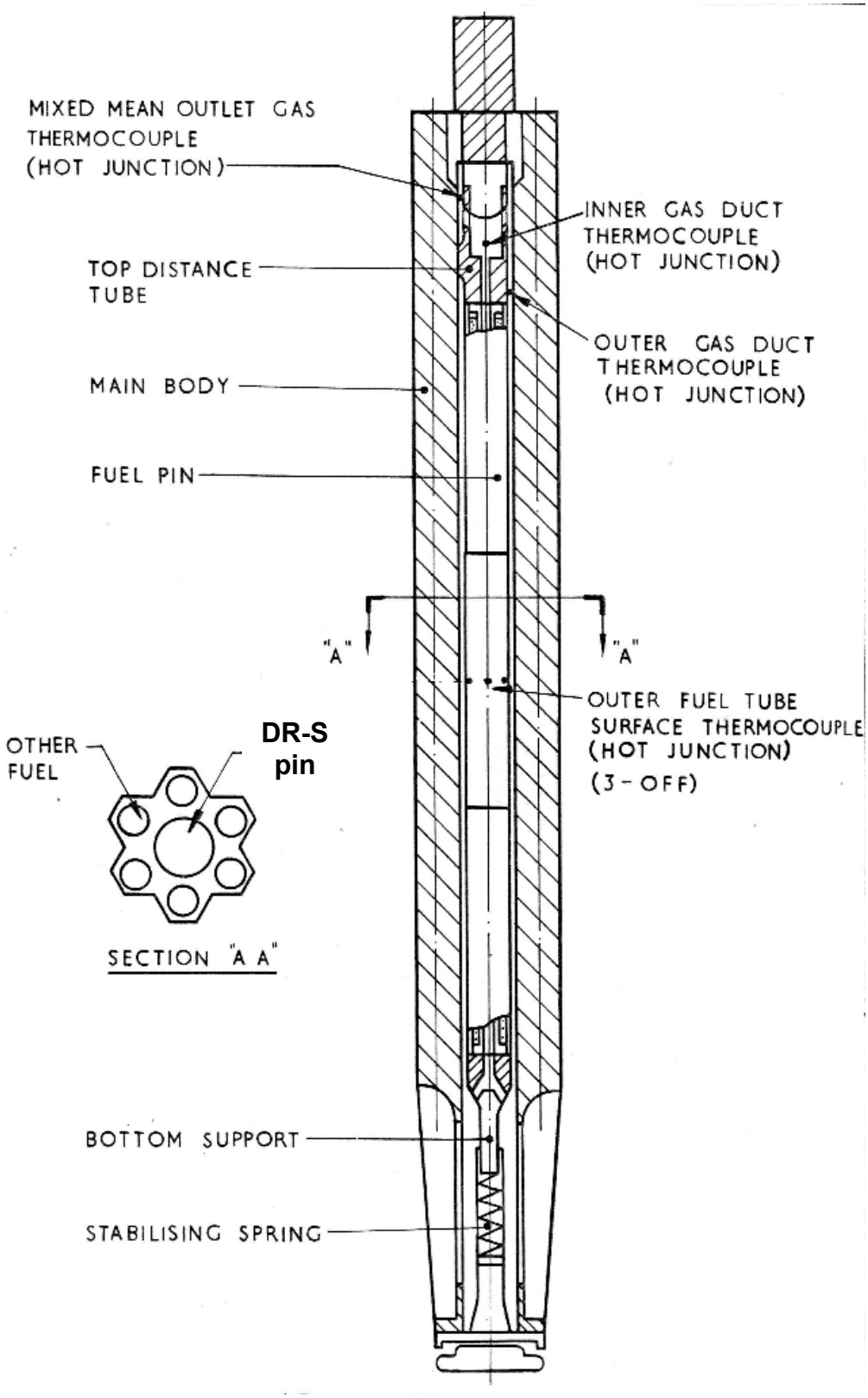

Figure 1: Dragon assembly design of DR-S experiment

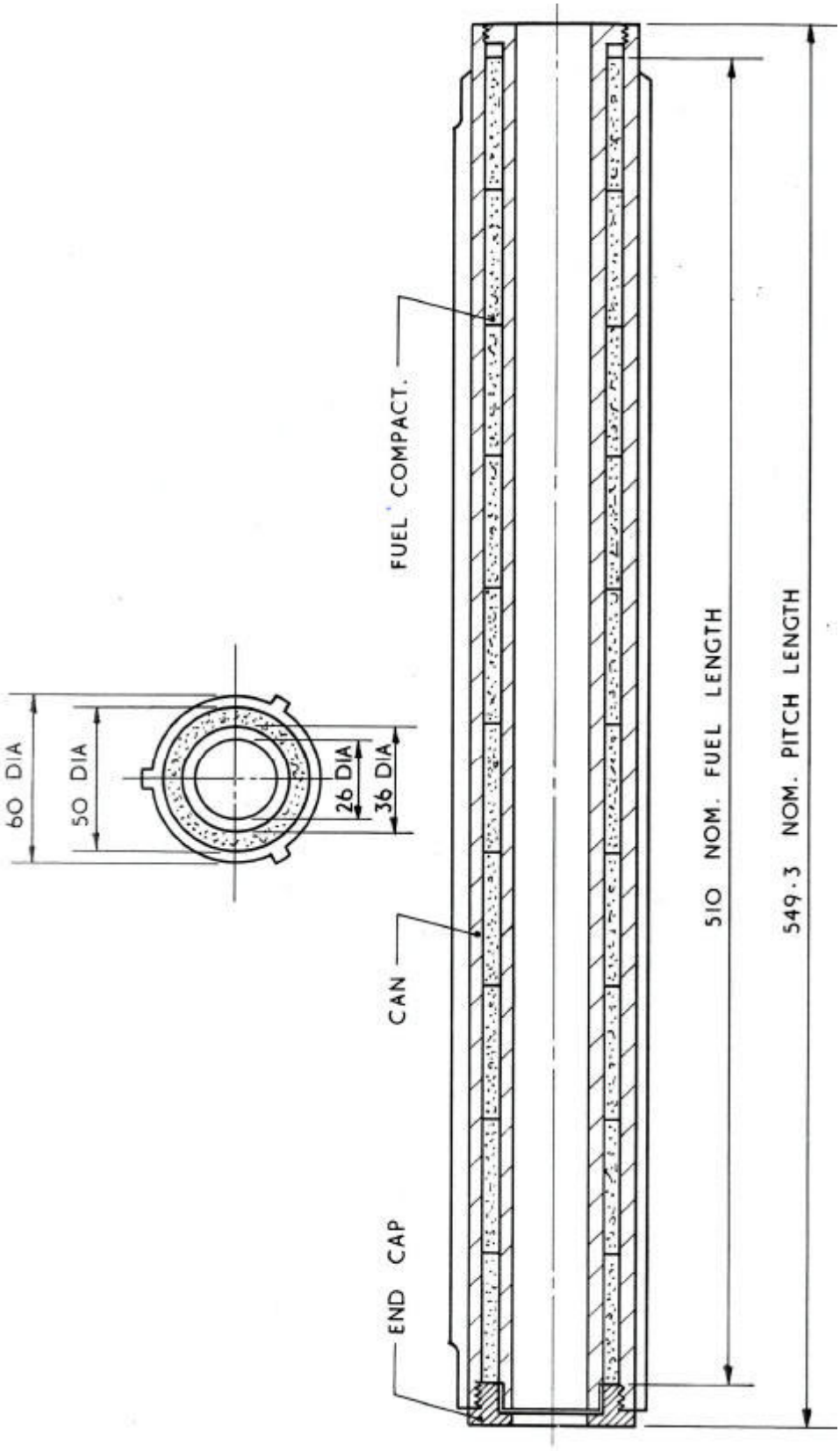

Figure 2: DR-S5 experiment fuel pin design

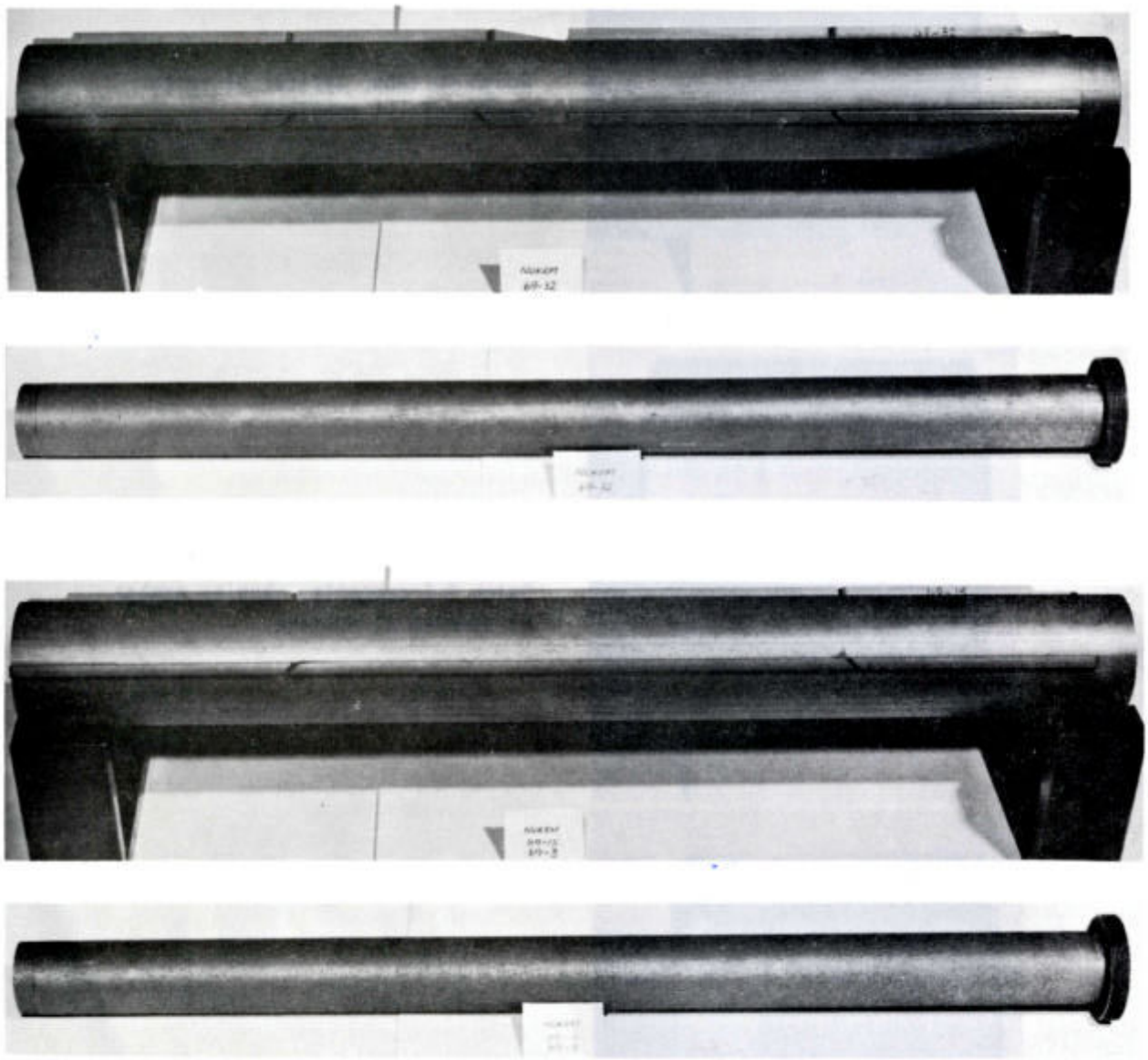

Figure 3: Graphite component for fuel pin DR-S5/5 and DR-S5/6

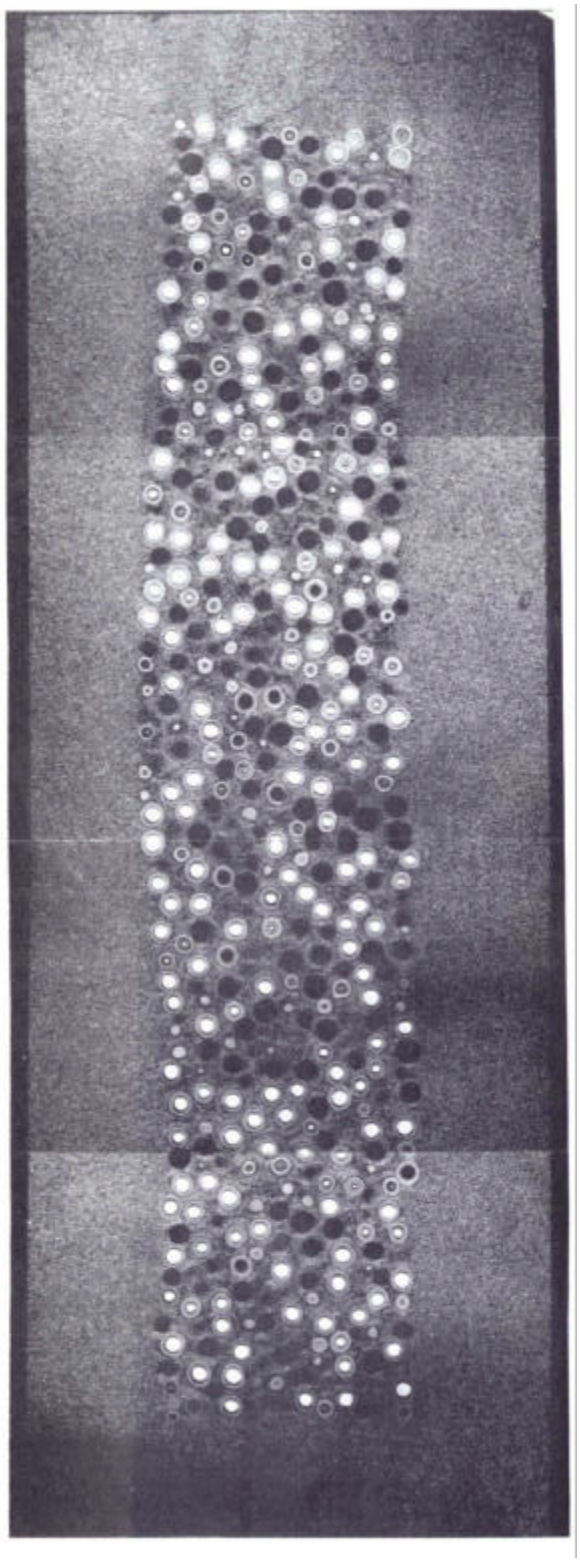

Figure 4: Compact for DR-S2 experiment (transversal cross section)

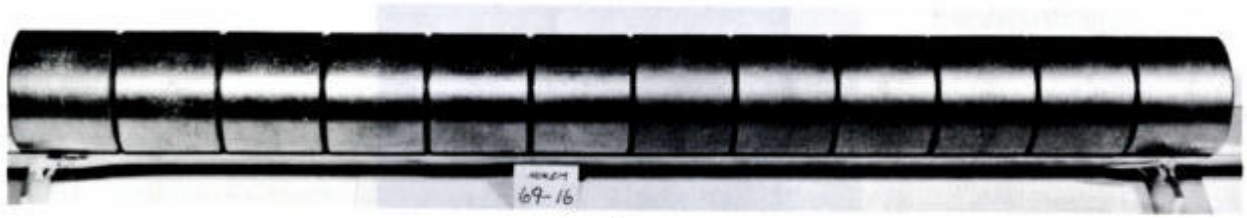

Batch 1-1. Shiny finish.
Rough surface is typical

Batch 2-1. Matt finish

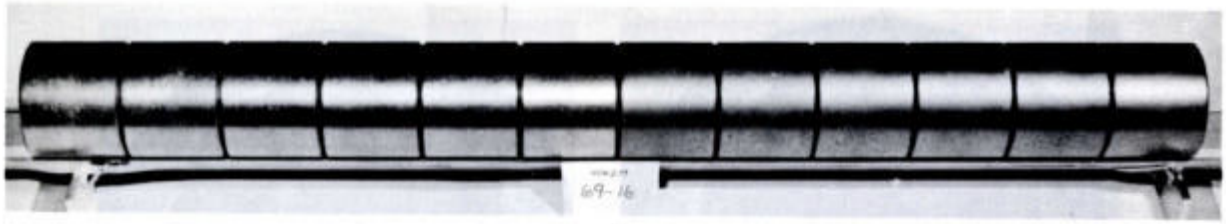

Batch 1-1

Batch 2-1

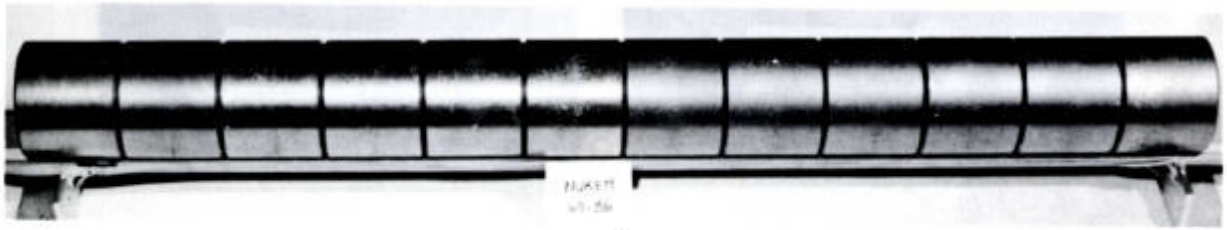

Batch 1-1

Batch 2-1

Figure 5: DR-S5 compact stacks

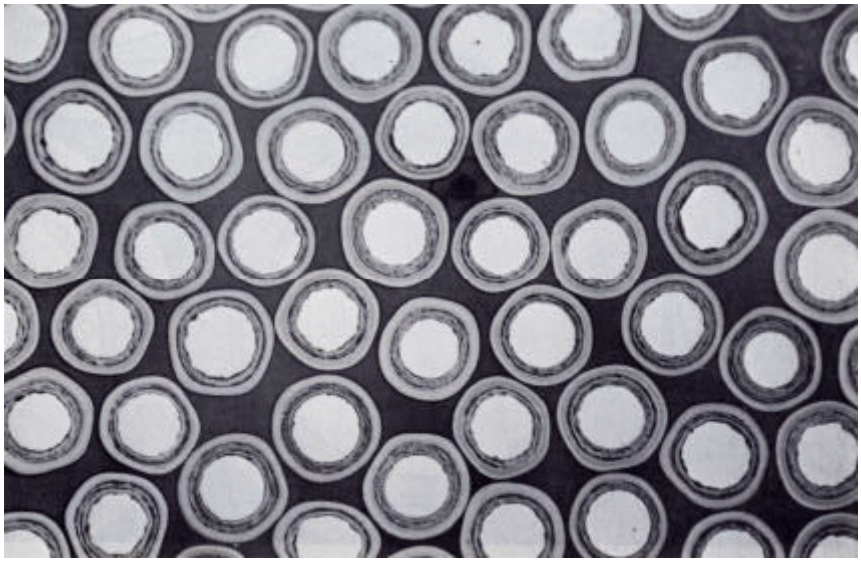

X15

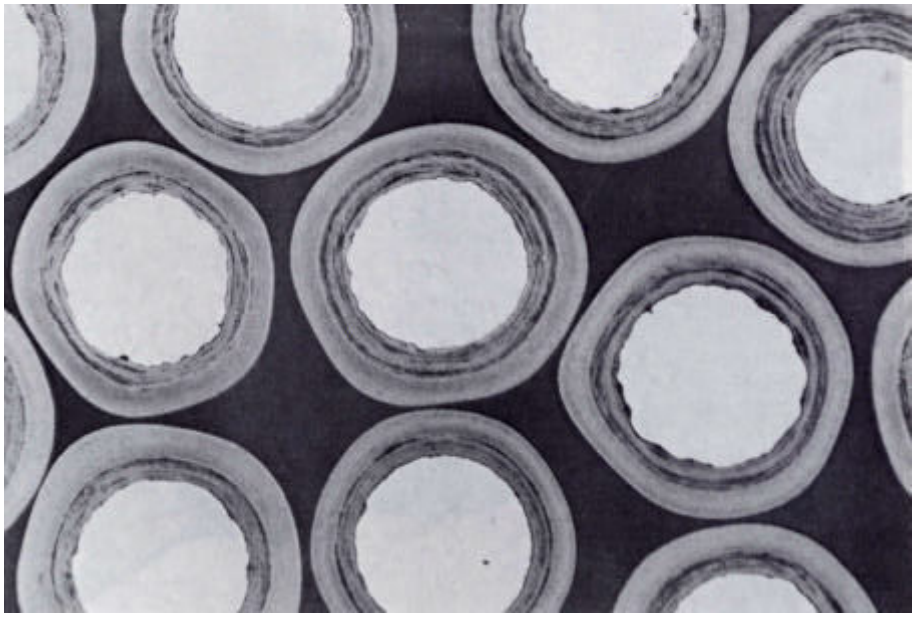

X40

Figure 6: General view of coated particles for DR-S2 (no SiC layer)

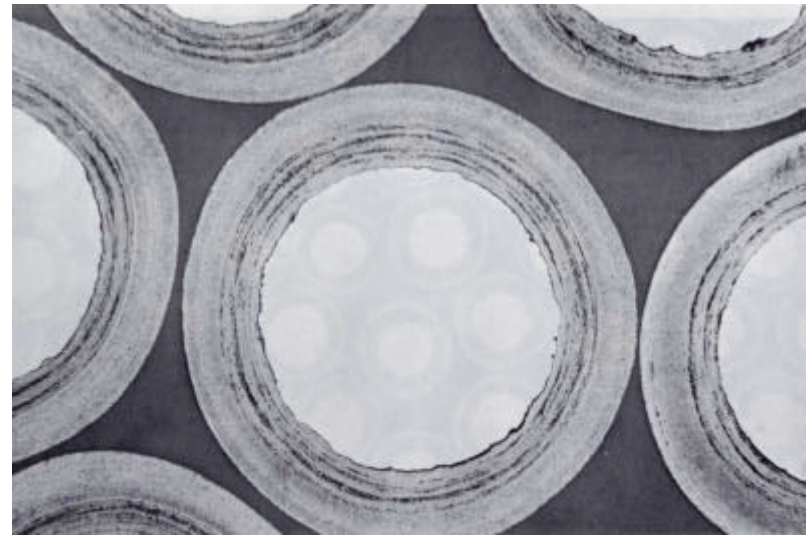

X70

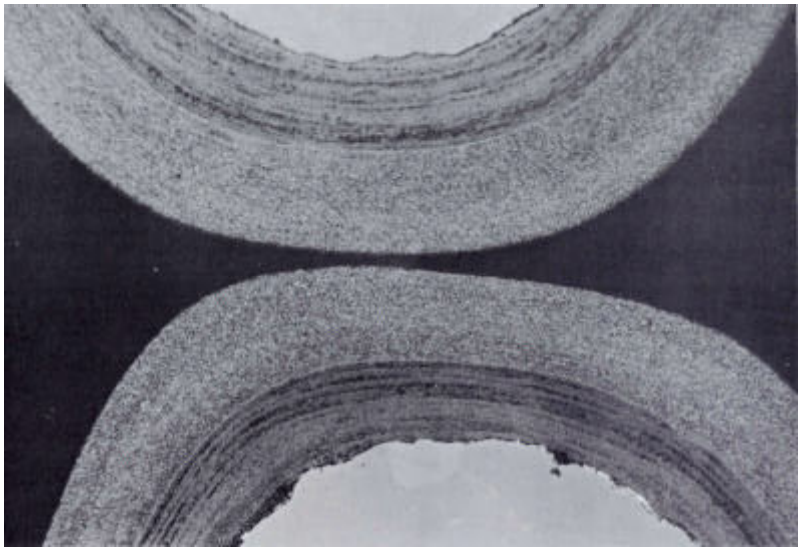

X140

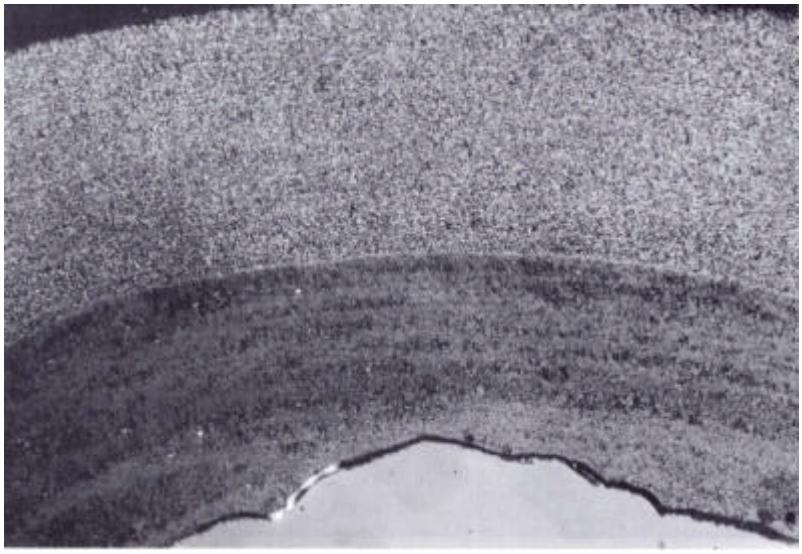

X350

Figure 7: Macrographies of DR-S2 coated particles

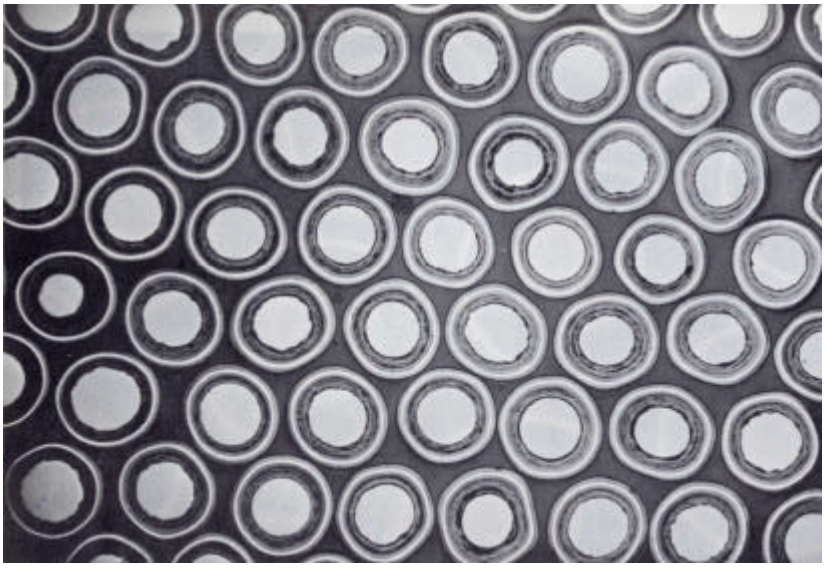

X15

Non polarised light

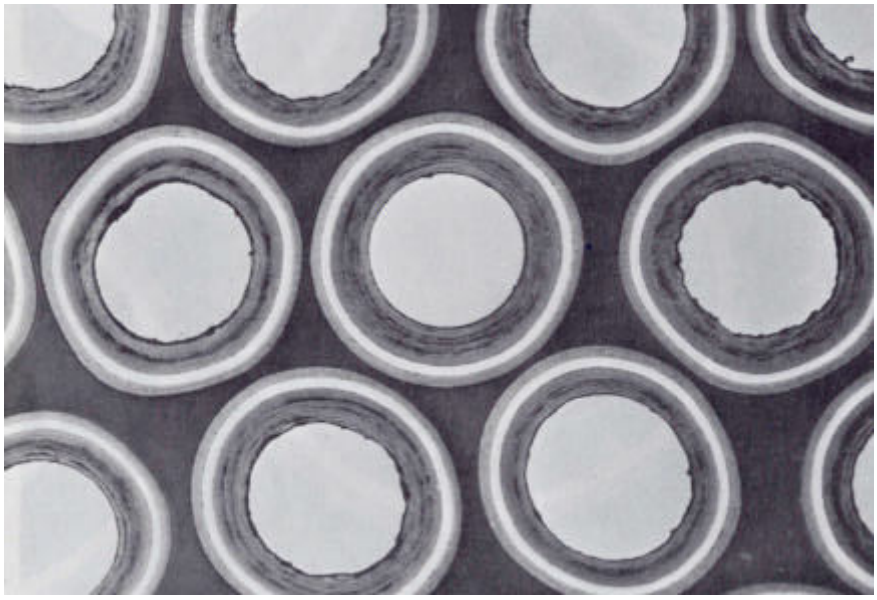

X40

15° polarised light

Figure 8: DR-S5 coated particles

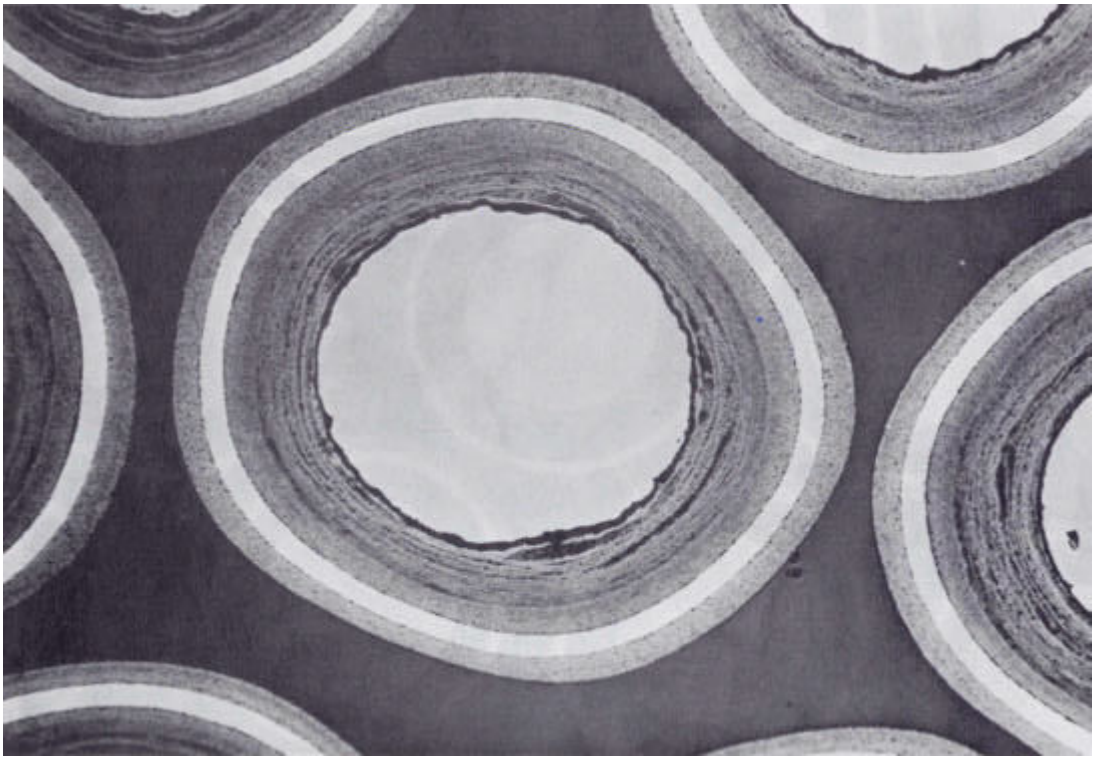

X100

12° polarised light

Figure 9: DR-S5 coated particles

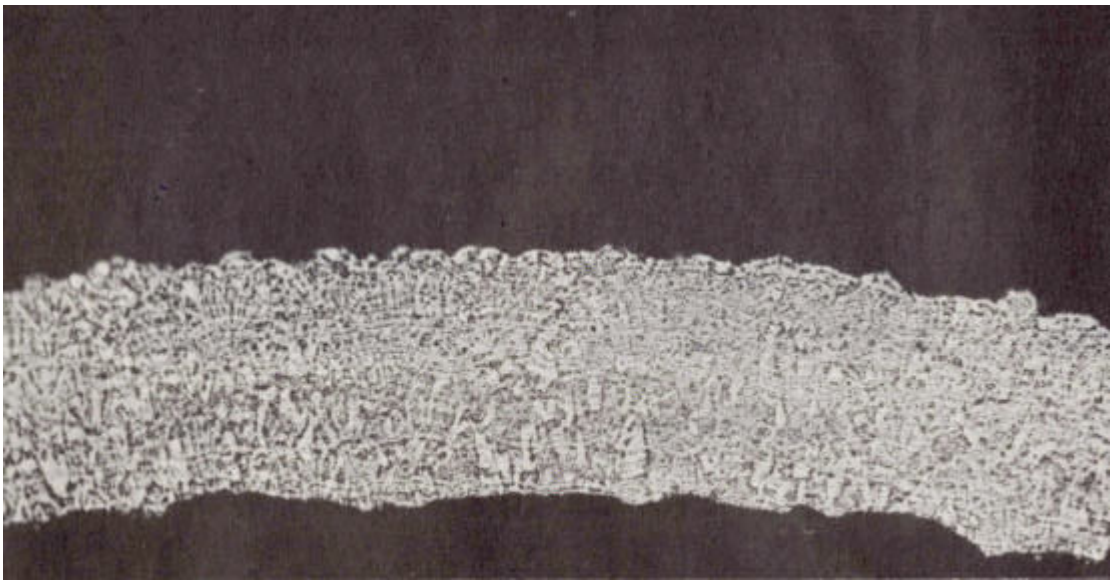

Figure 10: DR-S5 SiC layer of coated particle

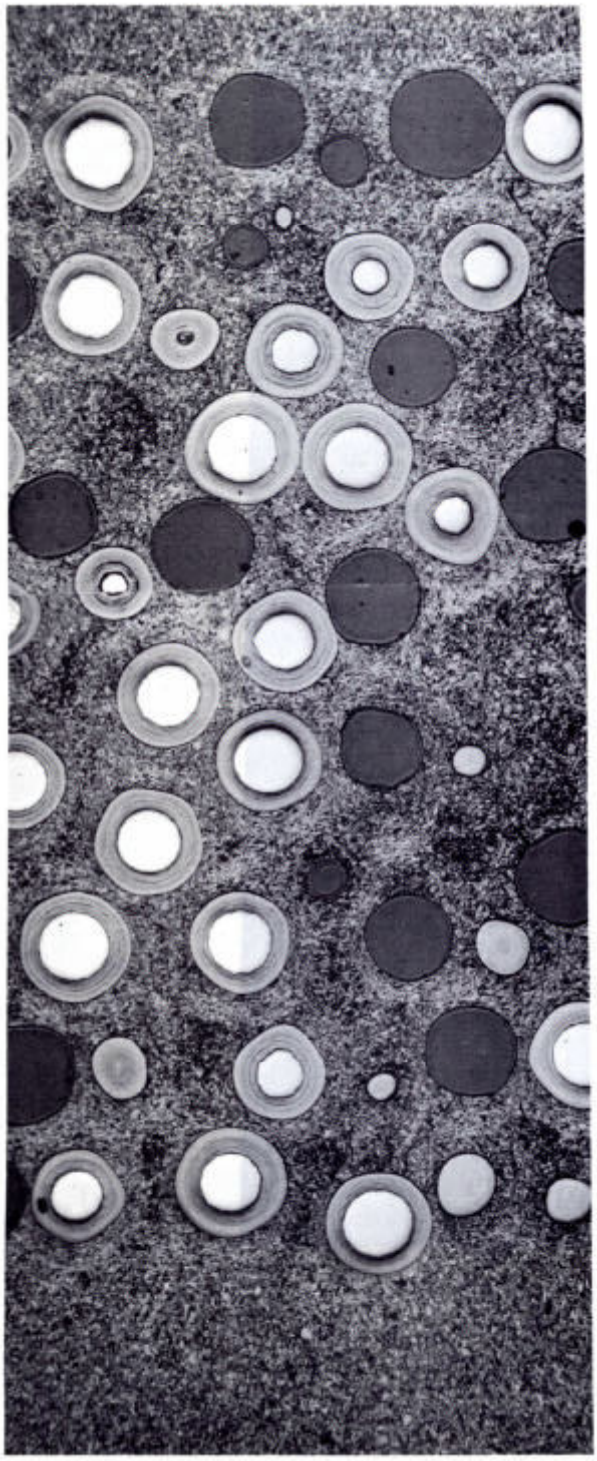

X 15

Figure 11: DR-S2 compact (transversal cross section)

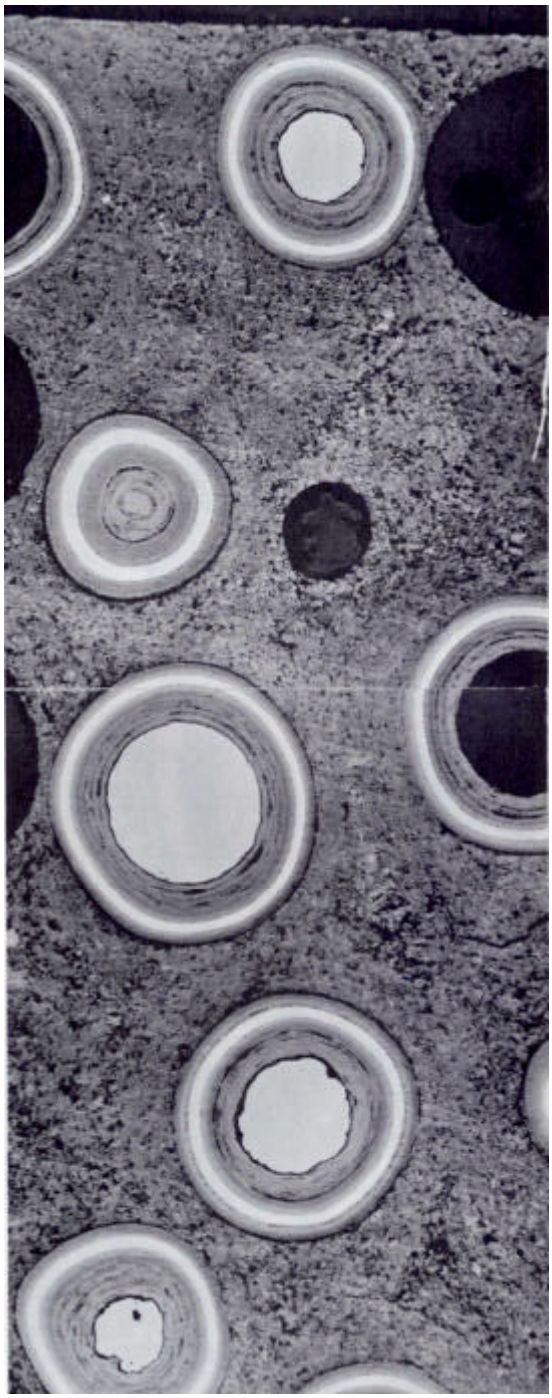

X40

Matrix 1/1

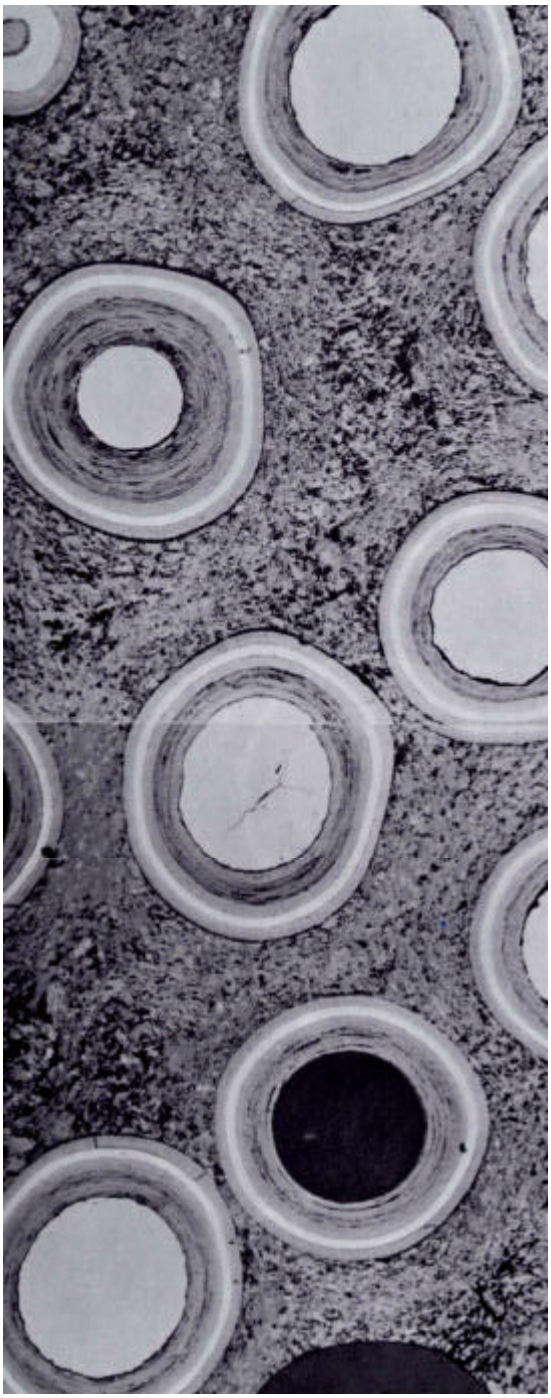

X40

Matrix 2/1
(Cracks in outer PyC developed supposedly during cutting and polishing)

Figure 12: Cross section of DR-S5 compacts

X40

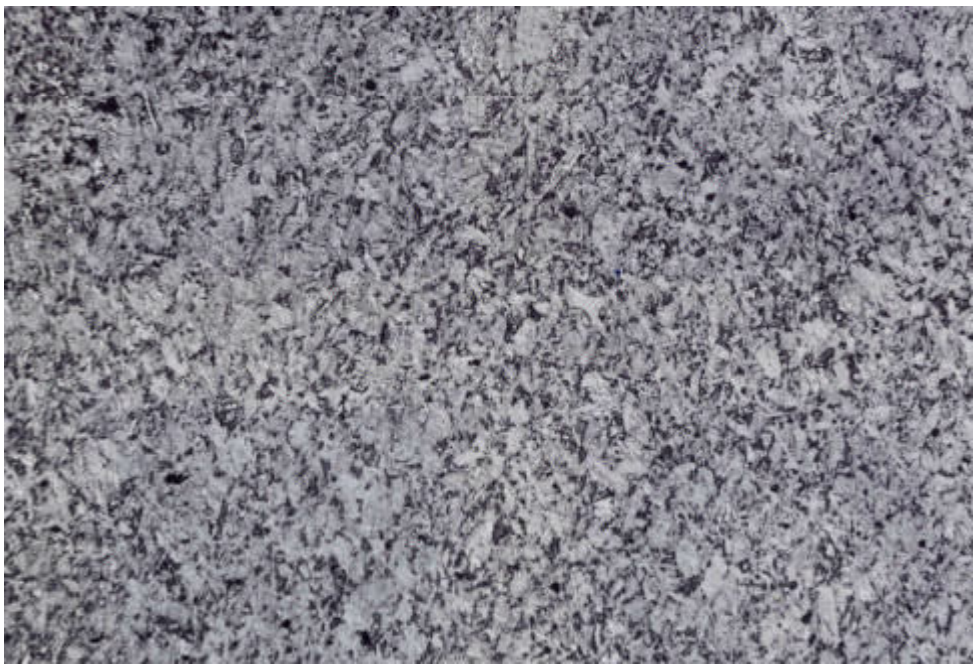

X80

Figure 13: DR-S2 compact matrix type 2/1

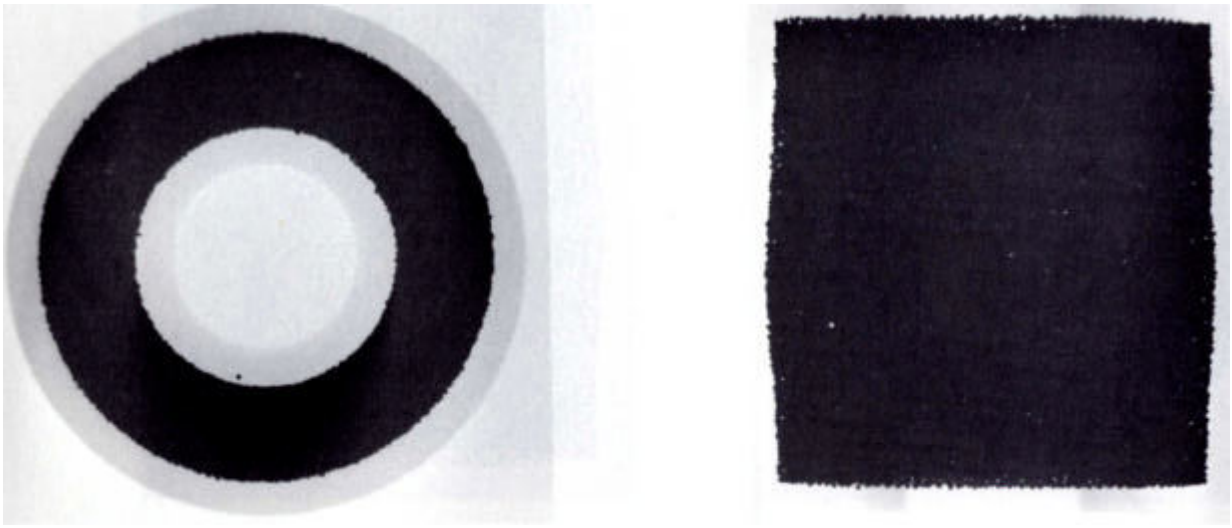

Compact 2103

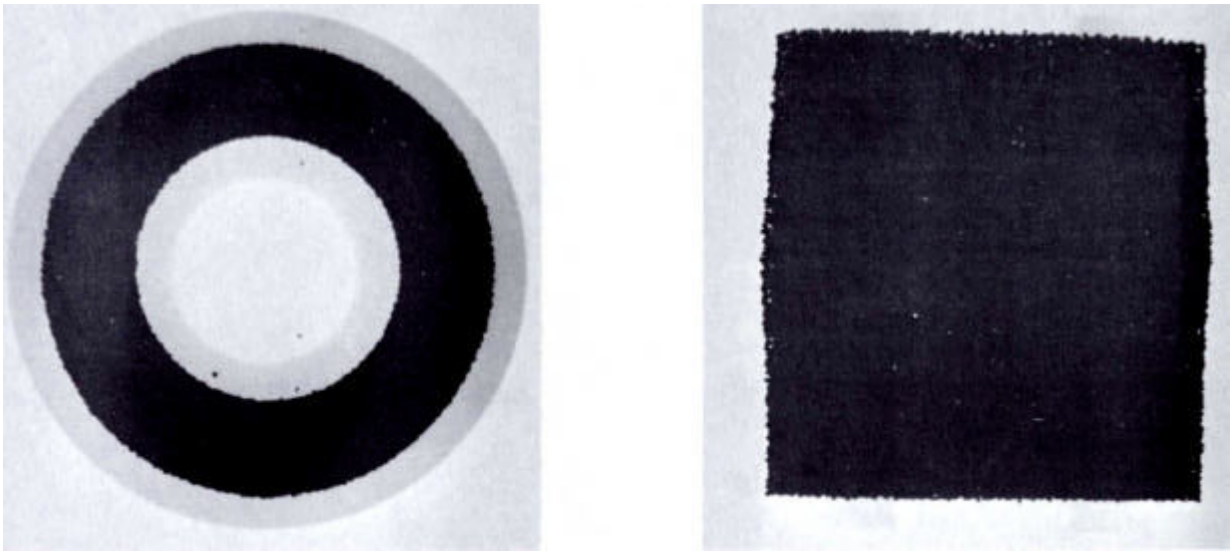

Compact 2081

Figure 14: X-ray of DR-S2 compacts

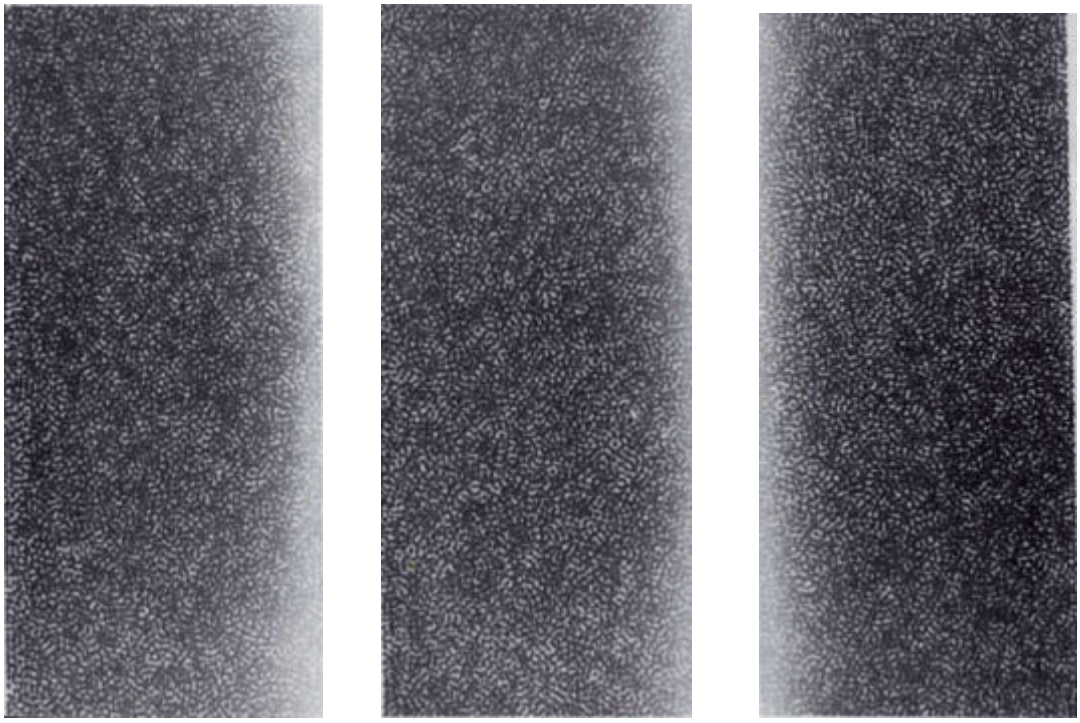

Compact 2194 Type 1/1 | **Compact 2220 Type 1/1** | **Compact 2261 Type 2/1**

Figure 15: Panoramic radiograph of DR-S5 compacts

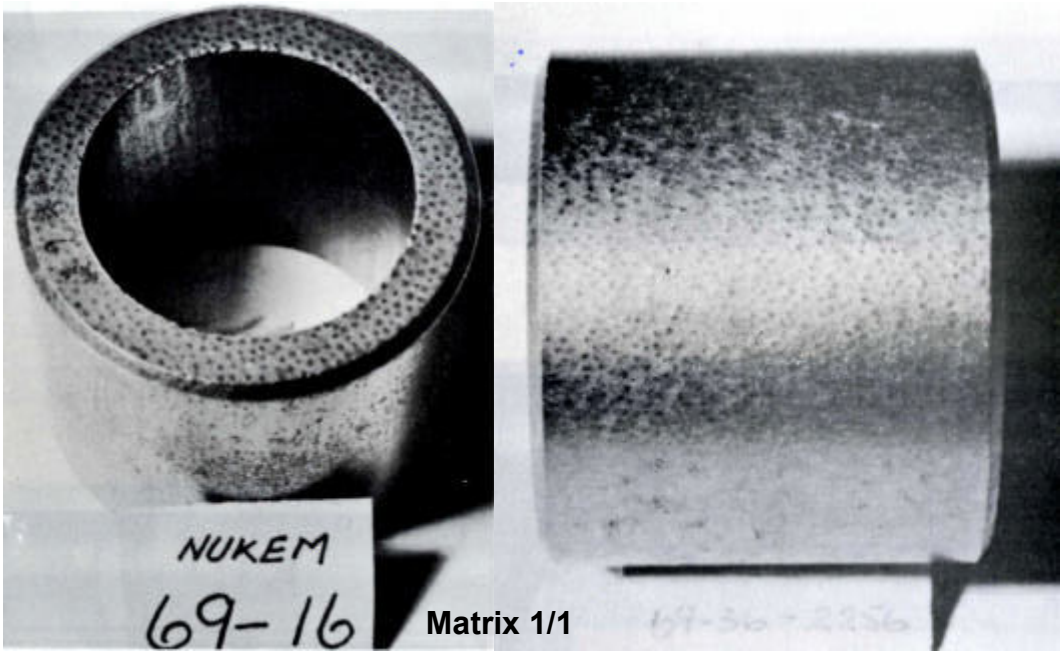

Figure 16: View of DR-S5 compacts

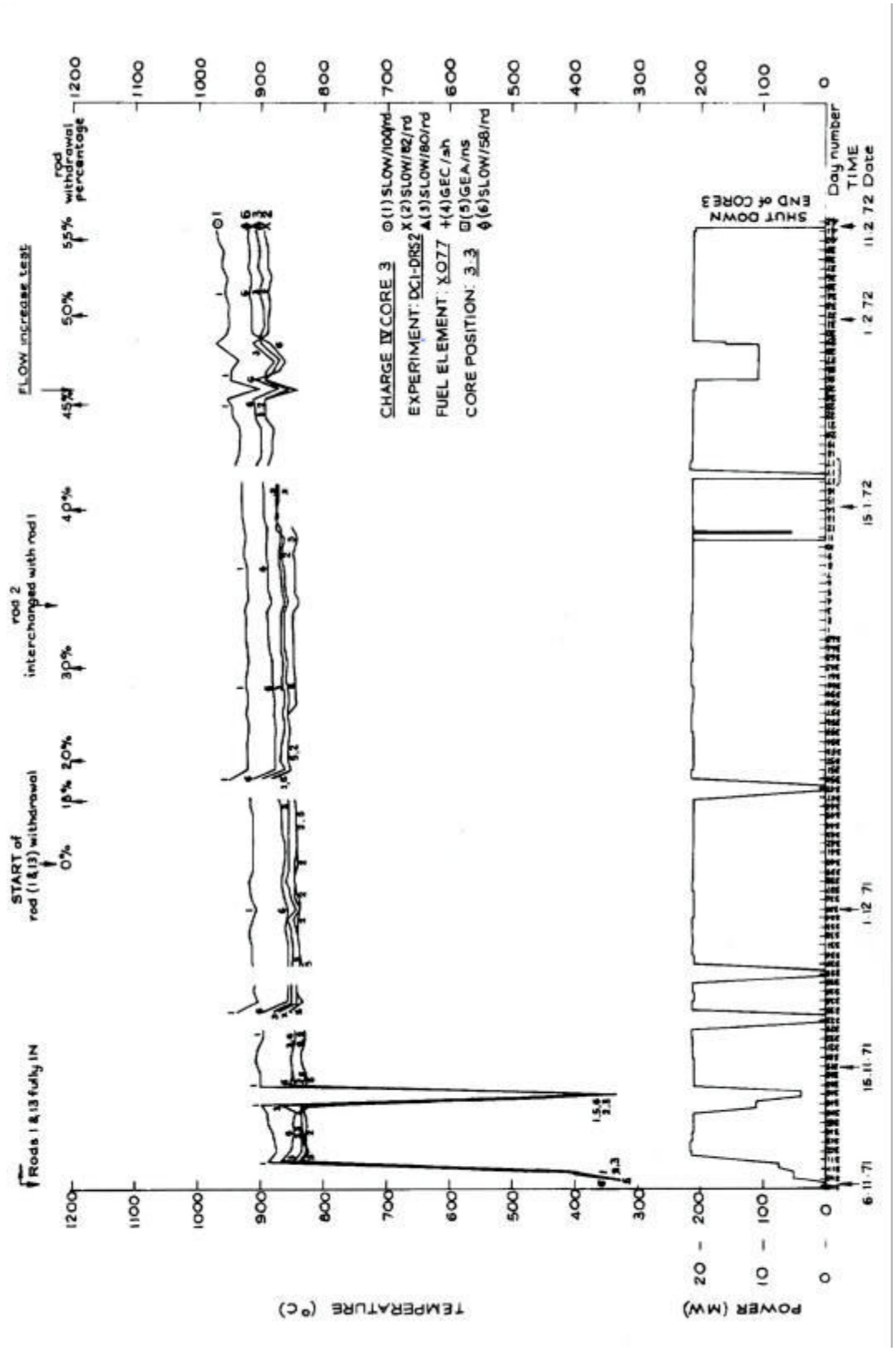

Figure 17: Irradiation history of DR-S2 experiment in Dragon Charge IV core 3

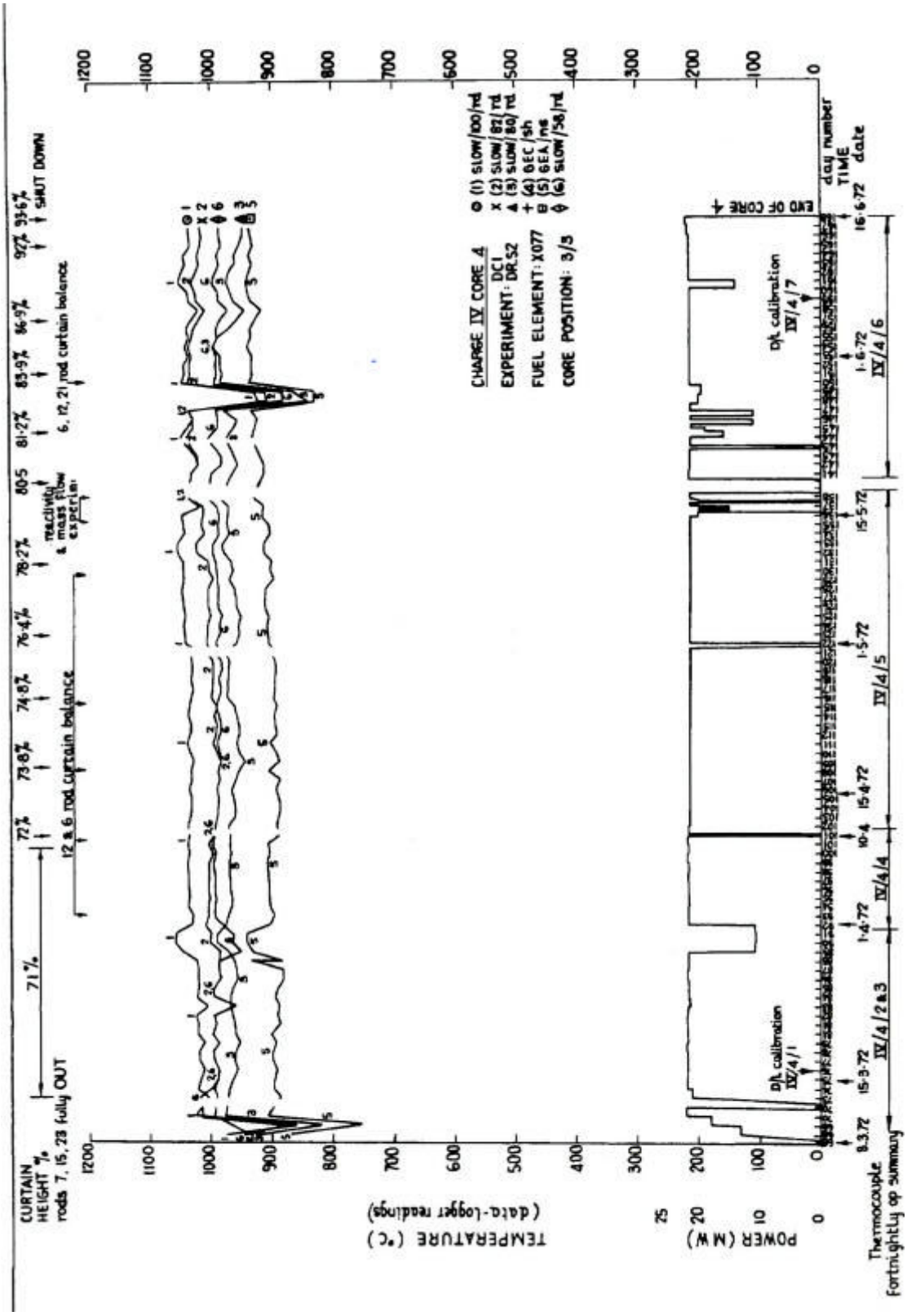

Figure 18: Irradiation history of DR-S2 experiment in Dragon Charge IV core 4

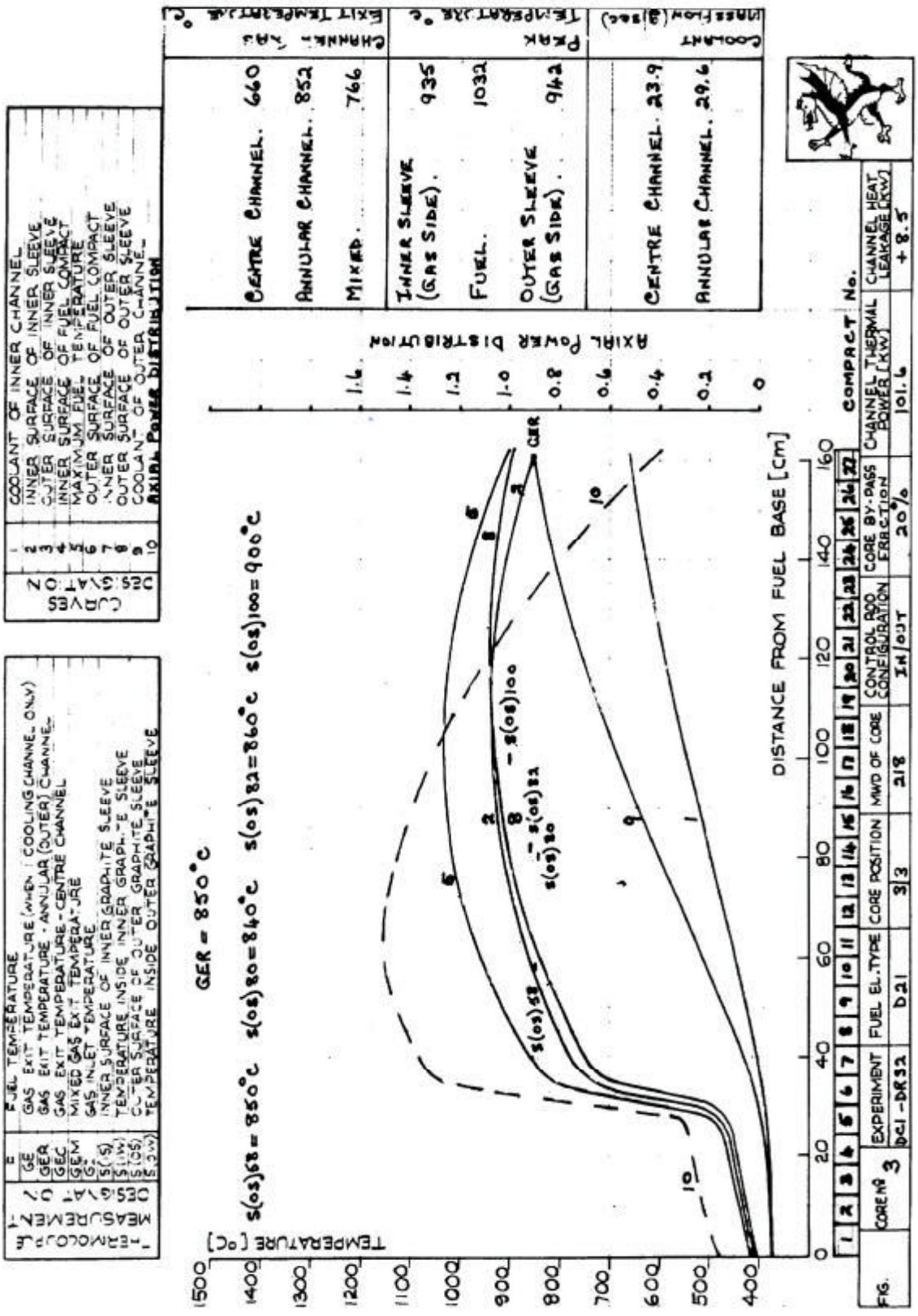

Figure 19: DR-S2 axial temperature and power profiles (Charge IV core 3)

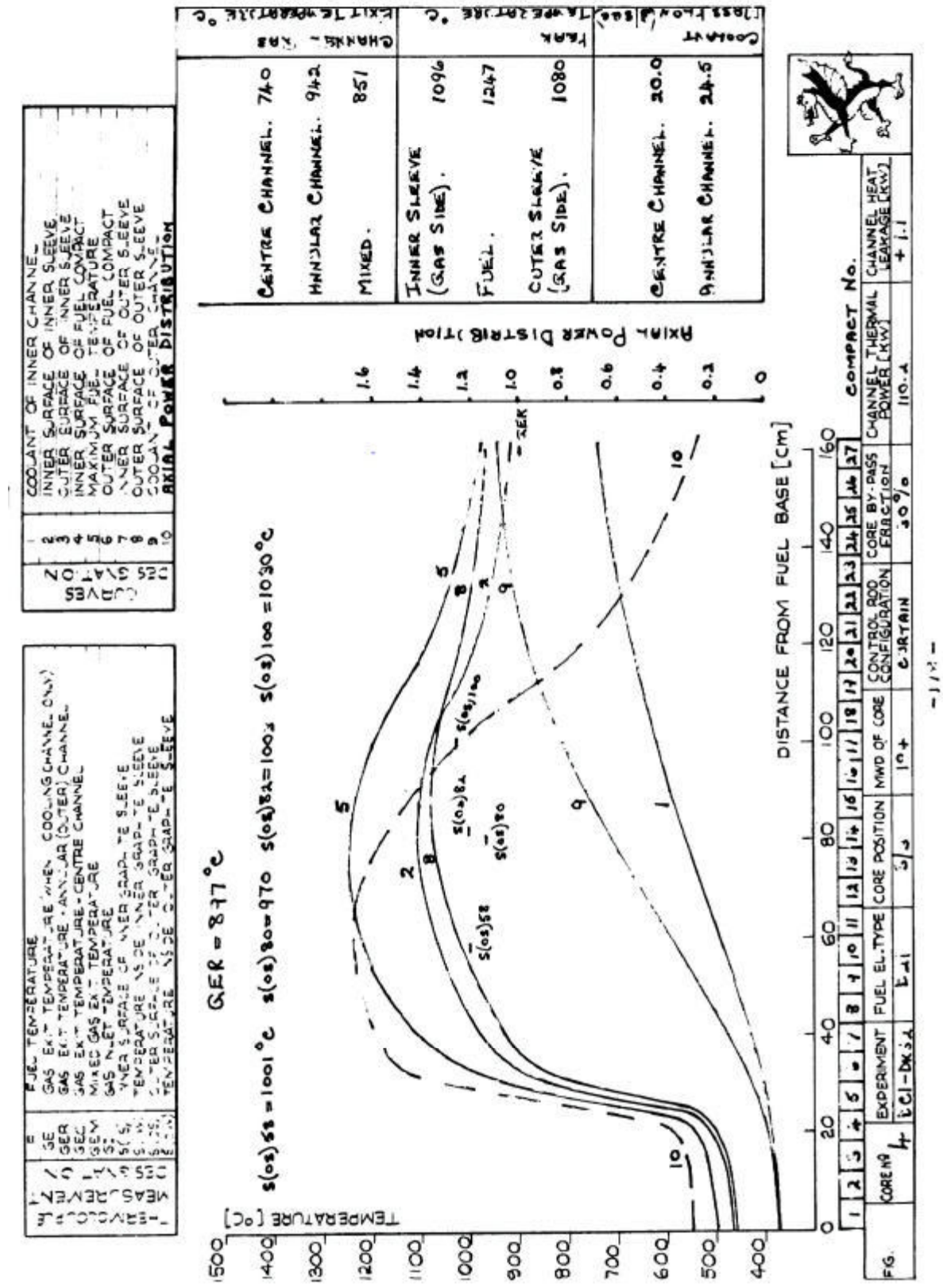

Figure 20: DR-S2 axial temperature and power profiles (Charge IV core 4)

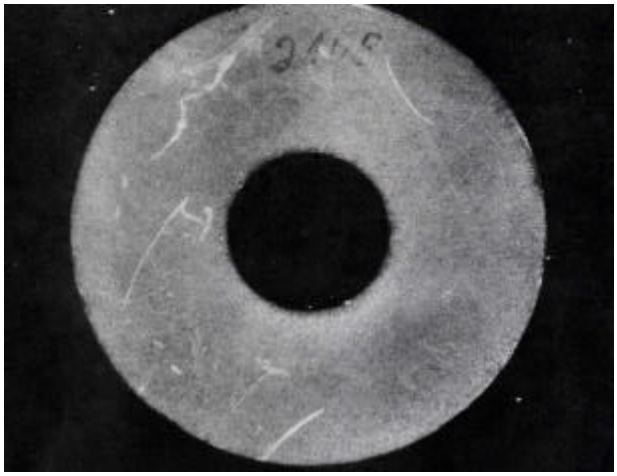

Top end face, Compact 2118, position 14

Top end, chipped edge, Compact 2110, position 18

Figure 21: DR-S2 irradiated compacts - top end

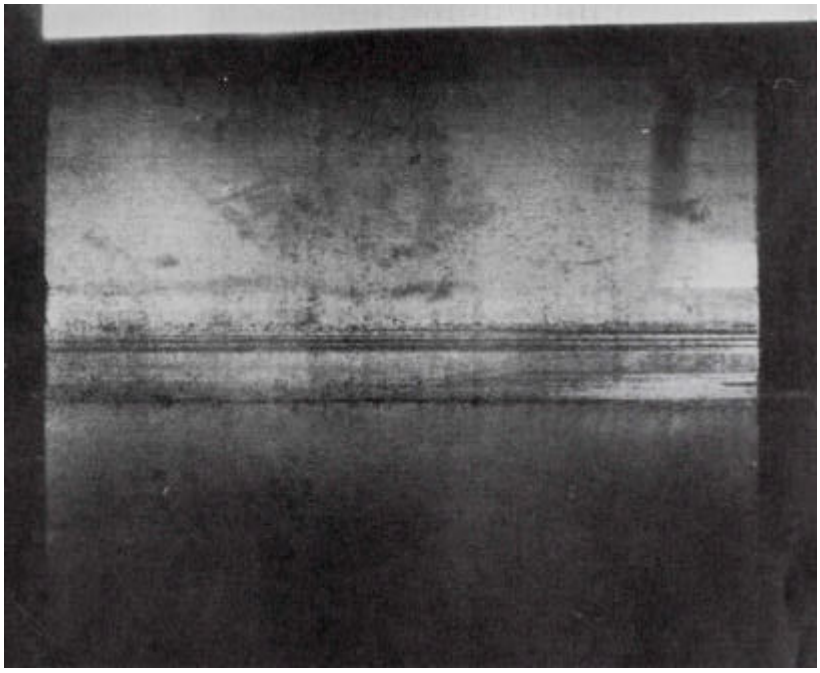

X1.5

Compact 2105, position 4

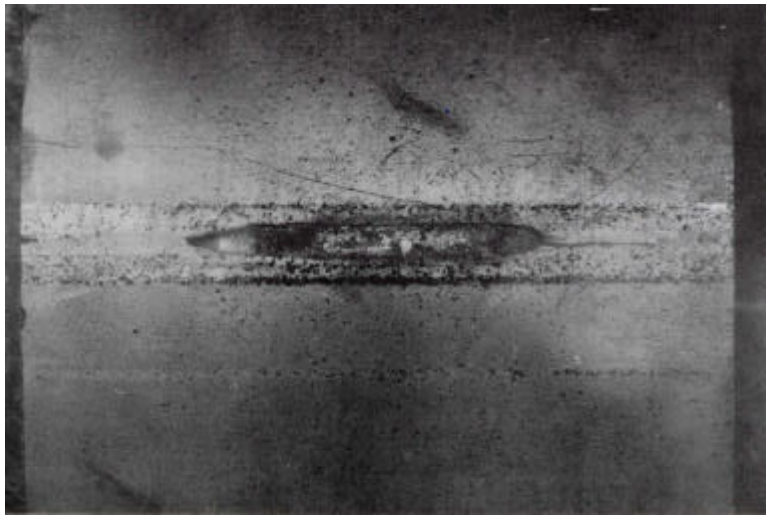

X1.5

Compact 2097, position 10

Figure 22: DR-S2 irradiated compacts - outer surface

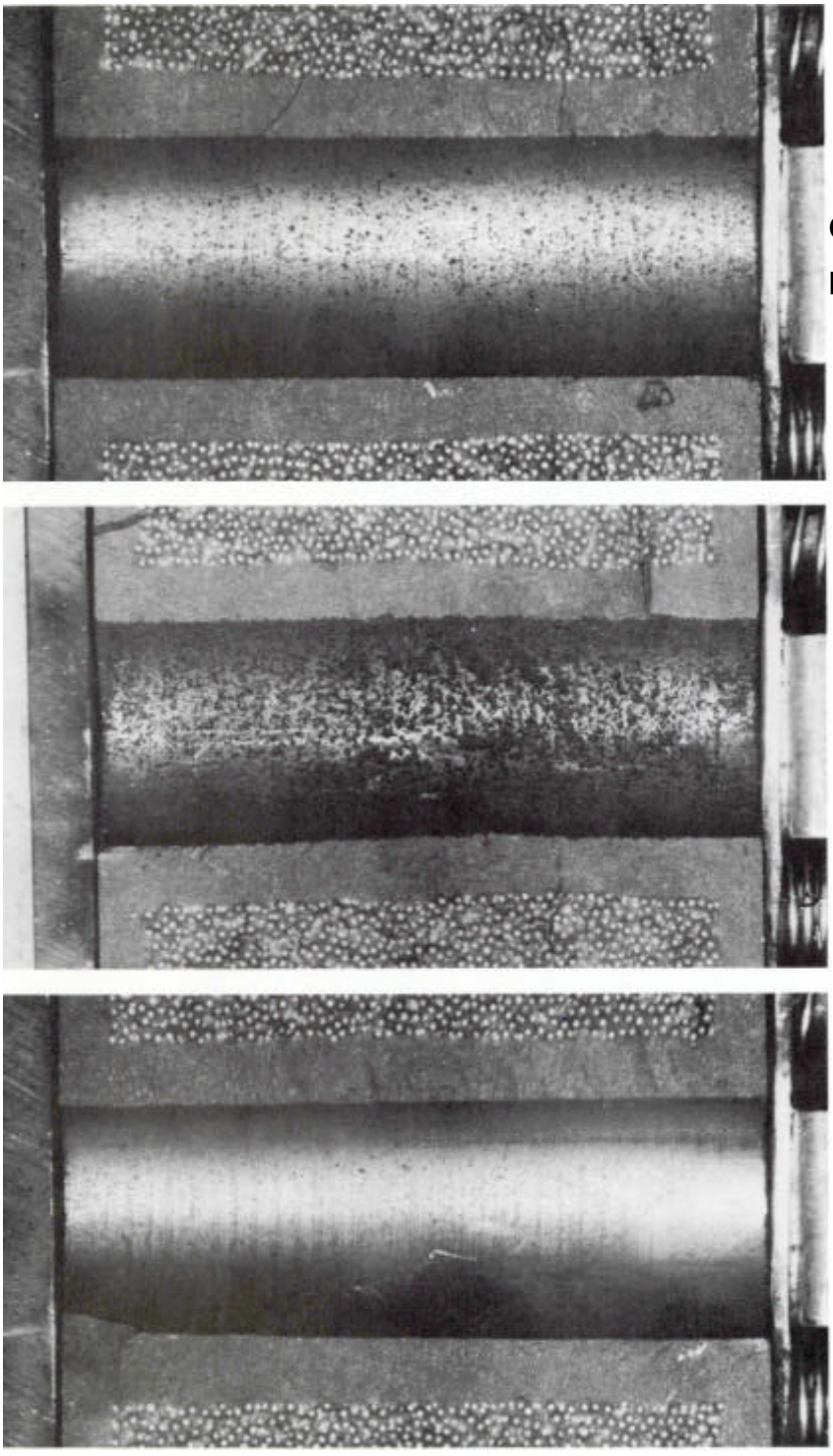

Figure 23: DR-S2 irradiated compacts – inner surface

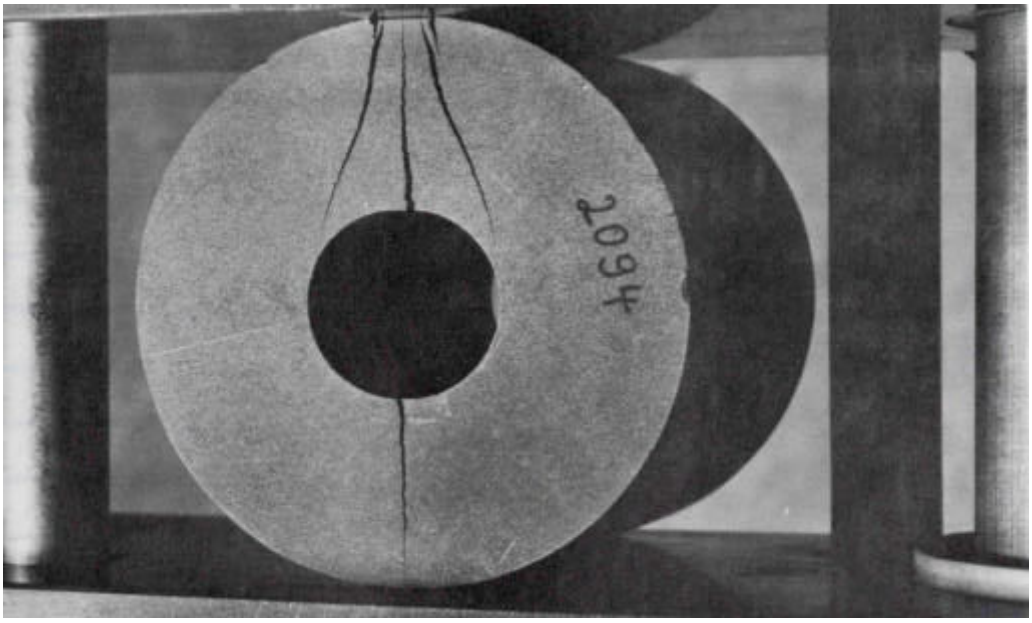

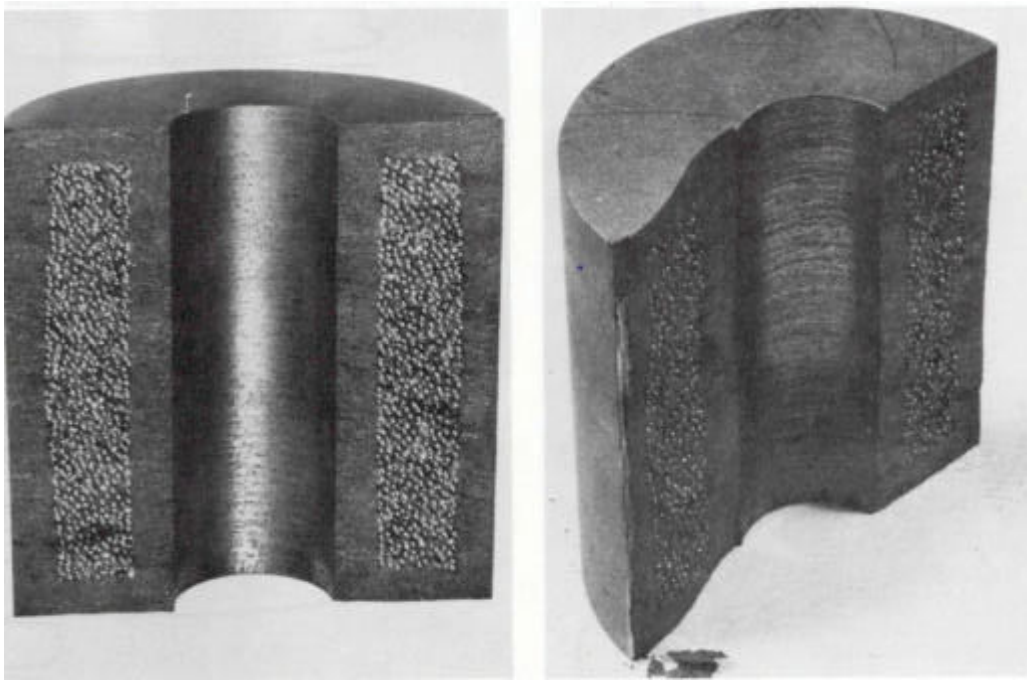

Figure 24: DR-S2 - Fracture of fresh compact by diametrical compression

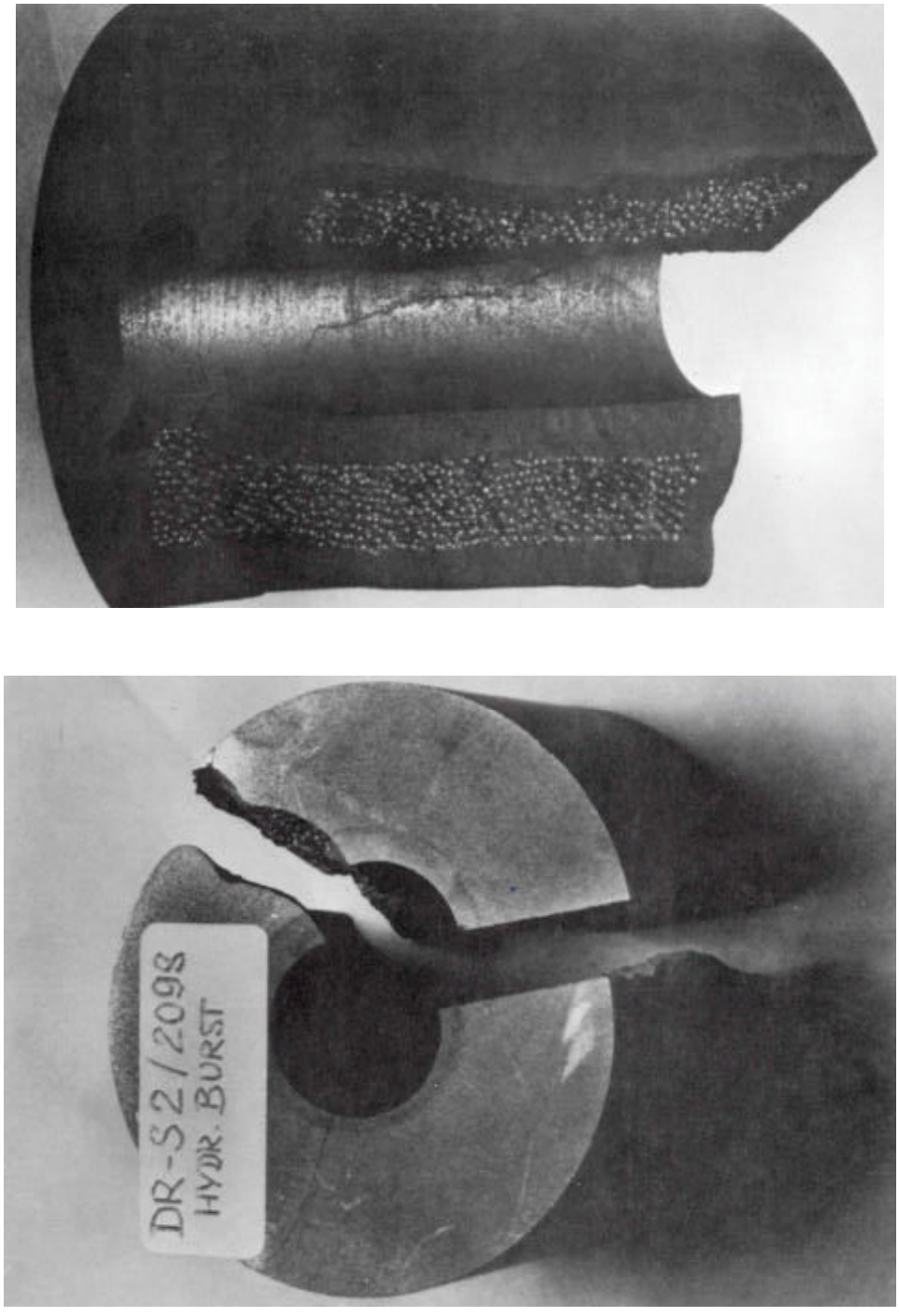

Figure 25: DR-S2 - Fracture of fresh compact by hydraulic burst test

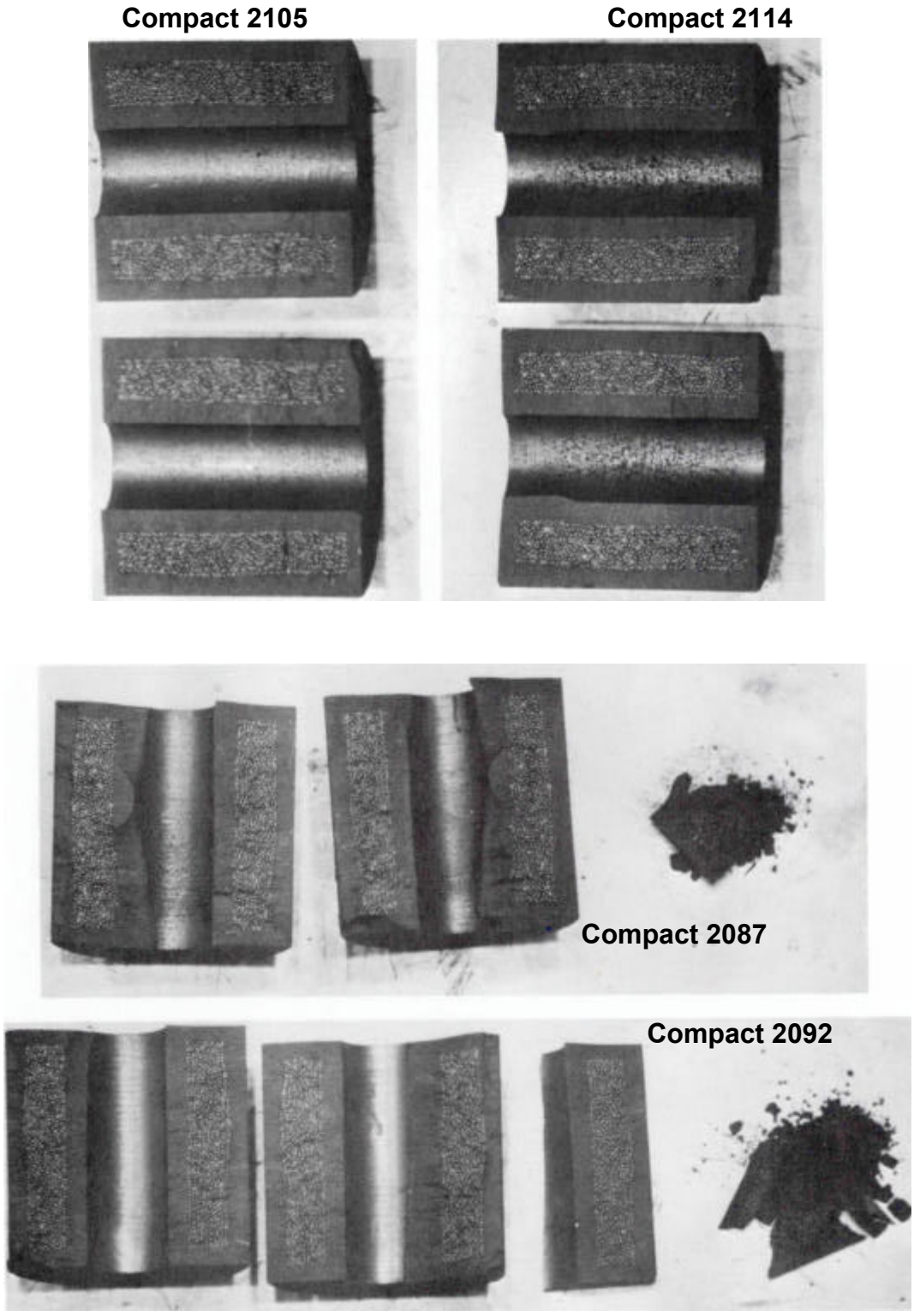

Figure 26: DR-S2 - Fracture of irradiated compact by diametrical compression

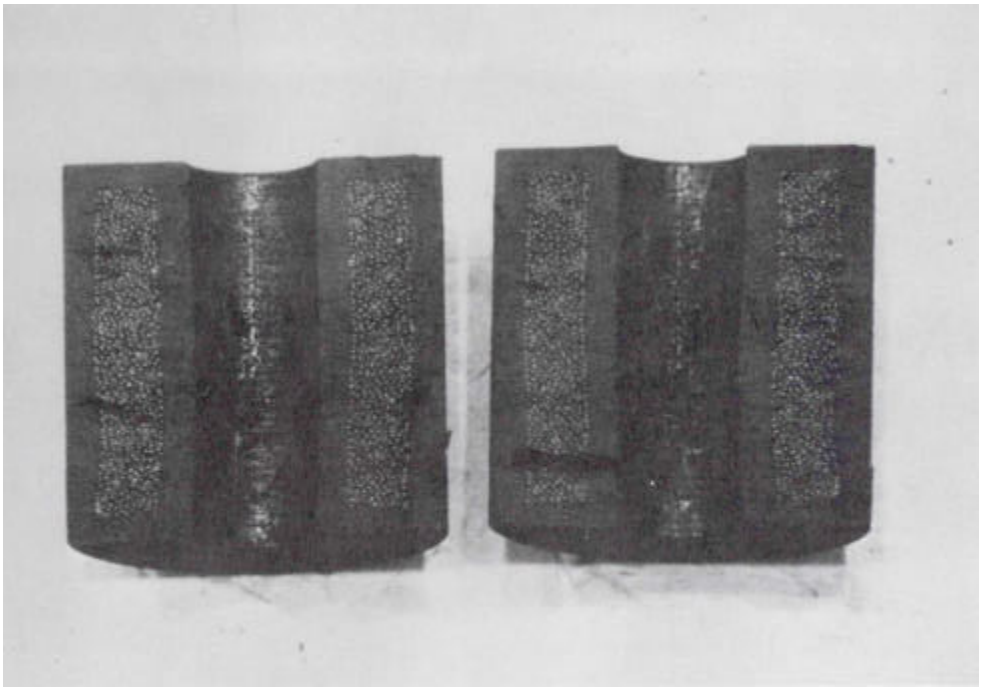

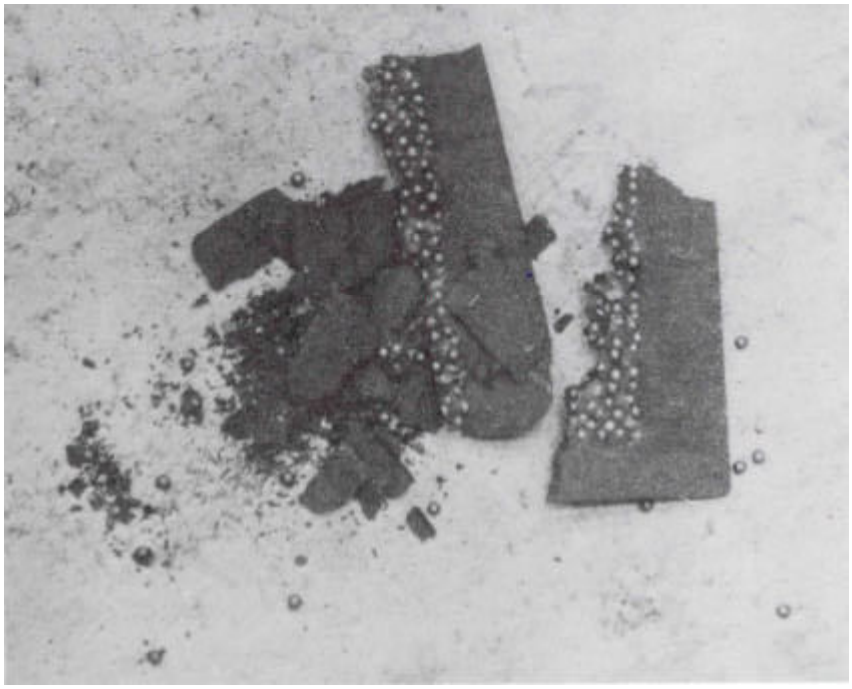

Figure 27: DR-S2 irradiated compact after diametrical compression (Compact 2089)

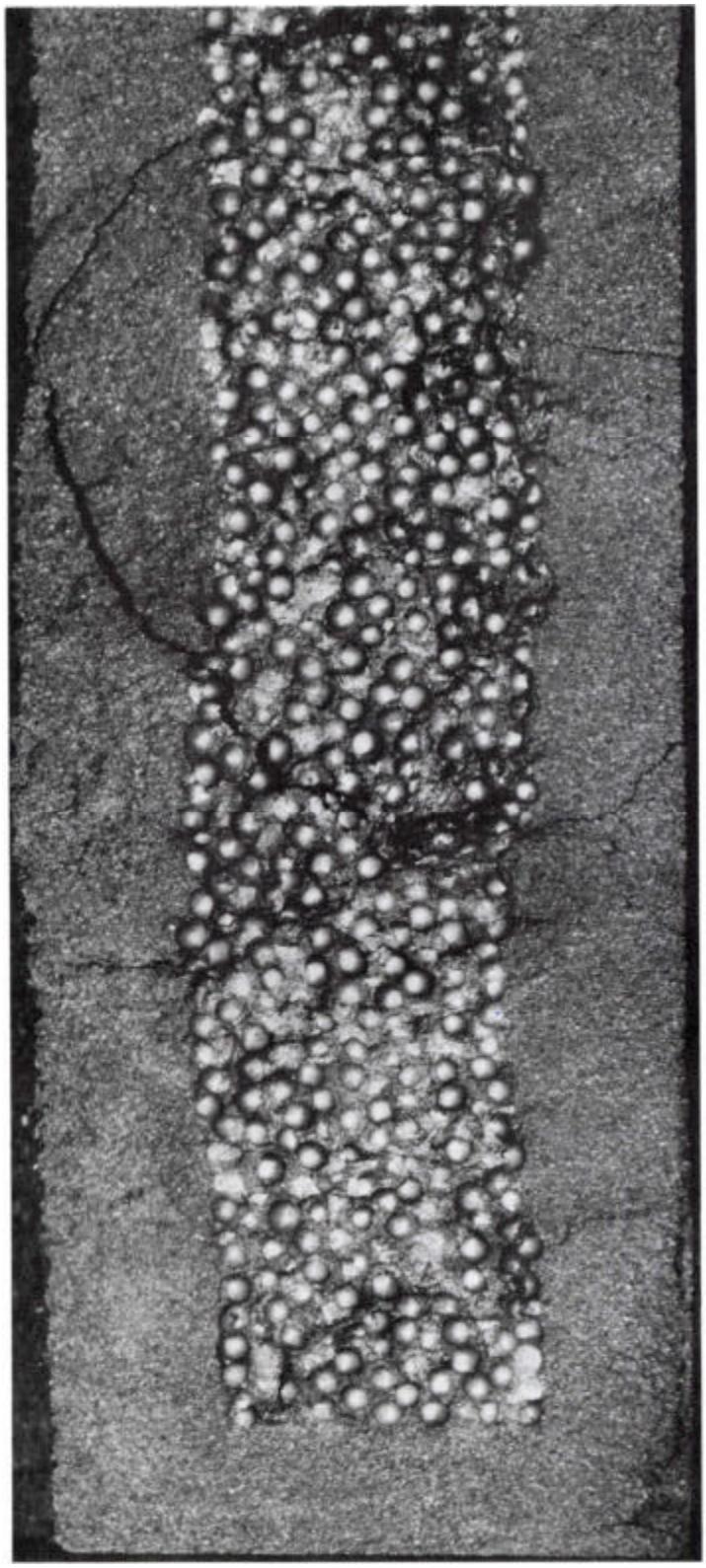

Figure 28: Fracture surface of irradiated compact after diametrical compression (Compact 2089)

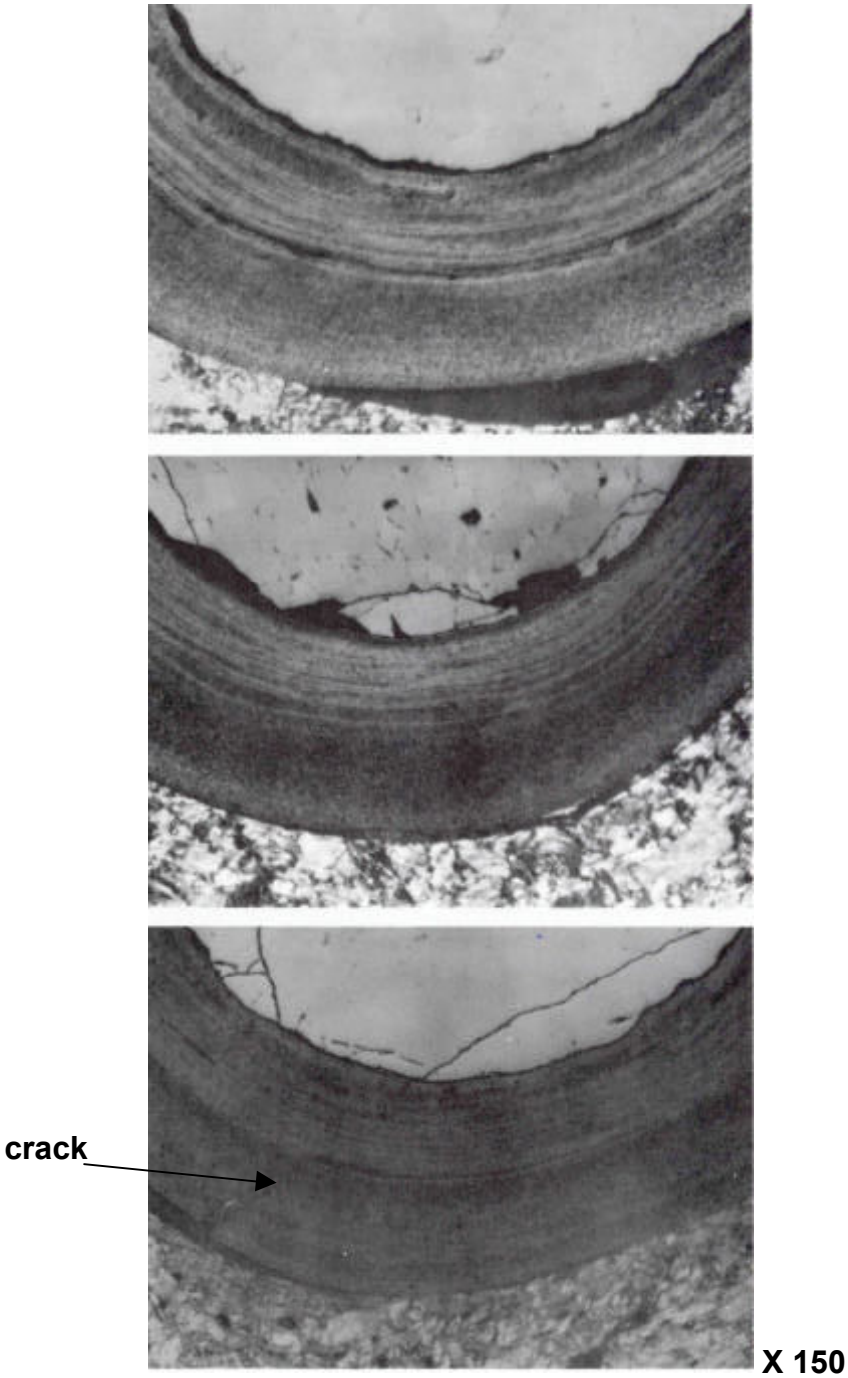

Figure 29: DR-S2 sections of irradiated particle coatings

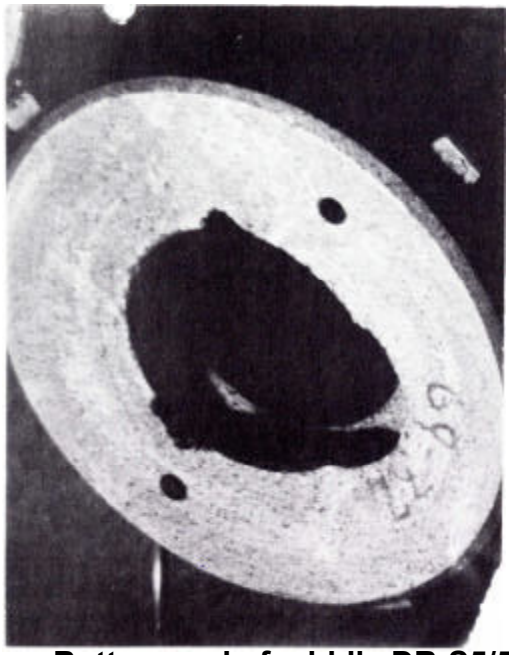

Bottom end of middle DR-S5/5, broken during unload

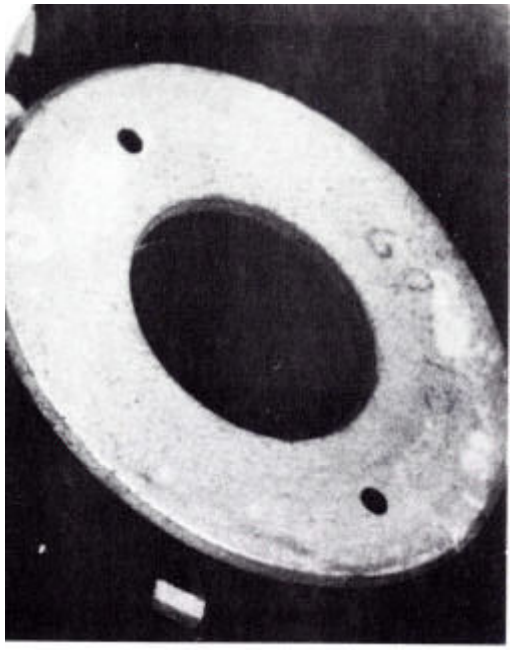

Bottom end top pin DR-S5/6

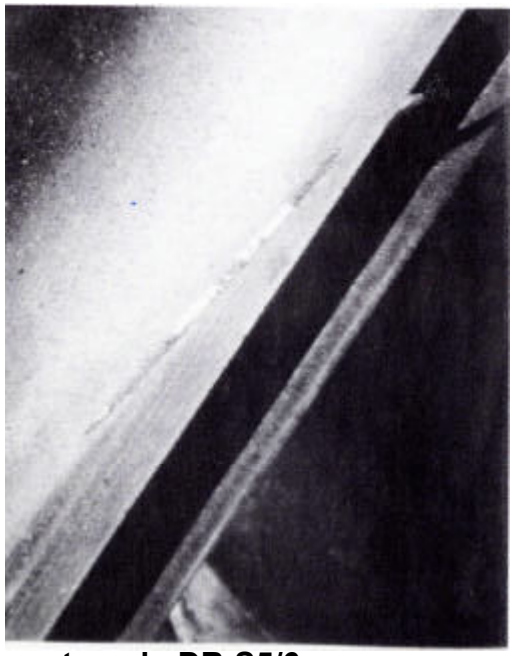

Thermocouple burn mark on top pin DR-S5/6

Figure 30: DR-S5 pins visual examination

General view of DR-S5

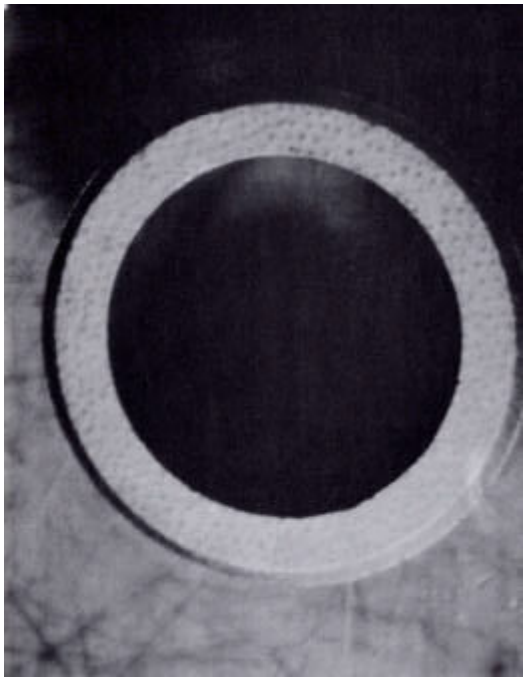

Top view of compact n°2229

Compact n°2229

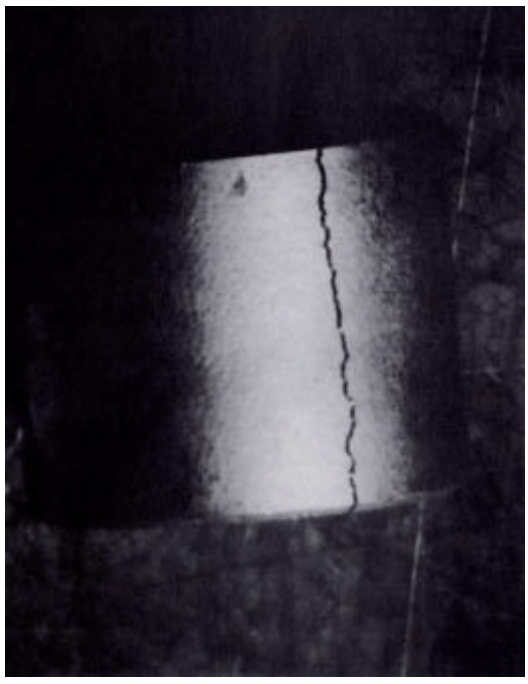

Compact n°2269

Figure 31: DR-S5 compacts visual examination after irradiation

Compact n°2210

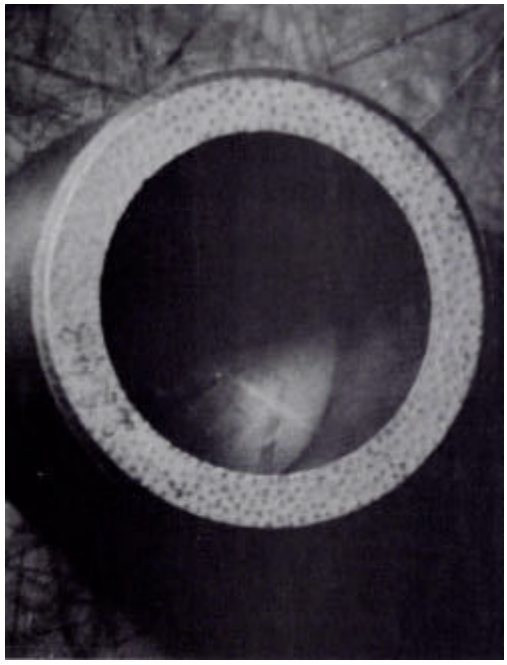

Compact n°2243 (bottom view)

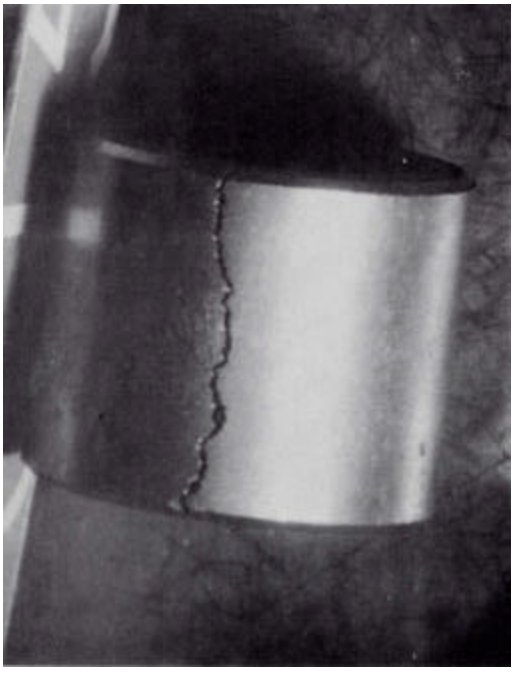

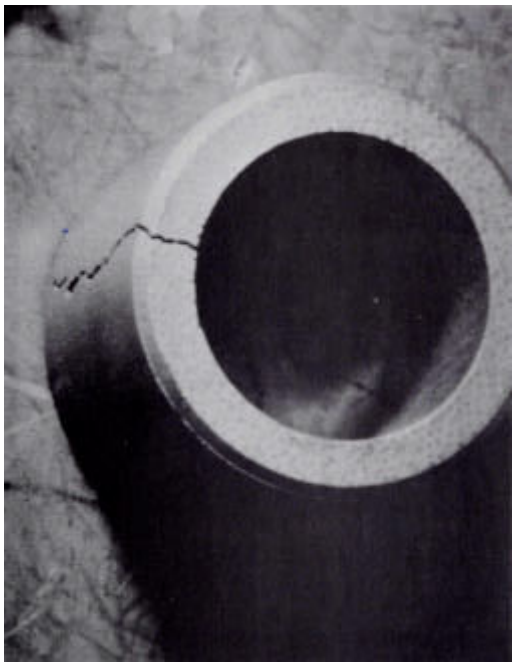

Compact n°2232

Figure 32: DR-S5 compacts visual examination after irradiation

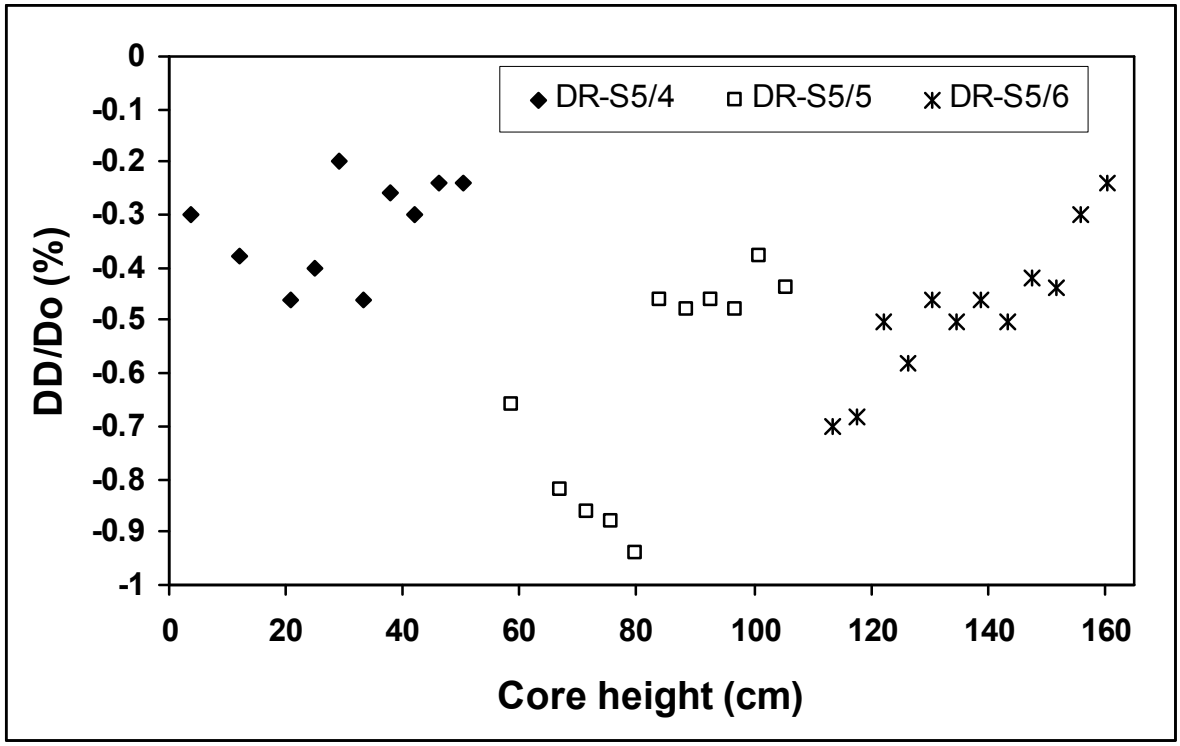

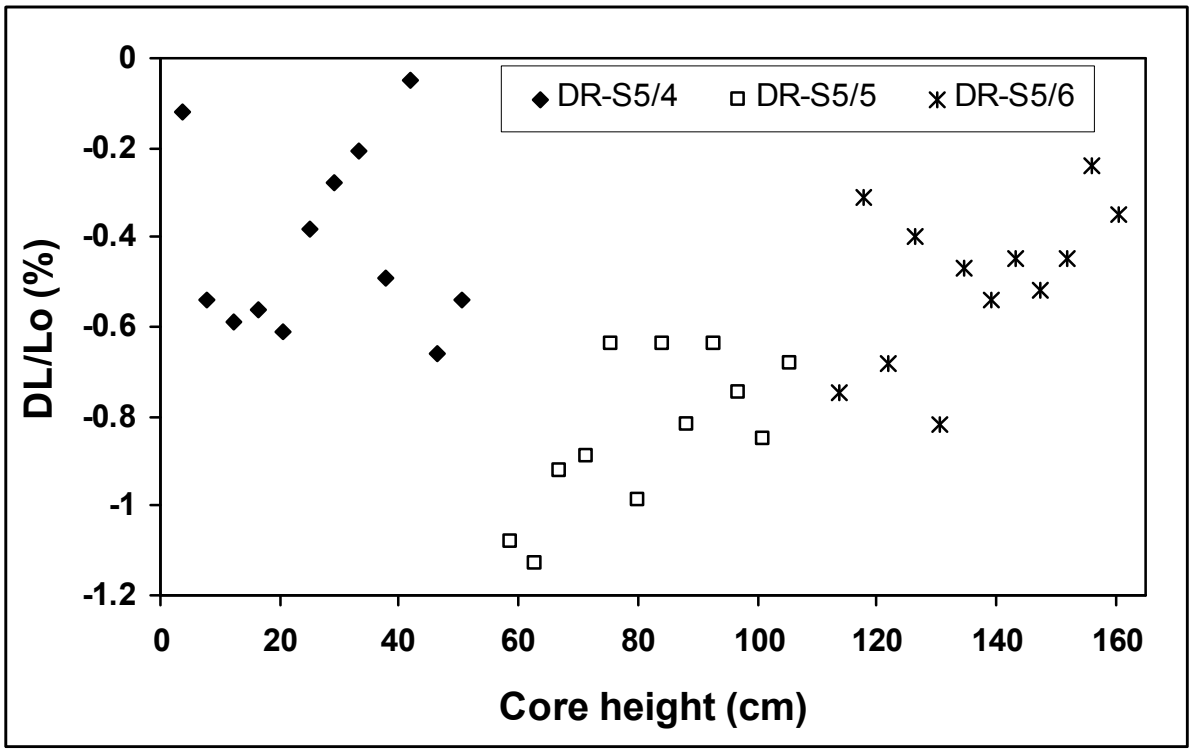

Figure 33: Irradiation induced dimensional changes of DR-S5 compacts

	Type of document:	Reference No / File - "Rev." - Page
	Technical Note	**0601019/220-"-"- 1**
		Other reference:

Client: EC	Author(s) G. TOURY
Project: Raphael IP – SP Fuel Technology WP-FT4 Performance Modelling	
Subject:	

HTR particles Irradiation Experiment BN database

FRJ2 Experiment

Rev.	Date	Chrono Filing No.	Status	Initials dactylo.	Author: Initials	Author: Visa 1	Verified by: Initials	Verified by: Visa 2	Approved by: Initials	Approved by: Visa 3	Q.A.: Initials	Q.A.: Visa 4	Issued by: Initials	Issued by: Visa 5	Number of pages
C															
B															
A															
-	17/05/06	0601019	Draft		GTY		SSH						GTY		76

Distribution:

RAPHAEL Project: Mr. OBRY (1 copy +1 CD)

BN: SSH, GTY

BELGONUCLEAIRE N.V.
Avenue Ariane, 4 - 1200 Brussels
TVA: BE 403.126.258
RCB: 271.300
TEL: 32-2774 05 11
FAX: 32-2-774 05 47

LIST of MODIFICATIONS		
DATE	**REVISION**	**OBJECT**
17/05/2006	-	Draft

NOTICE

PERSONNEL IN CONFIDENCE, NOT FOR PUBLICATION

This work is performed under the term and conditions of the Consortium Agreement of the RAPHAEL Project supported by the EC under contract n° 516508 (FI6O)

LIABILITY

This document was prepared by BELGONUCLEAIRE (BN). Neither BN, nor any person acting on behalf of BN:

a) gives any warranty, expressed or implied, with respect to the accuracy, completeness of the information contained in this document, or that the use of any information, apparatus, method or process disclosed in this document may not infringe third party rights, or

b) assumes any liabilities with respect to the use of, or for damage resulting from the use of any information, apparatus, method or process disclosed in this document.

	Type of document:	Reference No / File - "Rev." - Page
		0601019/220-"-"- 4
	Technical Note	Other reference:

Abstract:

Two types of plutonium oxide fuelled coated particles with carbon diluted 550 µm-kernels and dense 250 µm-kernels were irradiated for 45.4 full power days in FRJ 2 (Jülich) at about 1200°C. A burn up of about 18% FIMA and a fast dose of less than 10^{20} n/cm^2 DNE were accumulated. Postirradiation fission gas measurements have indicated that no particle was broken. The metallographic examinations have shown different behaviour of the inner pyrocarbon layers due to different plutonium migration into buffer layers during the coating process. Only small plutonium migration during irradiation could be found which has been stopped by the SiC layer.

Table of content

List of Tables

List of Figures

1. INTRODUCTION

Basically, the plutonium finds its best utilisation in the HTR's operating on the thorium cycle. In that cycle, the feed plutonium fuel will be subjected to a high burn-up and therefore will not be worth recovering. Since the aqueous reprocessing by the known techniques is complicated when plutonium is present, it is advantageous to separate the thorium breed particles from the plutonium feed particles so that the head-end of the reprocessing operation can mechanically screen the plutonium fuel to be discarded from the Th-U^{233} fuel to be recuperated.

In the HTR's working on the low enriched uranium cycle, it is also advantageous to segregate the plutonium particles from the uranium ones, in order to reduce the economic penalty inherent to handling plutonium. A further but minor advantage is to enable to recuperate only the fresh plutonium bred in the uranium particles from the depleted plutonium having essentially no commercial value due to its high burn-up and its isotopic degradation. The inconvenience in that cycle is to insure a proper distribution of the plutonium particles in order to reduce the technological peaking factor to acceptable levels. It is therefore not certain that in a low enriched uranium cycle the segregated fuel will be the best solution.

2. PREVIOUS BACKGROUND

Feed plutonium particles have been developed at Mol, partially under the sponsorship of the DRAGON Project, since 1964. The necessary voidage for the fission gases and the carbon monoxide expansion were provided mainly by the porosity of the kernel. Due to the high burn-up envisaged (600000 MWd/t_{Pu} corresponding to 65% FIMA) it was indeed necessary to dilute the fissile material in a support enabling to accumulate the voidage.

As in the driver fuel utilised in the DRAGON reactor, carbon was chosen as diluent. However, the attempts to manufacture a kernel consisting of a dispersion of a plutonium carbide in a carbon matrix, according to the concept retained by DRAGON at that time, had to be abandoned due to the high losses of fissile material experienced in the carbochemic reduction process.

The development was then focused towards a dispersion of oxide within the carbon matrix, based on the equilibrium of the two materials under a certain CO pressure, as had been developed in Mol earlier. This development lead to acceptable fuel which was irradiated in the R2 reactor at Studsvik Sweden, to extreme burn-ups of 200000 MWd/t and 360000 MWd/t at temperatures of 1850°C and 1200°C respectively.

Another test was carried out in the Second Charge of the DRAGON Reactor Experiment during the period, January 1967 to March 1968, when the central rods of the DRAGON fuel elements were constituted of plutonium fuel. The plutonium coated

particle fuel was placed loose inside a "telephone dial" arrangement of holes in graphite boxes. The number and size of holes were adjusted to give a constant fissile plutonium loading in each box using three batches of particles to deliberately vary the composition (Table 1). The average burn-up at the end of the irradiation (equivalent to 224 days at full power) was estimated to be 600000 MWd/t_M and the fast fluence $1x10^{21}$ n/cm^2 at 700 - 1100°C. The value of R/B for Xe^{85m} and Xe^{135} as measured via the helium purge for the two fuel elements, remained between 10^{-6} and 10^{-5}; these values indicated that there was no damage to the particles. Visual and ceramographic examinations of the particles after irradiation confirmed this.

3. PURPOSE OF THE FRJ2 EXPERIMENT

The good irradiation behaviour of the diluted kernels led to the desire of improving the utilisation of the plutonium fuel in a thorium cycle. In order to minimise the age factor, the plutonium should be concentrated. Therefore, it was decided to mount an irradiation to compare the behaviour of the following fuels:

- "diluted fuel" of the type tested earlier but with a kernel diameter of 550 microns (instead of 300) and the same carbon dilution. This already gives a higher plutonium self-shielding than the previous generation of particles;
- "undiluted fuel" consisting of particles containing the same amount of plutonium into the same shell but with all the fissile material concentrated in a small kernel of pure plutonium oxide. The voidage and the difference in dimension of the kernel are compensated by a thicker buffer layer to produce approximately the same internal voidage expressed as total void per gram of fissile plutonium.

This report describes in detail a comparative irradiation of those two types of particles.

The diluted fuel has been manufactured completely by BN-SCK/CEN; the undiluted kernels were manufactured according to a Sol-Gel technique by CCR - Karlsruhe and to the SNAM process by the CNEN (La Casaccia). All the coating work was performed by BN – SCK/CEN.

For sake of simplicity, the terminology utilised throughout the present report will be :

- "D" fuel, for the diluted fuel;
- "T" fuel, for the batch of Sol-Gel fuel;
- "C" fuel, for the batch of SNAM fuel.

Table 1 gives the main characteristics of the irradiated plutonium particles and of the irradiations in which they have been tested.

4. PREPARATION OF THE PLUTONIUM OXIDE KERNELS

The C and T kernels were made by Sol-Gel process, while the D kernels were elaborated by the powder agglomeration process. Both techniques are able to produce both types of kernels; the choice of techniques to be applied for each fuel specification was based on the following reasons:

- the small concentrated kernels of pure plutonium oxide (300 μm) are difficult to manufacture to a good shape specification by the powder agglomeration techniques;
- the diluted kernels are more fragile when fabricated by a Sol-Gel technique than by a powder agglomeration technique.

The isotopic composition of the plutonium batches utilised is given in Table 2.

The preparation of the different kernels can be summarised as follows:

4.1. CCR - KARLSRUHE SOL-GEL preparation (T fuel)

The process consisted of the following steps: precipitation of $Pu(OH)_4$ from a $Pu(NO_3)_4$ solution, by adding this solution to an ammonia solution; peptisation of the washed $Pu(OH)_4$ with HNO_3 at 85°C to form a plutonium sol approx. 1.5 M.
These operations have had to be carried out under severe control of pH. The sol was converted into droplets, which were gelled by dehydration in 2 ethylhexanol at room temperature.
This method for the production of microspheres was based on that developed at Oak Ridge National Laboratory which involves the water extraction of a sol low in nitrate with a long chain alcohol.
The gelled kernels were washed in a suitable organic medium, dried slowly, calcined 3 hours at 950°C, and finally reduced 4 hours in hydrogen at temperature between 1600 - 1720°C to get dense plutonium oxide kernels with an O/Pu < 2 (mixture of PuO_2 and Pu_2O_3).
One hundred grams of microspheres resulting from several batches have been produced for coating by this method. Under metallographic examination the kernels showed cracks (Figure 1).
The heating schedule of green particles and the properties of sintered kernels are given respectively in Tables 3 an 4 and the crystallographic density of the substoechiometric oxide was reported by CCR - Karlruhe as 10.9 g/cm³.

4.2. CNEN / SNAM SOL-GEL preparation (C fuel)

The 71 g PuO_2 particles were prepared at the Plutonium Laboratories of CNEN by a Sol-Gel process, which can be summarised by the following steps:

- Preparation of an oxide hydrosol solution :

by amine (Primene JMT) solvent extraction of nitric acid on freshly prepared Pu(IV) nitrate solution. 0.2 M solutions of $Pu(NO_3)_4$ were solvent extracted to get a NO_3/Pu

ratio ~ 1. The diluted sol was finally concentrated to 2 M by evaporation. This oxide hydrosol was mixed with tetrahydrofurfuryl-alcohol and a organic polymetric thickner.

- Conversion of the colloidal hydrosol into gel spherical particles :

Gelation was achieved by dripping the colloidal hydrosol into an ammonium hydrate solution and gelified spherical particles are washed with ammonium hydrate and deionized water. Green particles were then dried by azotropic distillation.
Organic material introduced in previous preparation steps was eliminated at this stage by firing at 450-500°C in air.

- High temperature treatment :

Firing of the gel product to the final high density oxide was carried out in furnace under an appropriate atmosphere (usually 4 v/o hydrogen in argon) according to a standard temperature cycle up to 1200°C.

Higher temperature and hydrogen concentrations could be used if an hypostoichiometric oxide was desired.

As the first coating was done at 1450°C, these microspheres would not have withstood the dropping in the coating furnace at 1450°C. Therefore a further heat treatment has been made up to 1450°C in carbon monoxide atmosphere at the plutonium facilities of the joint CEN - BN Plutonium Group in Mol (see Table 3). The heating rate was 20°C per hour while the cooling down rate was 150°C per hour.

4.3. Diluted kernel preparation (D fuel)

The procedure can be summarised as follows:

- the plutonium oxide powder was ground in a planetary mill in an agate pot, sieved (44 μm sieve), mixed with "united MT" carbon black ground again in a planetary mill and sieved (210 μm sieve);

- the mixture PUO_2/C was blended with furfurly alcohol [10 cm³/100 g ($Pu0_2$ + C)] in a hand mortar and then crumbed by passing it through a 297 μm aperture sieve

- the $Pu0_2$/C green crumbs were spheroidized in an aluminium pot rotated on a planetary mill and sieved (350 / 297 μm) and finally hardened by exposing them to formic acid vapour for 24 hours

The heat treatment is given in Table 3. A typical cross-section of the fuel is given in Figure 1.

5. COATING OF THE KERNEL

The coating of the three batches was based on a simplified "triso" concept PyC - SiC - PyC consisting of a porous pyrocarbon ("PyC") buffer layer, a dense inner PyC layer, a

SIC layer and a dense isotropic PyC. Only the thickness of the layers varied (Table 10) corresponding to the two different particle designs.

The coating furnace was a 40 mm diameter graphite resistance coater.

All the details of producing these layers are given in Table 5.

5.1. Porous PyC layer

The porosity should provide the voidage necessary for the fission products accommodation; the thickness chosen was determined according a free volume (voidage) of 2-3 % of the fuel kernel volume for each atomic percent burn-up.

This coating should also prevent mechanical stress resulting from the interaction between kernel and coating during irradiation.

Finally, to prevent damage of the structural layer by the fission product recoil, a buffer carbon layer of 2.82 mg/cm² was required.

Figure 2 gives, as a function of the buffer density, the minimum buffer thickness to fulfil this requirement. A 150% of this minimum thickness was used to avoid, for a non-perfectly spherical kernel, a too thin buffer in some direction and to compensate for the thickness dispersion within a batch; this type of coating was indeed produced within a few minutes in the coating apparatus.

In order to get the same voidage in the coated particles both for the diluted and undiluted fuels, it was necessary to raise the buffer thickness from 30 microns for the diluted to 160 microns for the undiluted fuel.

5.2. Dense inner PyC layer (sealing layer)

This coating is a vessel for the CO gas in equilibrium with the system oxide - carbon and a barrier for the diffusion of HCI gas produced during the pyrolysis of trimethychlorosilane (CH_3-Si-Cl_3) to form the SiC (next coating).

5.3. SiC layer

This coating is the diffusion barrier for the metallic fission products and is partially the pressure vessel.

In order to avoid excessive stresses due to differential thermal expansion during fabrication and initial irradiation, the SiC layer has further been surrounded by two flash layers (of a few μm) of porous PyC to compensate differential thermal expansion and prevent crack propagation.

5.4. HDI (High density Isotropic) PyC layer

This last layer is also part of the vessel of the fuel particle; it compresses the SiC layer during irradiation, by its fast dose induced shrinkage.

6. CHARACTERISATION OF THE COATED PARTICLES

Due to the small amount of material fabricated, a large scatter has been observed in the analytical results of the particles. They were deemed in most cases to be representative of sampling effects. In some circumstances however the difference between the results of the different samples could not be explained by a scatter in the properties of the product. For instance, the sintered "T" kernels were analysed both at Karlsruhe and Mol.
The results are presented in Table 4. It can be seen that the analytical data are consistently different. It might however indicate in this case an oxidation reaction of the kernels during the transport. Another example of the scatter in the data is given by the plutonium contents in Table 6.

The O/M ratio deduced from the relative intensity of two diffraction X-ray is characteristic respectively of the sesquioxide and the dioxide. The evolution apparent in Table 8 is probably realistic as a tendency. The scatter around this general tendency of each successive step is not representative of the average of the batch but due to the small sample size involved in the analytical technique.

The densities were measured both as bulk density and immersion density (Table 7). Here again a general tendency can be observed but the scatter of the individual values is not realistic. The layer density deduced from the particle density is obtained by difference and therefore not accurate.
For what the density of the SiC is concerned, it includes the two flash layers deposited in order to protect the coating from differential thermal expansion effects as mentioned in paragraph 5.3. The contamination of the particle was very low (Table 9) and has tended to decrease as the coating proceeds.

The coating thicknesses given in Table 10 are the results of cross-check between dimensional measurement and metallographic observations. Finally, Table 11 summarises the accuracy claimed for in various analytical results.

Figures 3, 4 and 5 show respectively metallographic sections of particles D, T and C after each coating step. For C type, a bulk plutonium diffusion has appeared after PyC deposition; this was also confirmed by the alpha autoradiography and polished section presented in Figure 6. In the T type, the plutonium migration was limited to plutonium concentration spots in the buffer layer; this was visible on the metallographic sections. Table 12 indicated the extent of the plutonium displacements, measured by X-radiography (Cf. Paragraph 8.6.) on 15 particles of each batch; by comparison with Table 10, it can be seen that the plutonium migration has proceeded to the dense inner PyC.

7. IRRADIATION

7.1. Irradiation capsule

The samples were irradiated as loose coated particles in 8 small graphite (material: Ringsdorf graphite type Kr 66) containers of 12 mm diameter which were deposited in a telephone dial type graphite (material : Ringsdorf graphite type Kr 60) cartridge of 74 mm diameter (Figure 7).
The graphite cartridge was inserted into a sealed stainless steel capsule which was enclosed in the irradiation rig JK 4 (Figure 8).
The rig was of LV-4 type normally used for irradiation of five spherical fuel elements of 6 cm diameter. In this case, the plutonium particle capsule was inserted instead of the lower fuel ball.
Three Ni/CrNi thermocouples had been put into small holes at the outer circumference of the cartridge. Another thermocouple was located at the outer stainless steel wall.

7.2. Capsule loading

Each of the 8 containers was filled with one of the three particle types.
Additionally, five individual radiographed particles of each batch had been filled into the center hole of containers 1. The particle quantities filled into the containers are given in Table 13 and Figure 7.

7.3. Irradiation conditions

The rig JK 4 has been irradiated in FRJ2 (DIDO) Jülich in position D1 for three reactor periods from January 27, 1970 till April 1st, 1970 The total irradiation time was 45.4 full power days at 15 W.

(1) Temperature.

The designed temperature profile is shown in Figure 9. However, the experimental temperatures remained about 150°C below the designed ones. Figure 10 shows the temperature history during the three reactor periods. The graphite temperatures were measured by three thermocouples; from this, the central temperature was calculated using the design temperature profile.

(2) Burn-up.

The axial profile of the perturbated thermal neutron flux in position D1 is given in Figure 11. The mean thermal flux in the plutonium particle - capsule was :

0.92×10^{14} cm^{-2} sec^{-1} during the first period

0.875×10^{14} cm^{-2} sec^{-1} during the second period

0.76×10^{14} cm^{-2} sec^{-1} during the third period

Using these flux values, the accumulated burn-up has been calculated. At the end of irradiation, the following burn-up values have been achieved:

Particle type	Burn-up (% FIMA)
D Fuel	17.0
T Fuel	18.7
C Fuel	18.3

(3) Particle rating.

The initial rating per coated particle has been calculated using the mean particle data given in Table 13 and the plutonium composition given in Table 2.

Particle type	Initial rating (W)
D Fuel	0.54
T Fuel	0.36
C Fuel	0.32

(4) Fast neutron dose.

The fast neutron flux (E > 1 MeV) monitored by nickel - wires in position D1 (-30 cm from core center), is about 1.35 x 10^{13} cm^{-2} sec^{-1}. From that, the accumulated fast neutron dose has been calculated to be about 5.3 x 10^{19} cm^{-2} (DIDO Nickel Dose).

8. POST-IRRADIATION EVALUATION

8.1. Fission gas release (KFA Jülich)

After extraction from the irradiation rig, the plutonium particle capsule was punctured in a vacuum chamber. A 100 cm^3 aliquot of the sucked gas was analysed by means of a germanium - detector. As a result of this, only Xe 133 was measurable. Calculated on the last irradiation day it has given a Xe^{133} quantity of 8.4x10^{11} atoms. Assuming that at the end of the last irradiation cycle equilibrium was reached between the release and the decay of Xe atoms, a R/B value was calculated for the last irradiation stage:

$$R/B = 4.2 \times 10^{-7}$$

8.2. Dismantling

After the puncture test the metallic capsule was cut at the base for cartridge extraction. One could notice black and white deposits on the inside of the metallic part and on the graphite.

8.3. Visual examination

Some difficulties have arisen with the unloading of the particles because they were stuck to each other and also on the wall of the graphite container. Apparently, this was due to a white coloured product deposited on the surface of the coated particles. Examination of the particles of the complete contents of capsules 1, 3, 4 using the hot - cell periscope, showed no cracks or other major structural damage.

8.4. Annealing test (in hot cell KFA Jülich)

Each type of particles has been heated up to 1350°C (containers 2, 5 and 8); a check has been made up to 1500°C (container 2). As a function of the long half-lives and the good condition of the particles, the measured release of Xe^{133} was very small and, in the case of container 5, practically not detectable. As no release of Kr^{85} was measurable, it can be assumed that the particles were not damaged.

The Table 14 gives the release rate of Xe^{133} in atoms/sec, after steady release had been reached. The figures refer to the date of the end of irradiation.

These results confirm that no particle was broken during irradiation.

8.5. Metallography

Microsections of each kind of irradiated particles were prepared first for one sample of each type of particles (containers 1, 3, 4) and then for the particles having been subjected to annealing test (2, 5 and 8).

The results can be summarised as follows:

(1) Container 1 (D particles) – No figure available

Apparently no change in the coating could be detected in spite of the high anisotropy of the sealing layer (see Figure 3). Even part or the sooty layers was still visible. Inside the kernel many cracks could be seen.

(2) Container 5 (D particles annealed at 1550°C) – No figure available

The same remarks as for container 1 are also valid as no major difference could be detected.

(3) Container 3 (T particles) - Figures 12 and 13

From the microsections, it appears that the kernel did not diffuse through the sooty layer to a markedly larger extent than what was due to fabrication. Quite an important delamination between the SiC and inner layers can be observed. The buffer layer is

cracked over the outer half of its thickness in approximately half of the particles. The segregation of metallic parts into the kernel is important (Figure 13).

(4) Container 8 (T particles after annealing at 1350°C) – Figure 14

The same general results as for container 3 are noticeable. Some particles show cracks, which have started from the kernel but were stopped at the SiC layer.

(5) Container 2, 4 and 7 (C particles) - Figure 15

The diffusion of the kernel into the porous layer resulting from the fabrication did not extend throughout the full layer. "Spearhead" attack is visible in the inner pyrocarbon coating whenever the plutonium is spread throughout all the buffer layer; it is not visible when the plutonium diffusion is limited to part of the buffer layer. The SiC and outer PyC layers remained in good condition.

(6) Container 2 (C particles after successive annealing at 1350°C and 1500°C) - Figure 16

No much difference could be found by comparison with container 4.

8.6. Investigations on marked particles

Marked particles which were introduced in the central hole of the sample container have been examined after fabrication and after irradiation.

The characterisation after fabrication consisted in X-radiography to indicate the plutonium location within the particle (cf.§6).

The postirradiation examination consisted in two different tests: an alpha-autoradiography of the coated particles, which indicates the evolution of the plutonium migration to be compared with the X-ray results and a polished section of these coated particles. These photographs are presented in Figures 17 to 23.

For the T particles (Figures 17 to 19), the plutonium migration to a few spots within the buffer layer during fabrication is emphasised by the X-ray examination. The alpha-autoradiography indicates that this preferential plutonium location has not changed during irradiation. However a densitometric analysis of the alpha-radiographies suggest a tendency to plutonium migration away from the spots. Outside the kernel, the α concentration for these particles varies between 5 and 15 % (particles 3-4-7). All these coated particles have an intact inner PyC layer and a partial discoupling of this layer from the SiC layer.

For the C particles, important plutonium diffusion is noticed in the buffer after fabrication. The alpha-autoradiography obtained for the C particle n° 6 shows a high plutonium penetration generalised in the buffer PyC coating. Its α-microdensimetry leads also to the same conclusion.

The destruction of the inner PyC coating is also noticed for particles n° 5, 9 and 13 (Figures 22 to 24). This damage of the inner PyC would be induced by the combined effect of shrinkage induced by fast neutron dose and spearhead attack induced by fission product recoil of the migrating plutonium. For particle n° 8 (Figure 20) the buffer

layer is completely discoupled from the inner PyC layer, which remained intact. Nevertheless, the plutonium migrated through the total thickness of the buffer.

For the D marked coated particle which was examined, one notices quite the same behaviour as for the D particles from container 1. The inner PyC layer remained intact and the dispersed kernel in a carbon matrix shrinked avoiding any mechanical interaction with the pressure vessel. Unfortunately, no X-ray has been done after fabrication on this type of fuel, but no plutonium migration has been noticed in the inner PyC layer by metallography and alpha-autoradiography.

8.7. Lattice parameters

The lattice parameters were measured by X-ray diffraction at CCR – Karlruhe. Table 15 gives the data obtained after irradiation. The lattice parameters of unirradiated PuO_2 and Pu (O,C) have been added for reference.

Within the sensitivity of the technique, no other structure than the fluorite one corresponding to PuO_2 was visible after irradiation. No attempt was made to correct for the presence of fission products dissolved in the lattice.

9. INTERPRETATION OF THE IRRADIATION RESULTS

9.1. Stress analysis

Considering the microphotographs of the concerned coated particles, it is possible to distinguish three different behaviours which are:

- Discoupling of the buffer layer from the inner PyC layer resulting in a pressure vessel constituted by the PyC/SiC/PyC layers;
- Discoupling of the inner PyC layer from the SiC layer resulting in a pressure vessel constituted by the inner PyC layer;
- Destruction of the inner PyC layer leaving a pressure vessel constituted by the SiC and the outer PyC layers.

These coated particle behaviours were differently distributed in the three batches. Table 16 based on the microphotographs gives for each of the three batches the number and the percentage of particles in regard of the above described behaviour type. For each behaviour type, a stress – strain analysis can be performed, giving the gas pressure evolution and the stress history in the layers constituting the pressure vessel.

The mathematical model COCONUT (Coating Computation for Nuclear Technology) developed by BN considers the irradiation effect on the mechanical properties of the coating, the PyC dimensional change induced by irradiation, the fuel swelling, the fission gas build-up and the CO produced. The calculations were performed using a time step procedure required by the use of an irradiation creep law for the PyC coating.

The CO pressure estimate versus temperature and stoechiometry was extrapolated for several plutonium oxides from free enthalpies data published by T.L. Markin and E.J. Metver (UKAEA – Harwell) [1] and L.M. Atlas and G.J. Sekelman (ANL) [2].

The variation of the fission gas release from the kernel has been considered as linear versus the burn-up. This release reaches 90 % for 18.0 % FIMA at 1200°C.

Since, some metallographies show adherence between the inner PyC and the SiC, the disconnecting effect of the PyC flash layers deposited between the inner PyC and the SiC and between the SiC and the outer PyC has not been considered in the mathematical analyses.

The gas pressure evolution, for the three coated particle behaviour types, is given in Figure 25 for a constant temperature of 1200°C. In the case where the pressure vessel is constituted by the inner PyC layer, the gas pressure is higher than in the other case where the void volume offered for the gas expansion is larger. For both cases, the gas pressure evolution is quite similar from one behaviour (PyC/SiC/PyC pressure vessel) to the other one (SiC/outer PyC pressure vessel), with a lower pressure for the last case according to the higher void volume induced by the inner PyC breakage.

For the neutron dose reached in this experiment, one remains in the region of volume shrinkage of the PyC (Figure 26). This shrinkage is anisotropic and occurs mainly following the "C axis" of the crystal (radial direction of the layer, Figure 27).

For the plain PyC pressure vessel, a compression of this layer is induced (at start of life) by its dimensional change under irradiation (Figure 28), this layer remaining attached to the buffer layer. At 0.3×10^{20} cm^{-2} DNE, the fuel swelling influences the stress level in this layer and thus the hoop stresses increase, being moderated by the PyC irradiation creep.

The hoop stress evolutions in both other cases (SiC/outer PyC and PyC/SiC/PyC pressure vessel) are quite similar for the SiC and outer PyC layers (Figures 29 and 30). On one hand, a decompression of the SiC layer results from the gas pressure build-up and the outer PyC dimensional change under irradiation; on the other hand, for the fast neutron dose reached, the outer PyC dimensional change under irradiation induced a reduction of the hoop stresses in the outer PyC layer which remains in contact with the SiC layer.

In the case where the inner PyC is the inner part of the pressure vessel, the irradiation dimensional change and the gas pressure induce an increase of the hoop stresses. The stresses in all the PyC layers are reduced by the PyC irradiation creep.

9.2. CO pressure evolution

The CO pressure evolution has been calculated for the particles having the highest O/Pu ratio at start of life, and burn-up e.g. for the particles type T.
The input data are given in Table 17
The CO pressure evolution as a function of burn-up is given in Figure 31.

9.3. PyC resistance to fission products bombardment

The damage to the PyC layers is not visible in the D particles and evident in the C particles.
On the basis of the evaluated plutonium concentration profiles, the damage to the non-fuelled inner coating can be calculated and related to an equivalent fast neutron dose. Table 18 gives the results of these calculations. It can be seen that the porous PyC is resistant to irradiation damage while the anisotropic inner PyC shows spearhead attack at a threshold somewhat lower than reported in the literature; mention is indeed made that the phenomenon starts between 2×10^{16} and 2×10^{17} FP/cm².

10. CONCLUSIONS

For the considered coated particle design and manufacture, the following remarks can be pointed out :

10.1. Plutonium displacement

10.1.1. Pu displacement before irradiation

An important plutonium migration occurred during the first two stages of coating for the dense kernels which led in one batch to a inner kernel relatively similar to the diluted kernel: i.e. the large buffer layer was completely impregnated with plutonium.

10.1.2. Pu displacement after irradiation

The migration of plutonium during irradiation continues but is rather small compared with the diffusion during coating: i.e. a maximum migration value of 20 μm for the T type has been found from X-rays and alpha-autoradiography micrographies of the irradiated kernels. The plutonium migration has been stopped by the SiC layer; this conclusion had to take account of the rather short irradiation time.

10.2. Irradiation damage

In the limit of the relatively low value of burn-up, no broken or cracked particle has been detected in the three batches. The extremely good behaviour of D fuel has already been proved in earlier irradiations and in this case even the anisotropic inner dense pyrolytic carbon layer (sealing layer) remains intact.

REFERENCES

[1] T. L. MARKIN, E.J. Mc IVER
Proc. 3rd Int. Conf. On Plutonium, London, 1965

[2] L.M. ATLAS, G.J. SCKELMAN
Thermodynamics II, IAEA, Vienna (1966) 407

Type of fuel	**Diluted**						**Undiluted**	
Batch	**P 352**	**P 353**	**P 372**	**P 373**	**P382**	**P 383 "D"**	**THP 311 "T"**	**THP 321 "C"**
Coated particle data :								
Diameter (μm)	700	600	600	700	800	890	790	850
Maximum HML(g Pu/cr	0.04	0.07	0.10	0.09	0.26	0.22	0.20	0.04
g Pu/cm³ CP	0.06	0.11	0.15	0.13	0.40	0.33	0.30	0.21
g Pu/cm³ kernel x μm diameter (self-shielding factor)	250	250	340	340	700	800	2300* (1400)	2200* (410)
Peak irradiation data :								
Temperature (°C)	1450	1850	1200			1300		
Burn-up (GWd/t)	360	200	600			200		
R/B for Xe 133	5.10^{-6}	10^{-2}	7.10^{-6}			4.10^{-7}		
Sponsored by :	BELGONUCLEAIRE CEN •SCK DRAGON Project					BELGONUCLEAIRE CEN •SCK KFA Jülich		

* Theoretical values (actual values resulting from Pu diffusion.

Table 1: Types of plutonium particles

Specimen	Batch n°	Isotopes of Pu in w/o				Activity Curies/g
		239	240	241	242	
D	P 3/8/1 (Pu 019)	79.4	17.1	3.05	0.4	3.6
T	THP 3/1/1 D	91.44	7.9	0.67	0.03	1.9
C	THP 3/2/1 D (Pu 020)	88.3	10.3	1.3	0.09	1.55

Table 2: Isotopic analysis and activities of Pu used for preparing the CP fuel

Batch n°	Temperature interval °C	Heating rate °C/h	Atmosphere
D (P 2/8/-)	20 - 200	200	CO
	200 - 1000	533	CO
	1000 - 1400	200	CO
	1400	0 (2h)*	CO
T (THP 2/1)	950	0 (3h)*	Air
	1600 - 1700	0 (4h) *	H_2
C (THP 2/2)	20 -		Air dried
	20 - 900	200	A - H2
	900 - 1450	200	CO
	1450 - 1000	- 150	CO

* ( ) : time at temperature.

Table 3: Heat treatment of green kernels

Batch n°	Hg Density g/cm³	Porosity %	Pu/C Ratio	O/M			Size (μm)		w/o Pu
				Chem.	X - ray		Sieve Range	Average	
					$\frac{I\ Pu_2O_3\ (222)}{I\ PuO_2\ (111)}$	O/M			
D (P 2/8) (b)	2.75	31	1 : 19.5	n.d.	0.23	1.9	450 - 572	500	47.6
T (THP 2/1) (a)	10.5	3.7	-	1.77	n.r.	1.75	227 - 331	280	89.5
(b)	10.2	8	-	1.90	0.25	1.9	254 - 312	270	88.73
C (THP 2/2) (b)	9.8	10	-	1.745	1.0	1.7	216 - 292	260	89.54

(a) Data received from CCR - Karsruhe
(b) Analytical data obtained at Mol

Table 4: Properties of sintered kernels

Fuel		Coating			Gas flows							
Type	**Identi-fication**	**Tempe-rature °C**	**Layer Type**	**Time (min)**	**Total (l/min)**	**C_2H_2 %**	**CH_4 %**	**H_2 %**	**CO Total**	**A %**	**% H_2 via Silane**	**Silane %**
D	P 3/8/1	1450	Soft PyC	8	4.325	23.1			76.9			
		1550	D PyC	80	4.125		17	32.7	50.3			
		1450	Flash	2	4.325	23.1				76.9		
		1450	SiC	62	5.646			35.4		21.7	35.4	
	P 3/8./2	1450	Flash	2	4.600	21.8				78.2		
		1800 2000	PyC HDI	8	4.100		12			88		7.5*
		2000	HD PyC	90	4.100		12			88		
	P 3/8/3	2000	HD PyC	120	4.100		12			88		

* Evaluation

Table 5: Coating conditions

Fuel		Coating			Gas flows							
Type	**Identi-fication**	**Tempe-rature °C**	**Layer Type**	**Time (min)**	**Total (l/min)**	**C_2H_2 %**	**CH_4 %**	**H_2 %**	**CO Total**	**A %**	**% H_2 via Silane**	**Silane %**
T	THP3/1/1A	1480	Porous	40	4620	50	-	-	50	-	-	8.3*
	THP3/1/1B	1550	D	80	4125	-	17	32.7	50.3	-	-	
	THP3/1/1C	1450	Flash	2	4625	28.1	-	-	-	71.9	-	
		1450	SiC	62	5699	-	-	35.1	-	21.5	5.1	
	THP3//1D	1450	Flash									
		1800 -2000	HDI	8	4.1	-	12.2	-	-	87.8	-	
		2000	HDI	210	4.1	-	12.2	-	-	87.8	-	

* Evaluation

Table 5: Coating conditions (continued)

Fuel		Coating			Gas flows							
Type	**Identi-fication**	**Tempe-rature °C**	**Layer Type**	**Time (min)**	**Total (l/min)**	**C_2H_2 %**	**CH_4 %**	**H_2 %**	**CO Total**	**A %**	**% H_2 via Silane**	**Silane %**
C	THP3/2/1A	1530	Porous	34	4.620	50.0	-	-	50.0	-	-	7.7*
	THP3/2/1B	1550	D	80	4.125	-	17	32.7	50.3	-	-	
	THP3/2/1C	1450	Flash	2	4.625	28.1	-	-	-	71.9	-	
		1450	SiC	62	5.759	-	-	35.3	-	21.7	35.3	
	THP3/2/1D	1450	Flash	2	4.9	25.5	-	-	-	73.5	-	
		1800 -2000	HDI	8	4.1	-	12.2	-	-	87.8	-	
		2000	HDI	210	4.1	-	12.2	-	-	87.8	-	

* Evaluation

Table 5: Coating conditions (continued)

Fuel		Plutonium calculated from the chemical analysis of the sintered particles				Pu content (w/o Pu) by analysis after coating		
						Chemical	Gamma-spectrometry	
Type	**Identifi-cation**	**In**	**Out**	**Pu Content in g**	**% Pu calcu-lated**		**Average**	**Standard Deviation % relative**
D	P 2/8/-	50	-	23.8	-	47.6	-	
	P 3/8/1	50	116.17	23.8	20.48	-	-	
	P 3/8/2	116	138.8	23.76	17.12	17.74	-	
	P 3/8/3	121.4	144.5	20.78	14.38	14.97	-	
T	THP2/1	50	-	44.365	-	88.73		
	THP3/1/1A	50	102.09	44.365	43.45		42.0	4.0
	THP3/1/1B	57.007	72.67	24.78	34.10		36.0	10.5
	THP3/1/1C	68.082	106.047	23.30	21.97		20.7	10.5
	THP3/1/1D	101.242	148.16	22.24	15.01	13.83	13.8	10.4
C	THP2/2	50	-	44.77	-	89.54		
	THP3/2/1A	50	127.233	44.77	35.18		30.2	4.2
	THP3/2/1B	57.052	70.273	20.07	28.16		-	-
	THP3/2/1C	66.927	108.09	19.11	17.68		14.3	11.9
	THP3/2/1D	100.7	148.68	17.80	11.97	9.9	9.94	11.6

Table 6: Plutonium content

Type	Identification	Bulk density		Particles density	Layer density
		g/cm³	% part. dens.	g/cm³	
D	P 2/8*	1.7	63	2.75	-
	P 3/8/2	1.5	66	2.3	n.d.
	P 3/8/3	1.3	59	2.2	2.0
T	THP2/1*	6	61	10.2	-
	THP3/1/1A	1.3	57	2.2	~ 1 (estim)
	THP3/1/1B	1.2	59	2.1	1.7
	THP3/1/1C	1.3	59	2.3	2.8 *
	THP3/1/1D	1.3	59	2.1	1.9
C	THP2/2*	7	71	9.8	-
	THP3/2/1A	1.1	61	1.85	~ 1 (estim)
	THP3/2/1B	1.1	64	1.8	1.6
	THP3/2/1C	1.3	61	2.1	2.9*
	THP3/2/1D	1.3	64	2.1	2.0

* Including the flash PyC layers.

Table 7: Densities of sintered and coated particles

Type	Identification	Chemical form of plutonium		$\frac{I\ Pu_2O_3\ (222)}{I\ PuO_2\ (111)}$	O/M
		Mean	Secondary		
D	Before coating	PuO_2	$\alpha\ Pu_2O_3$	0.23	1.9
	P 3/8/3	$\alpha\ Pu_2O_3$	PuO_2	1.3	1.75
T	Before coating	$Pu0_2$	$\alpha\ Pu_2O_3$	0.25	1.9
	THP3/1/1A	$\alpha\ Pu_2O_3$	PuO_2	2.3	1.6
	THP3/1/1B	$\alpha\ Pu_2O_3$	PuO_2	3.7	1.6
	THP3/1/1C	$\alpha\ Pu_2O_3$	PuO_2	2.4	1.6
	THP3/1/1D	$\alpha\ Pu_2O_3$	PuO_2	2.5	1.6
C	Before coating	PuO_2	$\alpha\ Pu_2O_3$	1.0	1.7
	THP3/2/1A	$\alpha\ PuO_{23}$	PuO_2	2.0	1.6
	THP3/2/1B	PuO_2	$\alpha\ Pu_2O_3$	0.6	1.8
	THP3/2/1C	PuO_2	$\alpha\ Pu_2O_3$	0.7	1.8
	THP3/2/1D	PuO_2	$\alpha\ Pu_2O_3$	0.8	1.75

Table 8: X-ray analysis of coated particles

Type	Identification	dis/s g *	FVC *
D	P383	670	3.4×10^{-8}
T	THP3/1/1A	123.000	1.5×10^{-5}
	THP3/1/1B	27500	3.3×10^{-6}
	THP3/1/1C	350	4×10^{-8}
	THP3/1/1D	4230	5×10^{-7}
C	THP3/2/1A	39700	7×10^{-6}
	THP3/2/1B	24300	4×10^{-6}
	THP3/2/1C	1200	2.0×10^{-7}
	THP3/2/1D	46980	8×10^{-6}

* dis/s g = disintegrations per second and per gram of particles.

FVC = Fraction of Visible core = ratio of alpha-count of the particle to alpha-counts of the fissile material included in the kernel.

Table 9: External alpha-contamination of coated particles

Type	Identification	Kernel diameter µm	Layer type	Layer thickness µm	Cumulative coated thickness µm	CP diameter µm
D	P 3/8/1	550 +22 -27-	Porous PyC	21	21	(590)
			Dense PyC	45 ± 5	66	(680)
			SiC	41 ± 4	107	(760)
	P 3/8/2		HD PyC	28 ± 10	135	(800)
	P 3/8/3		HD PyC	34 ± 10	169	888
T	THP3/1/1A	267 + 48 - 31	Porous	145 +20 -14	145	(560)
	THP3/1/1B		Dense PyC	31 ±1	176	(620)
	THP3/1/1C		SiC	32 +2 - 3	208	(680)
	THP3/1/1D		HDI	52 + 4 -7	260	787
C	THP3/2/1A	248 + 40 - 23	Porous	187 +30 -20	187	(620)
	THP3/2/1B		Dense PyC	29 ±2	216	(680)
	THP3/2/1C		SiC	32 ±2	248	(740)
	THP3/2/1D		HDI	53 ±5	301	850

Table 10: Kernel and coating dimensions

Analysis	Method	Accuracy In % relative
Hg density	Hg/vacuum	± 0.5
Bulk density	Weight of particles in know volume	± 5
Layer density	Computed from weight and volume gains	High density ± 5 Low density ± 20
Pu/C	Chemical calcinations	± 0.5
O/M	Gravimetric	± 0.5
$\frac{(Pu_2O_3)}{(PuO_2)}$	Ratio of the intensity of the 2.2.2. Pu_20_3 line and the intensity of the 1.1.1. $Pu0_2$ line	Indicative values
Particles sizes	X-ray photograph of Ni coated particles	± 4
Pu	Chemical calcination - dissolution - titration gamma-scanning	± 1
Alpha counting		± 10

Table 11: Accuracies of the different analysis

Transfer container Number	Particle		Kernel Before coating	After coating		After irradiation	
	N°	Type		Kernel	Diffusion zone	Kernel	Diffusion zone
1	3	T	267µm +48 -31	270	570	270	550
2	4			246	460	260	500
3	7			250	460	250	500
	8	C	248µm +40 -23	600	600	n.d.	
4	6			550	550	550	550
5	5			630	630	n.d.	
6	9			540	540	n.d.	
7	13			500	500	n.d.	
8	14	D	550µm +22 -27	n.d.			475
9				Wasted before examination			

Table 12: Outer diameter of the plutonium zone (µm)

	Pu particle type		
	D	**T**	**C**
Middle diameter in μm	888	787	850
Density of ended coated particle	2.23	2.14	2.08
Bulk density	1.3	1.26	1.33
% plutonium content (chemical)	14.97	13.83	9.9
Total plutonium content in one hole (1350°) (calculated with the various isotopic composition)	0.06633	0.0600	0.062 - 0.063
Volume 1 particle : x 10^{-4} cm³	3.69121	2.53284	3.21555
Weight of 1 particle : g x 10^{-3}	0.82314	0.54203	0.66883
Weight of plutonium in 1 particle : g x 10^{-3}	0.12322	0.074963	0.066214
Number of particles in one hole	538	800	936
Weight of coated particles in one hole in g	0.4430861	0.433839	0.6262626
Bulk volume of these particles in cm³	0.576	0.547	0.833

Table 13: Specifications of each batch for capsule loading

Container	Number of Particles	Particles Type	Temperature (°C)	R (Xe 133) (atom/sec)	Fraction Release R/B
2	930	C	1350 1500	3.0 x 107 1.1 x 107	8×10^{-5} 2.9×10^{-5}
5	540	D	1350	Less than background	-
8	800	T	1350	2.2×10^{7}	6×10^{-5}

Table 14: Annealing test results

Particles types	Unirradiated		After irradiation	
	Kernel	CP	Mean	Standard Deviation
Analytical data				
D	-	-	5.394	0.018
T	5.400	-	5.442	0.006
C	5.396	5.398	5.381	0.100
Theoretical values				
PuO_2	5.396			
$PuC_{0.2}O_{0.8}$	4.96			

Table 15: Lattice parameters (Å)

Type	Batch n°	Pressure vessel type					
		Inner PyC		SiC / outer PyC		PyC / SiC / PyC	
		Nb of particles	%	Nb of particles	%	Nb of particles	%
D	P 3/8/3	0	0	0	0	17	100
T	THP 3/1/1	15	33	24	52	7	15
C	THP 3/2/1	5	17	23	76	2	7

Table 16: Behaviour distribution versus discoupling mechanism

% FIMA	Irradiation Temperature	O/Pu ratio*
0	1200	1.9
4	1140	1.922
8	1080	1.945
12	1050	1.967
16	1010	1.99
19	1000	2.007

* The O/Pu evolution as a function of burn-up is taken from [18].

Table 17: Input data for the calculation of the CO pressure evolution

Particle type	D	T	C
Bombarded unfuelled coating	Porous PyC	Porous PyC	Inner PyC
FP / cm^2	$3.8x10^{16}$	$1.8x10^{17}$	$1.6x10^{16}$
$n.cm^{-2}$ DNE	$1.52x10^{21}$	$7.2x10^{21}$	$0.96x10^{21}$

Table 18: Fission product bombardment of the coating layers

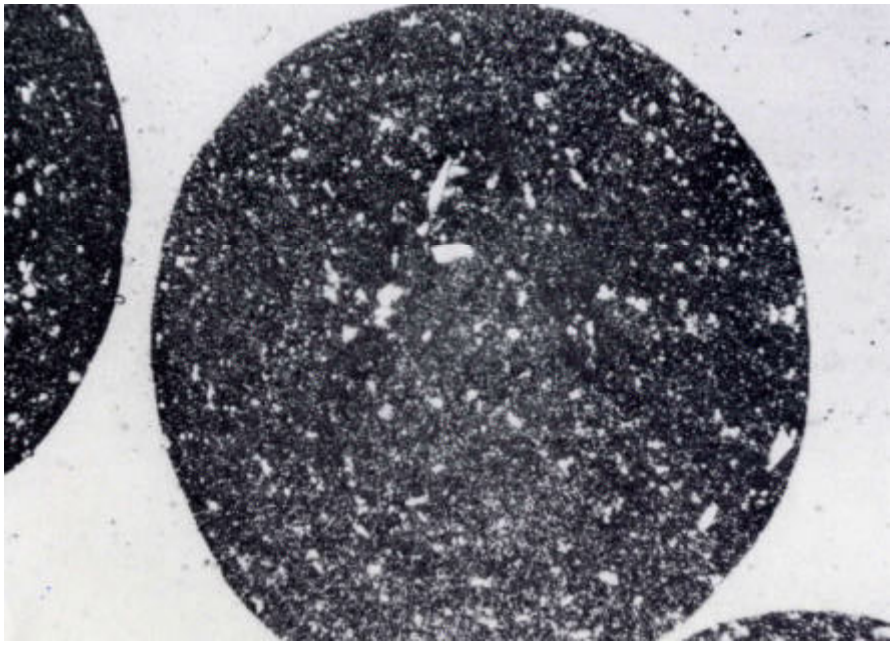

D Fuel X180

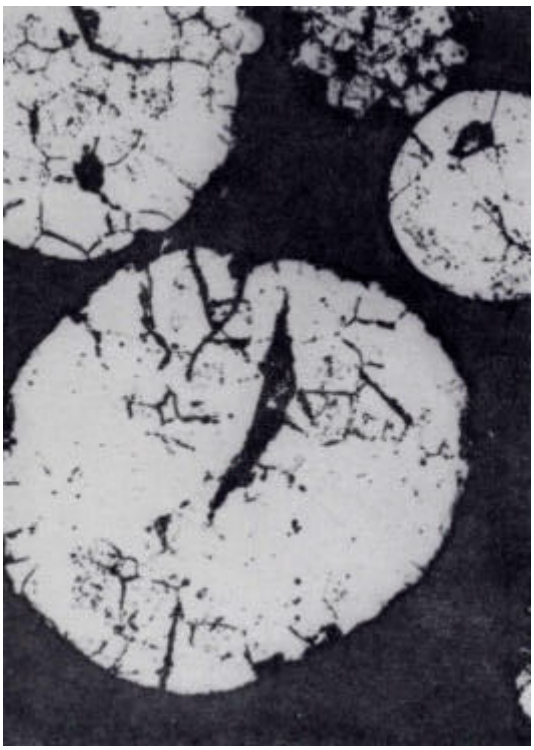

X180

T Fuel

Figure 1: Metallographic sections of undiluted and diluted Pu kernels

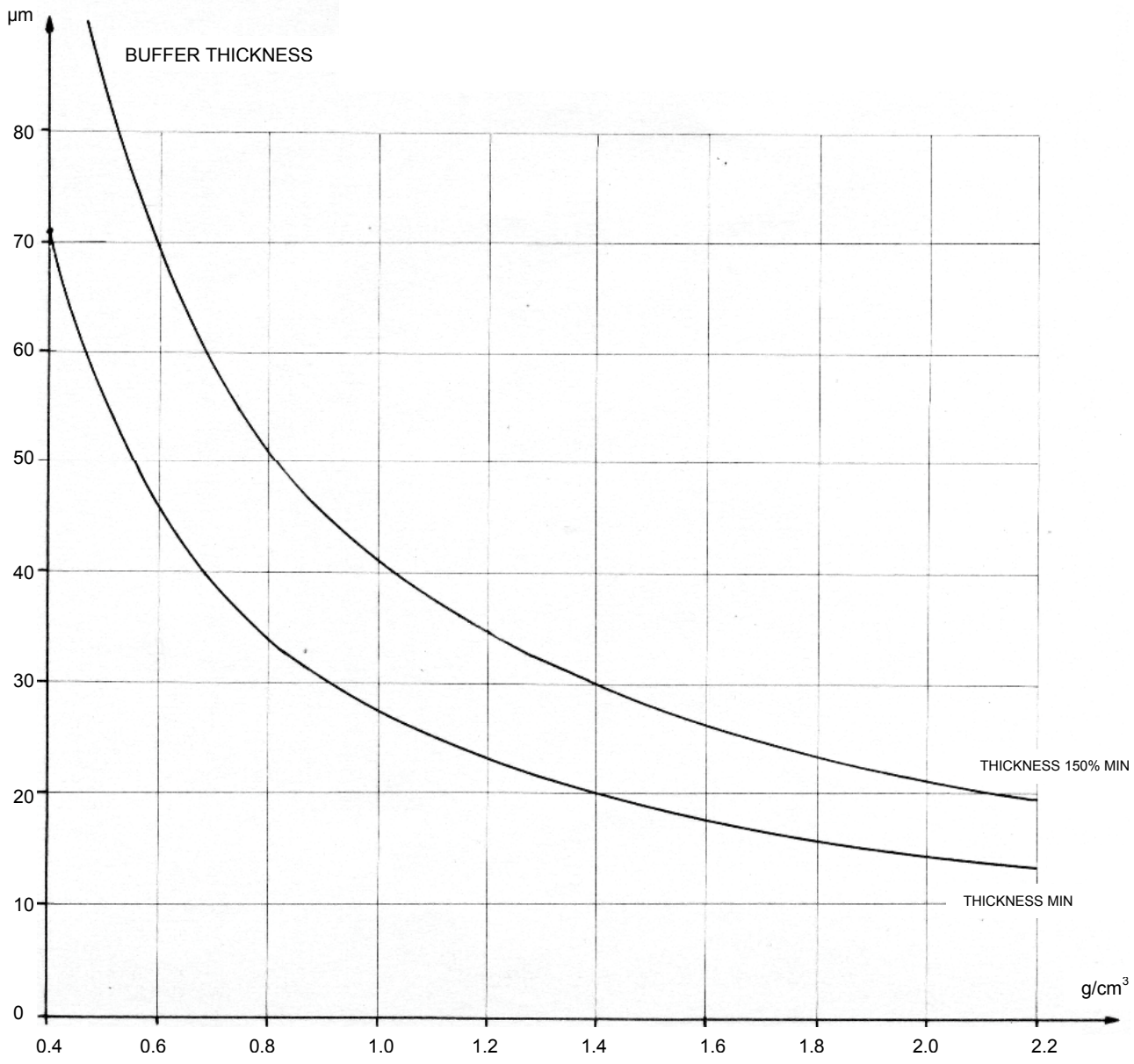

Figure 2: Buffer thickness required to attenuate fission recoils versus buffer density

X80

Figure 3: Cross section of the D particles

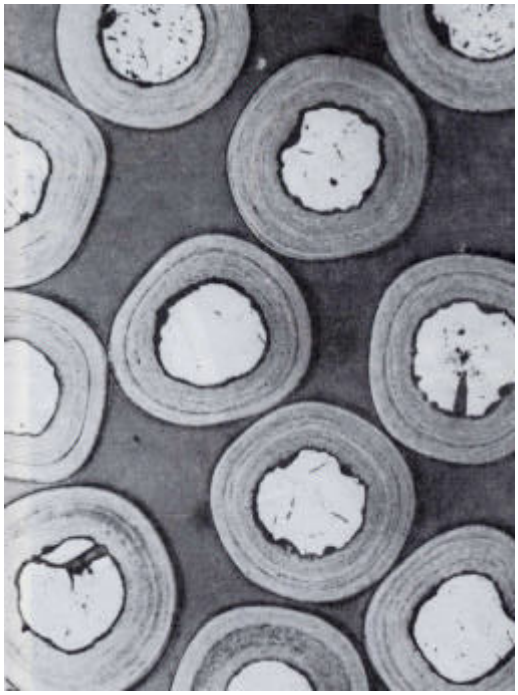

X50

THP 311A

THP 311B

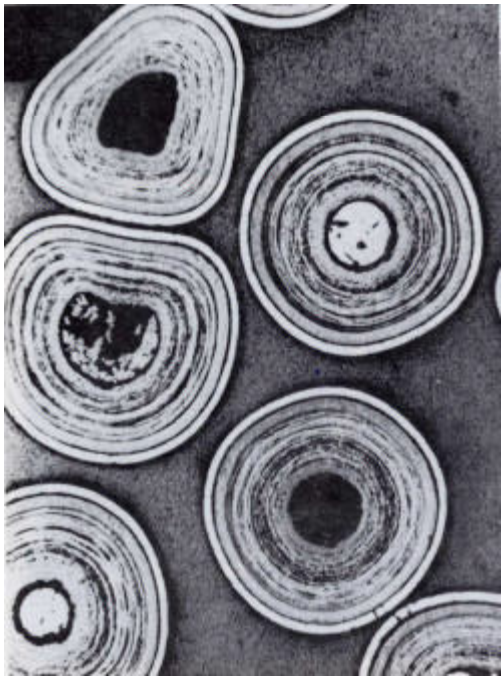

X50

THP 311C

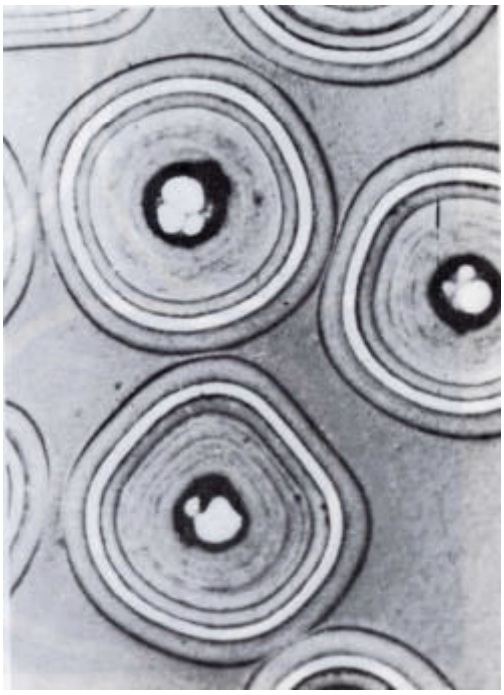

THP 311D

Figure 4: Cross sections of T particles after each coating steps

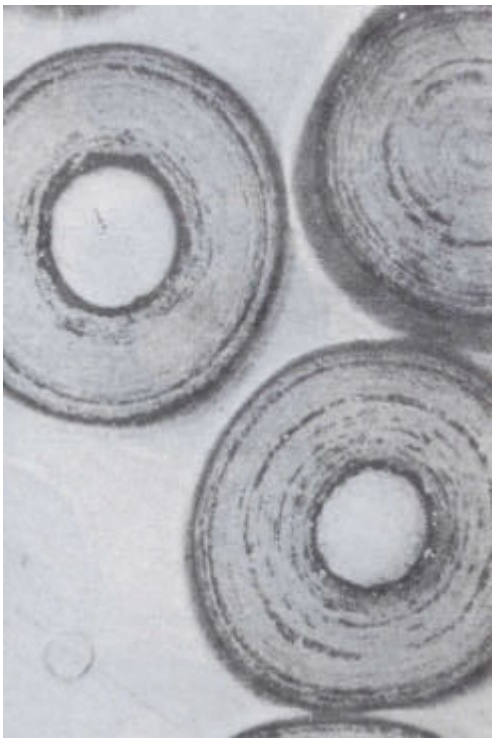

THP 321A

X80

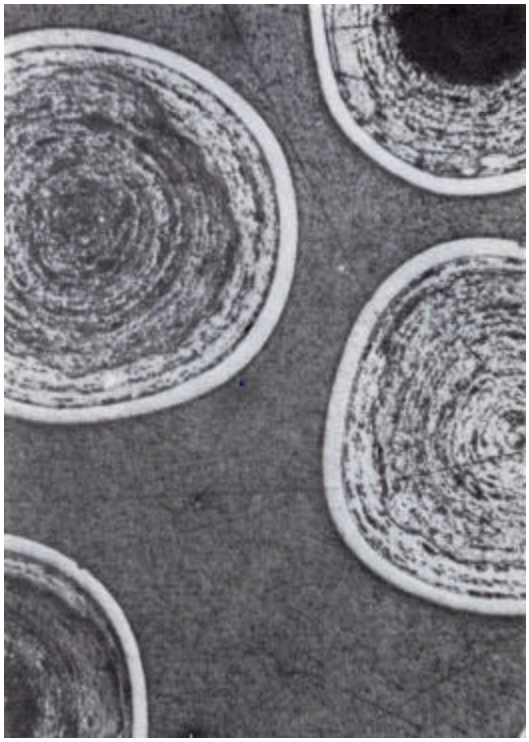

THP 321B

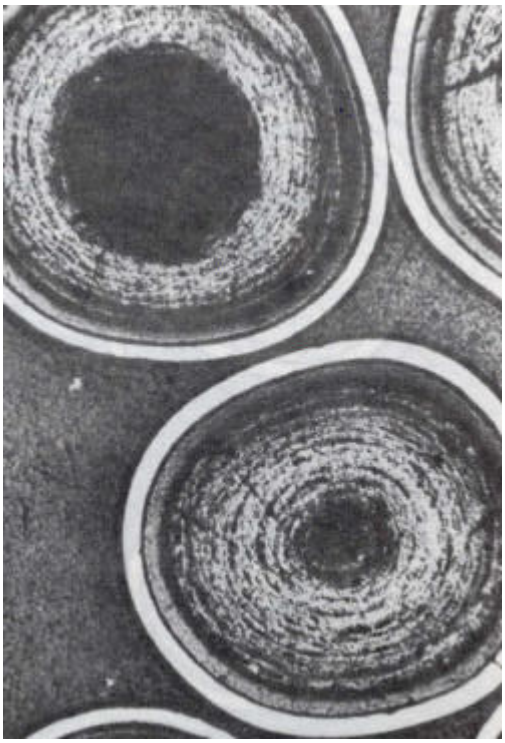

THP 321C

X80

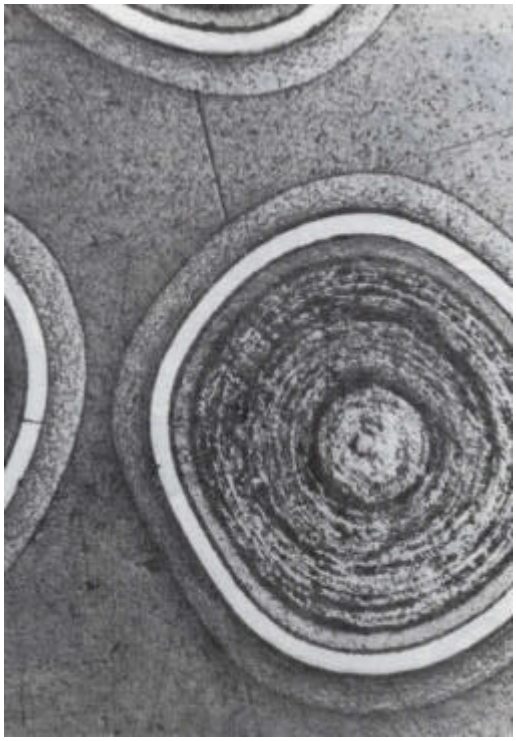

THP 321D

Figure 5: Cross sections of C particles after each coating steps

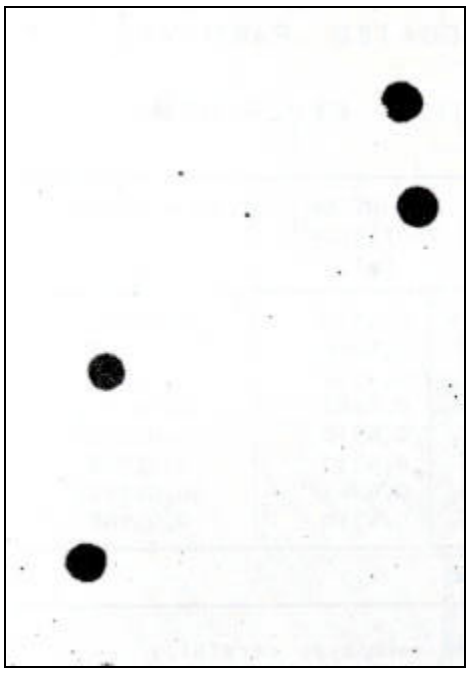

THP 321A

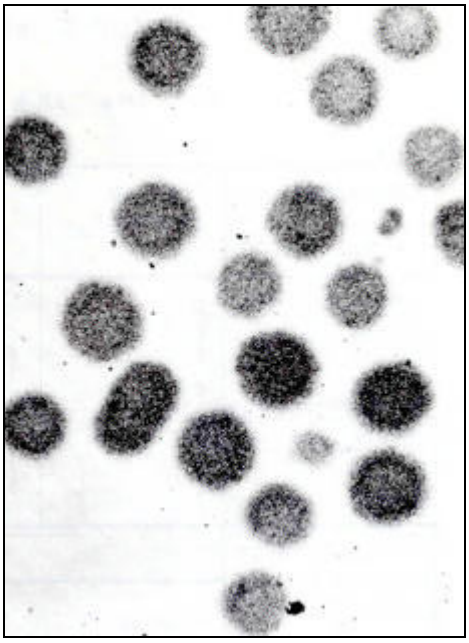

THP 321B

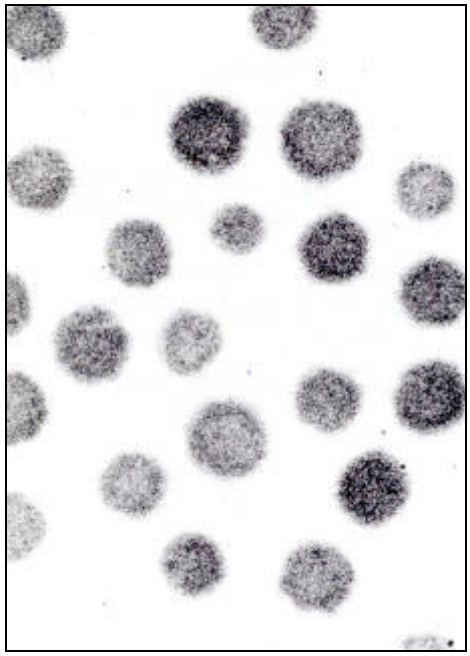

THP 321C

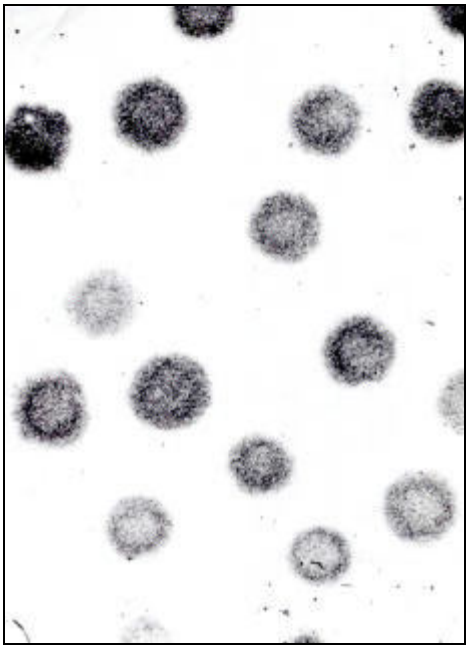

THP 321D

Figure 6: α-radiography of C kernel polished section after each carbon coating step

CONTAINER. Nr.	TYPE OF PARTICLE.	PARTICLE-DIAMETER. (mm)	WEIGHT OF PARTICLES (g)	Pu - WEIGHT. (g)
1	D	-	0,4330	0,06482
2	C	0,699	0,6260	0,061974
3	T	0,835	0,4330	0,05988
4	C		0,6262	0,061993
5	D	-	0,4330	0,06482
6	T	0,699	0,4330	0,05989
7	C	0,835	0,6261	0,061983
8	T		0,4330	0,05988
CONTAINER Nr.1 (MIDDLE HOLE)	LOADING.			
1a 1b 1c	DRAGON CNEN KARLSRUHE	5 Particles of each type carefully checked before irradiation.		

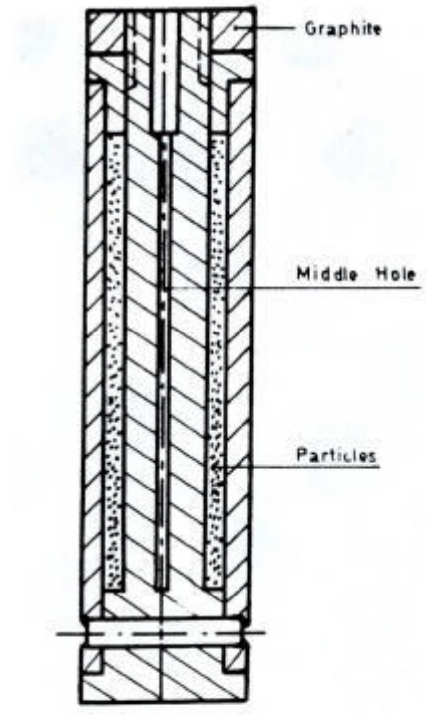

LOOSE PARTICLES CONTAINER
PERPENDICULAR CUT
ENLARGEMENT 2:1

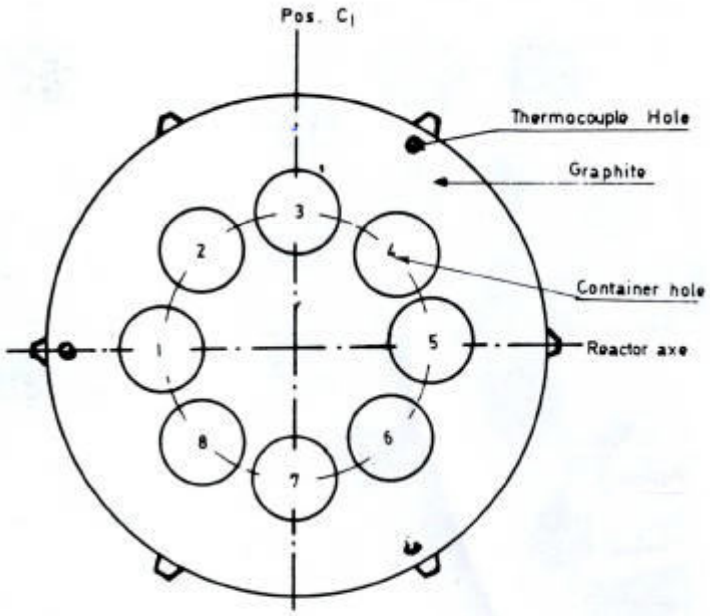

TELEPHONE DIAL TYPE GRAPHITE CARTRIDGE
UPPER VIEUW
ENLARGEMENT 1:1

Figure 7: Loading of the Pu coated particles for the JK4 irradiation experiment

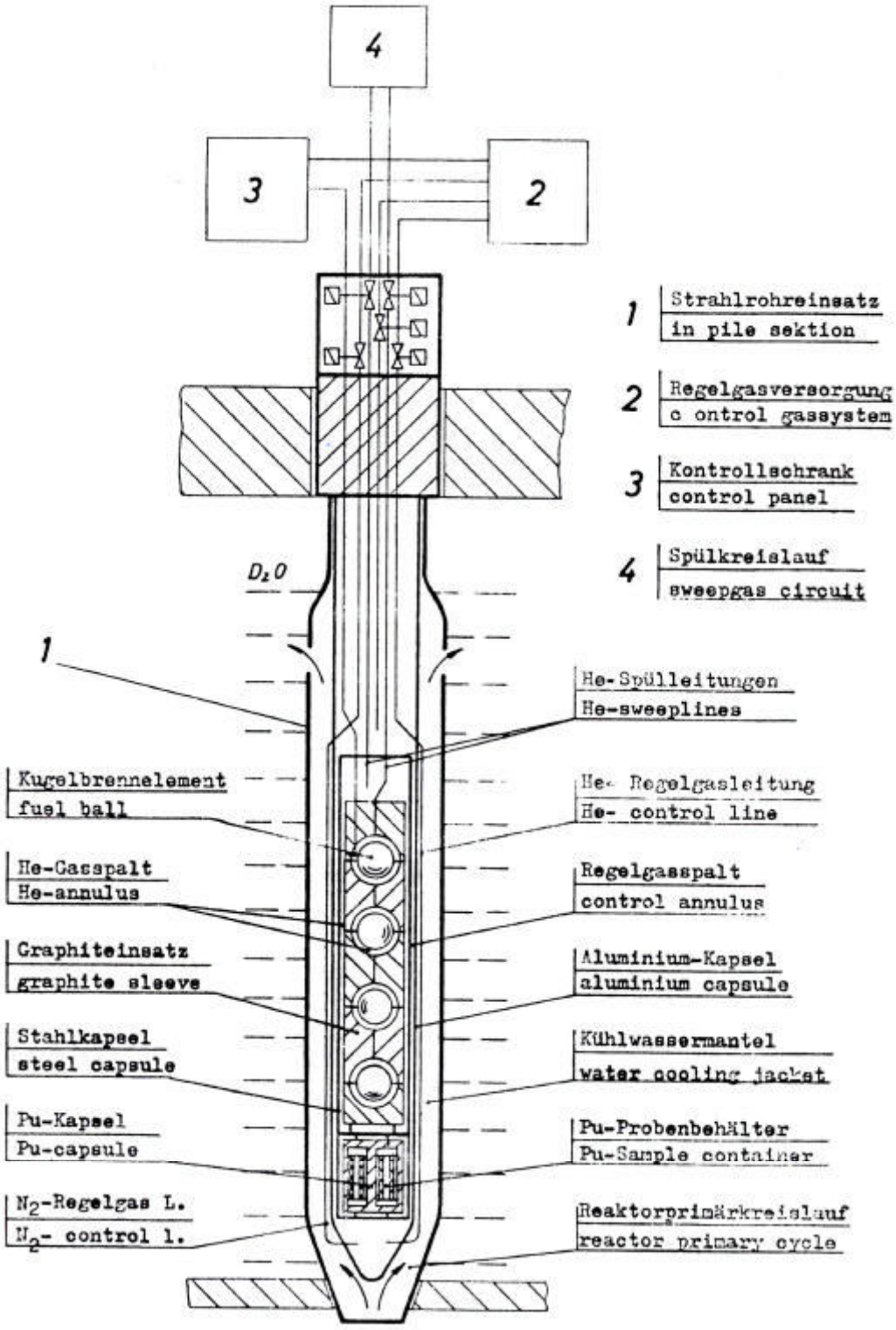

Figure 8: Irradiation Rig JK4

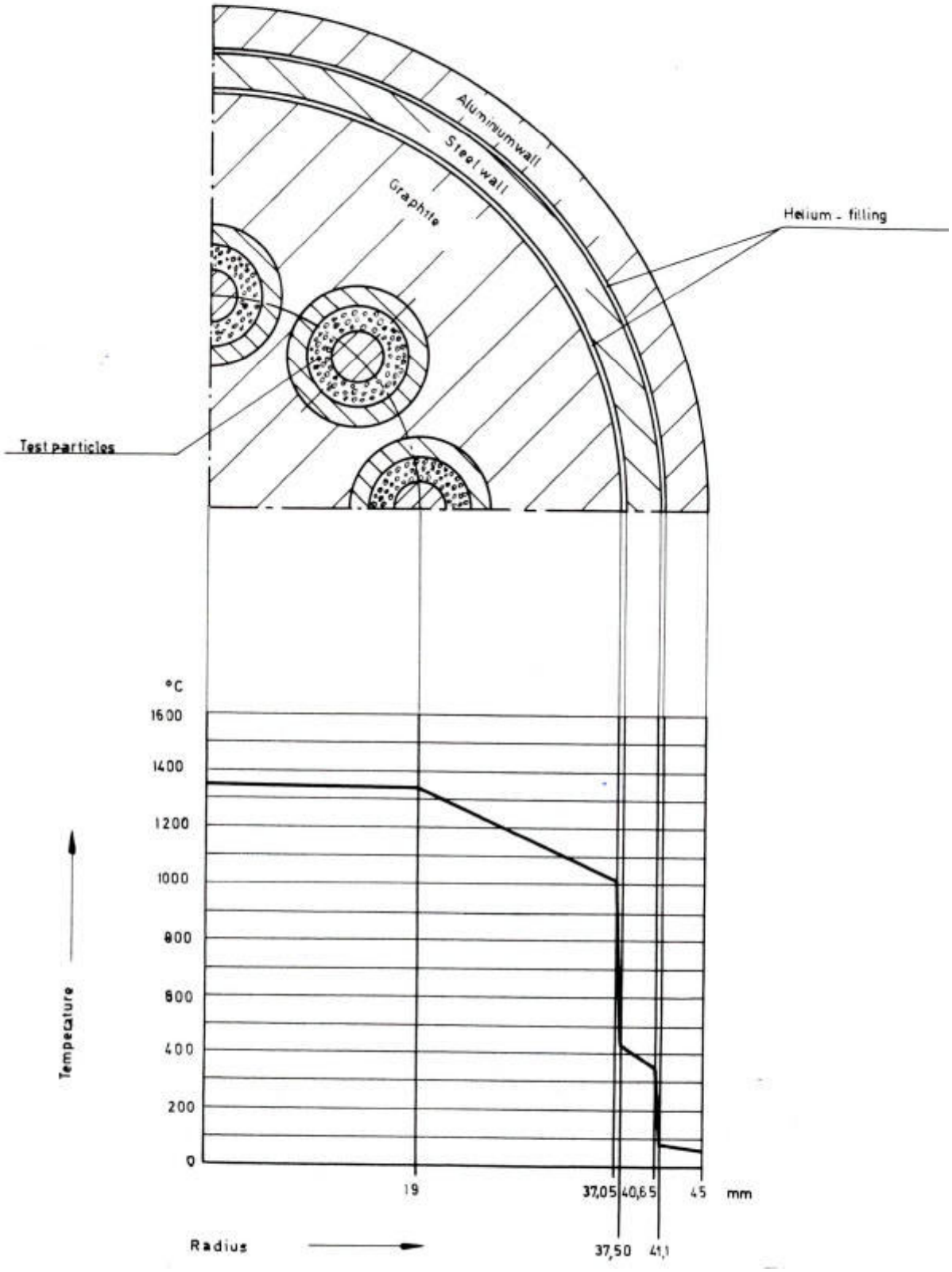

Figure 9: Radial temperature profile of the Pu capsule

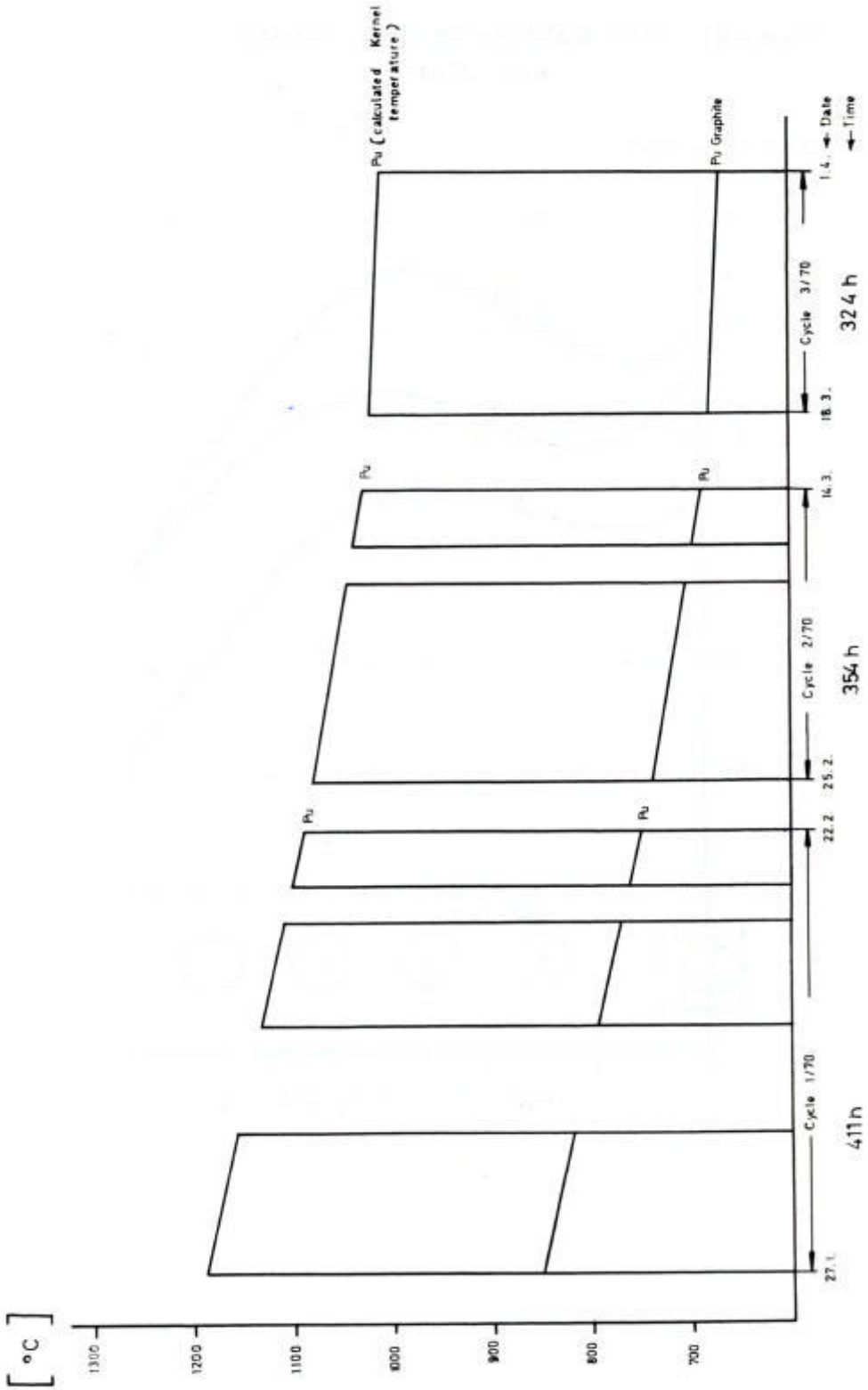

Figure 10: Temperature history of LV4/JK4 Pu kernel temperature (Calculated value ± 50°C)

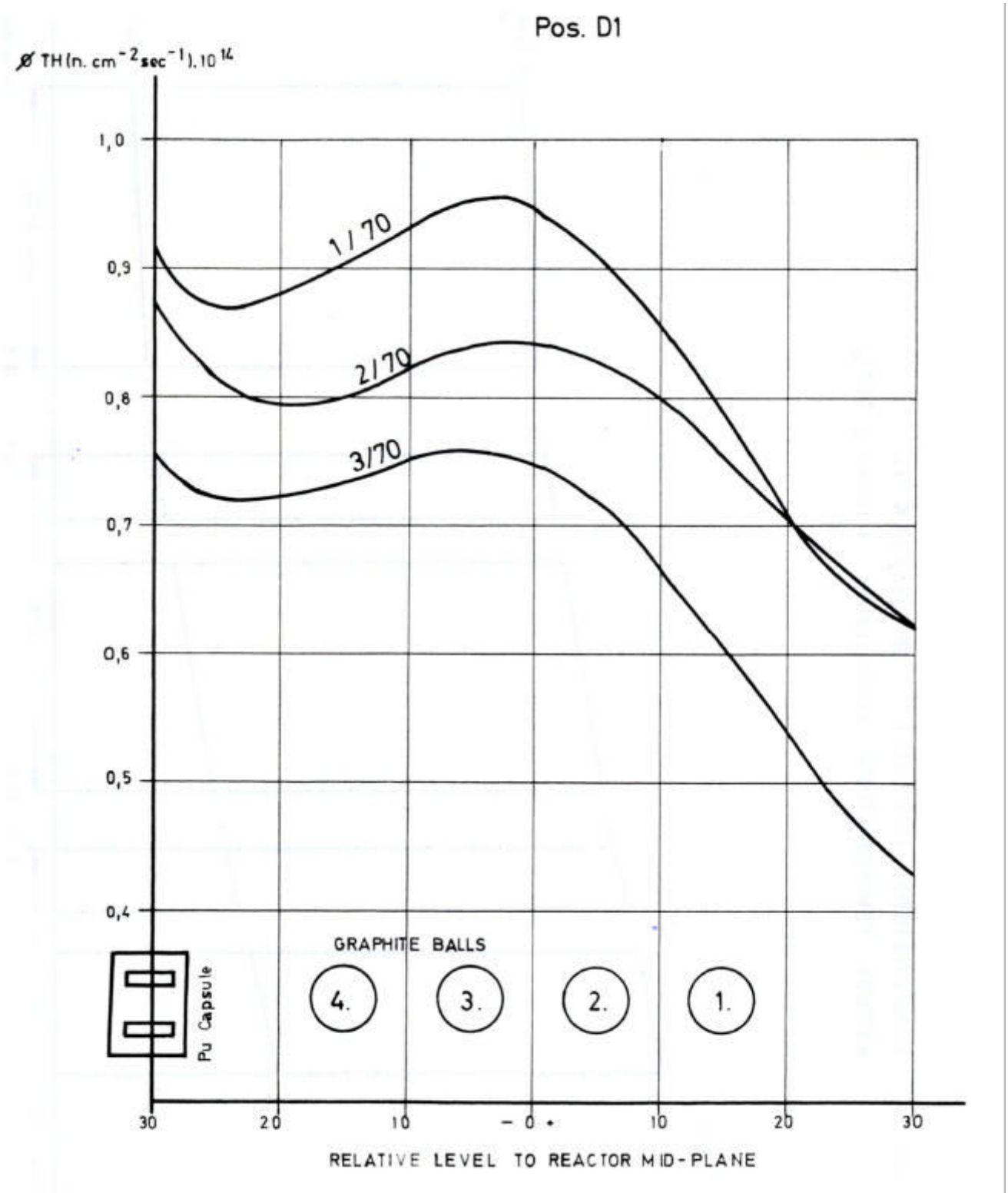

Figure 11: Flux distribution in experiment LV4/JK4 Pu

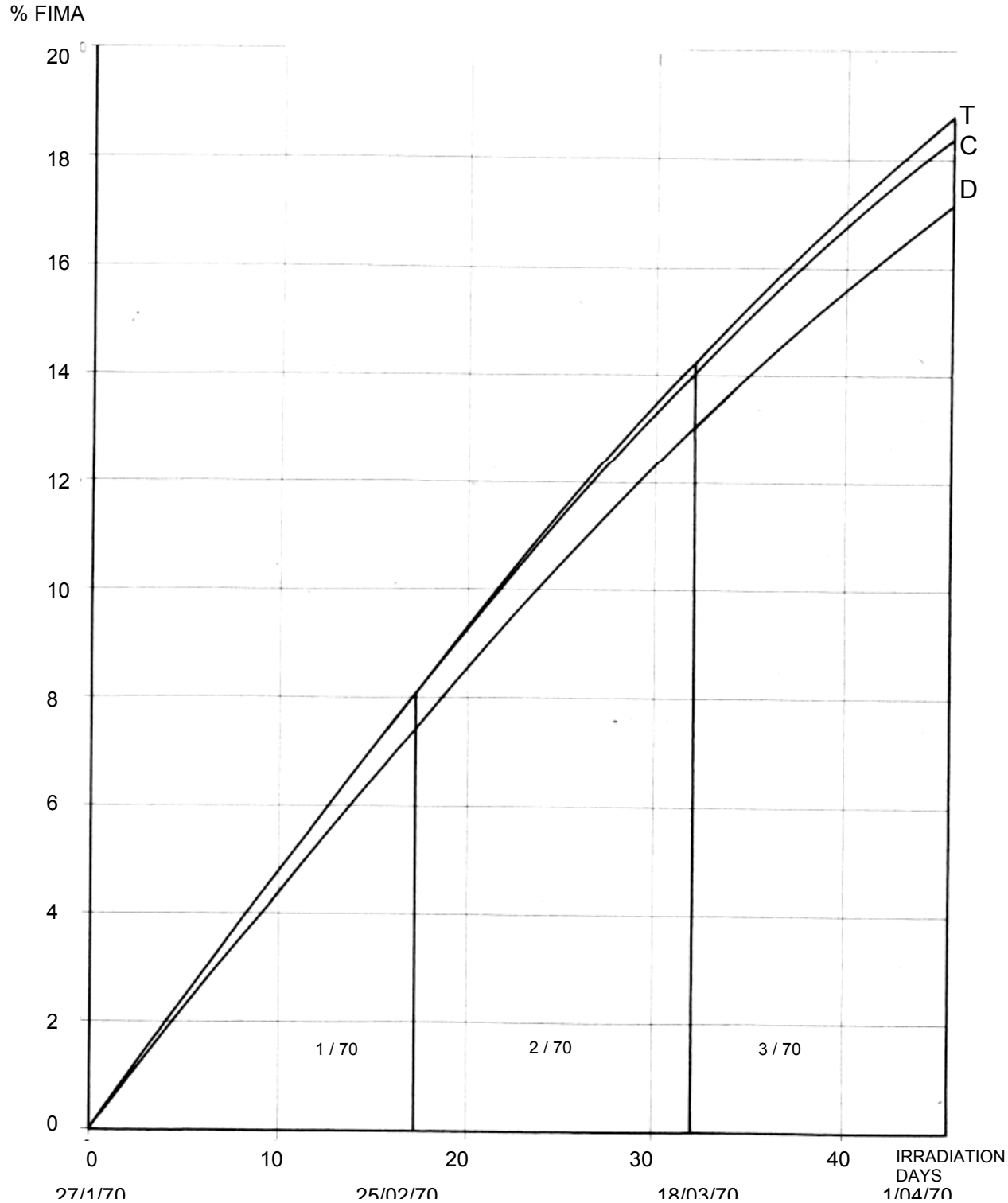

Figure 12: Burn-up diagram of AJK 4Pu
Begin of irradiation: 27/01/1970 - End of irradiation: 01/04/1970

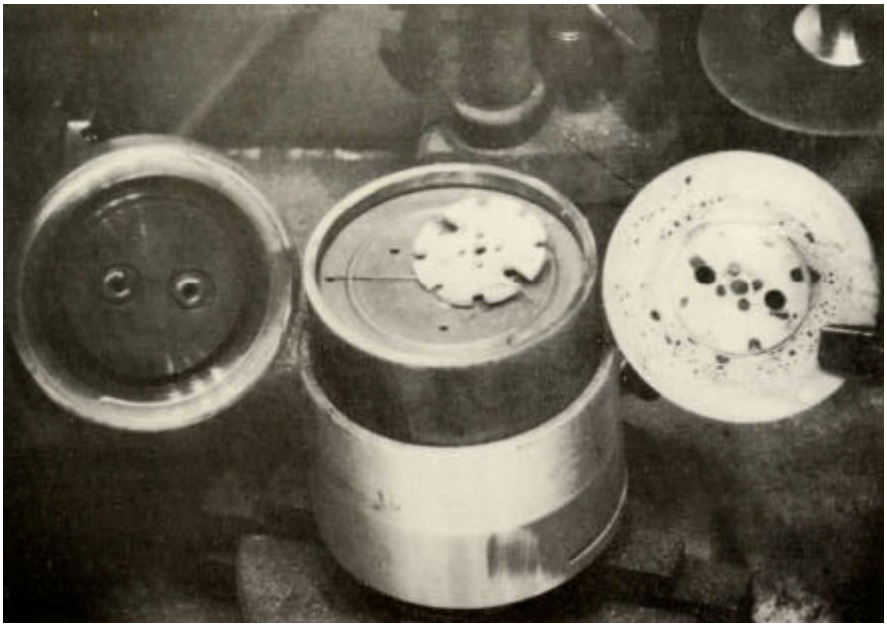

Figure 13: Cut aluminium capsule after irradiation

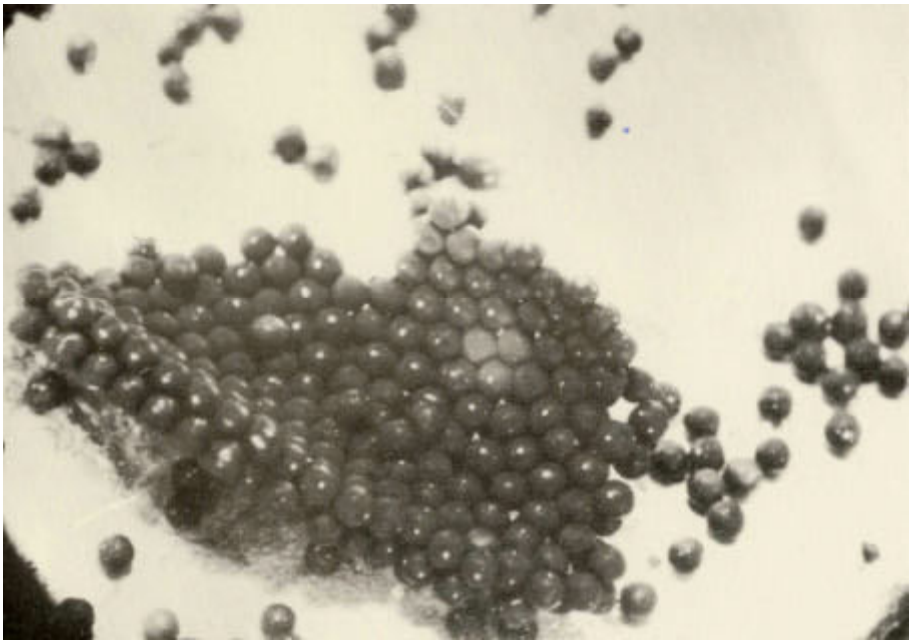

Figure 14: Irradiated coated particles in container 3

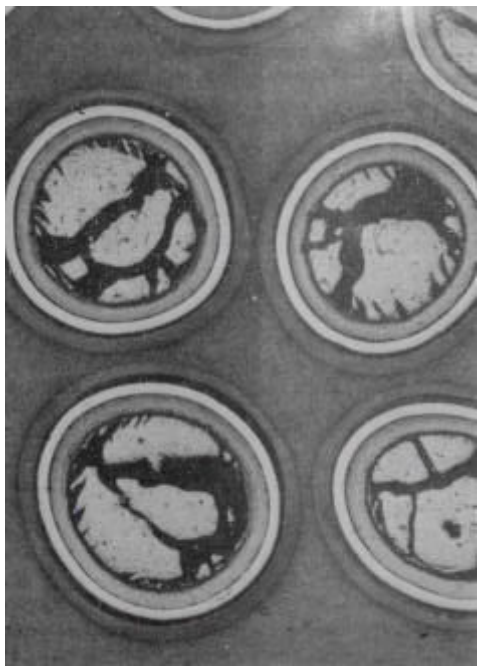

X40

Abb.1

X65

Abb.2

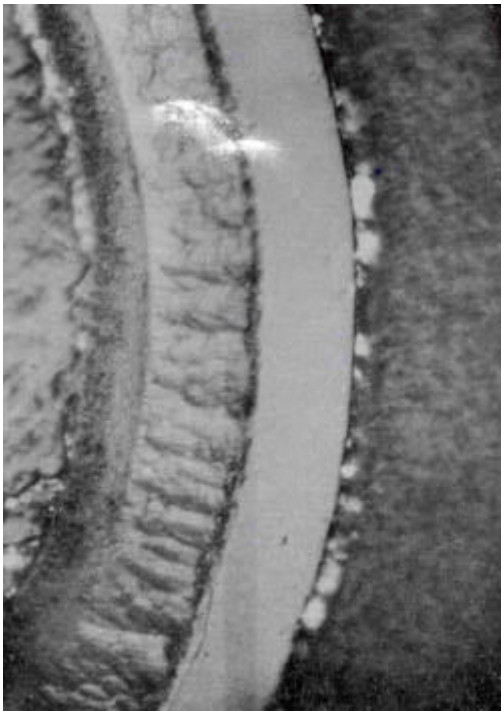

X425

Abb.3

Figure 15: D particles – Container 1

X90 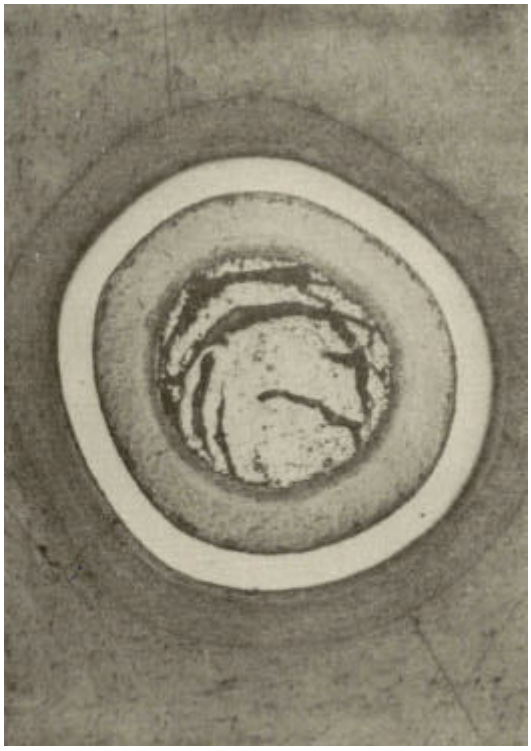 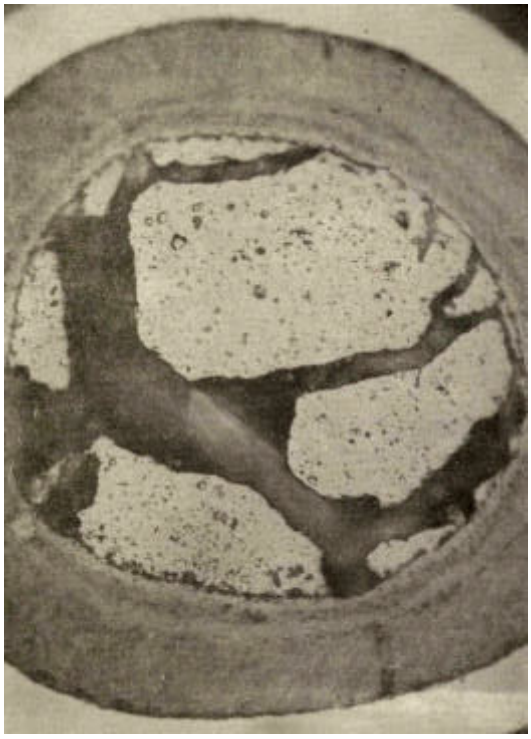 X180

X90 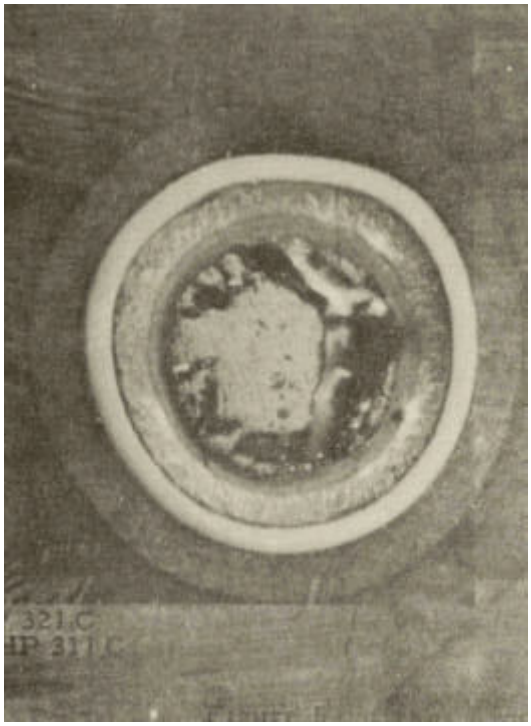 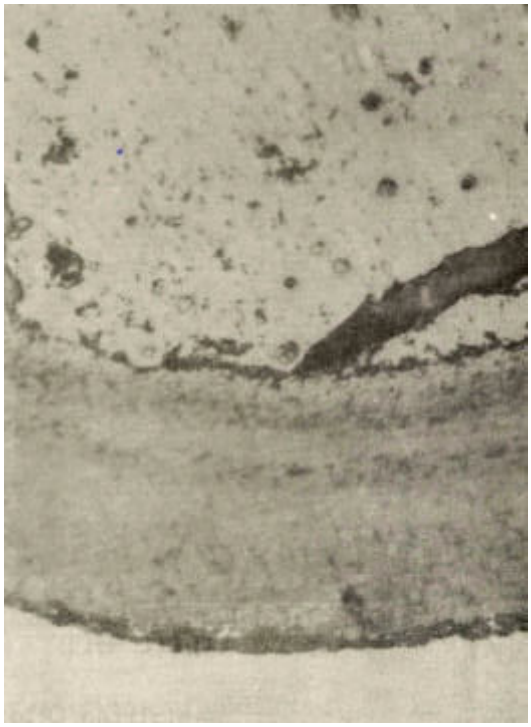 X180

Figure 16: C particles (container 5) after annealing at 1350°C

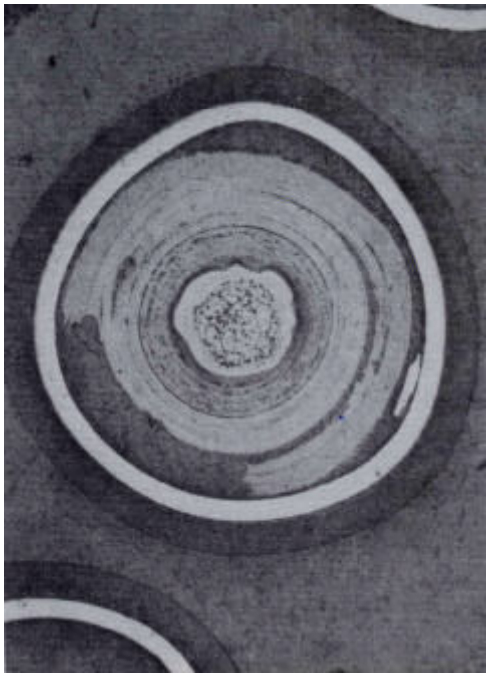

Abb.8

X80

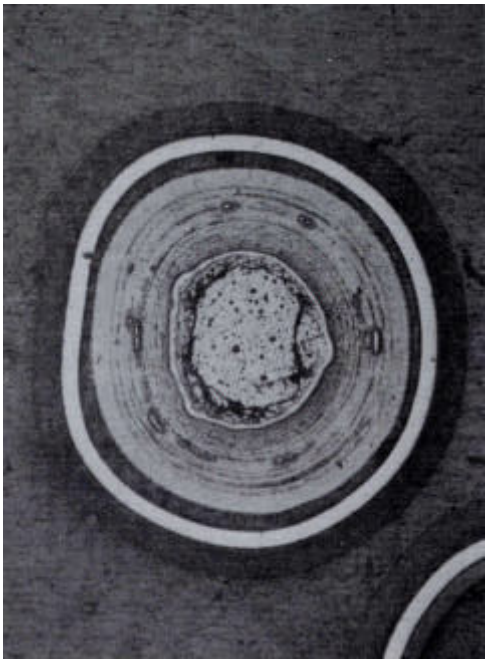

Abb.9

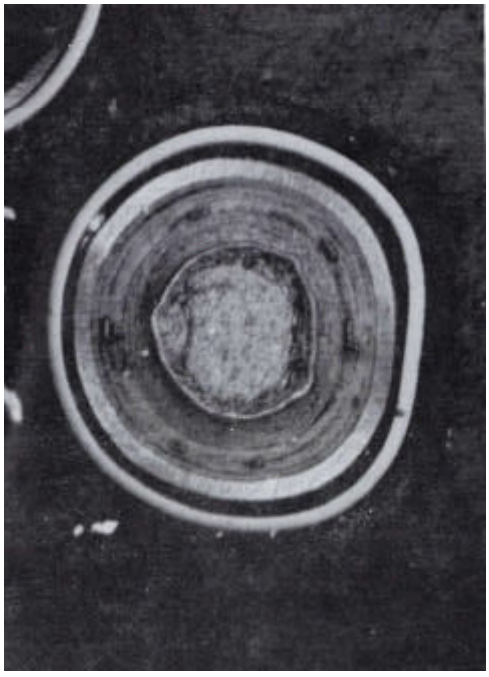

X80

Abb.10

Figure 17: T particles - Container 3

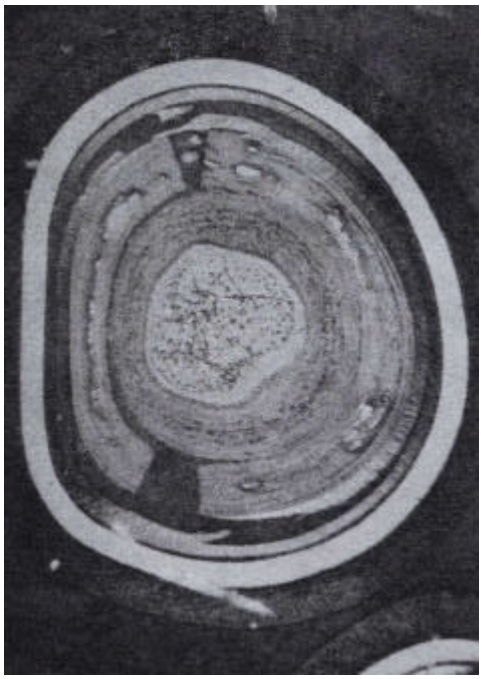

X80

Abb.11

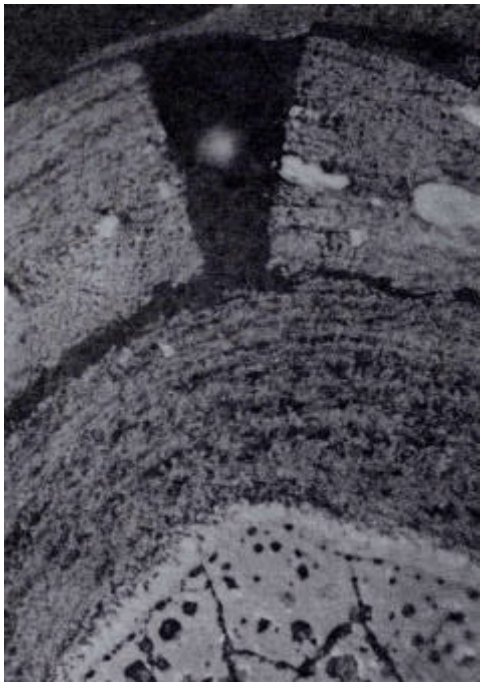

X400

Abb.12

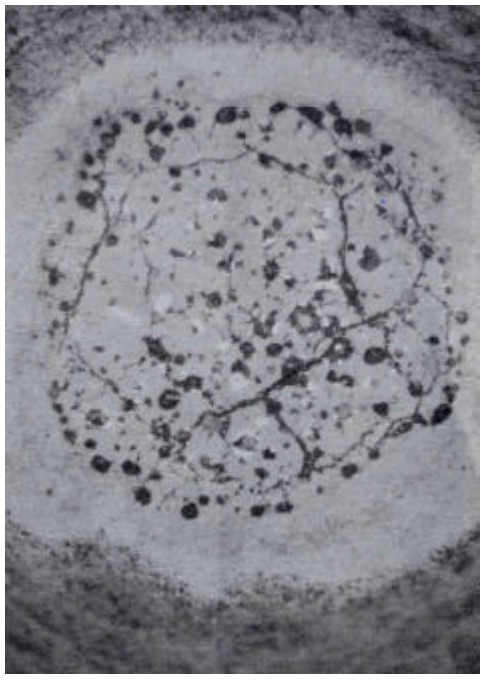

X400

Abb.13

Figure 18: T particles – Container 3

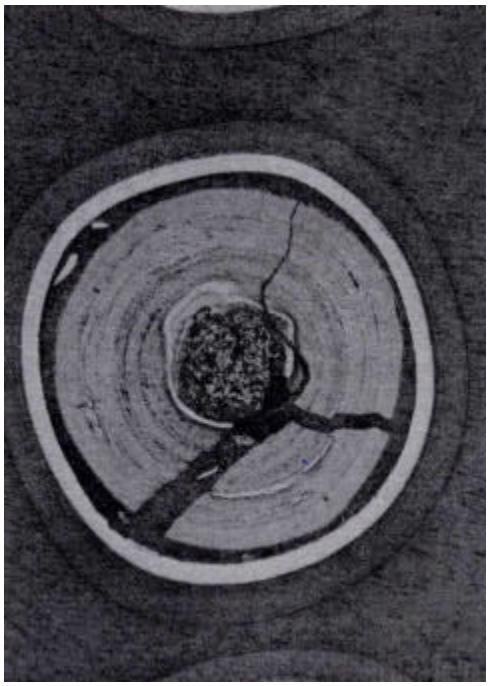

X80

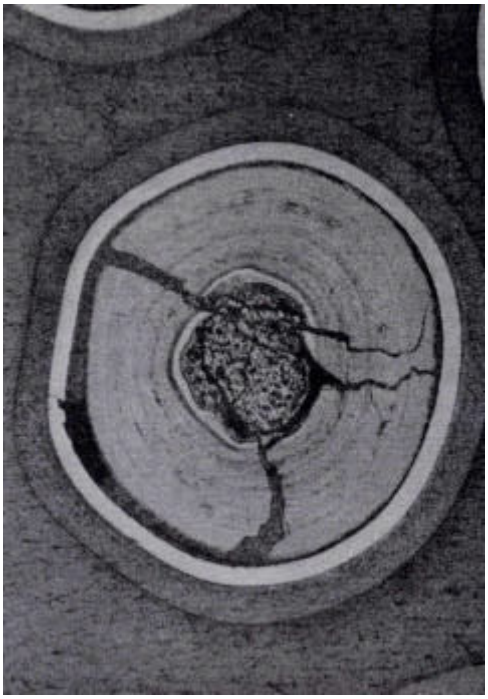

Abb.21

Abb.22

X80

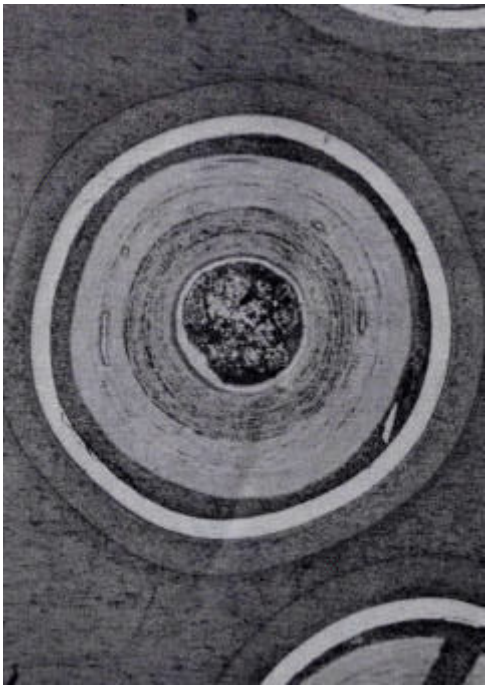

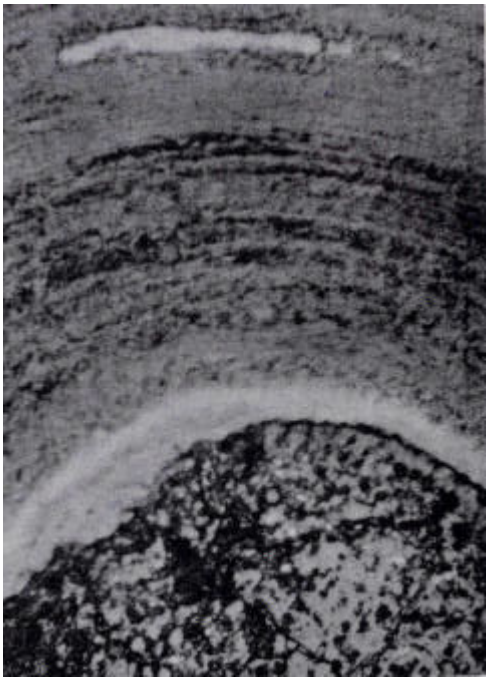

X400

Abb.23

Abb.24

Figure 19: T particles after annealing at 1350°C – Container 8

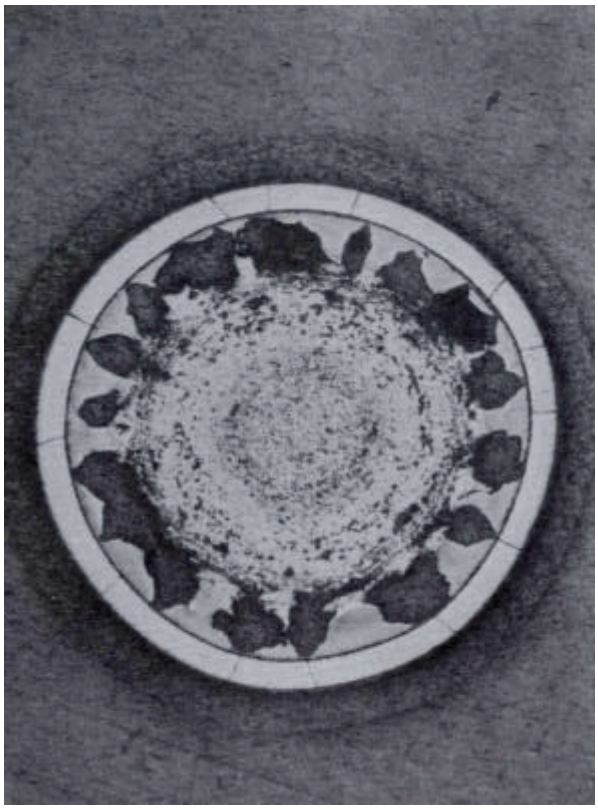

X100

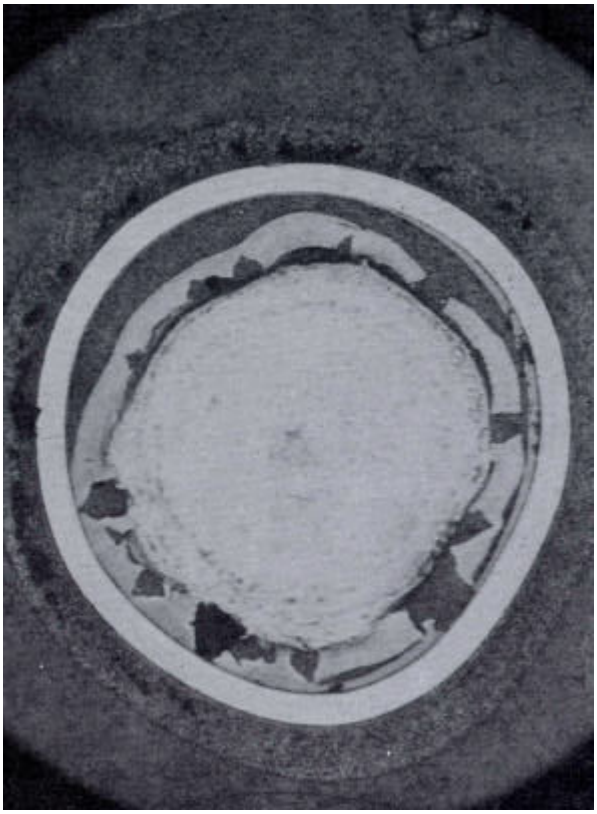

Abb.14 Container 4 Abb.15

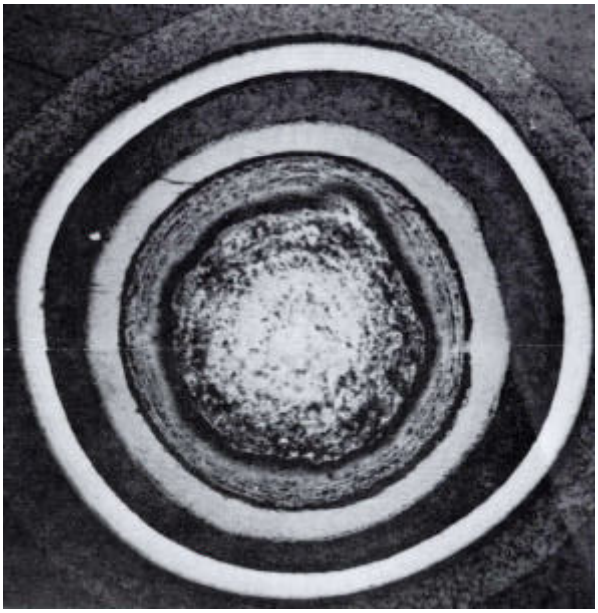

Container 7

Figure 20: C particles – Containers 4 and 7

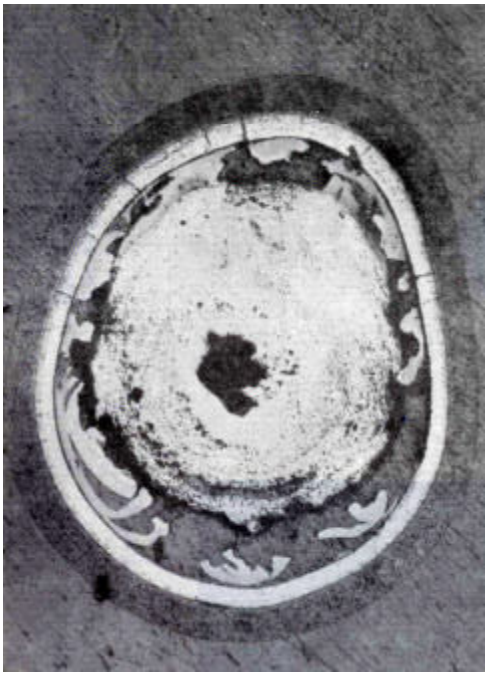

X80

Abb.4

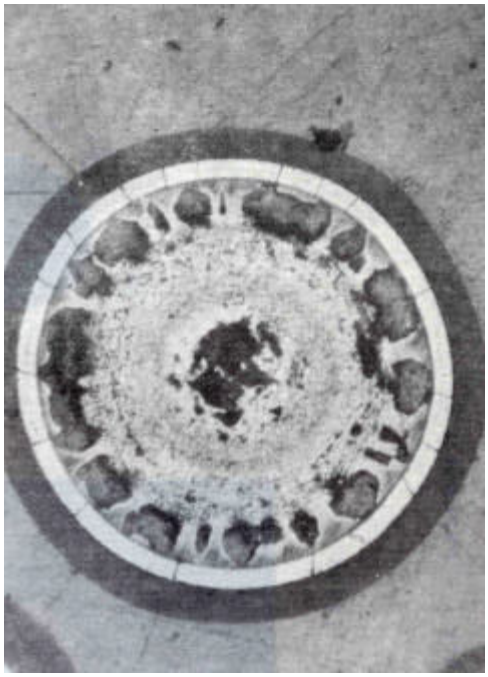

Abb.5

X400

Abb.6

X80

Abb.7

Figure 21: T particles after successive annealing at 1350°C and 1500°C (Container 2)

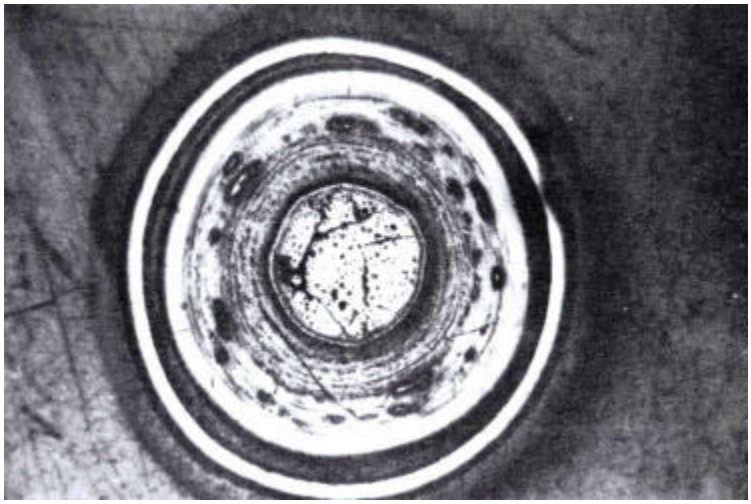

X90

Polished section

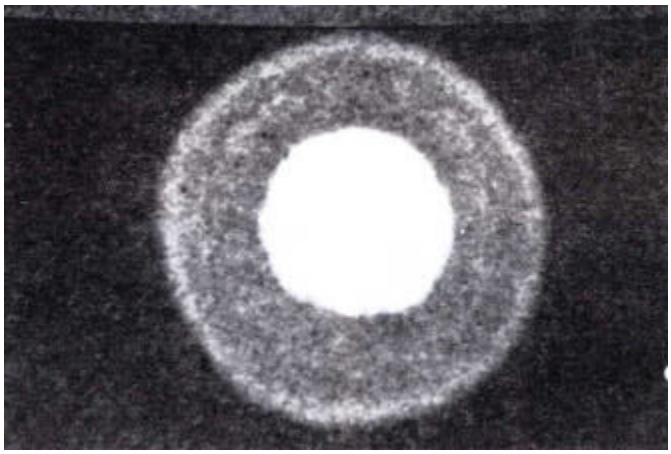

X90

X-ray after fabrication

X90

α-autoradiography after irradiation

Figure 22: Particle 3T – Container 1

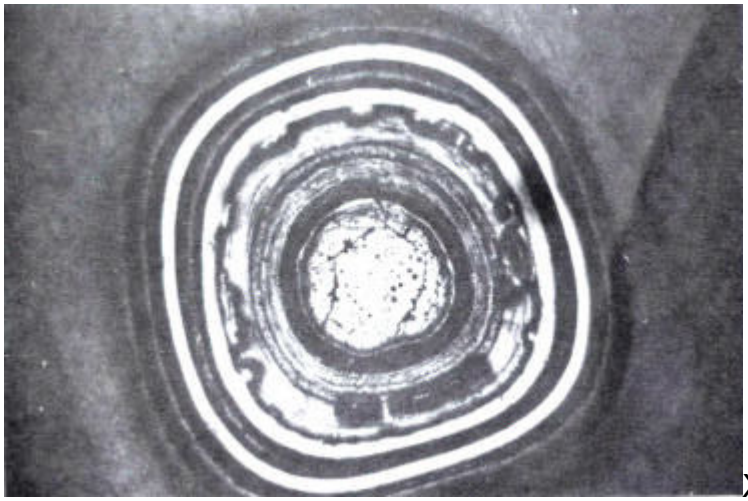

X90

Polished section

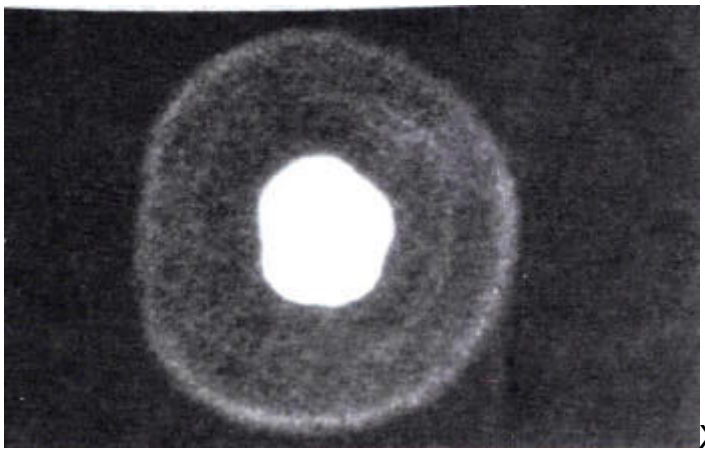

X90

X-ray after fabrication

X90

α-autoradiography after irradiation

Figure 23: Particle 4T – Container 2

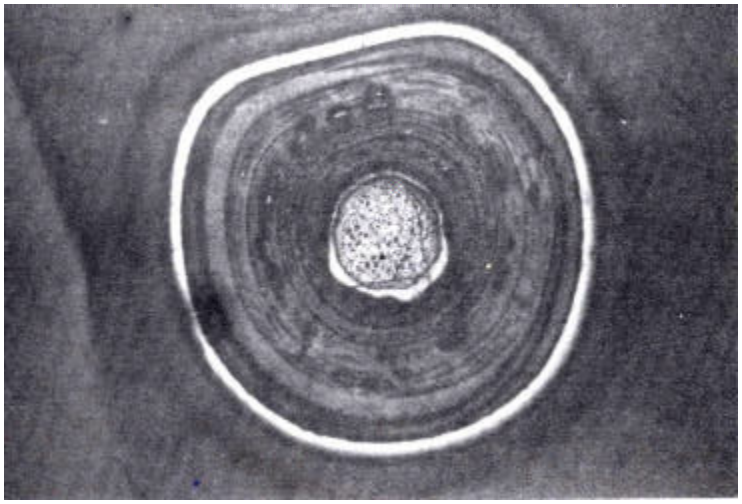

X90

Polished section

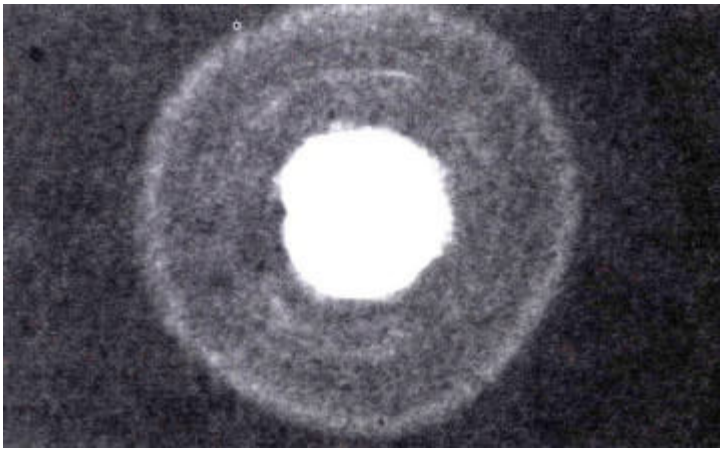

X90

X-ray after fabrication

X90

α-autoradiography after irradiation

Figure 24: Particle 7T – Container 3

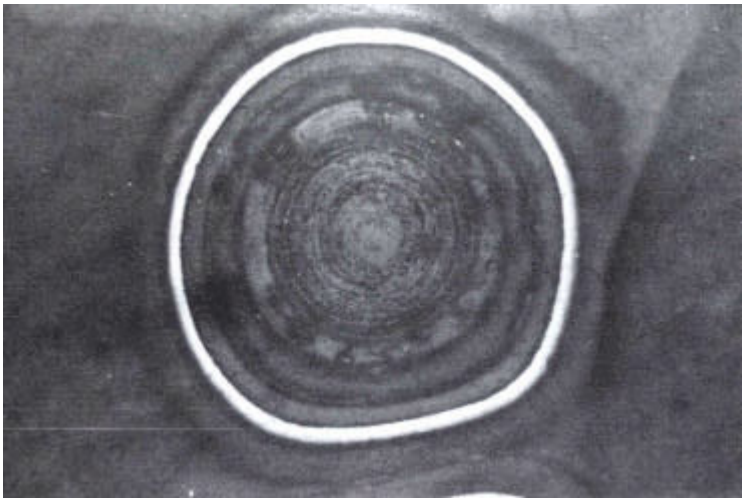

X90

Polished section

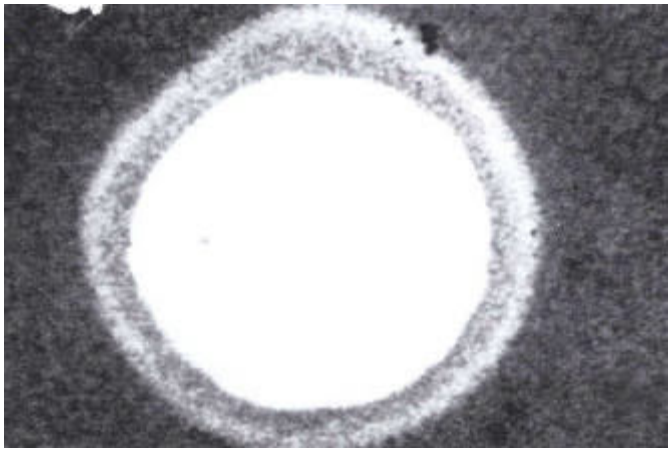

X90

X-ray after fabrication

Figure 25: Particle 8C – Container 3

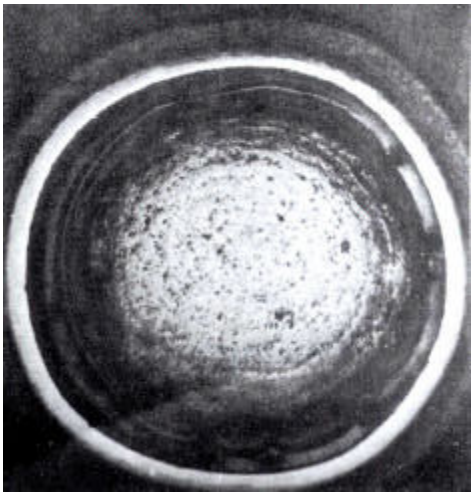

X90

Polished section

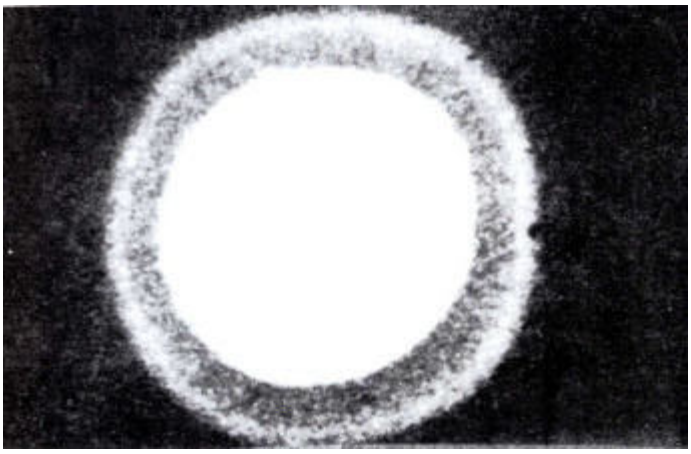

X90

X-ray after fabrication

α-autoradiography after irradiation

Figure 26: Particle 6C– Container 4

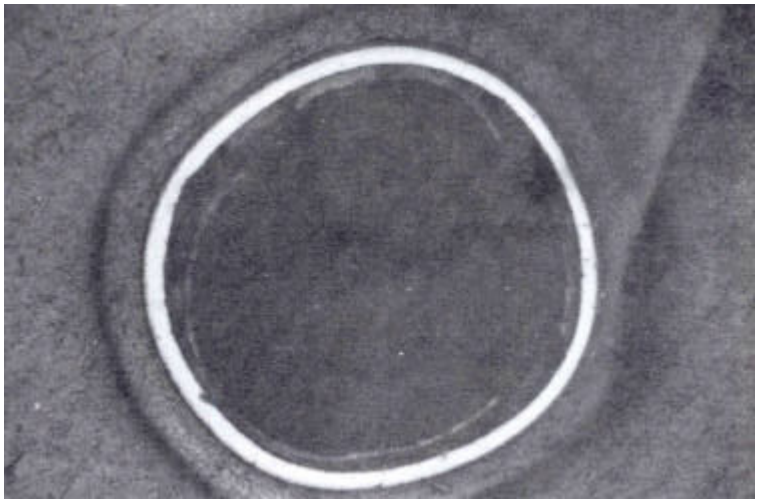

X90

Polished section

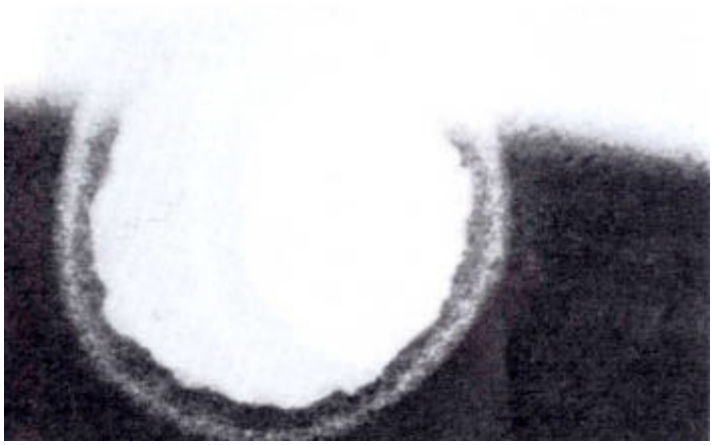

X90

X-ray after fabrication

Figure 27: Particle 5C – Container 5

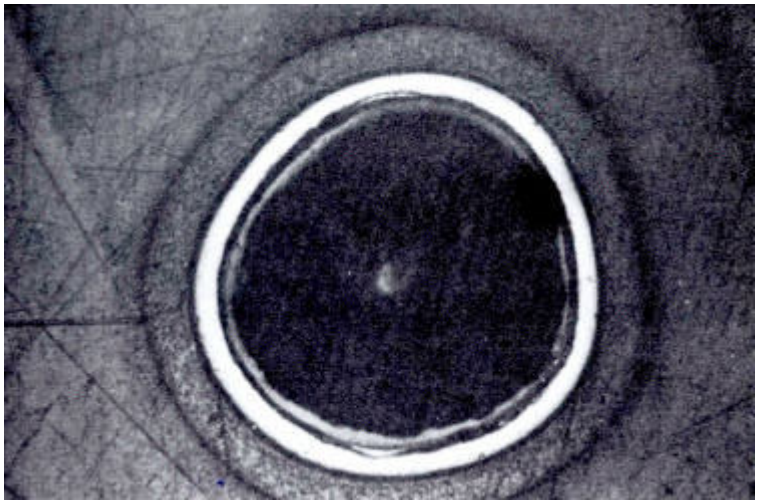

X90

Polished section

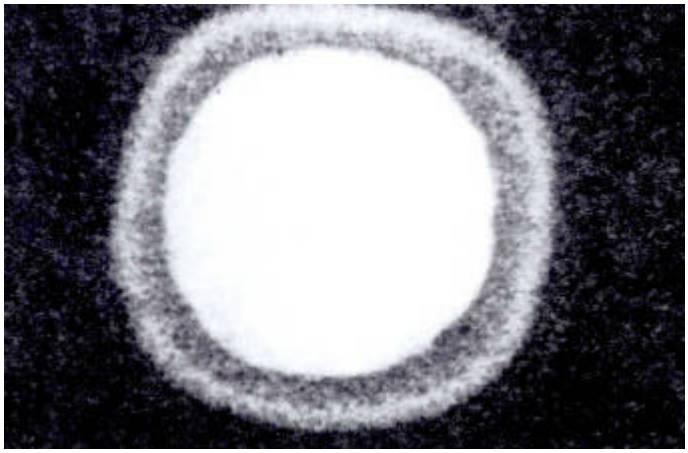

X90

X-ray after fabrication

Figure 28: Particle 9C – container 6

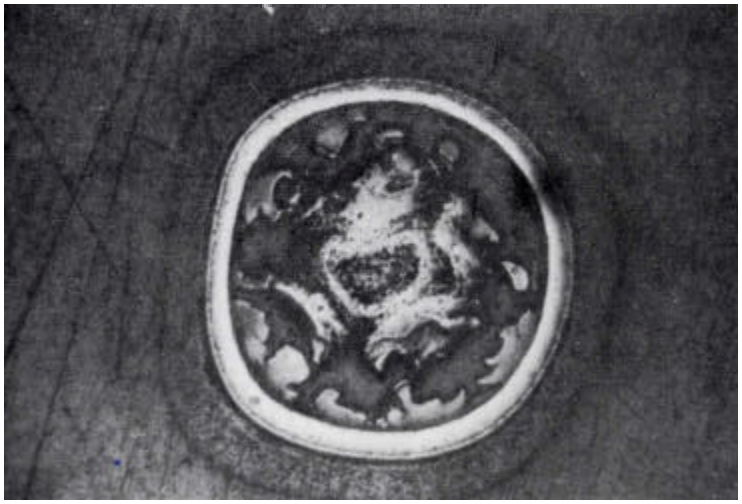

X90

Polished section

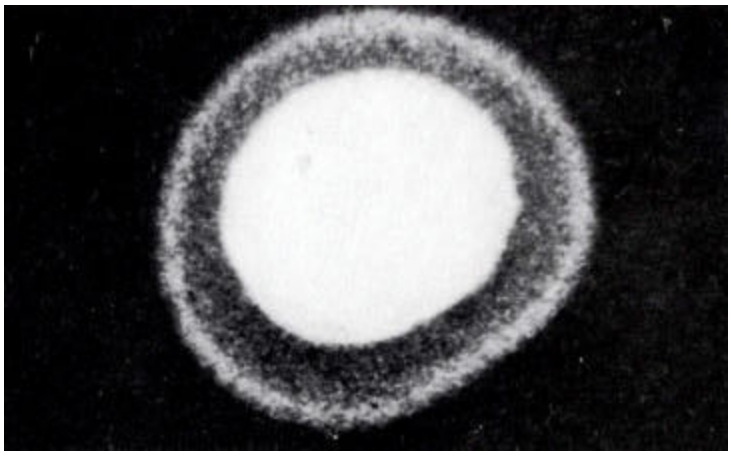

X90

X-ray after fabrication

X90

α-autoradiography after irradiation

Figure 29: Particle 13C – container 7

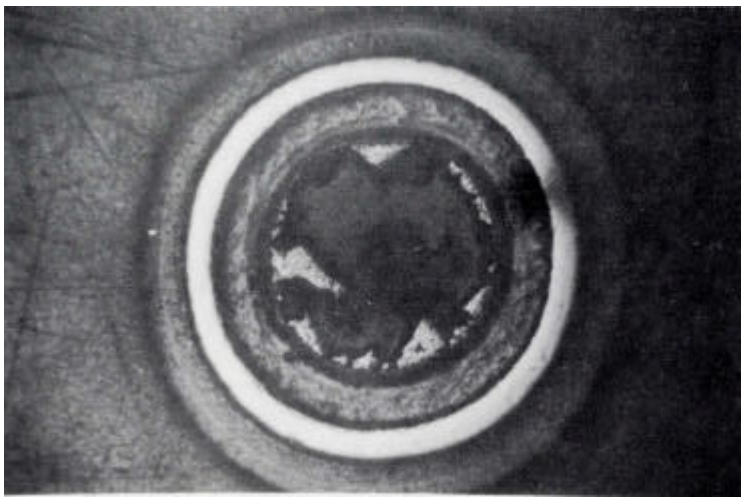

X90

Polished section

X90

α-autoradiography after irradiation

Figure 30: Particle 14D – container 8

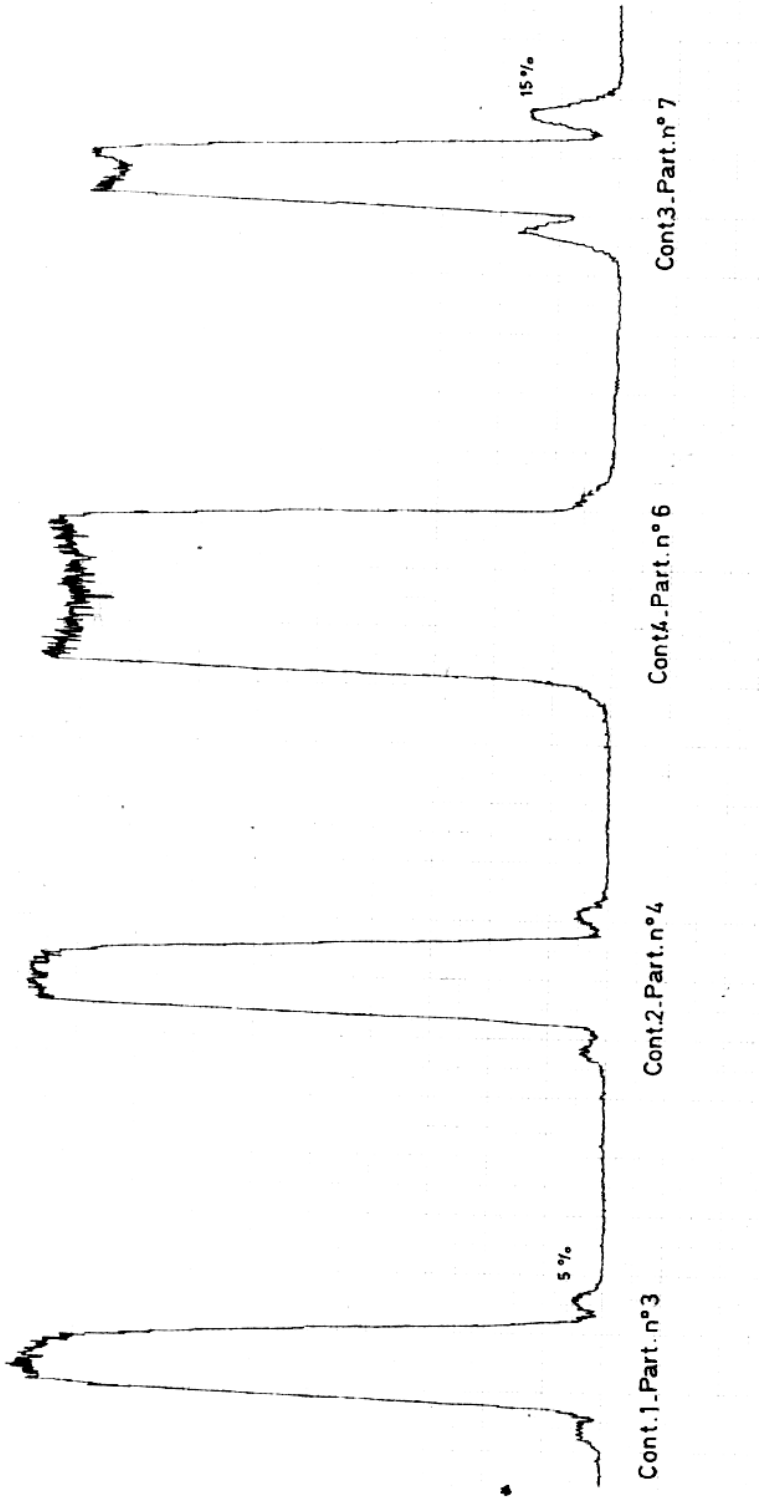

Figure 31: Microdensimetry of a-autoradiographies

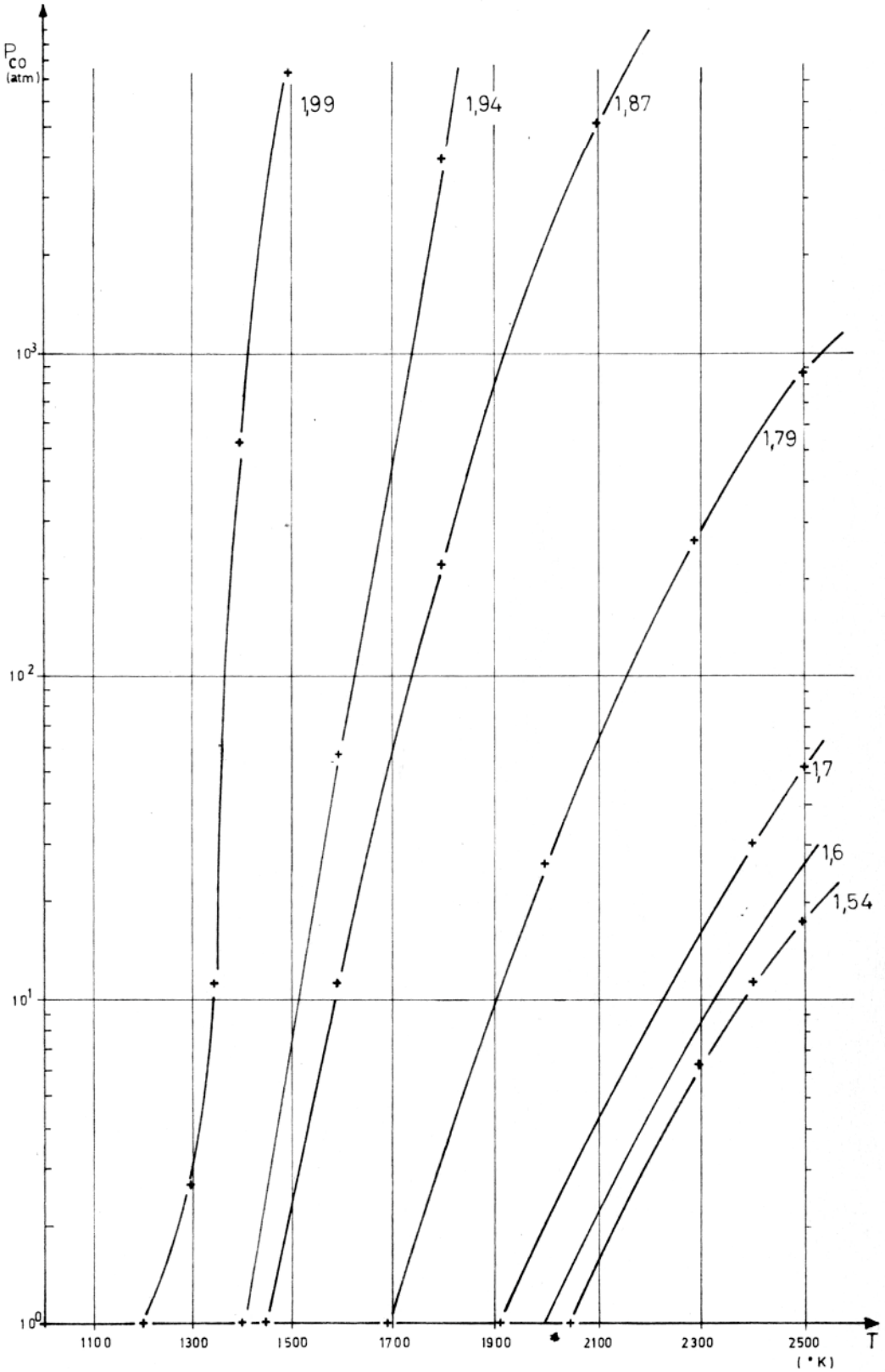

Figure 32: CO equilibrium pressure for several PuO_{2-x} stoechiometries

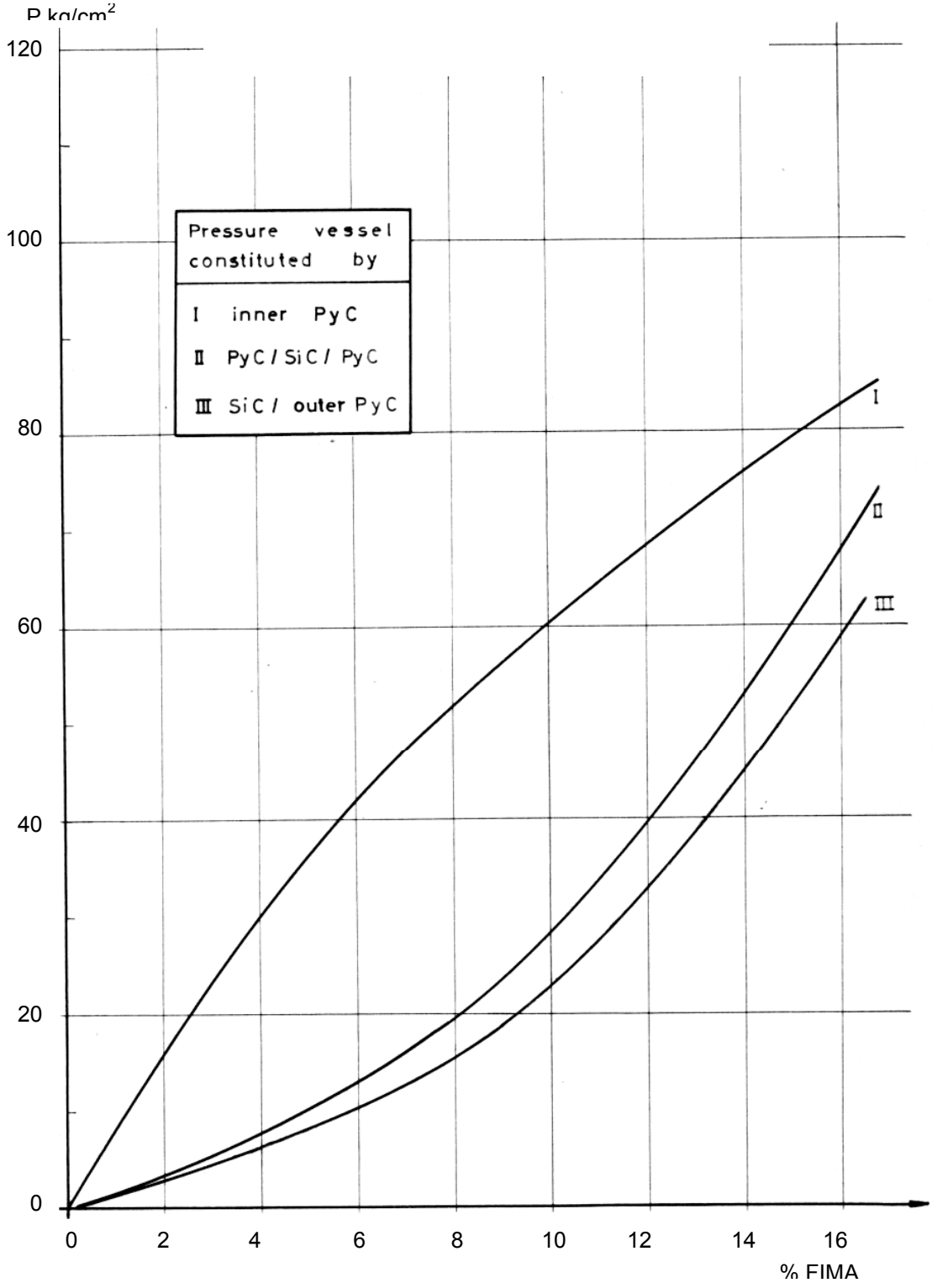

Figure 33: Gas pressure in the PuO_2 coated particles at 1200°C

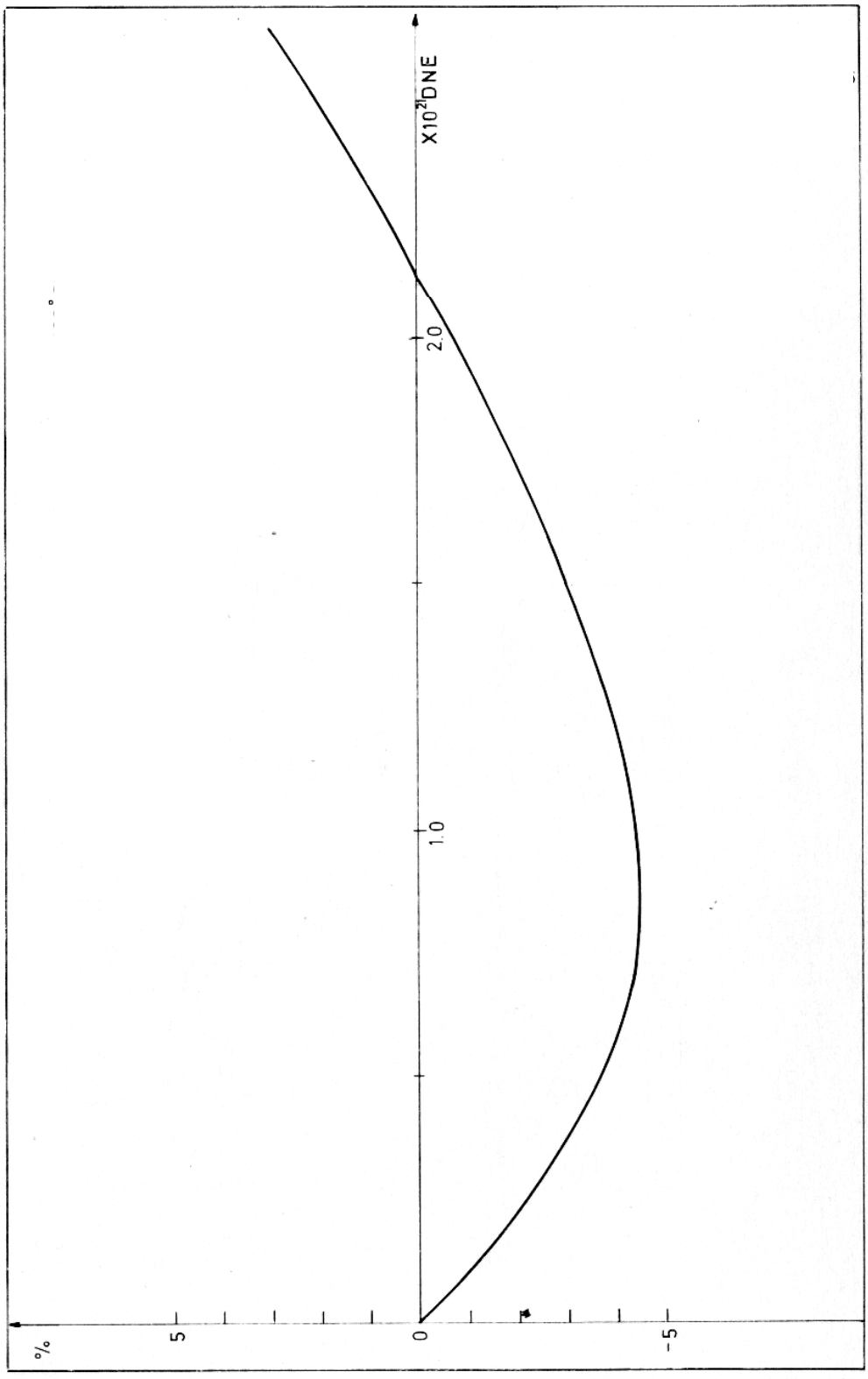

Figure 34: Volume change of PyC irradiated at 1200°C
(ρ= 2.08 g/cm^3)

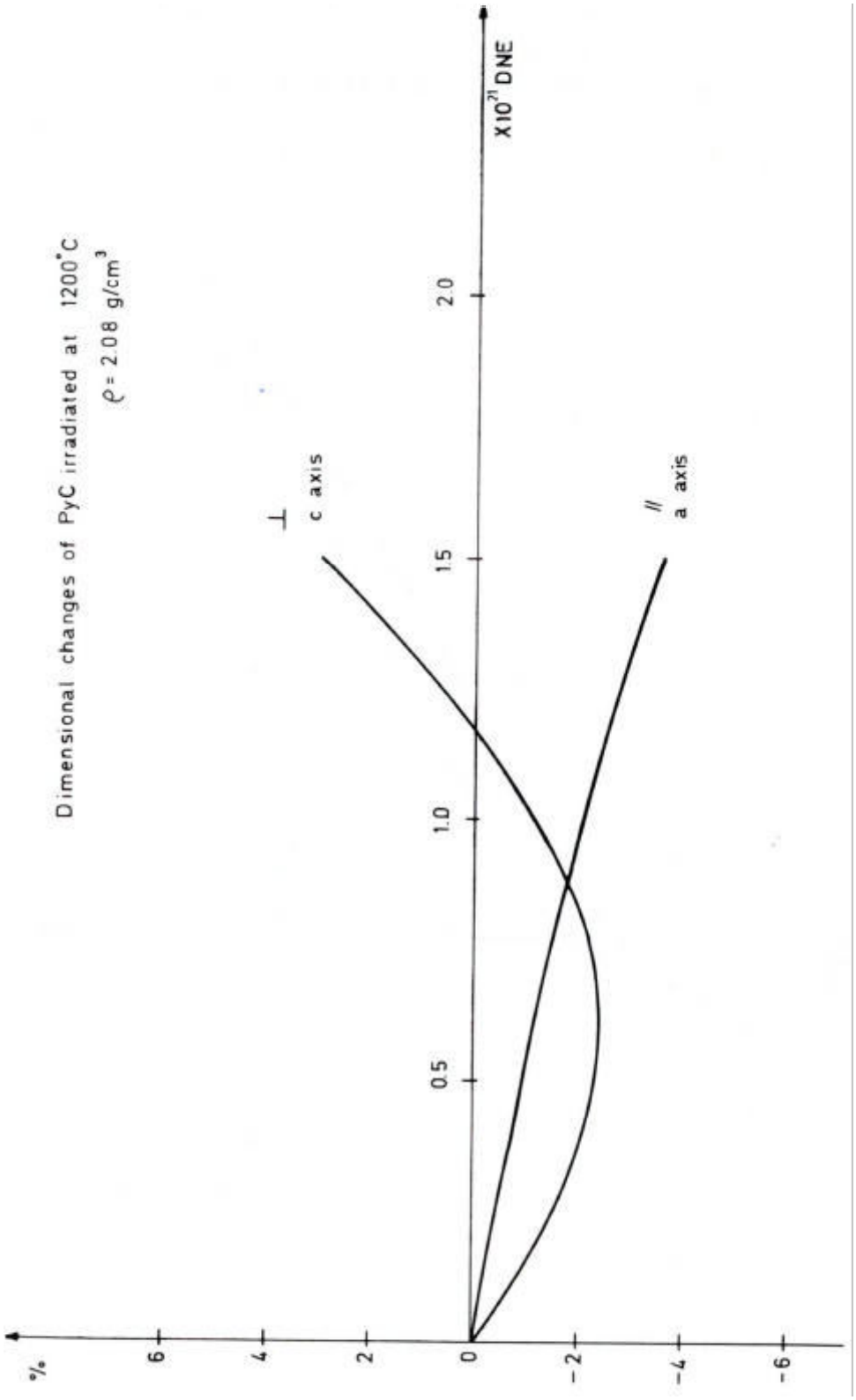

Figure 35: Dimensional change of PyC irradiated at 1200°C (ρ= 2.08 g/cm^3)

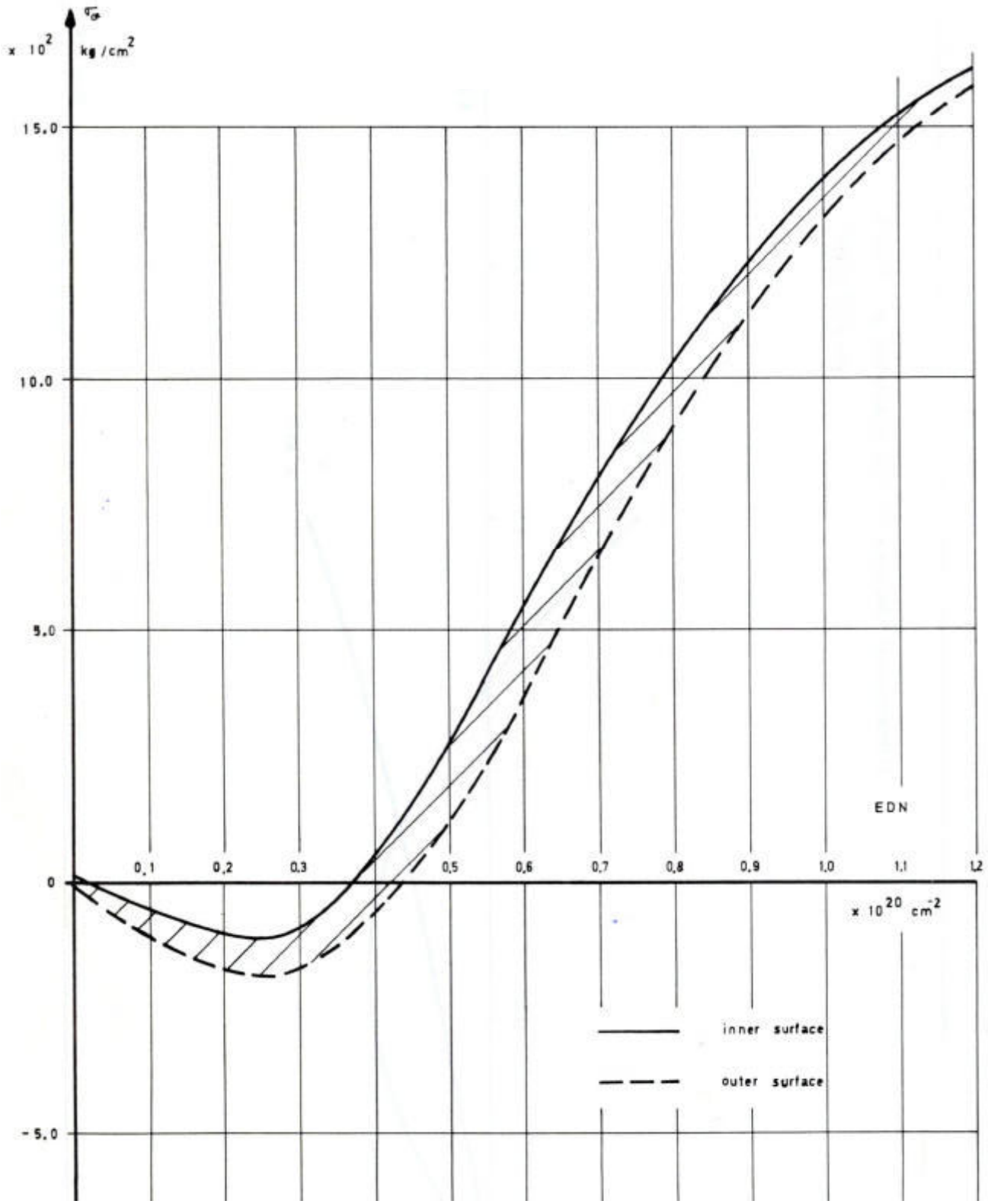

Figure 36: Hoop stress in the PuO_2 CPs at 1200°C for an inner PyC pressure vessel

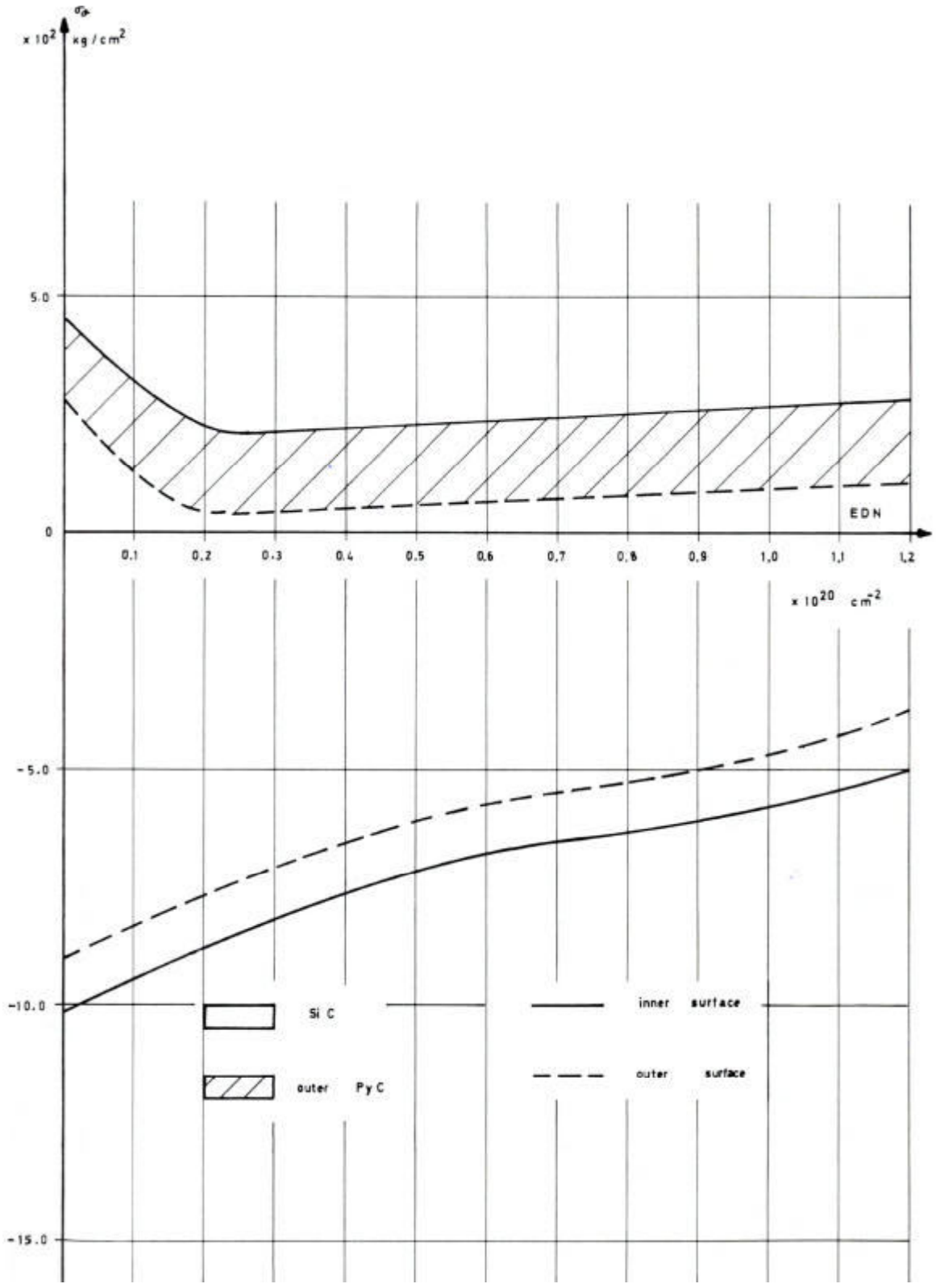

Figure 37: Hoop stress in the PuO_2 CPs at 1200°C for a SiC/outer PyC pressure level

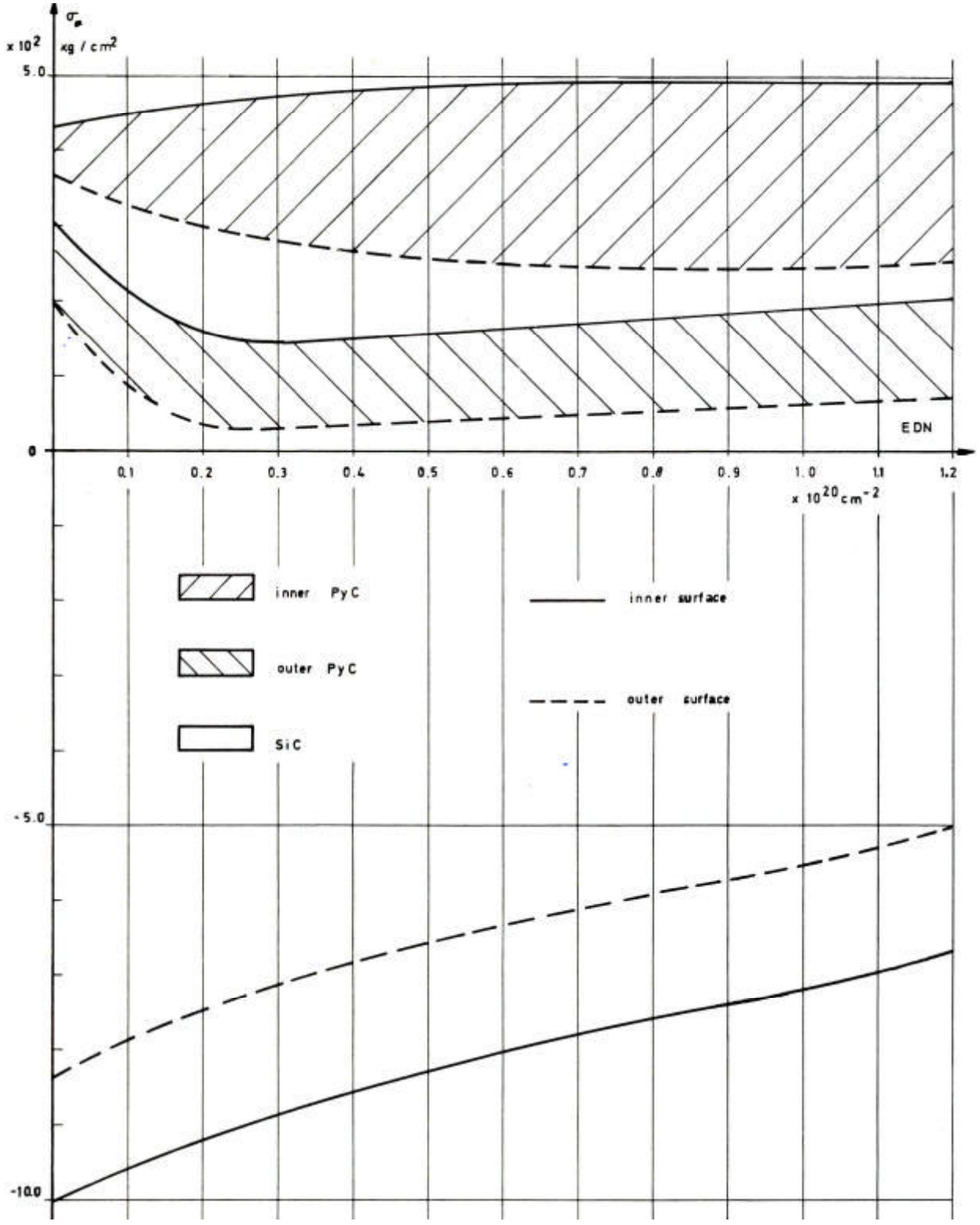

Figure 38: Hoop stress in the PuO_2 CPs at 1200°C for a PyC/SiC/PyC pressure level

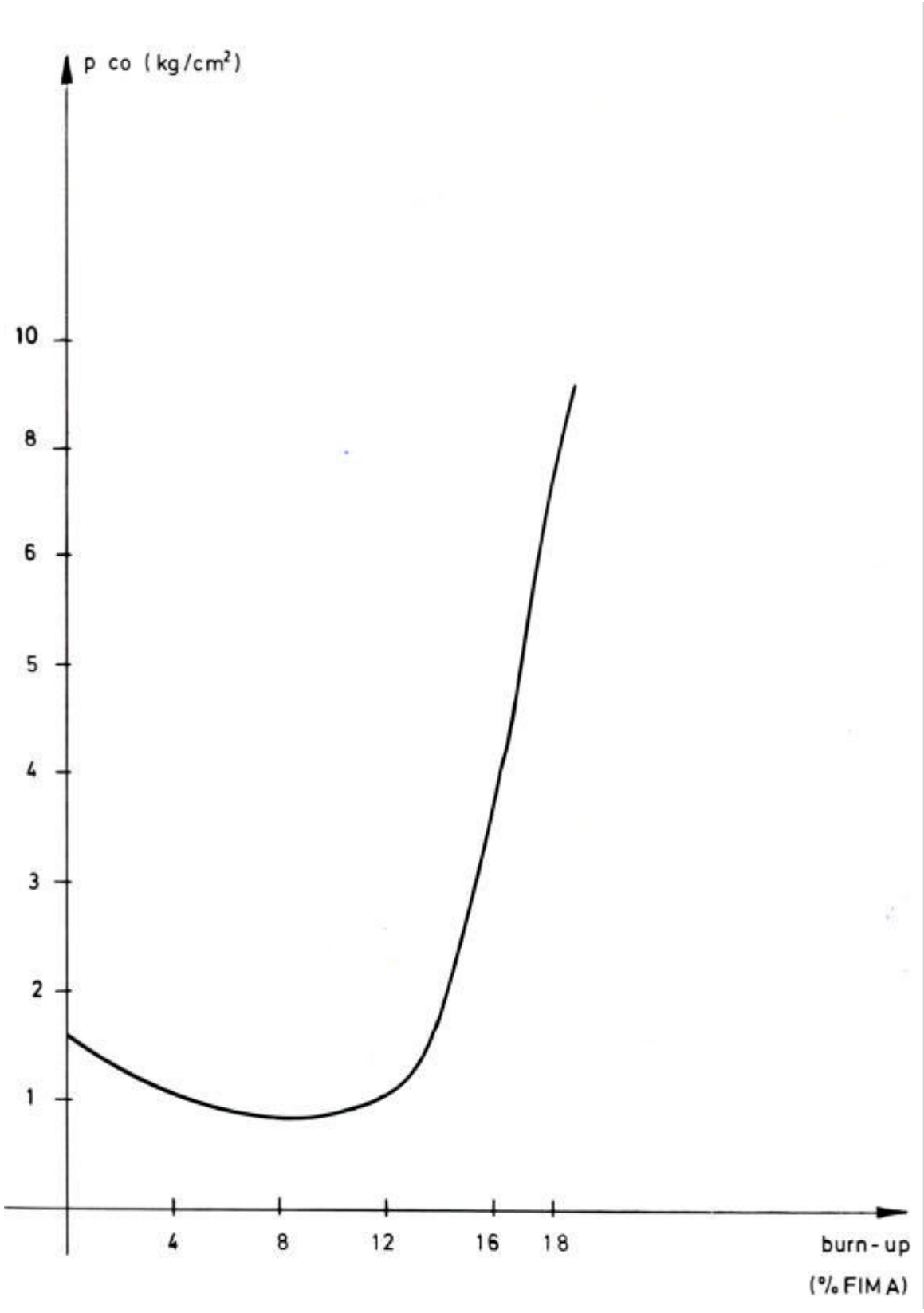

Figure 39: CO pressure versus burn-up in T type particle

	Type of document:	Reference No / File - "Rev." - Page
	Technical Note	**0601020/220-"-" - 1**
		Other reference:

Client: EC	Author(s) G. TOURY
Project: Raphael IP – SP Fuel Technology WP-FT4 Performance Modelling	
Subject:	

HTR particles Irradiation Experiment BN database

MET V Experiment

Rev.	Date	Chrono Filing No.	Status	Initials dactylo.	Author: Initials	Author: Visa 1	Verified by: Initials	Verified by: Visa 2	Approved by: Initials	Approved by: Visa 3	Q.A.: Initials	Q.A.: Visa 4	Issued by: Initials	Issued by: Visa 5	Number of pages
C															
B															
A															
-	17/05/2006	0601020	Draft		GTY		SSH						GTY		52

Distribution:

RAPHAEL Project: Mr. OBRY (1 copy +1 CD)

BN: SSH, GTY

	Type of document:	Reference No / File - "Rev." - Page
	Technical Note	**0601020/220-“-“ - 2**
		Other reference:

BELGONUCLEAIRE N.V.
Avenue Ariane, 4 - 1200 Brussels
TVA: BE 403.126.258
RCB: 271.300
TEL: 32-2774 05 11
FAX: 32-2-774 05 47

LIST of MODIFICATIONS

DATE	REVISION	OBJECT

15/05/2006	-	Draft

NOTICE

PERSONNEL IN CONFIDENCE, NOT FOR PUBLICATION

This work is performed under the term and conditions of the Consortium Agreement of the RAPHAEL Project supported by the EC under contract n° 516508 (FI6O)

LIABILITY

This document was prepared by BELGONUCLEAIRE (BN). Neither BN, nor any person acting on behalf of BN:

a) gives any warranty, expressed or implied, with respect to the accuracy, completeness of the information contained in this document, or that the use of any information, apparatus, method or process disclosed in this document may not infringe third party rights, or

b) assumes any liabilities with respect to the use of, or for damage resulting from the use of any information, apparatus, method or process disclosed in this document.

Abstract

The MET V experiment is a high temperature coated particle experiment sponsored by the DRAGON Project with the participation of DRAGON, UKEA, BELGONUCLEAIRE and CEA.

The BELGONUCLEAIRE objective of this experiment was the behaviour comparison at high temperature of standard uranium and plutonium coated particles.

Table of Content

List of Tables

List of Figures

1. INTRODUCTION

The MET V experiment, irradiated in the DRAGON reactor, was a serie of three high temperature experiments (900-1600°C in five temperature regions) which have all the same fuel loading but which differ mainly in the irradiation time (for 1, 2 and 4 irradiation cycles). It was a collaborative experiment between CEA, Dragon project, UKAEA, Kernforschungsanlage, and BN.
The purpose of this experiment was

- for all the participants except BN, the study of the suppression of the internal CO pressure in the carbon coated oxide particle by the variation of the chemical composition of the kernel,
- for BN, the study of the comparative behaviour at high temperature of standard uranium and plutonium coated particles.

This part reports only the behaviour of the Belgonucleaire particle fuel.

2. PARTICLES CHARACTERISTICS

2.1. Pu coated particles

Three types of different Pu particles according to their kernel fabrication have been irradiated during the MET experiment:

- Pu type T particles with undiluted kernels manufactured by TUI according to a SOL-GEL process;

- Pu type C particles with undiluted kernels manufactured by the CNEN according to the SNAM process;

- Pu type D particles with diluted kernels elaborated by BN-CEN/SCK according to a power agglomeration process.

All the coatings were performed by BN-SCK/CEN. Fabrication processes are detailed in the FRJ2 experiment.

Characteristics of the Pu coated particles are presented in Table 1.

Cross sections of the Pu particles are shown in Figure 1.

2.2. U coated particles

The characteristics of the U particles are presented in Table 2.

No pictures of U coated particles are available.

3. GEOMETRY DESIGN

The fuelled length in the DRAGON core was 1612 mm. This length was divided into five temperature regions and each temperature was divided amongst the five experiment participants of the MET V program.

The experimental specimens were arranged in 27 "nut and bold" carriers of 60 mm length (Figure 2). The active length of each bolt for the monolayer coupons or trays which carry the fuel particles was 47 mm.

The BN particles were loaded as loose particle in trays of 22 mm outside diameter and 10 mm inside diameter. The Pu particles have been loaded in 68 holes trays. The 40 holes of the outer ring only have been filled whereas the 28 holes of the inner ring have been left empty (Figure 3/A). The U particles were loaded in 52 holes trays (Figure 3/B).

The loading plan of the BN fuel carriers and trays identification for the three experiments are respectively given in Table 3 and 4.

4. IRRADIATION HISTORY

The irradiation of the MET V experiment was completed in three parts.

4.1. MET V (1)

The first part of the irradiation was launched in July 1972 during the charge IV core 5 in the fuel element n°521 for 88 days. The estimated accumulated maximum fast neutron dose was 3.6×10^{20} n.cm^{-2} DNE. The best estimate of the maximum average fuel temperature over the core length is given in Figure 4. The burn-up profile of the MET V (1) experiment is shown in Figure 5; the overall burn-up, calculated from the fission product inventory, was 11.8%FIFA.

4.2. MET V (2)

The second part of the irradiation was made during the charge IV cores 5 and 6 in the fuel element n°522 for 152 days.

The best estimate of the maximum averaged fuel temperature profiles at the start and the end of each cores are presented in Figures 6 to 9.

The estimated accumulated maximum fast neutron dose was 5.8×10^{20} n.cm^{-2} DNE. The axial distribution of the fast neutron dose is given in Figure 10.

The burn-up profile of the MET V (2) experiment, determined on 18% enriched particles, is given in Figure 11.

4.3. MET V (3)

The MET V (3) has been irradiated in the fuel element n°523 for 320 days during the charge IV cores 5 and 6 and during the charge V, cores 1, 2 and 3.

The best estimate of the maximum averaged fuel temperature profiles during the charge IV are presented in Figures 6 to 9.

The estimated accumulated maximum fast neutron dose was 1.25×10^{21} $n.cm^{-2}$ DNE. During the experiment, a decrease of the peak temperature from 1520°C to 1300°C for the fuel and 1000°C to about 950°C for the outer surface of the graphite sleeve has been measured.

The measurements carried out by the UKEA on the 18% enriched U particles have determined a peak burn-up about 48.8% FIFA.

The main characteristics of the three irradiations of the MET V experiment are gathered in Table 5.

5. POST-IRRADIATION EXAMINATIONS

5.1. PIE on MET V (1)

The post-irradiation examinations have been carried out in HARWELL and ISPRA for the MET V (1)

The visual examination of the trays did not reveal any damage of the graphite components or of the fuel particles. Pictures of the trays with the particles are shown in Figure 3.

However, the alpha-radiography of the emptied Pu trays has shown a significant contamination revealing a high fraction of broken Pu particles (Figure 12)

Metallographies of the 3%U5 enriched particles have shown a satisfactory behaviour, no coating damage could be seen (Figure 13).

Metallographies of the PuO_2 type T particles have revealed that the outer PyC remained intact but that some SiC damage has occurred (Figures 14-16). These damages could be due to the sample preparation but most probably to the rather poor quality of the coating, which had been deposited about six years before irradiation.

An important separation between the SiC and the inner layers can be observed (Figure 14), as well as a curling and progressive change of the structure of the inner PyC (Figures 15-17); the buffer layers present a significant densification and important cracks. These observations explain the contamination revealed by the alpha-radiography.

The pre-irradiation characterisation of the PuO_2 type T particles had revealed a Pu migration limited to plutonium concentration spots in the buffer layer. The micrographies did not show any significant extension of this migration under irradiation.

5.2. PIE on MET V (2)

The post-irradiation examinations of the MET V (2) fuel have been carried out in ISPRA and SCK.

The visual examination has been carried out on all the trays of the carriers (B2-11, B2-16, B2-21, B2-26):

- All the graphite components were intact,
- No broken particles could be detected in the carrier B2-26 irradiated at a relatively low temperature (1200°C)
- Broken Pu particles could be detected in the B2-21, B2-16 and B2-11 carriers, the number increasing with the irradiation temperature
- Only a few damaged U particles could be noticed.

A TRAY WITH PU PARTICLES IS SHOWN IN FIGURE 18.

The alpha-autoradiographies carried out on the trays of the B2-16 (Figures 19-20) and B2-26 carriers (Figure 21) confirmed the good behaviour of the uranium particles and the high fractions of broken Pu particles in the carrier B2-16 irradiated at high temperature (1495°C). This was confirmed by the γ-spectrometry carried out on the emptied trays 2, 6 and 8 of the carrier B2-16, that has shown a high radioactivity from the same fission products spectrum as from the particles.

The metallographic examinations have confirmed the good behaviour of the U particles: no evidence of coating damage or kernel coating interactions have been noticed. (Figure 22).

The metallographic examinations have been carried out on three types of Pu particles of the three carriers (Figures 23-25):

Carriers B2-16 (1495°C, 4.8x10^{20} DNE) and B2-11 (1495°C, 5.75x10^{20} DNE)

The particles of these two carriers present the same behaviour: the particles are badly damaged (Figures 23 and 24), the buffer and the inner PyC have almost disappeared, the SiC has been chemically attacked, the outer PyC only seems to have survived in some cases.

One should note that the fast neutron dose in the B2-16 carrier has been estimated to:

- 9.0x10^{21} DNE at the inner surface of the buffer layer for the D particles,
- 4.32x10^{22} DNE at the inner surface of the buffer layer for the T particles,
- 3.84x10^{21} DNE at the inner surface of the PyC layer for the C particles.

Carrier B2-26 (1200°C, 2.25x10^{20} DNE)

The particles of this carrier show less damage than those of B2-16: the buffer layers have densified significantly and present important cracks; curling-up of the inner PyC and chemical attack of the SiC can also be noticed and the outer PyC is generally intact (Figure 25).

5.3. PIE on MET V (3)

As for the MET V (2), the post-irradiation examinations of the MET V (3) fuel have been carried out in ISPRA and SCK.

Pictures of the trays with particles are shown in Figure 26. The fraction of broken particles has been determined for each tray, results are given in Table 6.

The behaviour of the Pu particles depends strongly on the irradiation temperature; the limit above which the performance of the Pu particles appear not satisfactory can be estimated at about 1300°C

At that time, the low initial stoechiometry has been considered as responsible for the behaviour although a clear correlation could not be established.

The uranium particles irradiated in the same conditions than the Pu particles were all found intact and did not show any effect of the irradiation temperature (in the range of the experiment).

The alpha-radiography of the empty trays (Figures 27-28) has confirmed the results of the visual examination although they lead to estimate of lower fractions of broken particles. This can be explained by the fact that some fractures concern the outer PyC layer only and do not, therefore, lead to any contamination.

The metallographic examination of the U particles confirm their good behaviour (Figure 29):

- no evidence of coating damage has been found;
- the absence of an outer PyC layer did not lead to an increase of the fraction of broken particle (Figure 30); this was explained by the low fission gas pressure reached in these particles and the corresponding low tensile stresses in the SiC layer;
- an interaction between the kernel and the buffer PyC carbon layers can be seen on many particles (Figure 31). This reaction seems to have increased the plasticity of the PyC, which has then flown into all cracks of the kernel; EPMA has confirmed that this phase was rich in fission products, mainly caesium.

The metallographic examinations of the Pu particles have confirmed the previous observations carried out on the MET V (1) and (2) experiment. The interaction of the plutonium with the buffer and inner PyC layers, has lead to the modification of the structure of these layers, to a significant increase of their plasticity and finally to their destruction. The predominant effect of the temperature on this phenomenon is also confirmed:

- on all the intact particles, the buffer and the inner PyC layers have almost disappeared (Figure 32); in some case, the beginning of the chemical attack of the SiC layer can be seen in Figure 33;

- the outer PyC shows generally a satisfactory behaviour and is the last layer to break;

- the high plasticity of the PyC after its interaction with the plutonium can be noticed on Figure 34;

- important concentrations of fission products (confirming the high burn-up achieved) and the importance of the chemical reactions and of the migrations within the kernel can be seen in many particles (Figure 33).

The isotopic compositions have also been determined on the samples analysed at SCK. Results are given in Table 7.

Microprobe analyses have been carried out on the fuel of MET V (3) experiment.
The first was performed on a 3% enriched U particle in order to investigate the nature of the phase filling the cracks of the kernels and the buffer zone. This analysis has shown that the phase was carbon at high concentration of cesium (Figure 35).
The second microprobe analysis was performed on a Pu type C particle to investigate the fissile material distribution in a high burn-up particle. The EPMA has shown a Pu uniform migration into the zone occupied by the buffer and inner PyC layers and a Pu depletion in the central zone of the kernel (Figure 36).

5.4. Burn-up measurements

The burn-up measurements of the MET V (2) and (3) experiment have been carried out:

- in ISPRA on the U and Pu particles of the carriers B2-16 and B3-26 using the Cs137 method

- in SCK on Pu particles of the carrier B2-11, and on u and Pu particles of the carriers B3-6 and B3-11 using the cerium and neodymium indicators.

The results are gathered in Table 8.

6. CONLUSION

The post irradiation examination s carried out on the fuel particles of the MET V experiment lead to the following conclusions:

- Plutonium particles with diluted and concentrated kernel of low stoechiometry have been irradiated at temperatures ranging from 1200°C to 1500°C, up to a fast neutron dose of 1.25×10^{21} DNE and up to a burn-up of 70% FIMA. The PIEs have

revealed a strong effect of the irradiation temperature, 1300°C being a limit above which their performances are not satisfactory. The metallic cross sections and the microprobe analysis have shown that the plutonium penetrates the porous or damaged buffer layers to react with the inner PyC, modify its structure and eventually break it; then it reacts with the SiC and causes a failure of the particles.

- The 3% and 9% enriched uranium particles irradiated in the same dose and temperature conditions but to a burn-up about 6.3% FIMA did not show any damage.

		Pu particles					
		Type D		Type T		Type C	
Kernel	Manufacturing method	Powder agglomeration		Sol-gel		Sol-gel	
	Chemical form	$PuO_{1.92}$ + 20C		$PuO_{1.91}$		$PuO_{1.7}$	
	Pu/C ratio	1 / 19.5		-		-	
	Diameter	550 $^{+22}_{-27}$		267 $^{+48}_{-31}$		248 $^{+40}_{-23}$	
	Wt% Pu	47.6		88.73		89.54	
	Wt of Pu per particle (mg)	~0.123		~0.075		~0.066	
	Hg density (g/cm^3)	2.75		10.22		9.79	
	Porosity (%)	31		8		10	
	Isotopic composition Pu^{239} Pu^{240} Pu^{241} Pu^{242}	79.37 17.14 3.05 0.44		91.44 7.85 0.67 0.03		88.3 10.3 1.3 0.09	
Coating		Thickness (µm)	Density (g/cm^3)	Thickness (µm)	Density (g/cm^3)	Thickness (µm)	Density (g/cm^3)
	Porous PyC	21	~1	145 $^{+20}_{-14}$	~1	187 $^{+30}_{-20}$	~1
	HD PyC	45 ±5	1.6	31 ±1	1.66	29 ±2	1.6
	SiC	41 ±4	NA	32 $^{+2}_{-3}$	2.79	32 ±2	2.88
	HDI PyC	62 ±10	1.99	52 $^{+4}_{-7}$	1.9	53 ±5	2.04
Coated particle diameter (µm)		888		790		870	
Trays	Type	68 holes, outer ring only filled					
	N° of coated particle per tray	40		40		40	
	Trays n°	1 and 2		3, 4, 5 and 6		7 and 8	
	Pu content per tray (mg)	4.925		3.0		2.65	

Table 1: MET V experiment - Plutonium particles characteristics

		U particles					
		9% U5, buffer layer between SiC and outer PyC ref. TI/3/10/1/F	9% U5 no outer HDI PyC ref. TI/3/10/1/E	9% U5 ref. TI/3/11/2/F	9% U5 no outer PyC ref. TI/3/11/2/E	3% UE ref. GI/3/1/2/F	3% U5 no outer HDI PyC ref. GI/3/1/2/E
Kernel	Manufacturing method	Powder agglomeration					
	Chemical form	UO_2					
	Diameter	780	780	746	746	777	777
	Fuel enrichment	8.90	8.90	8.897	8.897	3.025	3.025
	Porosity (%)	18	18	14.6	14.6	11.7	11.7
	O/U ratio	2.005	2.005	2.017	2.017		
Coating thickness	Porous inner HDI (µm)	96	96	93	93	96	96
	SiC	36	36	37	37	39	39
	Low density layer	5					
	Outer HDI (µm)	35		39		37	
	Total (µm)	172	132	169	130	172	135
Coating densities	SiC (g/cm^3)	3.2	3.2	3.17		3.2	3.2
	Outer HDI (g/cm^3)	1.7		1.79		1.72	
	Outer HDI anisotropy	Very low		1.03		1.01	
Coated particle diameter (µm)		1098	1018	1062	1083	1106	1026
Trays	Type	52 holes completely filled					
	Trays n°	13	15	14	16	9 and 10	11 and 12
	U^{235} per tray (mg)	8.46	8.46	7.96	7.96	3.12	3.12

Table 2: MET V experiment - Uranium particles characteristics

N° Carrier / position in rod	Carrier identification		
	MET V (1)	MET V (2)	MET V (3)
26 (top) / 150-156 cm	B1-26	B2-26	B3-26
21 / 120-126 cm	B1-21	B2-21	B3-21
16 / 90-96 cm	B1-16	B2-16	B3-16
11 / 60-66 cm	B1-11	B2-11	B3-11
6 (bottom) / 30-36 cm	B1-6	B2-6	B3-6

Table 3: MET V experiment - BN fuel carrier – loading plan

Position Tray n°	Fuel ref.	N° of particles per tray
16	TI/3/11/2/E	52
15	TI/3/10/2/E	52
14	TI/3/11/2/F	52
13	TI/3/10/1/F	52
12	GI/3/1/2/E	52
11	GI/3/1/2/E	52
10	GI/3/1/2/F	52
9	GI/3/1/2/F	52
8	PuO_2 C	40
7	PuO_2 C	40
6	PuO_2 T	40
5	PuO_2 T	40
4	PuO_2 T	40
3	PuO_2 T	40
2	PuO_2 D	40
1	PuO_2 D	40

Table 4: MET V experiment - BN fuel trays identification

Experiment	Charge and core numbers	Irradiation time (days)	Peak fast neutron dose ($n.cm^{-2}$) DNE	Peak fuel T (°C)
MET V (1)	Charge IV, core 5	88	$3.6x10^{20}$	1380
MET V (2)	Charge IV, cores 5 and 6	152	$5.8x10^{20}$	1520
MET V (3)	Charge IV, cores 5 and 6 Charge V cores 1, 2 and 3	320	$1.25x10^{21}$	1520

Table 5: MET V experiment – Characteristics of irradiation

Carrier (irrad. T)	B3-6 (1300°c)	B3-11 (1400°C)	B3-16 (1500°C)	B3-21 (1350°C)	B3-26 (1200°C)
Tray number (particle type)					
1 (Pu-D)	17.5	72	77.5	12.5	2.5
2 (Pu-D)	12.5	27.5	65	20	2.5
3 (Pu-T)	12.5	10	23	7.5	0
4 (Pu-T)	0	12.5	27.5	9.21	0
5 (Pu-T)	7.5	10	12.8	5.3	0
6 (Pu-T)	10	15	17.5	2.5	0
7 (Pu-C)	50	60	74.4	10	0
8 (Pu-C)	42.5	60	62.5	17.5	2.5
9 (U-3% PyC)	0	0	2	0	0
10 (U-3% PyC)	0	0	0	0	0
11 (U-3% no PyC)	0	0	0	0	0
12 (U-3% no PyC)	0	0	0	0	0
13 (U-9% PyC)	0	0	0	0	0
14 (U-9% PyC)	0	0	0	0	0
15 (U-9% no PyC)	0	0	0	0	0
16 (U-9% no PyC)	0	0	0	0	0

Table 6: MET V (3) – Fraction of broken particles in the trays (%)
(Determination based on visual examination)

Particle	Sample	Pu^{238}	Pu^{239}	Pu^{240}	Pu^{241}	Pu^{242}
Pu type T	Initial	<0.01	91.44	7.85	0.67	0.03
	B3-6 tray 4	0.623	23.825	46.746	22.236	6.57
	B3-11 tray 4	0.931	13.503	44.377	29.137	12.052
Pu type C	Initial	<0.01	88.3	10.3	1.3	0.09
	B3-11 tray 7	1.836	10.751	31.849	36.561	19.003
U-9%		U^{234}	U^{235}	U^{236}	U^{238}	Pu/ U+Pu (%)
	initial	0	9	0	0	0
	B3-11 tray 13	0.057	4.929	1.122	93.892	2

Table 7: MET V (3) - Isotopic composition

	Carrier	Sample N°	Particle type	Burn-up (GWd/t_M)	Temperature (°C)
METV (2)	B2-16	Tray 10	3% U-235 enriched 3% U-235 enriched	5.7 [1] 5.6 [1]	1495
		Tray 14	9% U-235 enriched 9% U-235 enriched	8.7 [1] 10.3 [1]	1495
		Tray 6	Pu type T Pu type T Pu type T Pu type T	387 [1] 280 [1] 586 [1] 412 [1]	1495
	B2-11	Tray 3	Pu type T Pu type T Pu type T	420 [1] 426 [1] 425 [1]	1495
MET V (3)	B3-26	Tray 6	Pu type T Pu type T Pu type T	280 [1] 373 [1] 280 [1]	1200
		Tray 10	3% U-235 enriched 3% U-235 enriched 3% U-235 enriched 3% U-235 enriched	7.3 1 6.3 1 8.3 1 6.8 1	1200°C
		Tray 14	9% U-235 enriched 9% U-235 enriched 9% U-235 enriched	16.8 1 11.5 1 13.5 1	1200
	B3-6	Tray 4	Pu type T	540 [2] 561 [3] 560 [4]	1300
	B3-11	Tray 4	Pu type T	582 [2] 623 [3] 620 [4]	1400
		Tray 7	Pu type C	630 [2] 678 [3] 671 [4]	1400
		Tray 13	9% U-235 enriched	601 [2] 588 [3] 390 [4]	1400

Burn-up measure on [1]: Cs^{137} [2]: Ce^{144} [3]: Nd^{148} [4]: Nd^{tot}
Conversion %FIMA GWd x9.6

Table 8: MET V (2) and (3) - Burn-up measurements

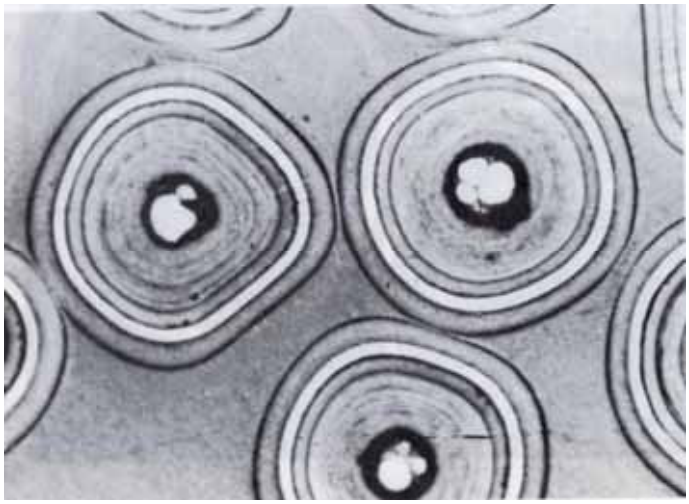

X50

T particles

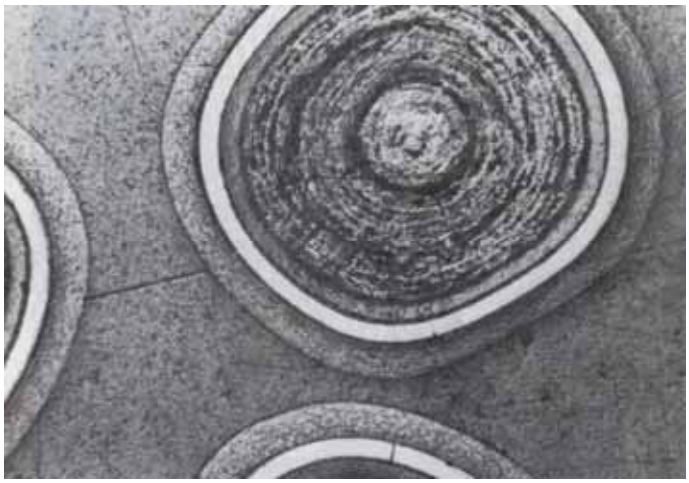

X75

C particles

X70

D particles

Figure 1: As fabricated Pu coated particles

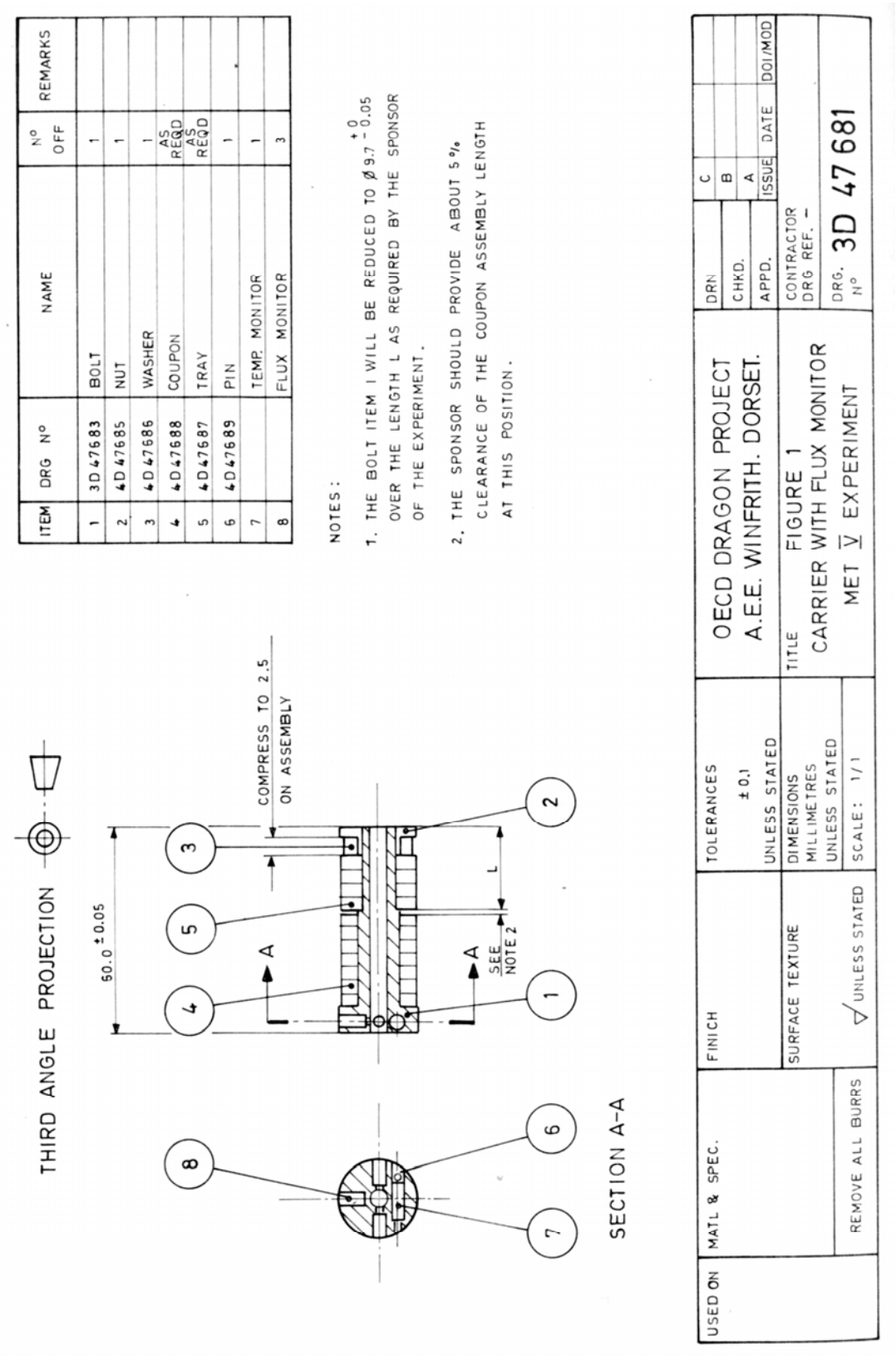

Figure 2: Design of the carrier of MET V experiment

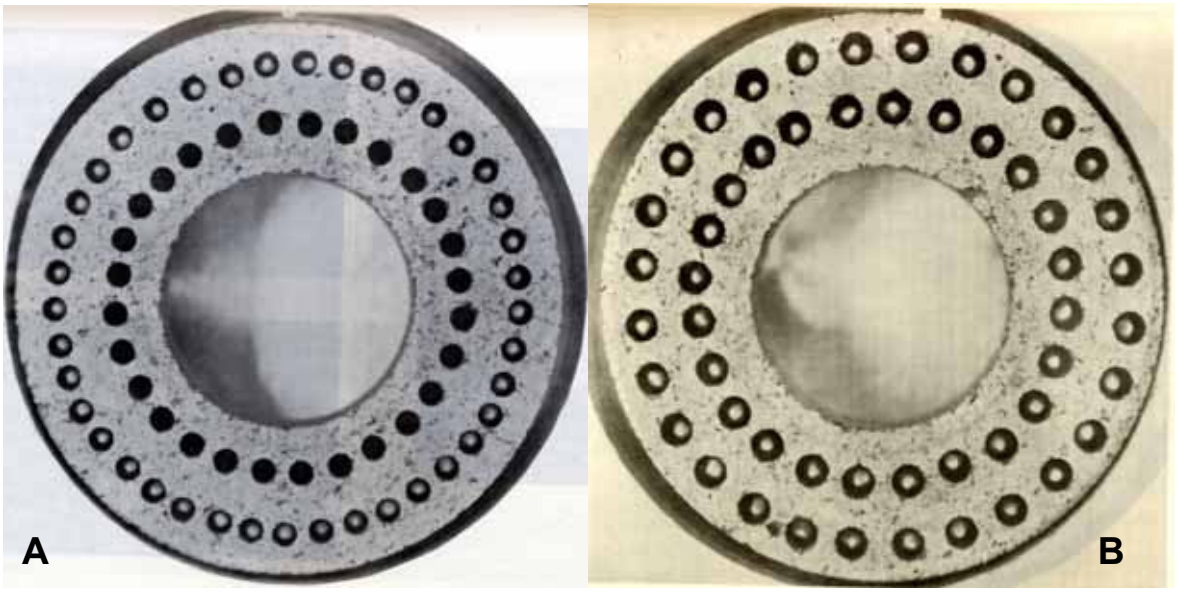

Figure 3: MET V (1) – Photographs of trays
A/ Tray 7 of the carrier B1-26 – Pu type C particles
B/ Tray 11 of the carrier B1-26 - (3.025%U235 enriched particles batch GI/3/1/2/F)

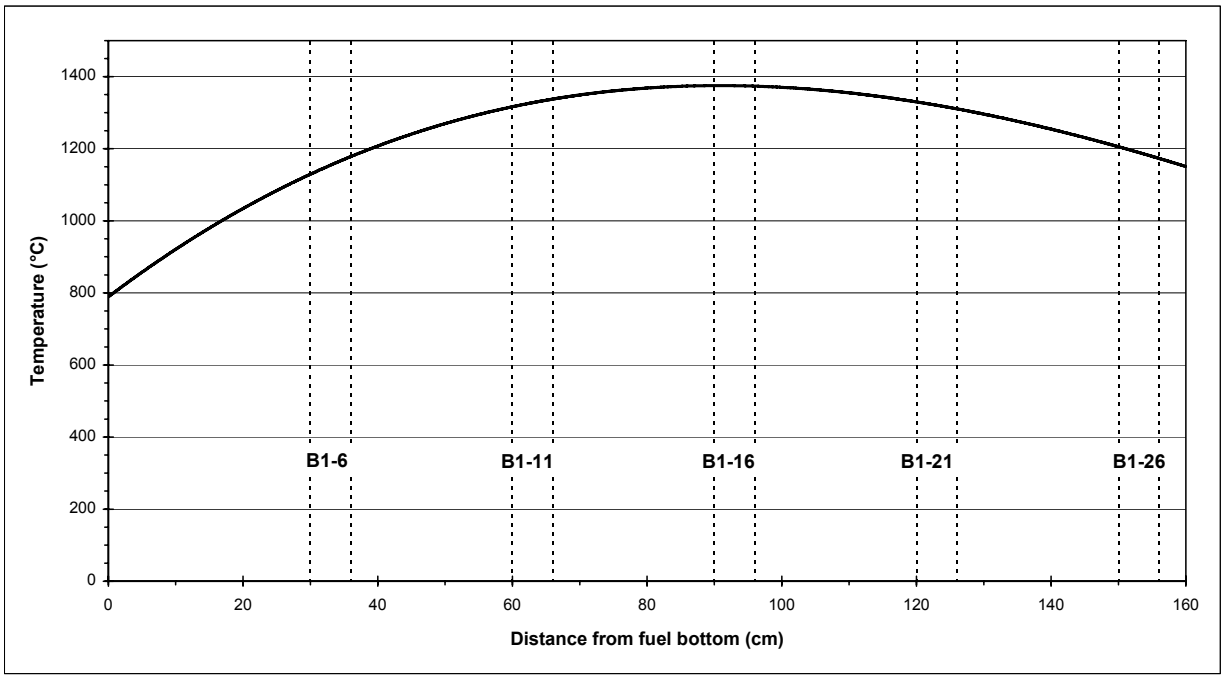

Figure 4: MET V (1) - Maximum fuel temperature averaged over core length (Charge IV end of core 5)

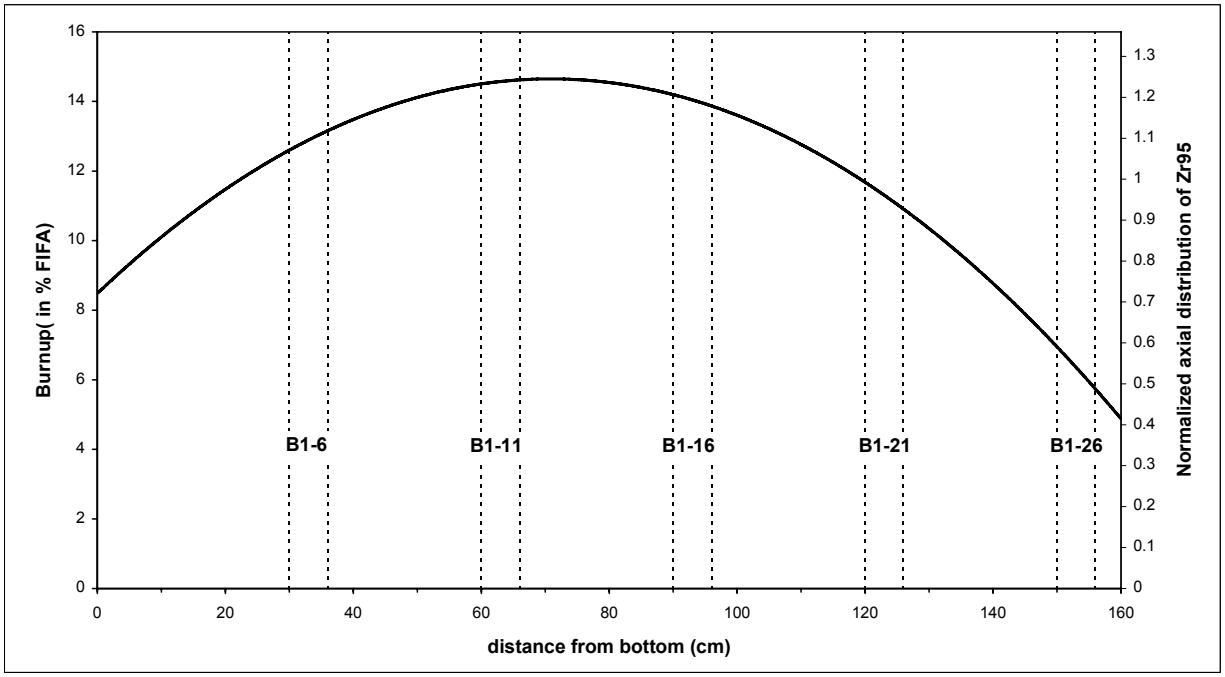

Figure 5: MET V (1) - Burn-up profile from gamma spectrometric measurements

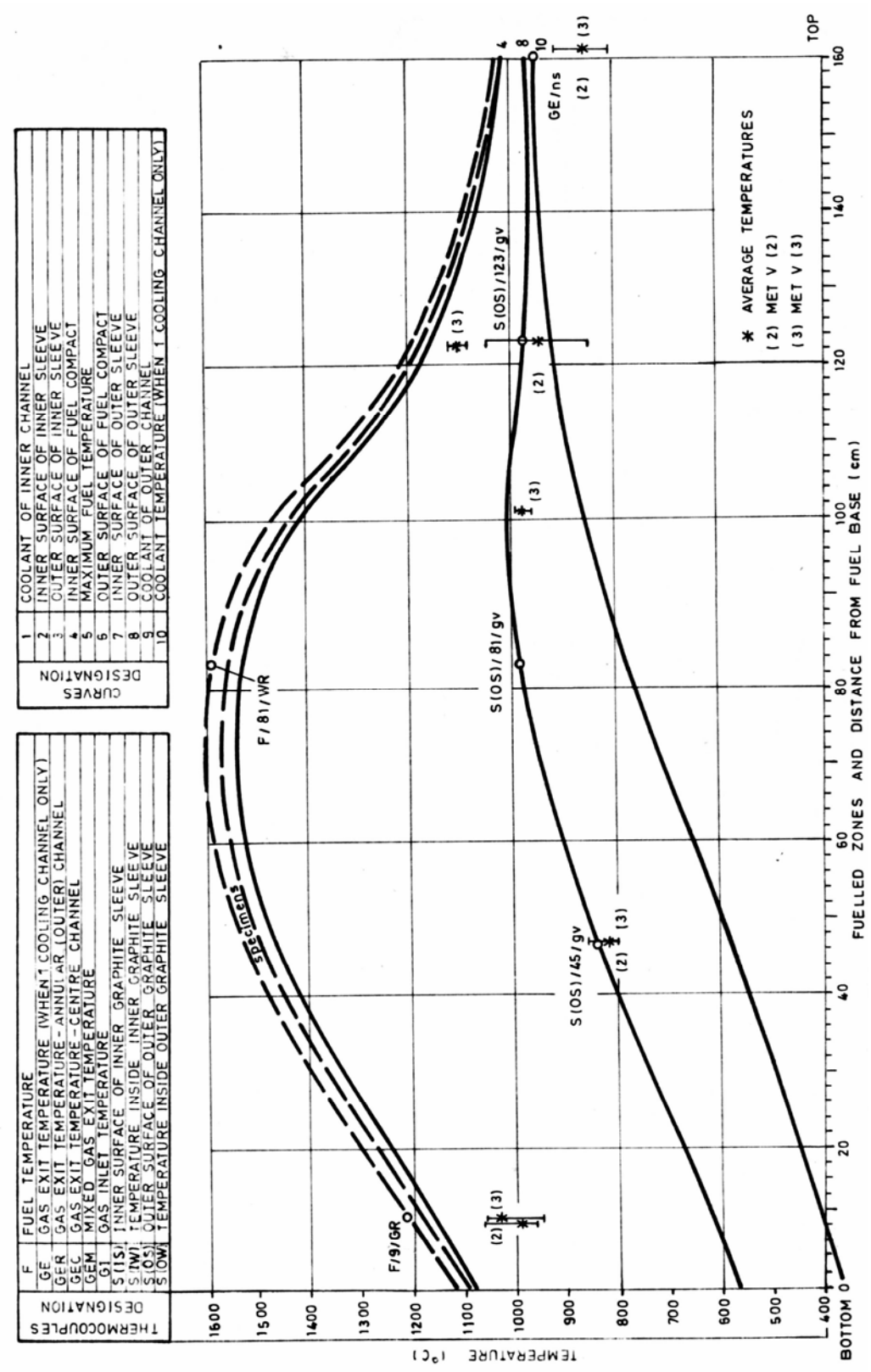

Figure 6: MET V (2)-(3) Maximum fuel temperature averaged over core length (Charge IV Start of core 5)

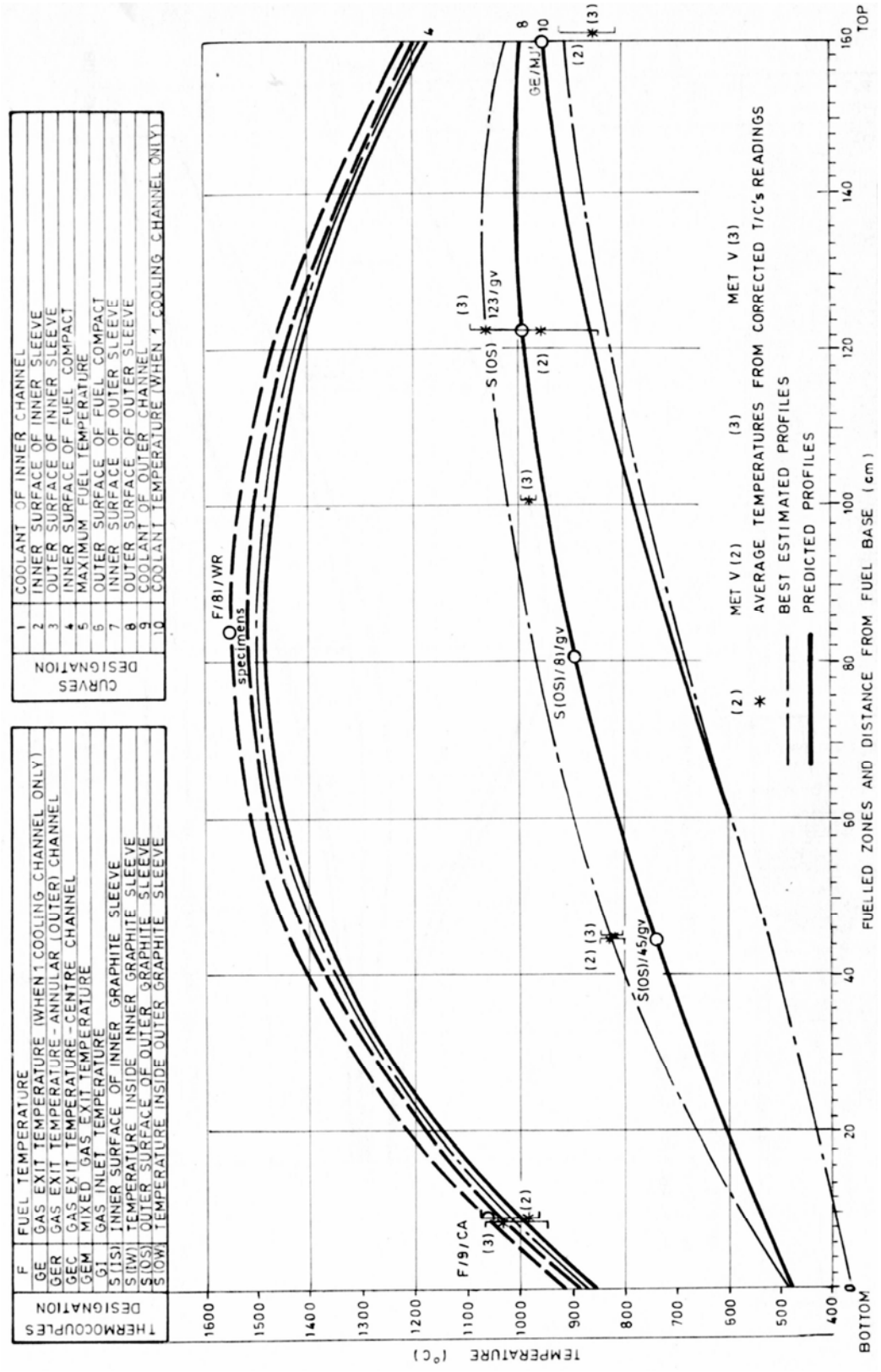

Figure 7: MET V (2)-(3) Maximum fuel temperature averaged over core length (Charge IV end of core 5)

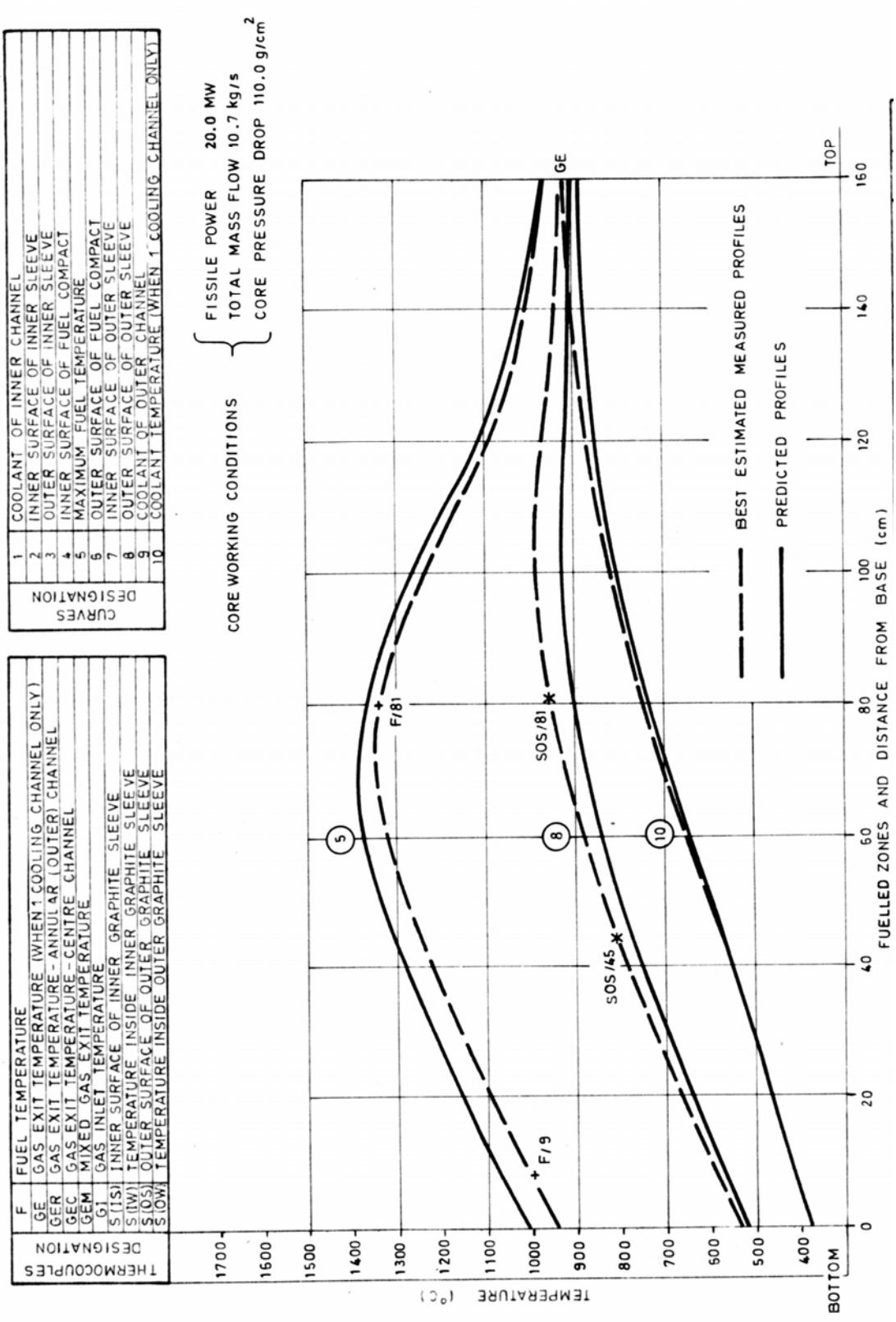

Figure 8: MET V (2)-(3) Maximum fuel temperature averaged over core length (Charge IV start of core 6)

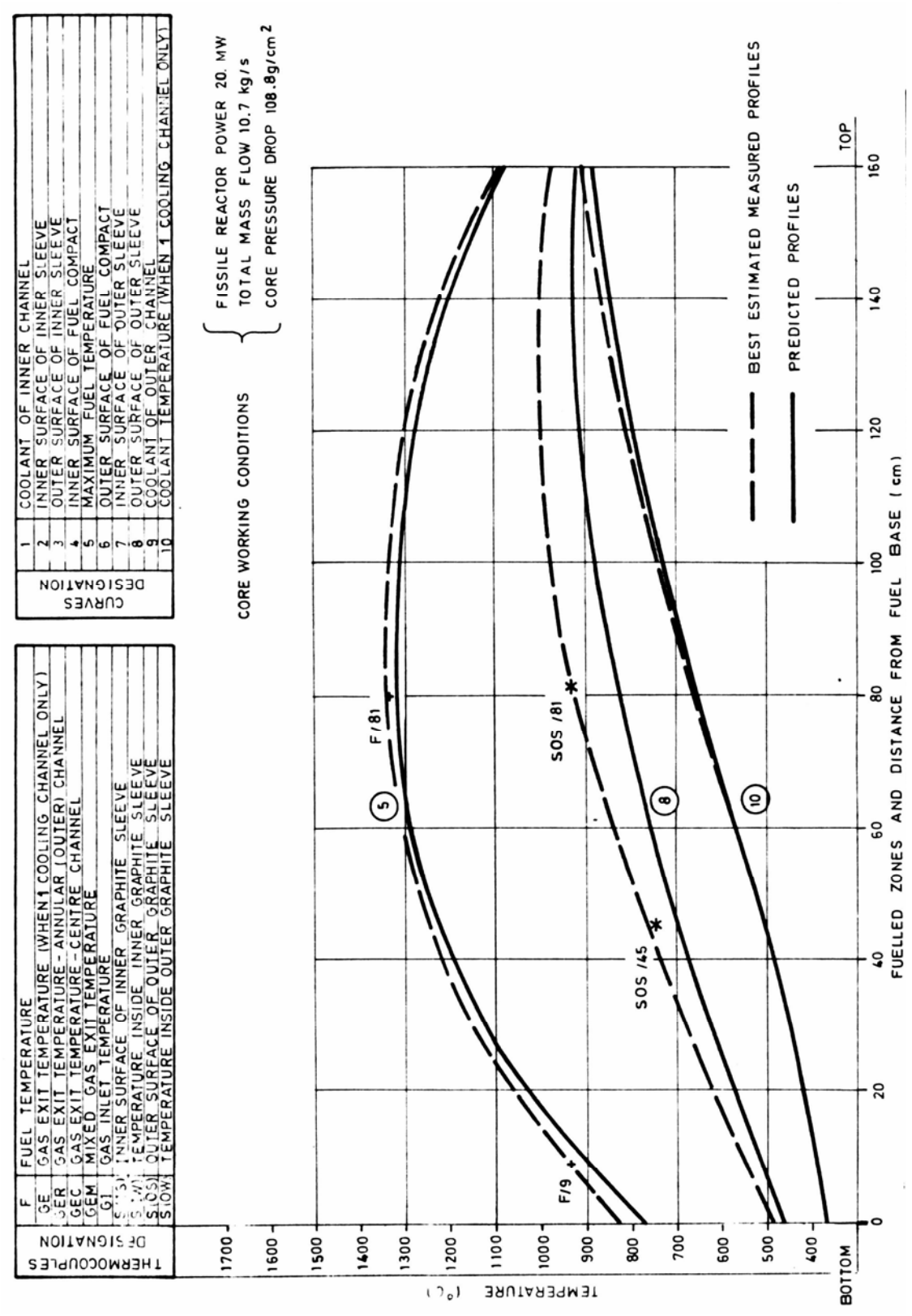

Figure 9: MET V (2)-(3) Maximum fuel temperature averaged over core length (Charge IV start of core 6)

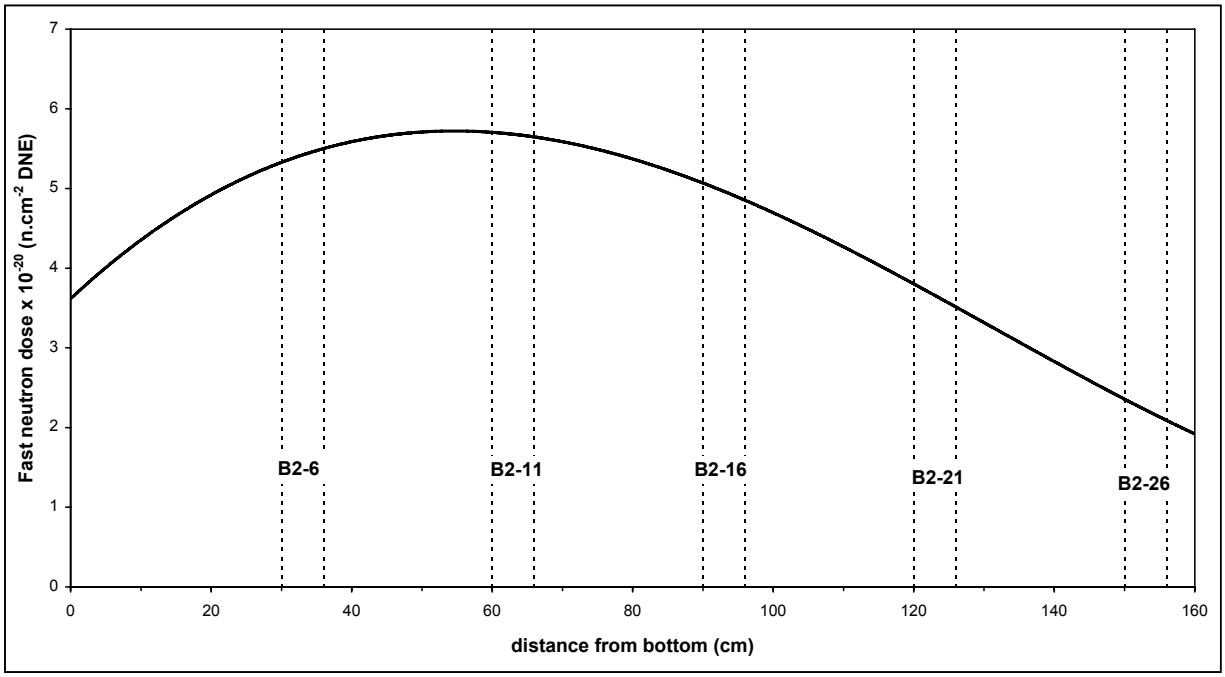

Figure 10: MET V (2) – Profile of the Neutron dose accumulated (Charge IV core 5 and 6)

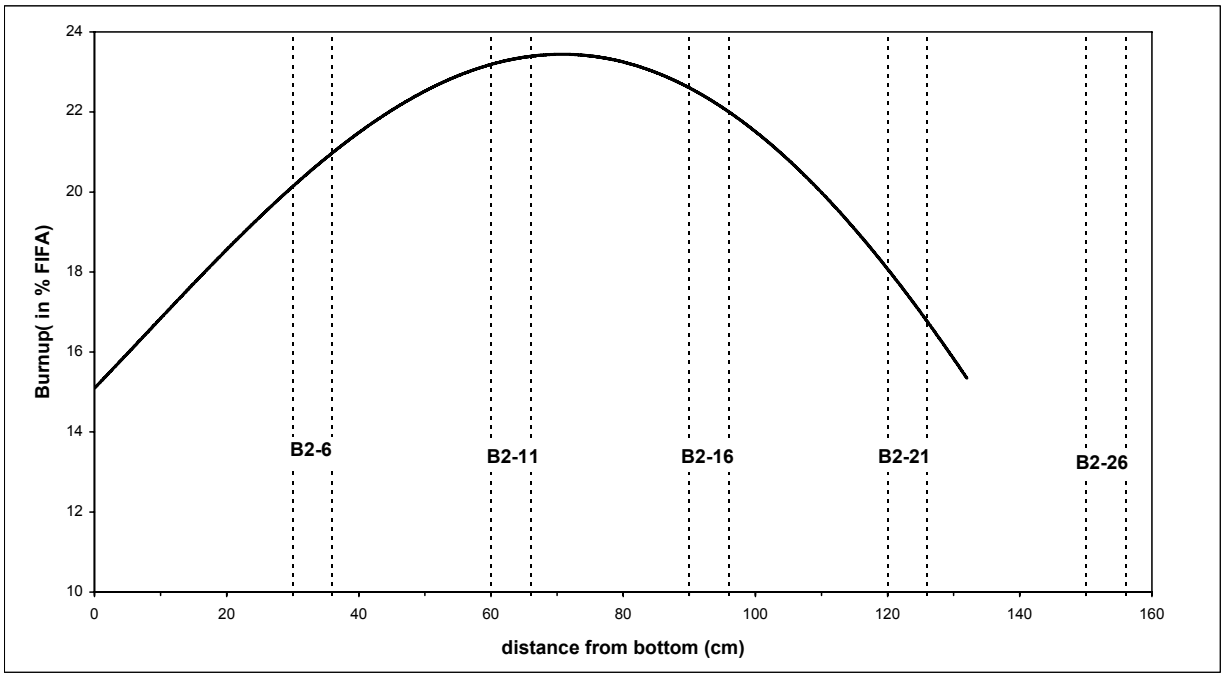

Figure 11: MET V (2) – Burn-up profile (Determined on 18% enriched U particles)

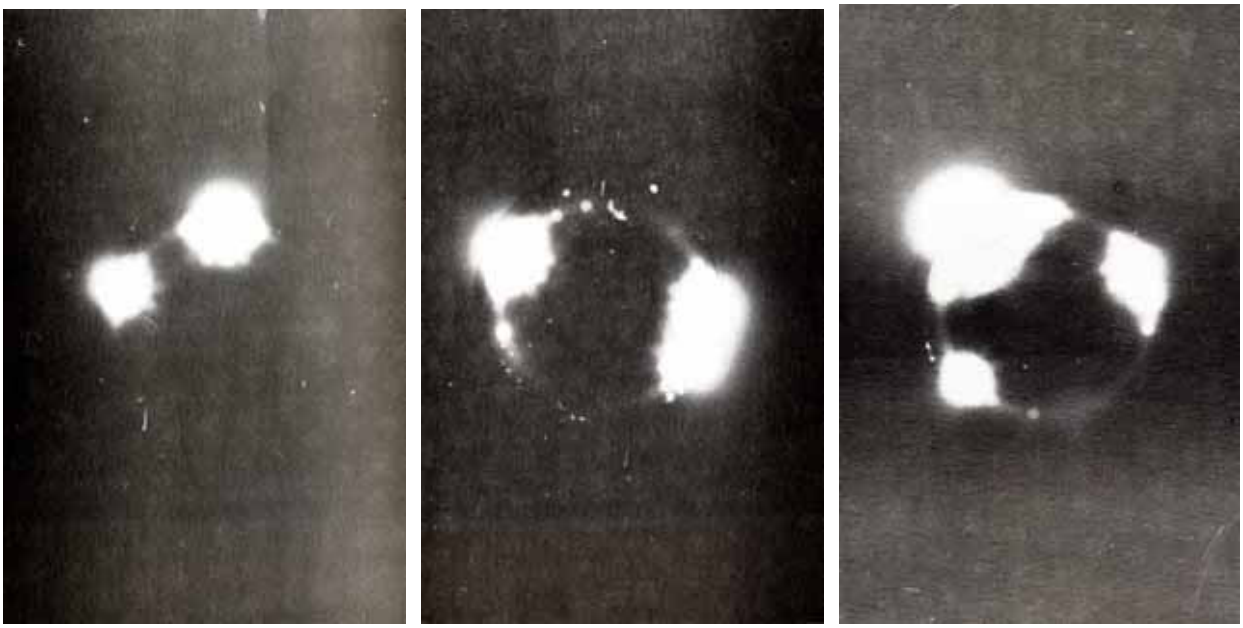

Figure 12: MET V (1) – α-autoradiography of the empty Pu trays (Carrier B1-16)

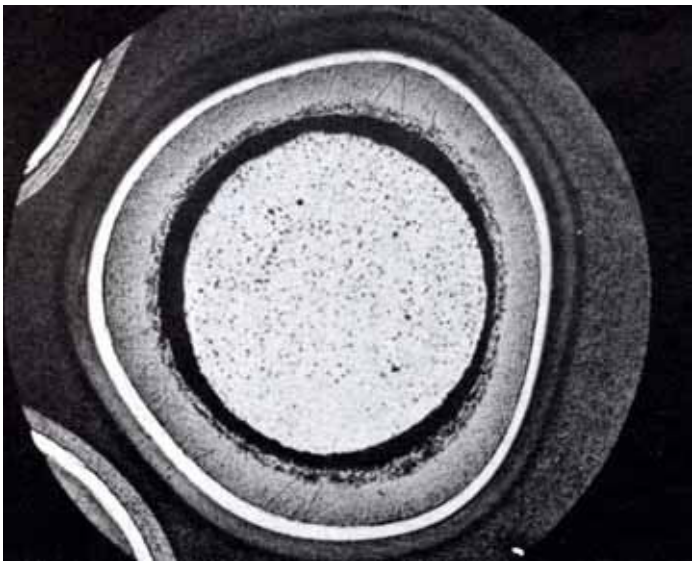

X 65

X 350

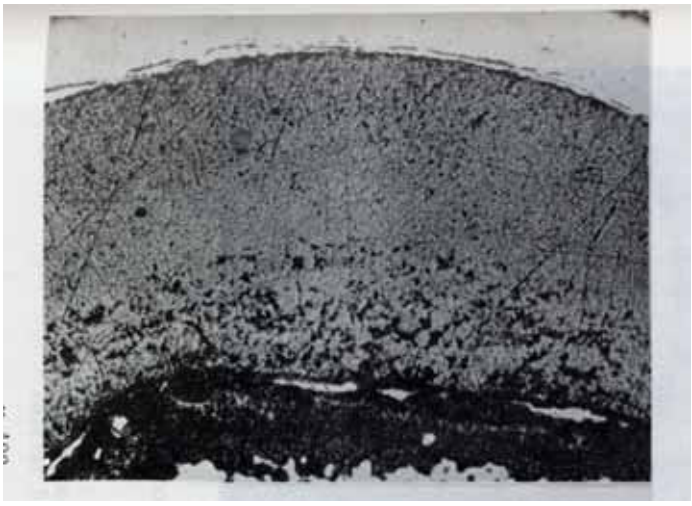

X 350

Figure 13: MET V (1) – Ceramography of 3% enriched UO_2 particle (Carrier B1-11, tray 13)

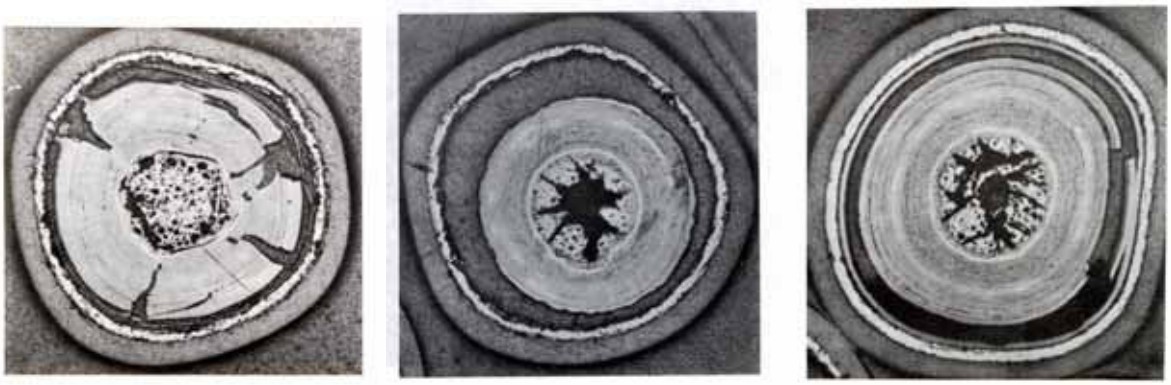

X60

Figure 14: MET V (1) – Pu type T particles from tray 16 of carrier B1-6

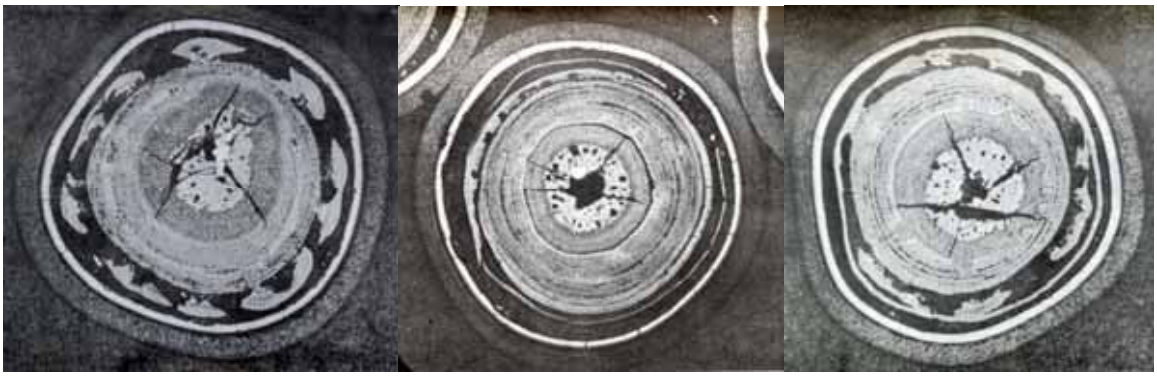

X60

Figure 15: MET V (1) – Pu type T particles from tray 16 of carrier B1-11

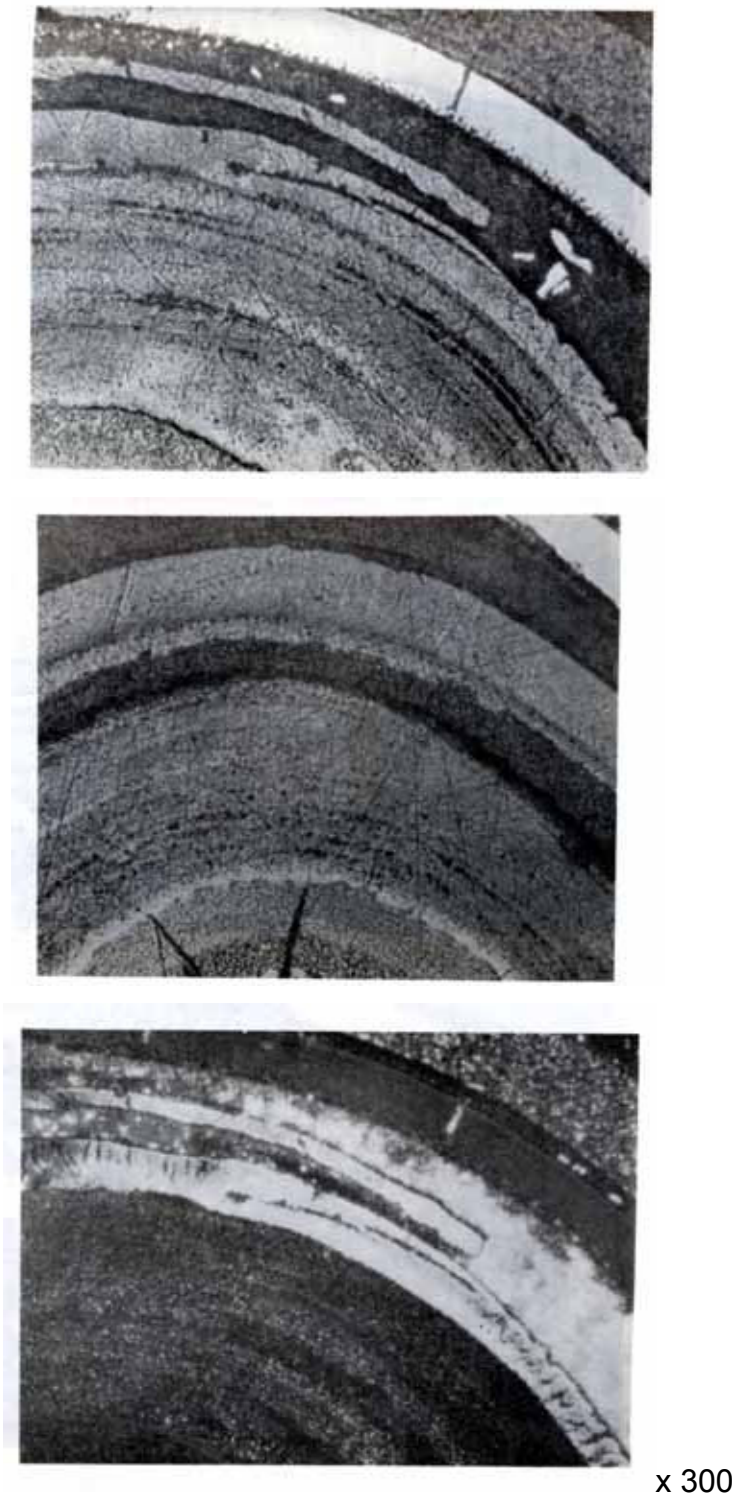

x 300

Figure 16: MET V (1) - Pu type T particles (Carrier B1-11, tray 6)

X 80 X 245

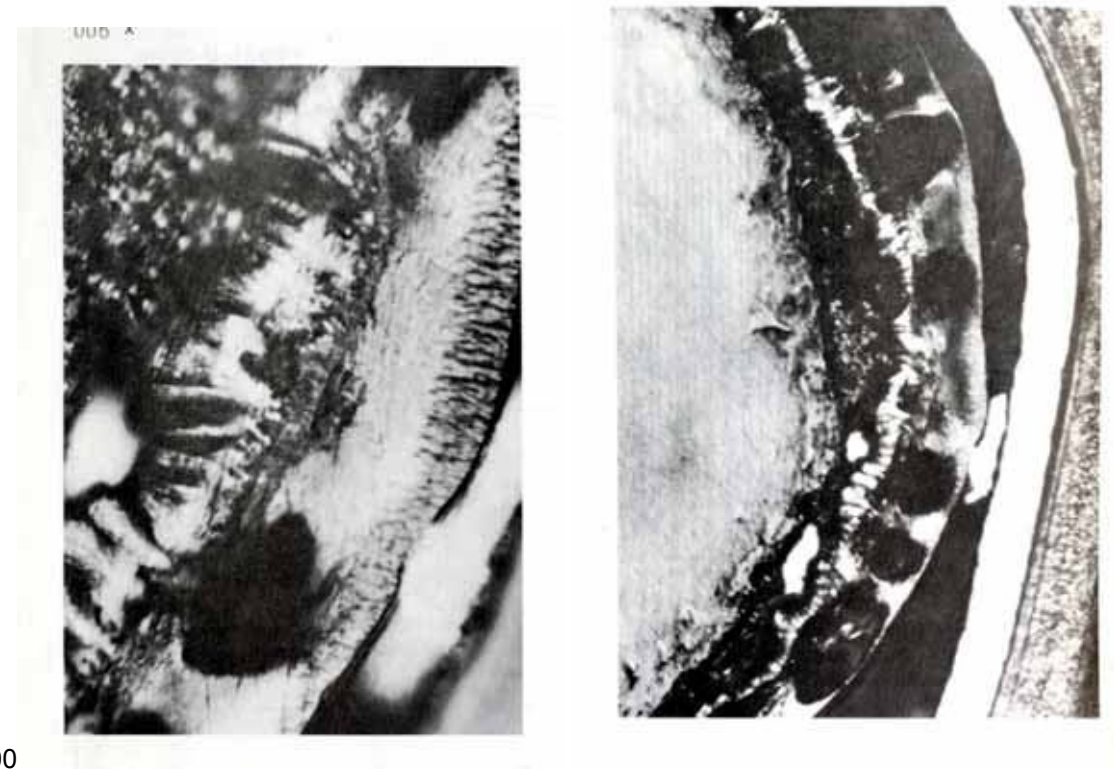

X 700 X 245

Figure 17: MET V (1) – Pu type D particles from tray 1 of carrier B1-16

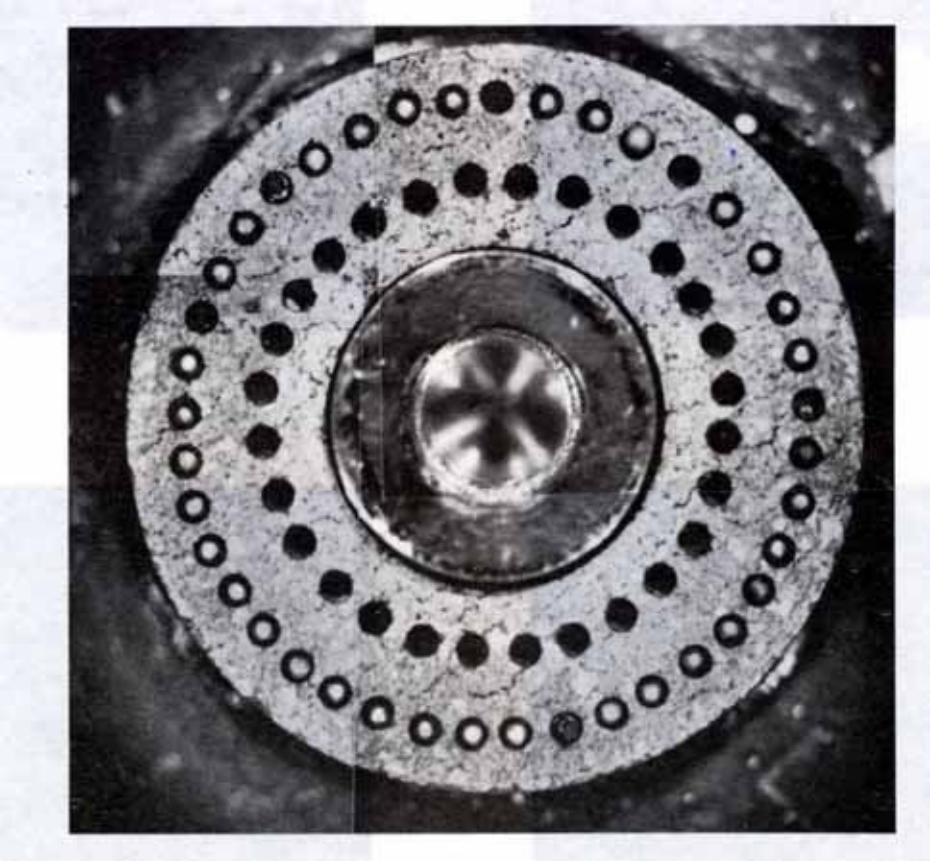

Figure 18: MET V (2) – Photograph of tray 7 of carrier B2-11 - Pu type C

Tray 10 (B2-16) - 3% enriched particle

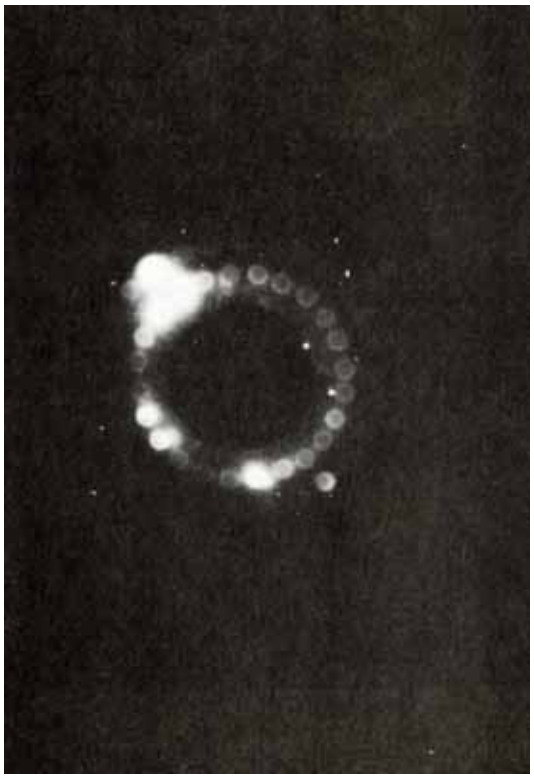

Tray 12 (B2-16) – 3% enriched particle

Tray 14 (B2-16) - 9% enriched particle

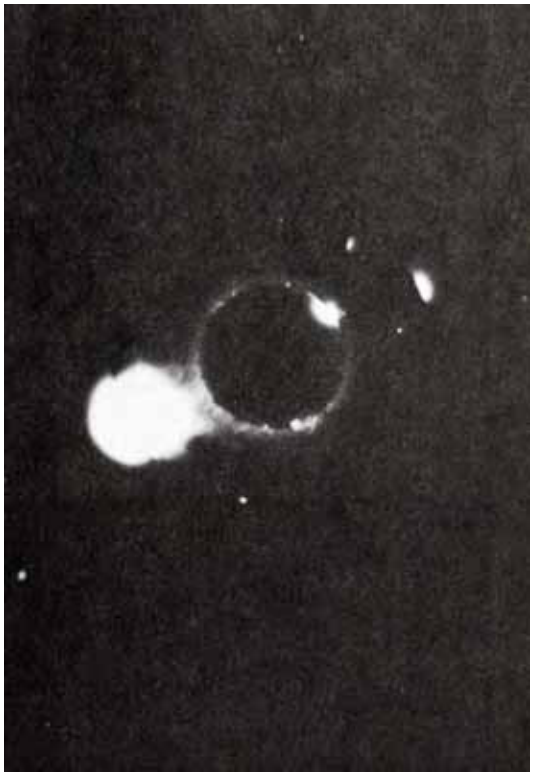

Tray 16 (B2-16) – 9% enriched particle

Figure 19: MET V (2) - α-autoradiographies on U particles

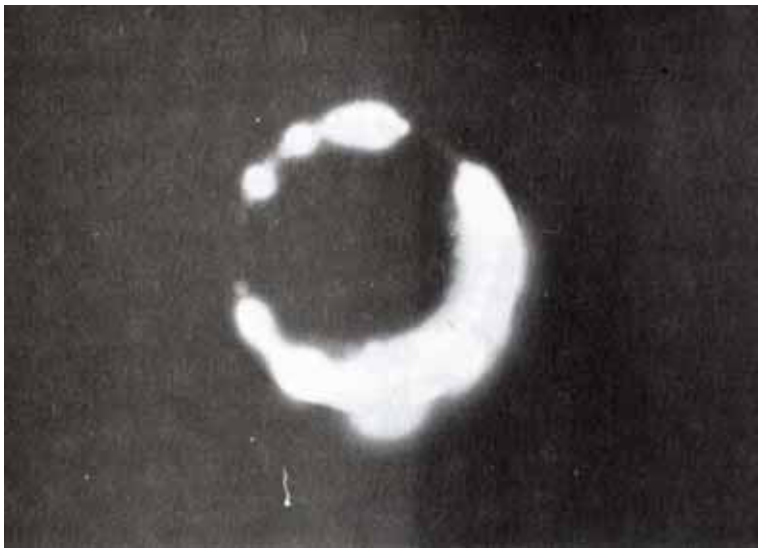

Tray 2 (B2-16) - Pu type D

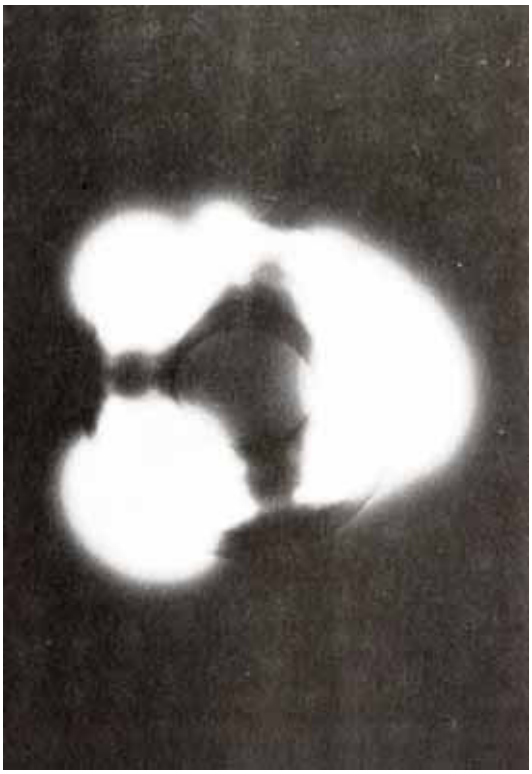

Tray 6 (B2-16) – Pu type T

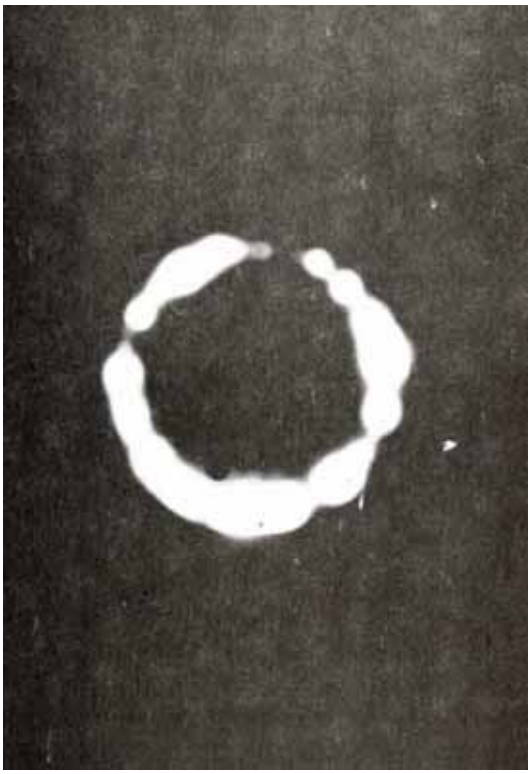

Tray 8 (B2-16) – Pu type C

Figure 20: MET V (2) - α-autoradiographies on Pu particles (T=1495°C)

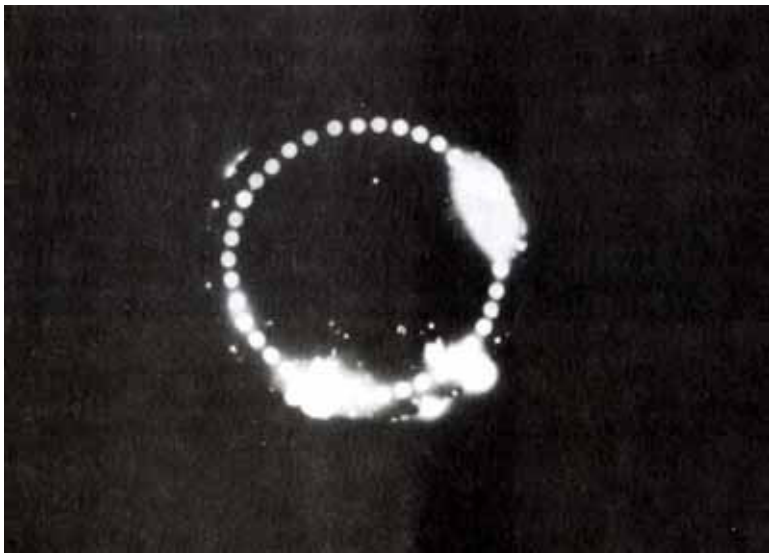

Tray 2 (B2-26) - Pu type D

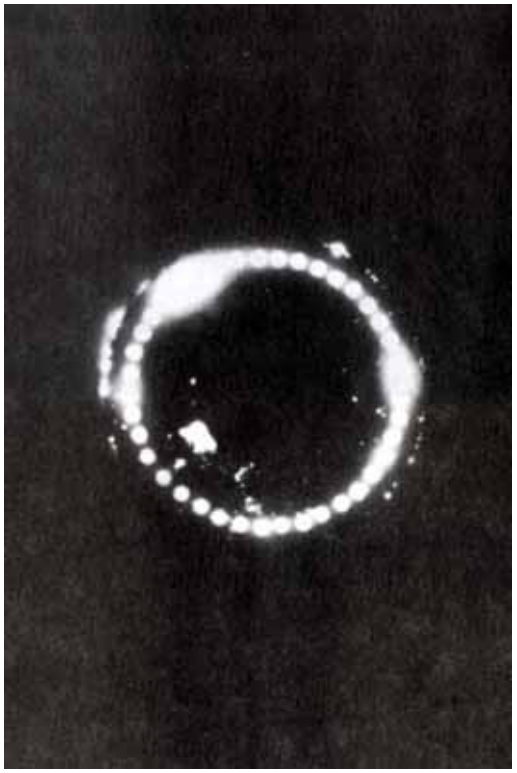

Tray 6 (B2-26) - Pu type T

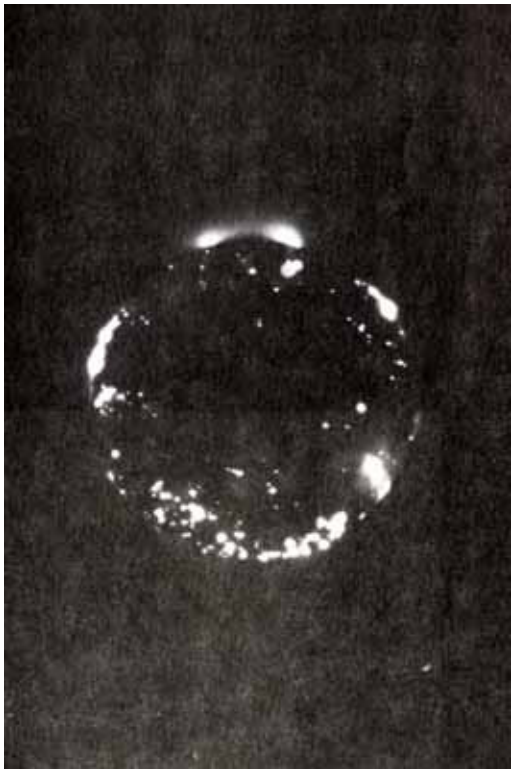

Tray 8 (B2-26) - Pu type C

Figure 21: MET V (2) - α-autoradiographies on Pu particles (T=1200°C)

Figure 22: MET V (2) - Metallography of the 3% enriched U particle

Tray 5 – Pu type T (X70)

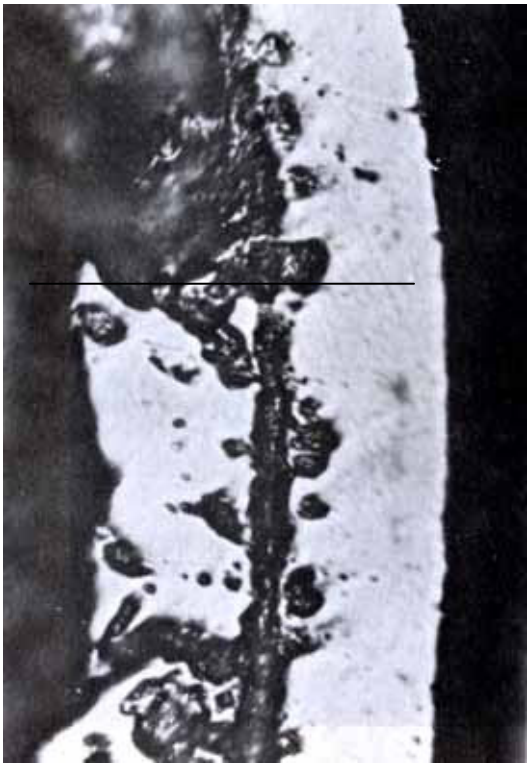

Tray 5 – Pu type T (X960)

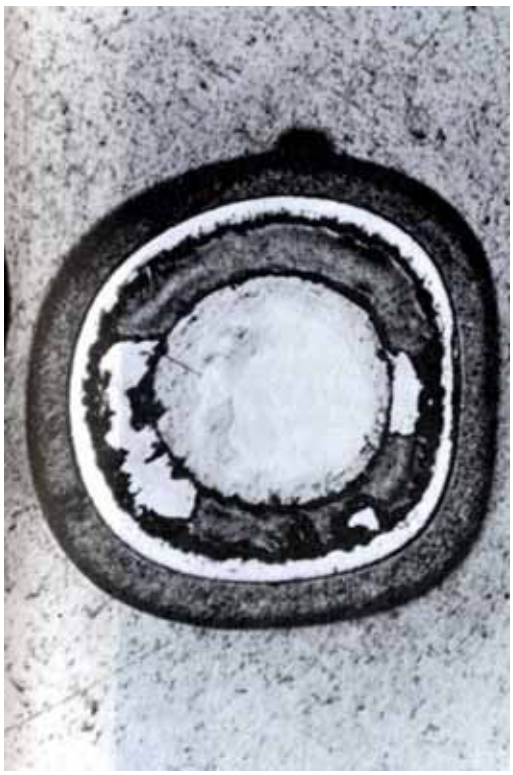

Tray 7 – Pu type C (X80)

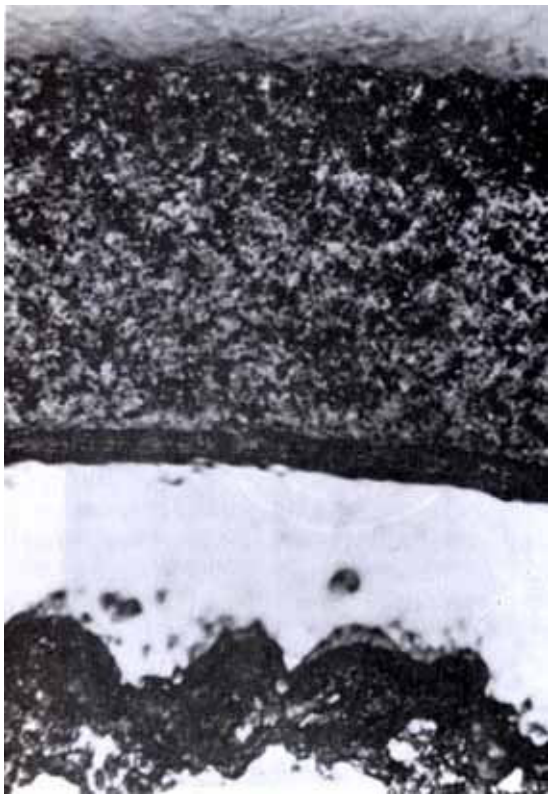

Tray 7– Pu type C (X960)

Figure 23: Met V (2) – Metallography of Pu particles of carrier B2-16

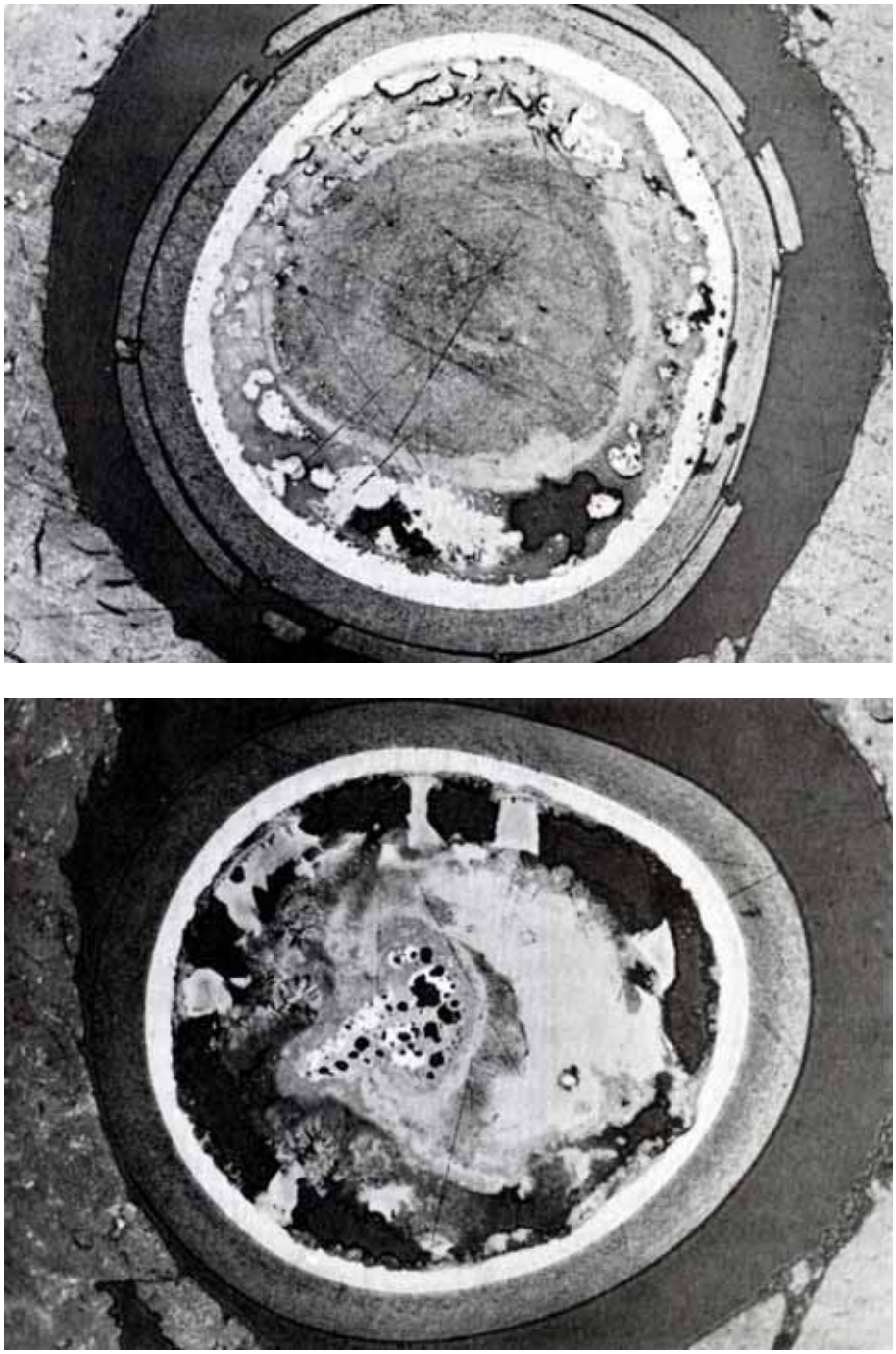

Figure 24: Met V (2) – Metallography of Pu type D particles of carrier B2-11 (Tray 2, T=1495°C)

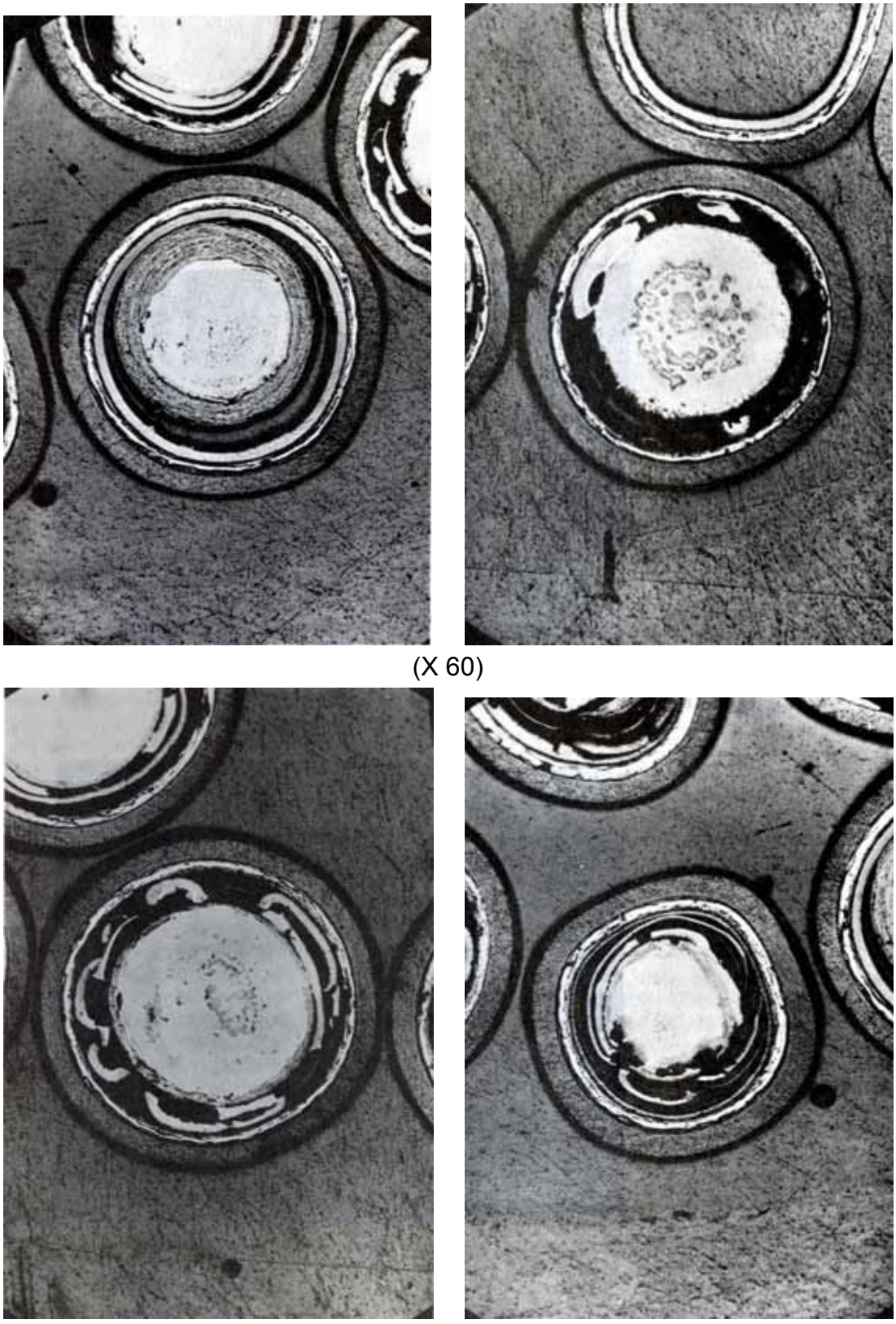

(X 60)

Figure 25: Met V (2) – Metallography of Pu type C particles of carrier B2-26 (Tray 8, T=1200°C)

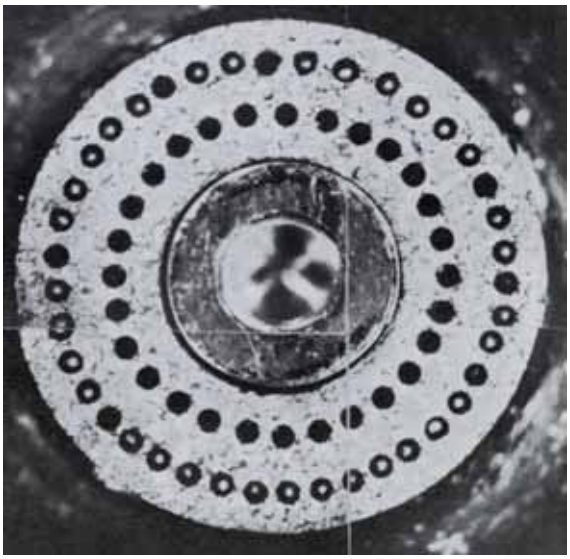

Carrier B3-11 tray 6 - Pu Type T particles

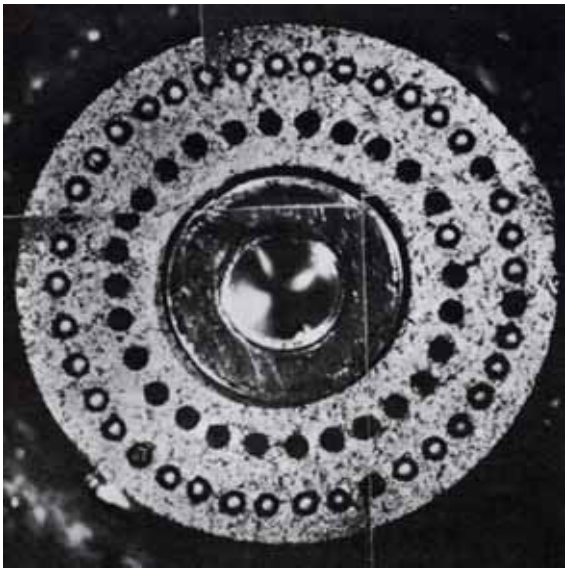

Carrier B3-6 tray 1 - Pu Type D particles

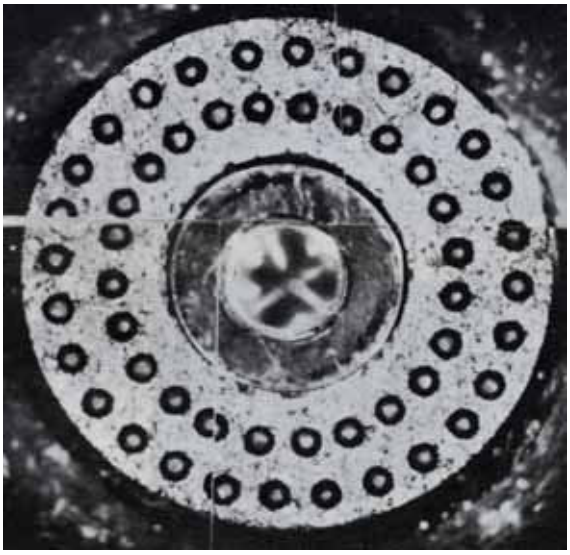

Carrier B3-11 tray 10 – 3% enriched U particles

Figure 26: MET V (3) – Photographs of trays

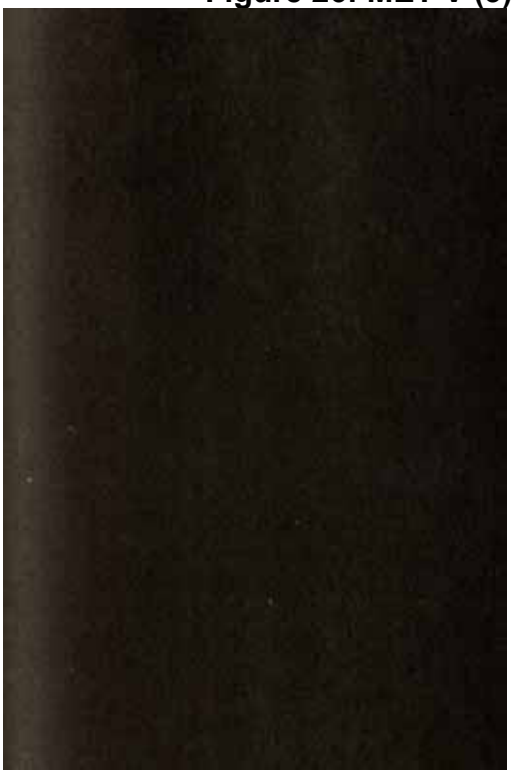

Tray 13 – 9% enriched particles

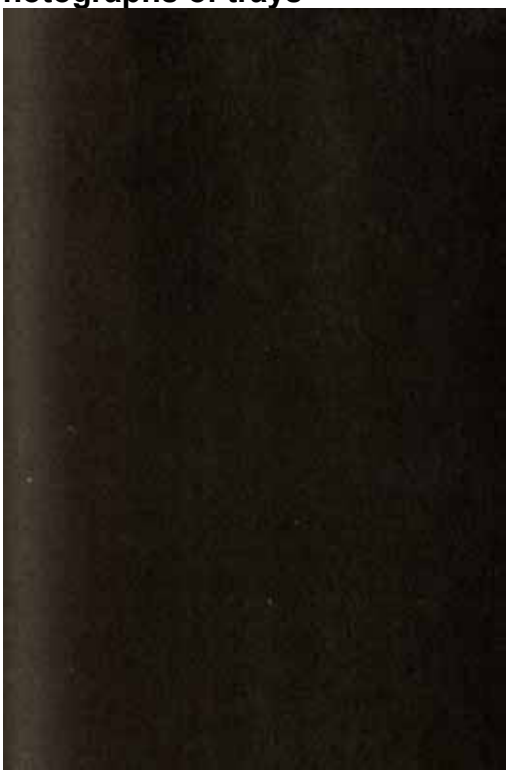

Tray 9 – 3% enriched particles

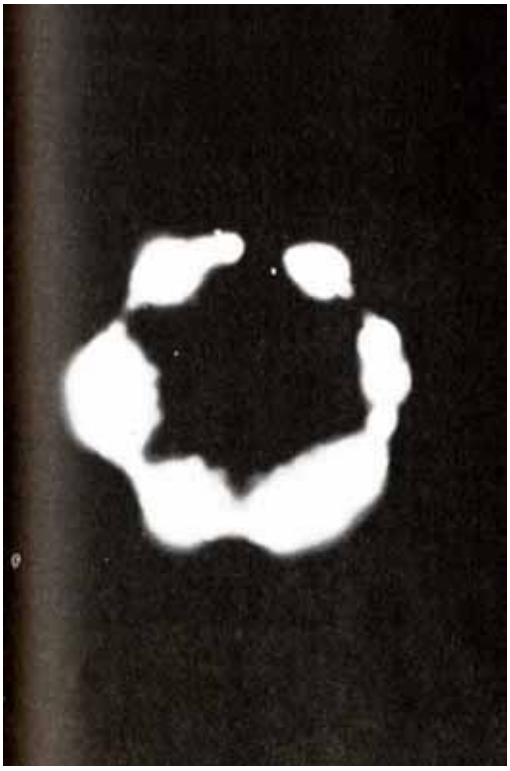

Tray 2 – Pu type D particles

Tray 6 – Pu type T particles

Figure 27: MET V (3) - α-autoradiography of empty trays

(Carrier B3-16, T=1500°C)

Tray 8 (B3-26, T=1200°C) Pu type C particles

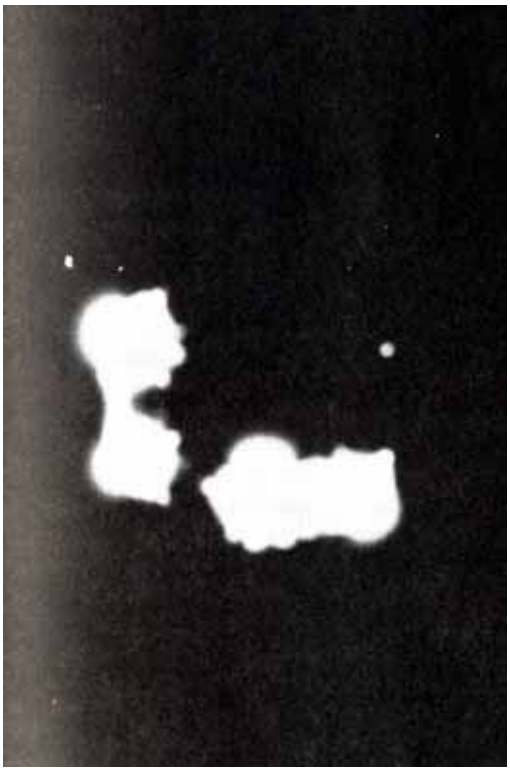

Tray 8 (B3-16, T=1500°C)
Pu type C particles

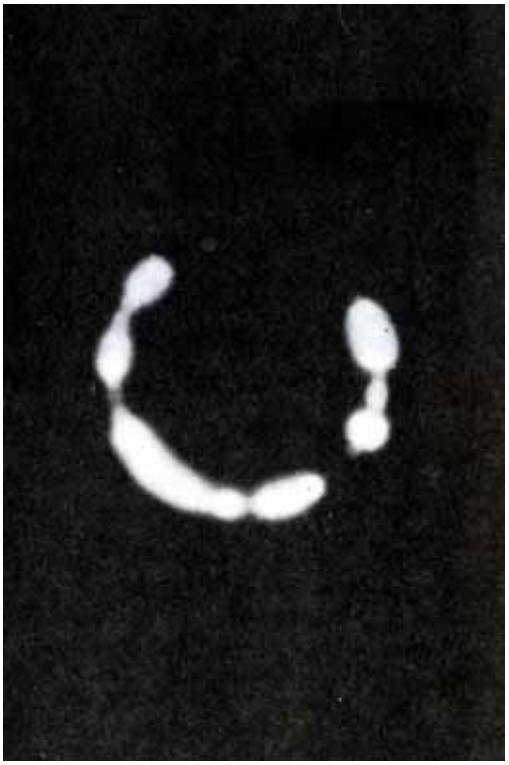

Tray 8 (B3-21, T=1350°C)
Pu type C particles

Figure 28: MET V (3) - α-autoradiography of empty trays

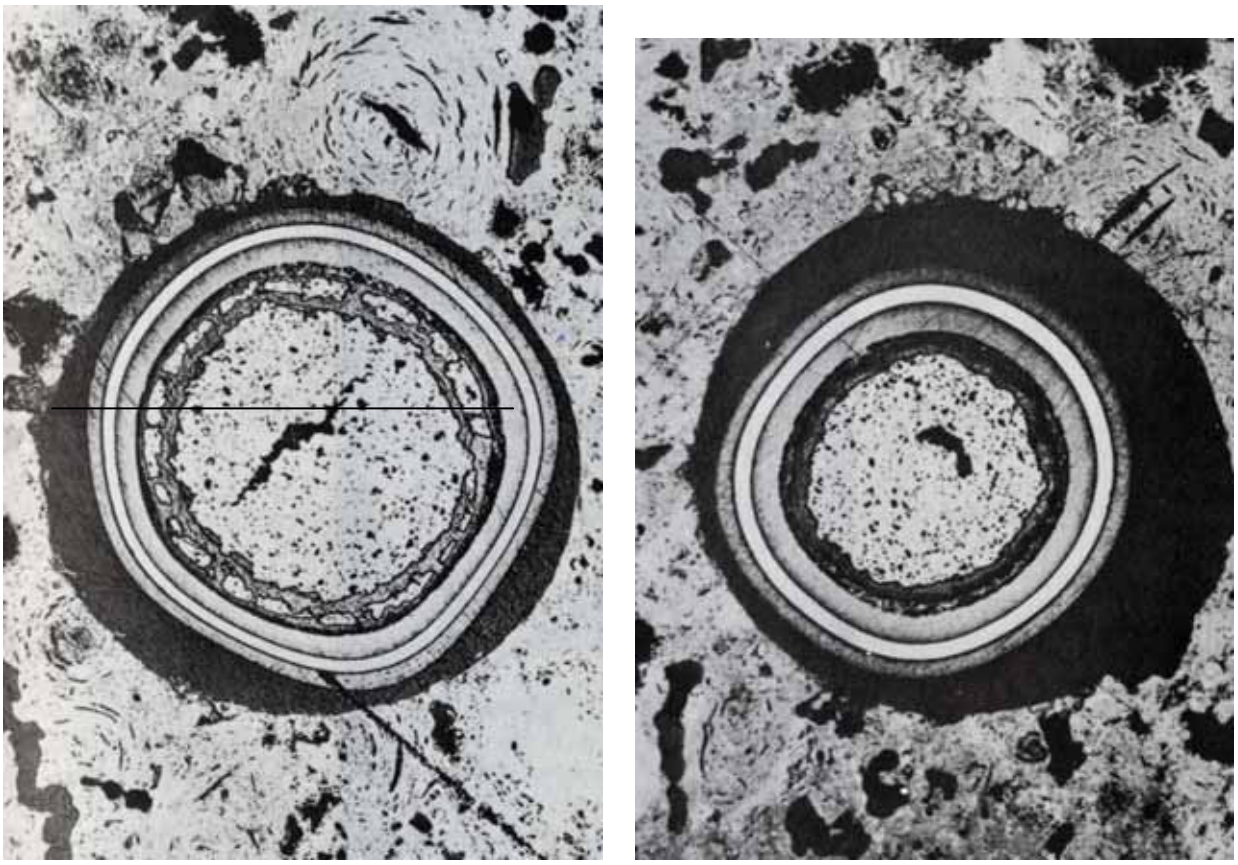

X 50

Figure 29: MET V (3) – Metallography of 3% enriched U particles (Carrier B3-11, tray 10)

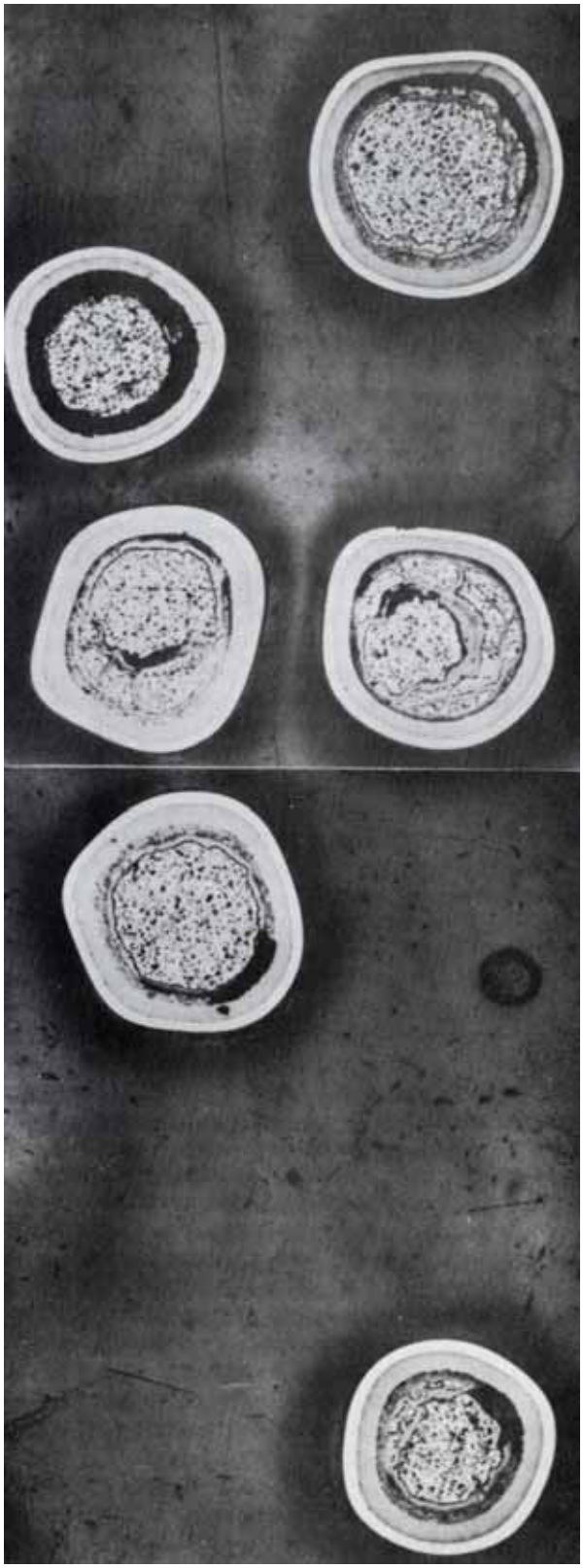

Figure 30: MET V (3) – Metallography of 3% enriched U particles without outer PyC

(Carrier B3-11, tray 12,T=1400°C)

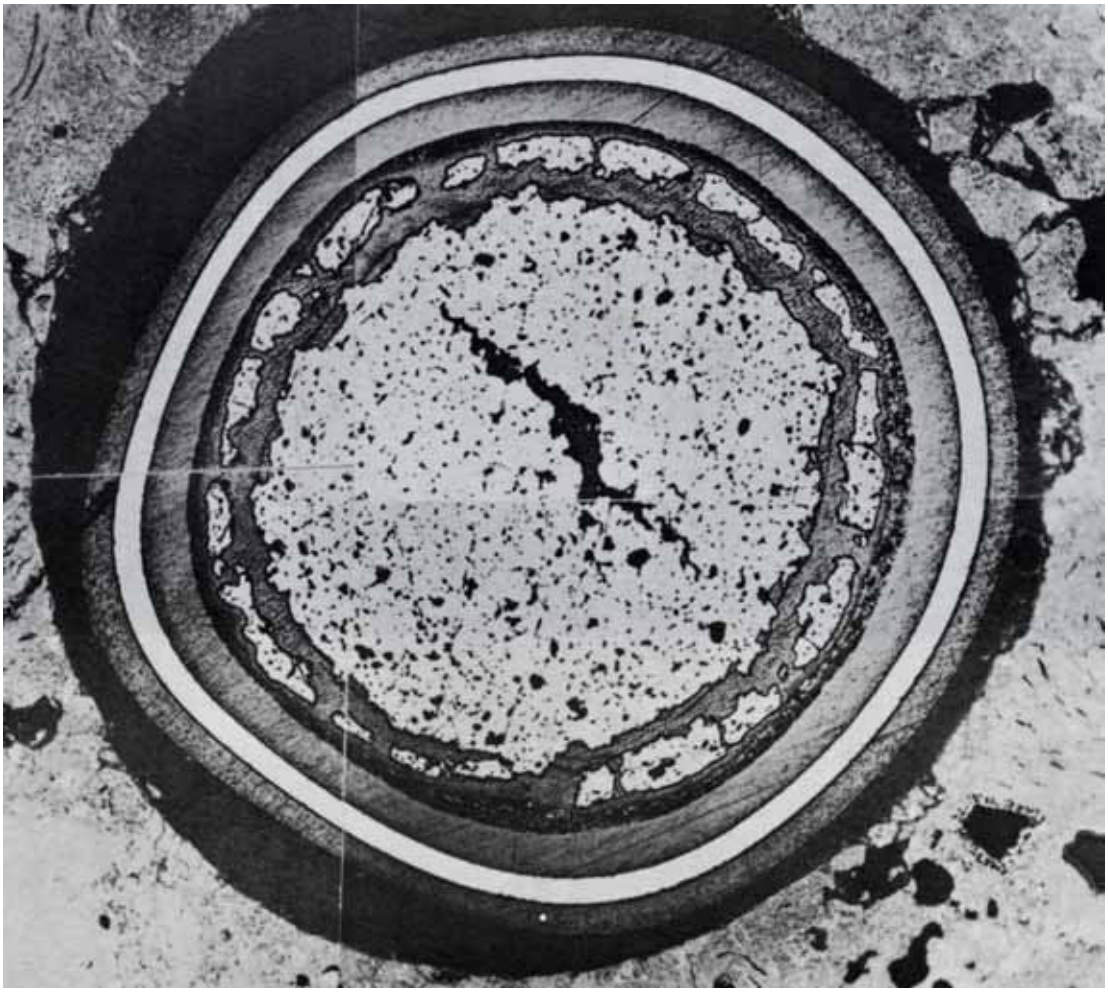

X 100

Figure 31: MET V (3) – Metallography of 3% enriched U particle (Carrier B3-11, tray 10, T=1400°C)

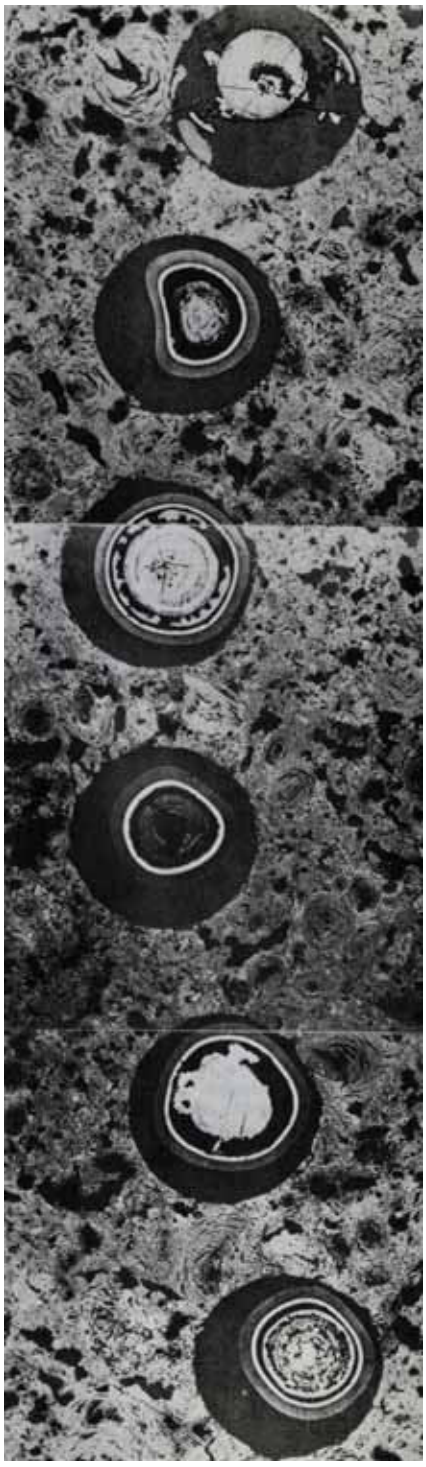

X 24

Figure 32: MET V (3) – Metallography of Pu type T particles (Carrier B3-11, tray 6, T=1400°C)

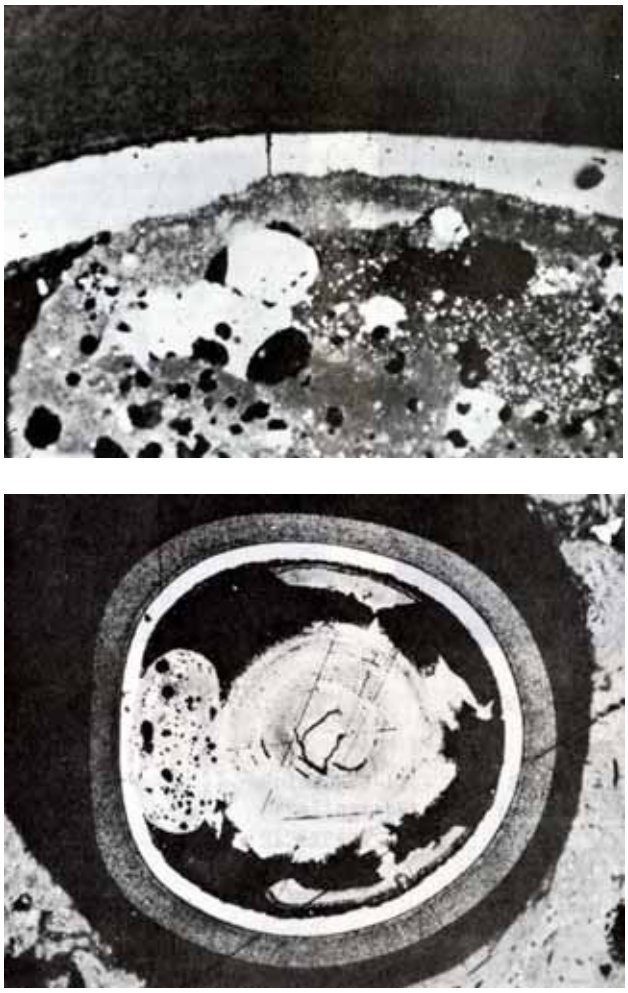

Figure 33: MET V (3) – Metallography of Pu type T particles (Carrier B3-11, tray 6, T=1400°C)

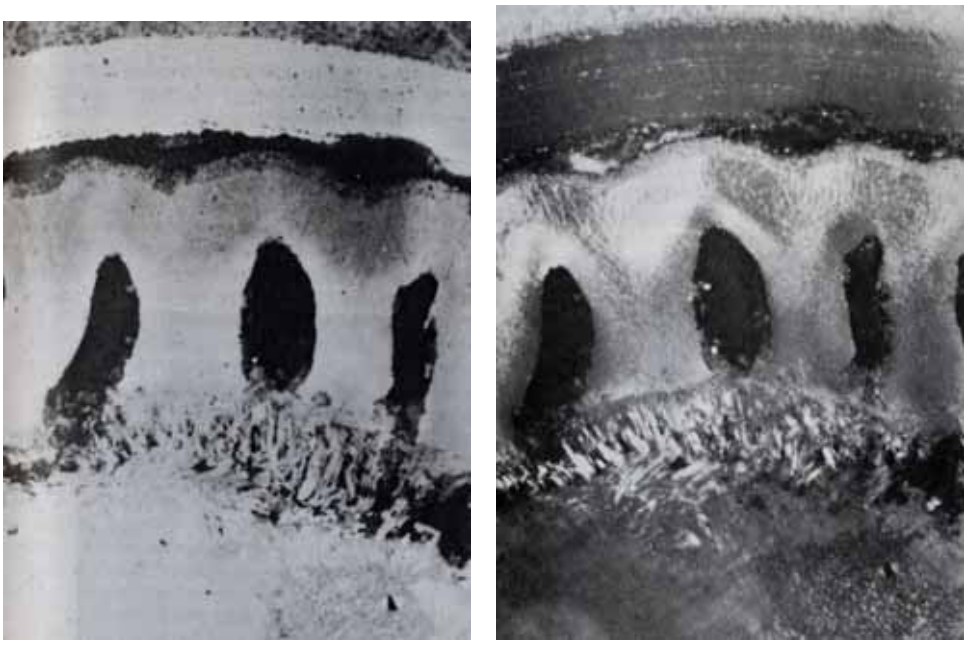

Figure 34: MET V (3) – Metallography of Pu type C particle (Carrier B3-11, tray 8, T=400°C)

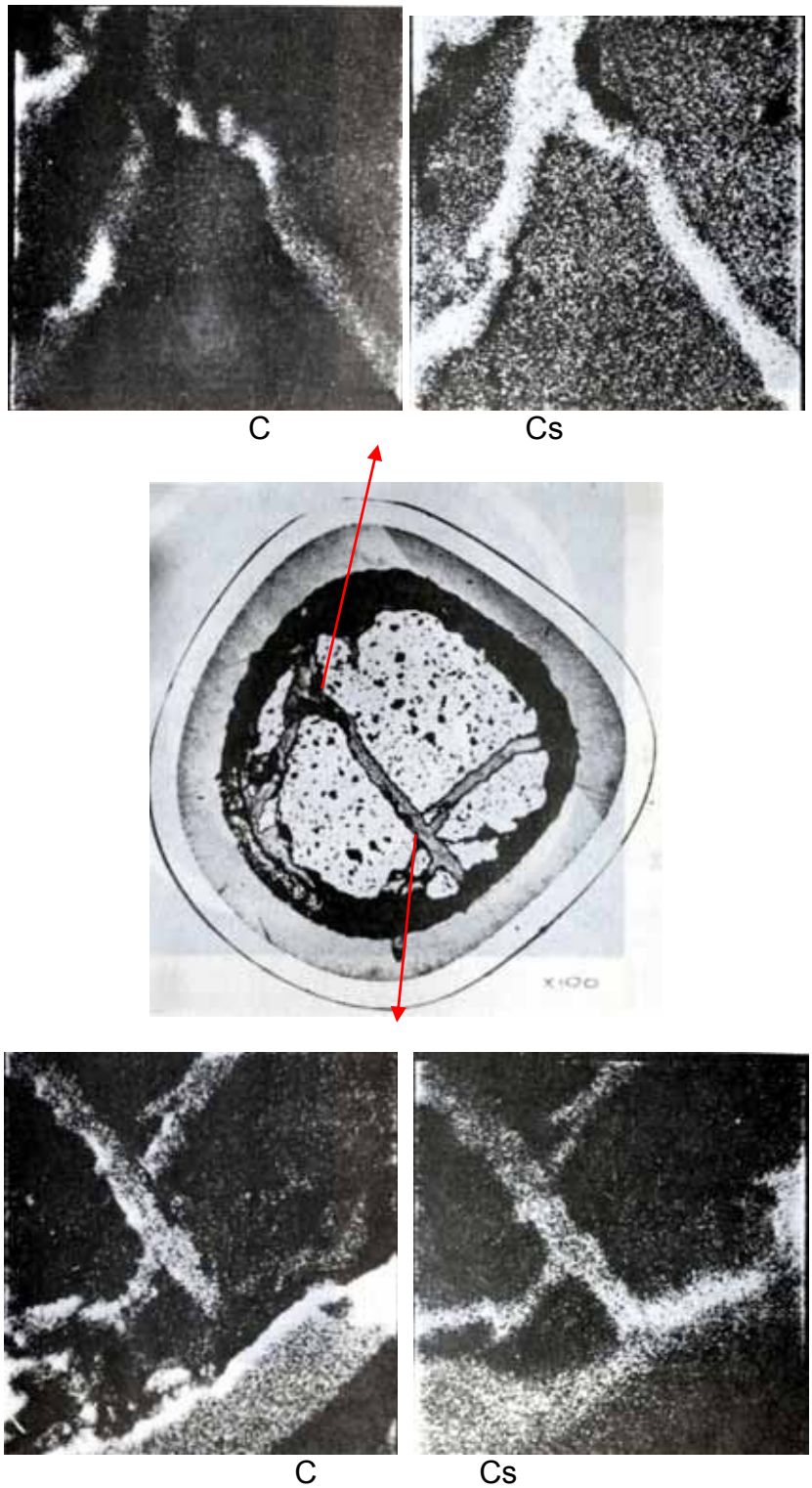

Figure 35: MET V (3) – Microprobe analysis on U particle -C and Cs distribution in the kernel cracks- (Carrier B3-11, tray 12)

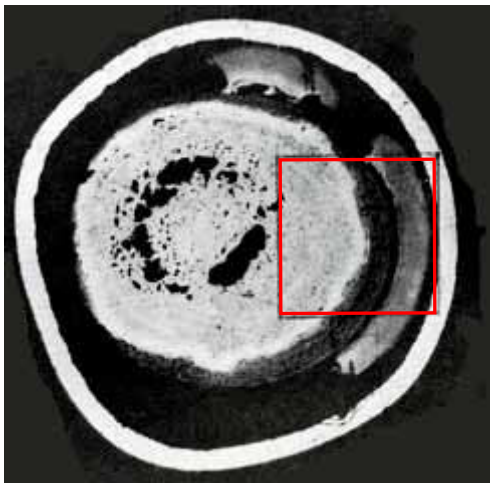

C

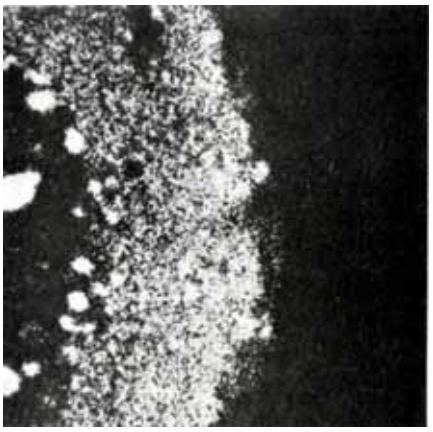

Pu

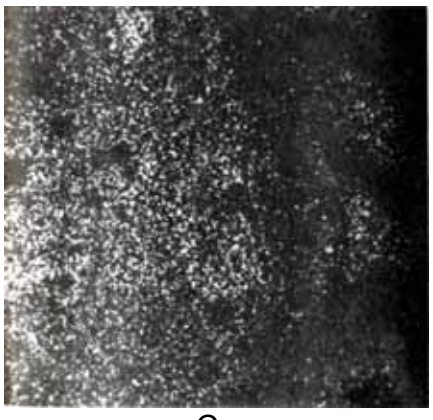

Cs

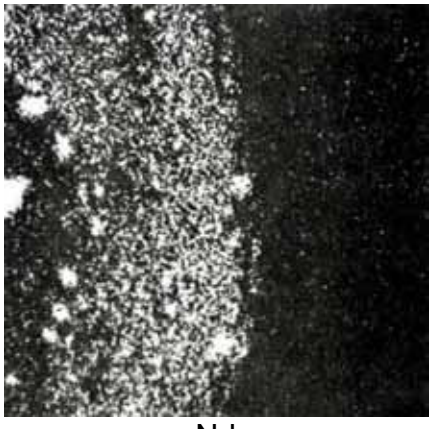

Nd

Figure 36: MET V (3) – Microprobe analysis on Pu type C particle (Carrier B3-6, tray 8 T=1300°C)

	Type of document:	Reference No / File - "Rev." - Page
	Technical Note	**0601020/220-“-“ - 54**
		Other reference:

	Type of document:	Reference No / File - "Rev." - Page
	Technical Note	**0601018/220-"-" - 1**
		Other reference:

Client: EC	Author(s) G. TOURY
Project: Raphael IP – SP Fuel Technology WP-FT4 Performance Modelling	
Subject:	

HTR particles Irradiation Experiment BN database

Misc. Met experiment

Rev.	Date	Chrono Filing No.	Status	Initials dactylo.	Author: Initials	Author: Visa 1	Verified by: Initials	Verified by: Visa 2	Approved by: Initials	Approved by: Visa 3	Q.A.: Initials	Q.A.: Visa 4	Issued by: Initials	Issued by: Visa 5	Number of pages
C															
B															
A															
-	17/05/2006	0601018	Draft		GTY		SSH						GTY		14

Distribution:

RAPHAEL Project: Mr. OBRY (1 copy +1 CD)

BN: SSH, GTY

	Type of document:	Reference No / File - "Rev." - Page
	Technical Note	**0601018/220-“-“ - 2**
		Other reference:

BELGONUCLEAIRE N.V.
Avenue Ariane, 4 - 1200 Brussels
TVA: BE 403.126.258
RCB: 271.300
TEL: 32-2774 05 11
FAX: 32-2-774 05 47

LIST of MODIFICATIONS

DATE	REVISION	OBJECT

15/05/2006	-	Draft

NOTICE

PERSONNEL IN CONFIDENCE, NOT FOR PUBLICATION

This work is performed under the term and conditions of the Consortium Agreement of the RAPHAEL Project supported by the EC under contract n° 516508 (FI6O)

LIABILITY

This document was prepared by BELGONUCLEAIRE (BN). Neither BN, nor any person acting on behalf of BN:

a) gives any warranty, expressed or implied, with respect to the accuracy, completeness of the information contained in this document, or that the use of any information, apparatus, method or process disclosed in this document may not infringe third party rights, or

b) assumes any liabilities with respect to the use of, or for damage resulting from the use of any information, apparatus, method or process disclosed in this document.

Abstract

The main purpose of the experiment was the study of the effect on the particle performance of a layer of overcoating. Coated particles with and without overcoating were loaded separately in the element n°370 of the Dragon reactor and their microstructure has been compared after irradiation.

Table of Content

List of Tables

List of Figures

1. INTRODUCTION

Two kind of coated particles, with and without overcoating layer, have been manufactured by BN then irradiated in the element 370 of the "Miscellaneous Metallurgical Elements" experiment.
The main purpose of the experiment was the study of the effect of a layer of overcoating on the particle performance.

2. EXPERIMENT CHARACTERISTICS

The irradiation characteristics of the experiment are summarised in Table 1.

Element Type	D3 (Sigri S2 graphite)
Element Number	370
Core position	4/3B
Irradiation Time	80 days
Burn-up	1.3% FIMA
Power	0.29 W/part.
Dose	0.4. 10^{21} DNE
Temperature	1250°C ±50°C

Table 1: Main experiment characteristics

The coated particles were loaded into concentric grooves of graphite trays, which were covered by a graphite lid. The trays have been loaded in rod n°7 of the element n°370 according to Figure 1. The contribution of the fuel trays loading to the power generation of the element was less than 2%. The temperatures in the rod position were therefore essentially determined by the driver fuel. The temperature rise from the inner surface of the tray to the fuel particles was about 25°C including γ-heat in the graphite (about 2W/cm^3).

The fuel particle data are given in Table 2.

Batch ref.	Kernel diameter (µm)	Layer coating thickness (µm)				Nominal enrich^{nt}	U content (%)	Hg density (g/cm^3)	α-count (c/g ks)
		Internal PyC	SiC	External PyC	Over-coating				
TN3//8/2F	835 +54 -49	102	40	40	-	12	63.8	4.57	20
TN3/8/2FO	834 +79 -53	102	40	40	36	12	63.8	3.95	8

Table 2: Coated particles characteristics

3. IRRADIATION RESULTS

The particles in tray n°71 (without overcoating) have reached a burn-up from 1.45 to 1.55% FIMA; the irradiation temperature was 1270°C ±55°C.

The particles from tray 72 (with overcoating) have reached a burn-up from 1.35 to 1.45% FIMA; the irradiation temperature was 1280°C ±20°C.

4. POST-IRRADIATION EXAMINATION

Metallographic sections of particles with overcoating layer are shown in Figures 2 to 4. Some particles are still intact, but some show radial cracks straight through the overcoating layer, the outer PyC and the SiC layer. Small circumferential cracks can also be seen at the inner surface of the SiC layers. Some particles show both effects (Figure 2-b). Higher magnification photographs show attacks of the SiC on both inner and outer surfaces (Figure 3-c).

Metallographic sections of particles without overcoating layer are presented in Figures 5 and 6. The behaviour of these particles is very similar to the behaviour of the particles with overcoating layer. The SiC layer shows radial cracks (Figures 5-d and 6-a), and circumferential cracks (Figure 5-c), radial cracks are apparent in the outer PyC layer as seen in Figure 6-b.

5. CONCLUSION

This experiment has shown that the addition of an overcoating layer does not seem to improve the behaviour of the particles.

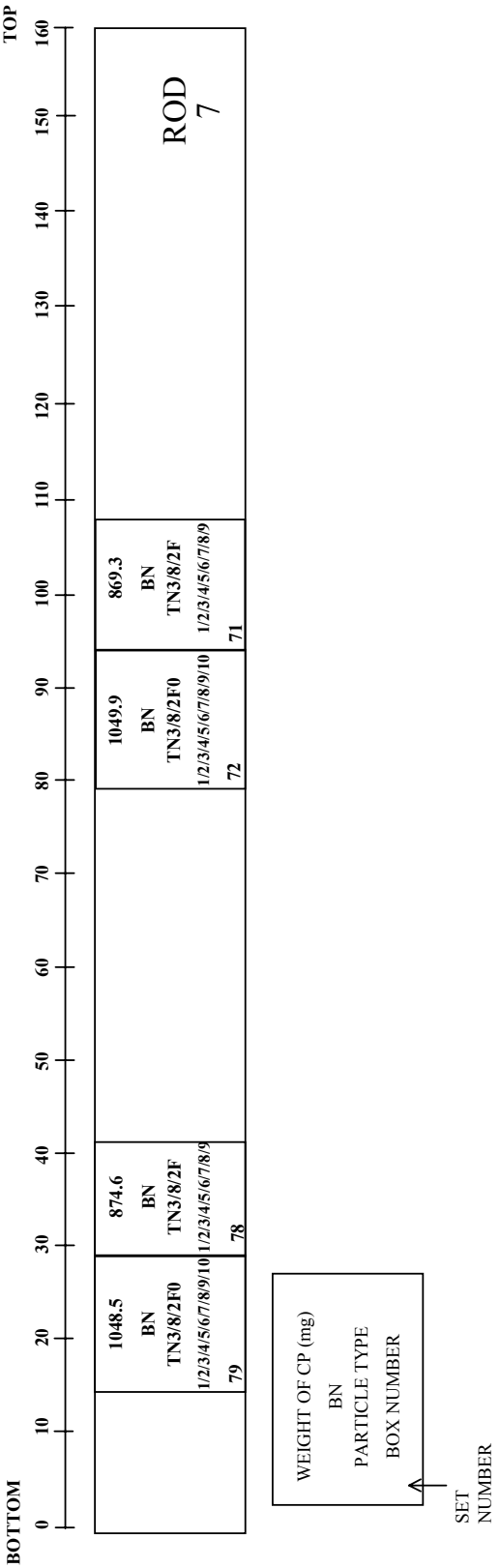

Figure 1: Loading diagram

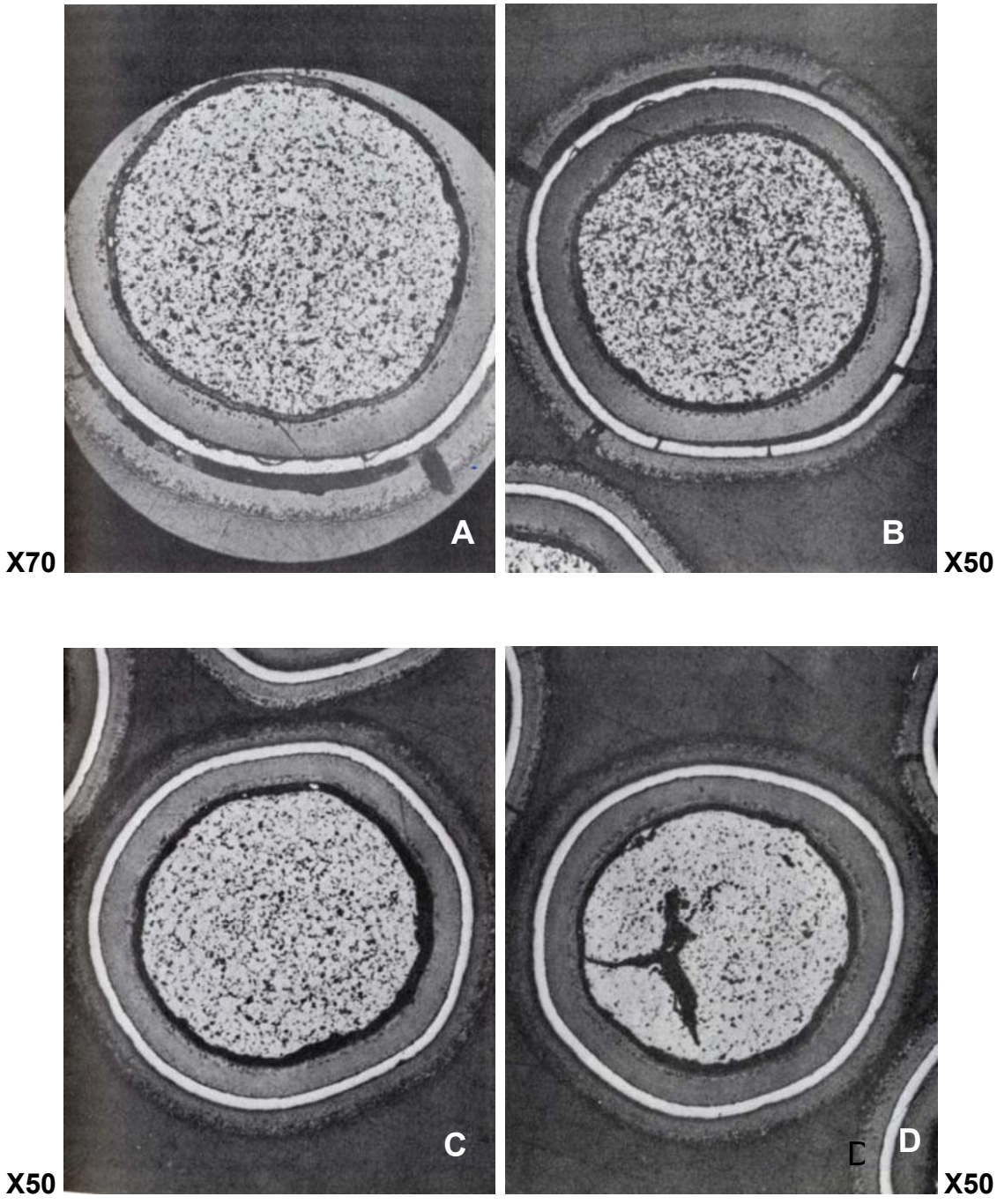

Figure 2: Metallographic cross section of coated particles with overcoating (Batch TN 3/8/2F0, 1.55-1.45 %FIMA 1270 ±85 °C)

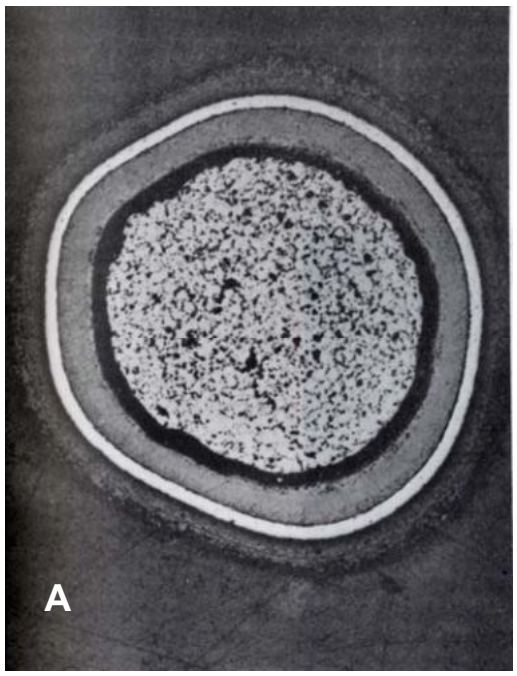

X50

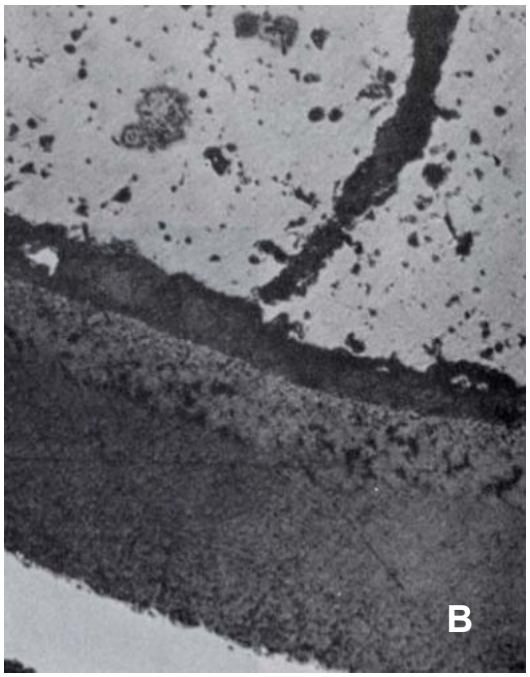

X335

X335

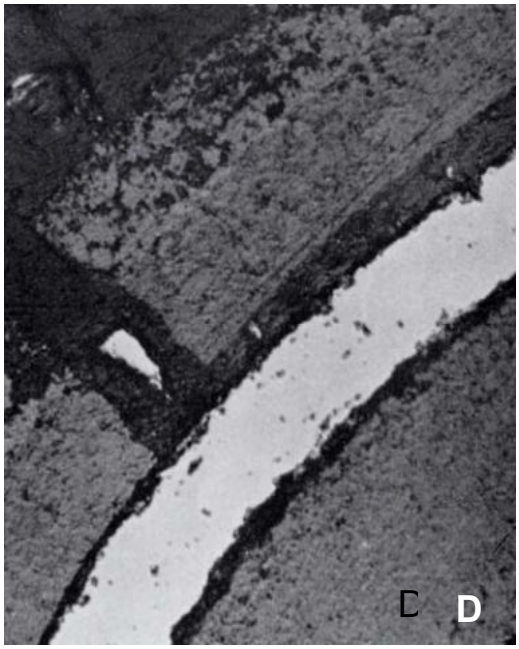

Figure 3: Metallographic cross section of coated particles with overcoating (Batch TN 3/8/2F0, 1.55-1.45 %FIMA 1270 ±85 °C)

X400

Figure 4: Metallographic cross section of coated particles with overcoating (Batch TN 3/8/2F0, 1.55-1.45 %FIMA 1270 ±85 °C)

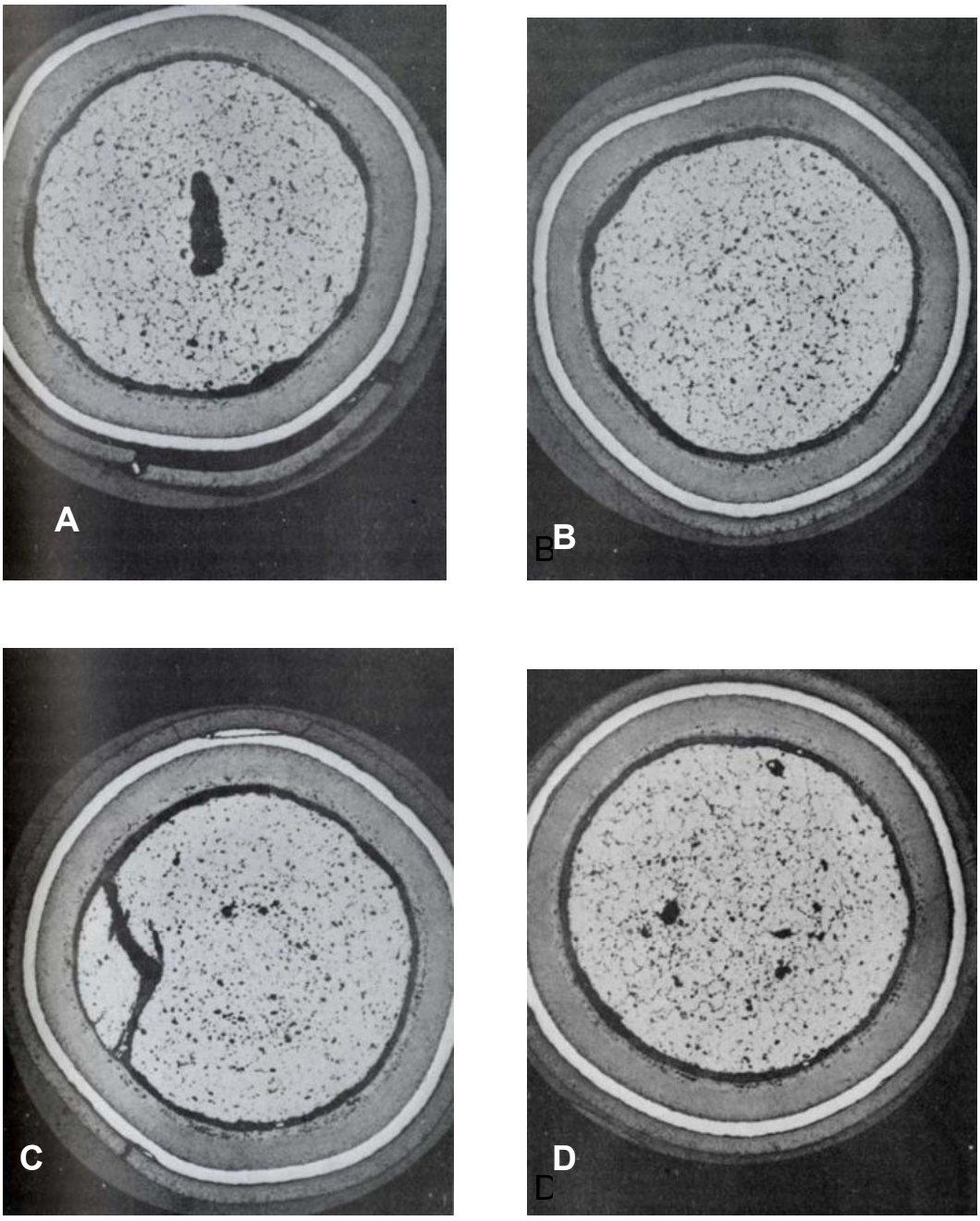

Figure 5: Metallographic cross section of coated particles without overcoating (Batch TN 3/8/2F, 1.45-1.34 %FIMA 1280 ±90 °C)

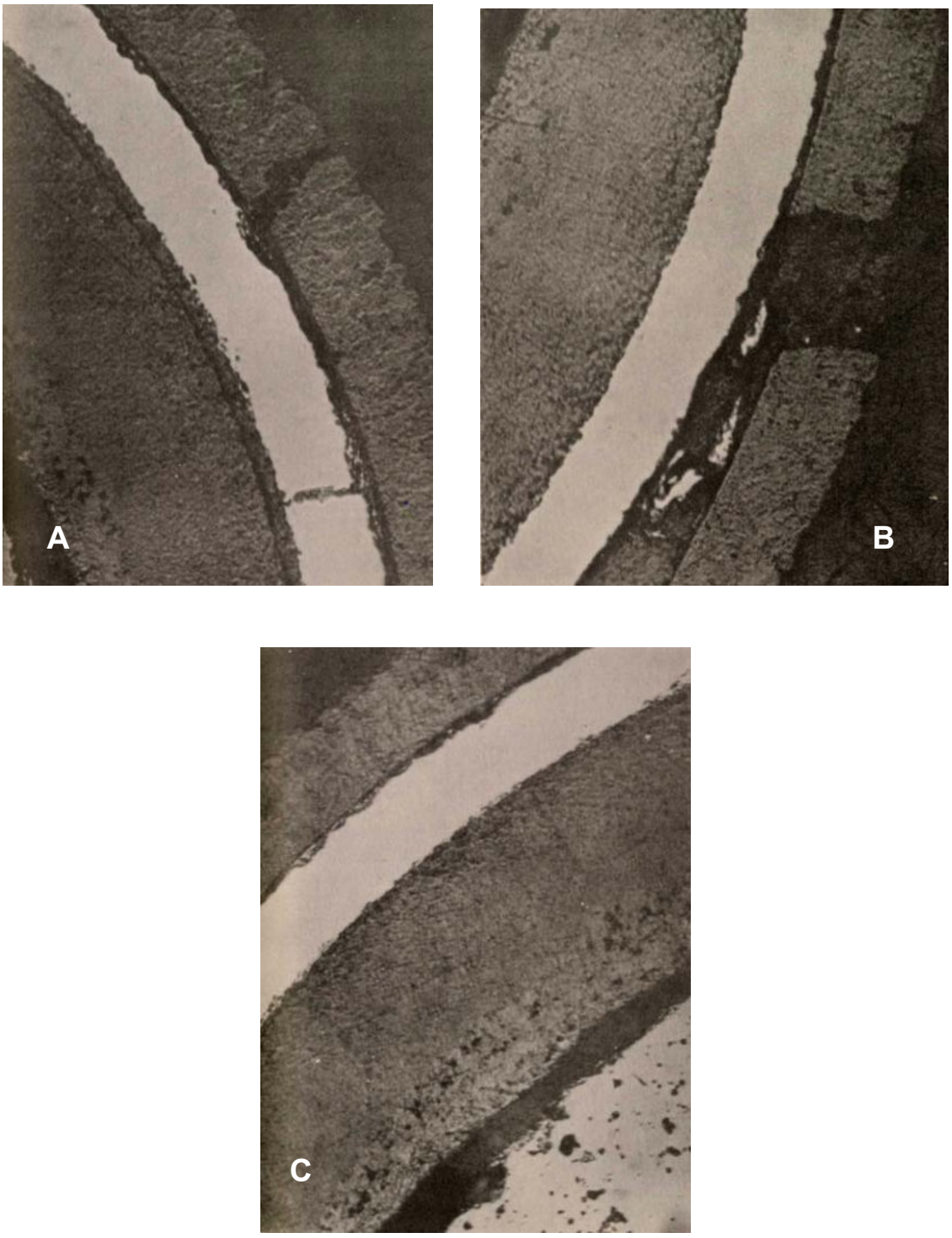

Figure 6: Metallographic cross section of coated particles without overcoating (Batch TN 3/8/2F, 1.45-1.34 %FIMA 1280 ±90 °C)

	Type of document:	Reference No / File - "Rev." - Page
	Technical Note	**0601022/220"-" - 1**
		Other reference:

Client: EC	Author(s) G. TOURY
Project: Raphael IP – SP Fuel Technology WP-FT4 Performance Modelling	
Subject:	

HTR particles Irradiation Experiment BN database

VC Experiments

Rev.	Date	Chrono Filing No.	Status	Initials dactylo.	Author: Initials	Author: Visa 1	Verified by: Initials	Verified by: Visa 2	Approved by: Initials	Approved by: Visa 3	Q.A.: Initials	Q.A.: Visa 4	Issued by: Initials	Issued by: Visa 5	Number of pages
C															
B															
A															
-	18/05/2006	0601022	Draft		GTY		SSH						GTY		38

Distribution:

RAPHAEL Project: Mr. OBRY (1 copy +1 CD)

BN: SSH, GTY

BELGONUCLEAIRE N.V.
Avenue Ariane, 4 - 1200 Brussels
TVA: BE 403.126.258
RCB: 271.300
TEL: 32-2774 05 11
FAX: 32-2-774 05 47

LIST of MODIFICATIONS		
DATE	**REVISION**	**OBJECT**
17/05/2006	-	Draft

NOTICE

PERSONNEL IN CONFIDENCE, NOT FOR PUBLICATION

This work is performed under the term and conditions of the Consortium Agreement of the RAPHAEL Project supported by the EC under contract n° 516508 (FI6O)

LIABILITY

This document was prepared by BELGONUCLEAIRE (BN). Neither BN, nor any person acting on behalf of BN:

a) gives any warranty, expressed or implied, with respect to the accuracy, completeness of the information contained in this document, or that the use of any information, apparatus, method or process disclosed in this document may not infringe third party rights, or

b) assumes any liabilities with respect to the use of, or for damage resulting from the use of any information, apparatus, method or process disclosed in this document.

Abstract

The purpose of these experiments was to study the irradiation behaviour of compacts with coated particles manufactured by different production methods. Both irradiation experiments consisted of an irradiation rig containing two capsules each. The mechanical behaviour, dimensional change and gas release during irradiation were analysed.

Table of content

List of Tables

List of Figures

1. INTRODUCTION

Among several rigs of the BR2 reactor located in Belgium, the vented capsules have been used extensively for the HTR irradiation programme.

They fulfilled the following requirements:

- allow a large variation of experimental parameters, such as target material, target dimensions, heavy metal loading, fuel enrichment, irradiation temperature and fission rating;
- temperature and power rating could be adjusted in a large range by varying the He_3-Ne mixture (which was used as an absorbent screen to modulate the local power) and by varying the in-pile section position in reactor;
- the fission gas release could be measured continuously.

This part presents the results of the two first experiments in the vented capsule VC01 and VC02 that were carried out by BN in collaboration with KFA.

In the irradiation experiment VC01 the upper vented capsule contained 12 hot pressed compacts (1350°C) manufactured by BN, while the lower non vented capsule contained four hot pressed compacts (1200°C) and two isostatically pressed compacts (1100°C) manufactured by Nukem. The BN fuel has consisted of compacts containing 9% enriched UO_2 coated particles, with kernel obtained by powder agglomeration (low density). The purpose of the VC01 experiment was to assess the proper behaviour of the rig under high fuel rating conditions (1.1 W/part.).

The VC02 experiment was made in the identical rig as the VC01, but the BN fuel was loaded in the non vented part. The compacts in the VC02 contained two different types of particles, namely low density coated UO_2 particle identical to VC01 and low porosity coated UO_2 particles, which kernel was manufactured according a sol-gel process. The objective of the VC02 experiment was to compare the behaviour of the two kinds of particles, and in particular their gas release.

2. FUEL CHARACTERISTICS

Two types of UO_2 coated particles were tested:

- batch TI/3/3/3F0, 7.98% U235 enrichment, which kernels were manufacturing according a powder agglomeration process (low density);
- batch S/S/S/3/2/14Fo, 4.7% U235 enrichment, kernels manufacturing by sol-gel process (low porosity).

The characteristics of the coated particles are gathered in Table 1. Microview and cross sections of the two types of particles are shown in Figures 1 and 2.

The fuel in VC01 consisted of coated particles from the batch TI/3/3/3F0 whereas in VC02, the fuel was a blend of the two batches of coated particles.

Compacts (with central hole to allow the insertion of a thermocouple for the measurement of the peak fuel temperature) and pellet were manufactured with Gilsonite as matrix material. High pressures were needed to reach the required density (120-240 kg/cm^2). The number of broken particles was systematically low after compaction.

Microviews of compacts are presented in Figures 3 and 4.

The characteristics of the fuel compacts are presented in Table 2.

The dimensional measurements of each individual compact are given in Tables 3.

3. IRRADIATION HISTORY

Five thermocouples have been installed in the upper capsule: one to measure the fuel centre temperature at the level –25 mm, two to measure the graphite sleeve temperature at the level +27mm and two to measure the graphite sleeve temperature at the level –23mm. No thermocouples have been installed in the lower capsule.

Two pairs of Co and Fe detectors have been inserted in the graphite sleeve of the upper capsule (level +85mm and +10mm) and three detectors in the graphite sleeve of the lower capsule (level –217mm, -274mm and –331mm).

The loading plan of the fuels bodies is presented in Table 4.

The irradiation was made in the BR2 reactor during 142 effective full power days (EFPD) for VC01 and 247 EFPD for VC02.

The irradiation has been carried out with a constant peak fuel temperature of 1350°C for VC01 (level of compact n°30) and about 1000°C for the VC02 compacts (from 1062°C at the start to 818°C at the end of the irradiation).

The temperature and temperature gradient distribution has been calculated for VC01 considering an uniformly distributed heat source, a thermal conductivity of 0.13 W/cm°C, the peak fuel temperature measured by a thermocouple located in the central hole of compact 30 and using the temperature of the primary coolant. The results are given in Figures 5 and 6 for the compact n°30 and in Figures 7 and 8 for the compact n°32.

The average power density has been estimated to be 209 W/cm^3 for compact n°30 and 206 W/cm^3 for the compact n°32.

A peak burn-up of 8.7%FIMA and a peak fast neutron dose of 1.27×10^{21} DNE have been reached in VC01.

The fast fluence in VC02 was estimated to 3.9×10^{21} DNE and the mean burn-up was about 7% FIMA for CPs with powder agglomeration kernel and 4.5% FIMA for CPs with sol-gel kernel.

4. POST-IRRADIATION EXAMINATIONS

4.1. Dimensional measurements

The results of the irradiation induced dimensional changes of compacts are plotted in Figure 9 and 10.

All the compacts VC01 being in a region were the flux distribution is very flat, no significant effect of the axial position was noticed.

For the VC02 experiment, the results showed a strong dose dependence of the compacts dimensional changes.

4.2. Annealing test

The annealing test carried out on the compacts n°28 and 35 up to a temperature of 1500°C has given a R/B for Kr85 and Xe133 lower than 10^{-4}.

4.3. Burn-up determination

The calculation of the burn-up was based on the quantitative measurement by gamma spectrometry of the mean Cs137 activity of individual particles.

The results of the gamma-spectrometric measurements has shown a leak of fission products at around 50% of the particles from compact n°31 (VC01 experiment) whereas the particles from compact n°19 (VC02 experiment) seemed to be intact after irradiation, though there were powder agglomeration-type particles in both compacts.

For the calculation of the Cs137 activity of particles in VC01, only particles, which have shown no leak of fission products, were considered.

In order to differentiate between high and low enriched particles in compact 19 of VC02, two facts were considered:

- the fission yields for Ce144, Ru106 and Cs137 are different for U235 fissions and Pu239 fissions;
- there are about twice more U235 fissions within the 9% U235 enriched particles than within the 4.7% U235 enriched ones.

The results of the burn-up calculations are :

VC01, compact 31, particles type TI/3/3/3F0: 8.7% FIMA

VC02, compact 19, particles type TI/3/3/3F0: 7.0% FIMA

VC02, compact 19, particles type S/S/S/3/2/14F: 4.5% FIMA

Though the irradiation time of experiment VC01 was shorter than that of the VC02 experiment, the TI/3/3/3F0 type particles have shown a slightly higher burn-up in compact 31 compared with the same particles type in compact 19.

4.4. Metallographic examinations

VC01

A longitudinal and a radial cross-sections of compacts n°30 and 32 have been prepared and examined (Figures 11 and 12). The results of these examinations may be summarized as follows:

- the matrix was porous and not homogeneous but was mechanically stable under irradiation;
- all the particles suffered from the Amoeba effect; the reaction front is radially orientated but it never reached the outer PyC layer. The particles located near the outer surface of compacts where the radial temperature gradient is the highest, are more deeply damaged;
- fragments of fissile material were reported to be found in the buffer layers;
- the intergranular fission product inclusions in the kernel indicate a high burn-up and a high irradiation temperature.

VC02

After irradiation, the amoeba effect was visible in both types of particles (Figures 13-14) as well as irradiation induced cracking.

The periphery of the sol-gel kernels has retained the original dense structure; its average thickness is 30 µm, as before irradiation. Microcracks are apparent along all grain boundaries, resulting frequently in larger cracks isolating one or a few grains. The grain size is approximately 100µm, with a pore-free periphery 20µm thick. The porosity within the grain has a spherical shape (Figure 14).

The powder agglomeration kernels appeared as a spongy structure, with a randomly distributed porosity (Figure 13). The pores are elongated tangentially which was a remembrance of the manufacturing technique. A breakage of the kernel was common, resulting in fragments corresponding typically to one third of the kernel.

In principle, the fragmentation mode observed in the sol-gel kernels is more favourable, but the important porosity-free zone at the periphery of the kernel and of the grains might indicate a lower in-pile densification of the fuel.

4.5. Gases measurements

The procedure for the fission gases and CO measurements in the coated particles of VC experiments are described as follow.

- First, the compacts are disintegrated by anodic oxidation; after disintegration, the residue consisting of matrix graphite and coated particles was washed several times with distilled water and then dried with acetone; the matrix graphite and the coated particles were then separated by sieving;
- The theoretical quantities of fission gas in fuel particle were calculated from the absolute content of Cs137 determined by gamma spectrometry on individual particle.

This Cs137 activity was converted into theoretically total produced Xenon and Krypton quantities taking into account the relative fission yields.

- The theoretical quantity of CO was calculated under the assumption of two oxygen atoms being released from the UO_2 or PuO_2 molecule during fission of the respective uranium or plutonium atom, leading to the formation of two CO molecules. In this hypothesis the formation of fission products oxide was neglected.

- The gas determination in the particles has been carried out as follows: the temperature has been increased at a rate of approximately 50°C/min, up to 1250°C; this temperature has been maintained during 20 minutes. After this heating time the particles have been crushed mechanically, and the release gases quantities have been measured.

- A fraction of the released gases has then been fed to the mass-spectrometer for isotopic composition measurement.

- The fractional release values have been determined by comparison of measured released and theoretical gas amounts produced.

- The gas pressures in the coated particles have then been calculated from the internal free volumes and the released gases quantities using the Redlich-Kwong equation

$$p_i = \frac{RT}{\frac{v}{n} - b} - \frac{a}{\frac{v}{n}\sqrt{T}\left(\frac{v}{n} + b\right)}$$

The constant a and b have the following numerical values:

	a	b
Co	1.73×10^7	27.2
Xe	7.25×10^7	35.3
Kr	3.45×10^7	27.4

R= 82.06 $cm^3.atm.C^{-1}.Mol^{-1}$
V= free volume inside the particle (cm^3)
N= number of moles of gas in equation

For the calculation of the gas pressures in different types of particles, the mean value of the measured gas amounts and the theoretical free volumes of the unirradiated particles have been used. For pressure calculation only the free volume of the buffer layer has been taken into account as theoretical free volume, assuming a porosity of 50%. The kernel porosity has not been added.

The main results of the gas determination and fractional gas release for the VC01 and VC02 experiments are presented in Table 5. The gas release is primarily dependent upon the irradiation temperature, i.e. the specific kernel temperature of the particles. Therefore locally different temperatures in the compact result in different gas release of the individual particles.

The results of irradiation experiment VC01 show for particles 1-7 fission gas release of Xe resp. Kr amounting to 73.9% resp. 59.8% and for the particles 8-11 amounting to more than 100%. The particles 1-7 have a mean Cs137 activity of approximately 541 µCi, but the particles 8-11 show a mean Cs137 activity of approximately 350 µCi, though the absolutely measured fission gas amounts do not show a difference. Therefore, it can be assumed that there were Cs137 losses in the particles 8-11. It can be assumed that in these particles the SiC layer had cracked during irradiation and consequently the created Cs had diffused through the PyC layer into the matrix. A damage of the PyC layer can be excluded since the same fission gas amounts have been measured in undamaged particles. The particle n°7 exploded after having been heated for 1 min at 1250°C. The released gas amounts corresponded with those in intact particles. The gas release values of particles 8-11 are only theoretical values and would converge to the same values as in intact particles, when the measured Cs137 activity is corrected for the Cs137 loss of approximately 30%.

Because of the low thermal rating in sol-gel particles, the fission gas release from these particles is lower than for powder agglomeration-type particles containing twice the amount of U235. Furthermore, it was shown within the same particle type, major differences in the fission gas release occurred, as shown in Table 6. This is less pronounced with the high-enriched particles, because of the relatively high gas release.

The CO releases of the examined particles are in good correspondence. The particles of experiment VC01 (powder agglomeration kernel) with the highest burn-up showed also the highest CO amount (0.88×10^{-3} cm^3). The same type of particles, but in experiment VC02, which had an approximately 20% lower burn-up than identical particle in VC01, showed only a CO amount of 0.679×10^{-3} cm^3. The sol-gel particles in VC02, having less fissions, showed a CO-amount of 0.270×10^{-3} cm^3.

The results of the gas pressures are presented in Table 6. The total pressure due to Xe, Kr and CO has been determined in 7 intact particles in VC01: a mean value of 811 atm has been found at 1250°C (pressure is mainly due to the Xe), whereas the inner pressure in identical particles in experiment VC02 are about 700 atm. The inner pressures in sol-gel particles are lower (about 400 atm). These different gas pressures were also reflected in the burst ratio of particles.

4.6. Anisotropy

The anisotropy profiles have been measured on 10 different particles from compact n°31 at a position of mean coating thickness. The aperture was 4µm x 40µm (4µm in radial direction), the distance between two measuring points was also 4µm. Each scan was started at the inner side of the layer.

Results are given in Table 7 and a typical profile is shown in Figure 15. In Figure 16, the mean anisotropy values of the irradiated particles as well as for unirradiated particles are plotted against the coating thickness at measuring position. Contrary to experience that showed that the anisotropy values of irradiated particles (under the same conditions) fit into one curve, the values obtained in this experiment can be

divided into two groups with a different increase of the anisotropy (particles 4,7,8,9 and particles 1,2,3,5,6,10). This different behaviour could be caused by the following reasons:

- the measured particles were a mixture of at least two coating batches;
- the particles were irradiated in different positions under different conditions;
- the outer PyC was supported differently by an overcoating or by the matrix;
- the stresses in the coating layers could be different to cracks in the coating.

4.7. Kernel migration measurement

On the macroscopic cross-sections of the compacts 30 and 32 (VC1), the coated particles, which show their equatorial planen, were chosen for the kernel migration measurements. The thickness of the internal PyC layers was measured at the hot side (t_h) and at the cold side (t_c) of these coated particles. The migration length X was then calculated as follows:

$$X = \frac{t_c - t_h}{2}$$

The results are given in Table 8 in connection with the radial location and the thermal characteristics of these coated particles. The measured migrations versus the coated particles radial positions in the compacts are presented in Figure 17 for the compact 30 and in Figure 18 for the compact 32.

5. CONCLUSION

The VC01 compacts irradiated at a temperature of 1350°C and up to a burn-up of 8.7%FIMA have shown a good mechanical stability under irradiation.

Relatively high fission and reaction gases pressures were measured on the irradiated particles, which have shown also a significant increase of the outer PyC anisotropy.

Most of the particles suffered from the amoeba attack, but this effect did not jeopardise the lifetime of the fuel, the R/B for Xe133 increase observed at the end of the irradiation being due mainly to the pressure failure of a limited number of particles.

Concerning the VC02 compacts irradiated at a range temperature of 800-1100°C and up to a burn-up range of 4.5-7%FIMA:

- the dimensional changes and mechanical behaviour depended strongly on the accumulated fast neutron dose and on the irradiation temperature;

- amoeba effect and irradiation induced cracking have been noticed on some particles;

- fission and reaction gases pressures of 800 and 450 atm have been measured respectively on the highly and low enriched particles.

KERNELS	**Manufacturing process**		**Powder agglomeration**		**Sol Gel**	
	Enrichment U235 (%)		8.98		4.7	
	Mean Diameter (µm)		762		760	
	Min / Max diameters		709 / 819		730 / 790	
	Sphericity[1]		1.033		1.032	
	Typical sphericity defect		Irregular shape, flats		Ovality	
	Surface condition		Orange peel , macroporosity, low abrasion resistance		Glossy, high abrasion resistance	
	O/U	Chromatography Gravimetry	2.001 1.999		2.005	
	Porosity by Hg immersion (%)		8.5		1.5	
	Type of porosity		Macroporosity, homogeneously distributed to concentrated in the centre		Microporosity, very dense surface layer (30 to 60µm), homogeneous distrib. on porosity in the centre	
	Isotopic composition		U^{234} 0.09% U^{235} 8.98% ±0.005 U^{236} 0.27% U^{238} 90.66%		U^{234} 0.02% U^{235} 4.715% U^{236} 0.036% U^{238} 95.229%	
COATINGS	Gap kernel – inner PyC		~ 5 µm		~ 3 µm	
	Layers		Thickness (µm)	Density (g/cm^3)	Thickness (µm)	Density (g/cm^3)
	Porous PyC		36 +5 -0	1.05 ±0.05	32	1.1
	Transition PyC		30 ±5	1.65 ±0.05	30	1.5
	Inner HDI PyC		30 ±5	1.80 ±0.05	34	1.75
	B.A.F.[2]		1.08			
	SiC		40.5	3.18 ±0.02	34	3.15
	Outer HDI PyC		35.5	1.8 ±0.05	33	1.75
	B.A.F.[2]		1.17			
	Mean total coating layer		183	1.88	163	
Batch number			**TI/3/3/3F**		**SSS 3/2/2F**	
Mean kernel diameter (µm)			757		163	
Mean overall diameter (µm)			1125		1086	
Mean mercury density (g/cm^3)			4.38		4.90	

[1] sphericity: $D_{max.mean}/D_{min.mean}$

[2] Bacon's Anisotropy factor

Table 1: Coated particles characteristics

		VC01		VC02
OVERCOATED PARTICLES	Batch number	TI/3/3/3F0		2.7 Ti/3/3/3F0 / 1 S/S/S/3/2/14F0
	Material	Gilsonite resin bonded graphite		
	% coated particles / overcoated particle	30.26		34.64
	%U in overcoated particle	18.44		21.430
FUEL BODIES		Compacts	Pellet	Compact
	Outer diameter (mm)	15	15	15
	Inner diameter (mm)	4	No hole	4
	Height (mm)	20	20	20
	Number	6	6	10
	Heavy metal loading (g U/cm^3)	0.387	0.392	0.463
	Linear enrichment (mg U235 /cm)	55.9	61.8	58
	Nb of particles	620	690	690
	Uranium weight	1.25	1.38	1.455
	U235 weight (g)	0.112	0.124	0.113
	Matrix density (g/cm^3)	1.60 ±0.2		

Table 2: Fuel bodies characteristics

	N°	Height (mm)		Diameter (mm)		Weight (g)	RX
		Max	Min	Max	Min		
VC01 Total uranium = 15.78g Total U235 = 1.44g							
	Compacts*						
	25	20.05	20.01	14.86	14.85	6.50	g
	26	20.21	20.18	14.85	14.83	6.49	g
	27	20.06	20.02	14.86	14.84	6.49	g
	28	20.28	20.22	14.85	14.84	6.49	g
	29	20.05	20.02	14.85	14.83	6.48	g
	30	20.15	20.10	14.85	14.84	6.50	g
	Pellets						
	31	20.27	20.25	14.85	14.85	7.17	g
	32	20.04	19.98	14.86	14.85	7.18	g
	33	20.46	20.39	14.85	14.84	7.16	g
	34	20.70	20.62	14.85	14.83	7.16	g
	35	20.32	20.26	14.85	14.84	7.17	g
	36	20.22	20.20	14.86	14.85	7.17	g
VC02 Total uranium = 14.55g Total U235 = 1.13g							
	Compacts*						
	15	19.65	19.60	14.85	14.86	6.75	g
	16	19.67	19.66	14.85	14.86	6.75	g
	17	19.65	19.63	14.85	14.87	6.75	g
	18	19.44	19.40	14.86	14.87	6.75	g
	19	19.50	19.48	14.85	14.86	6.75	g
	20	19.93	19.92	14.85	14.86	6.75	g
	21	19.37	19.35	14.86	14.87	6.75	g
	22	19.19	19.16	14.85	14.87	6.75	g
	23	19.35	19.35	14.85	14.87	6.75	g
	24	19.68	19.64	14.85	14.86	6.75	g

g: good

* compacts contain central hole of 4 mm

Table 3: Individual fuel bodies dimensional measurement

	Fuel body n°	Fuel body type	Length (mm)
VC01 Vented part of the capsule	Top of reactor		
	28	Compact	
	26	Compact	
	27	Compact	120.8
	25	Compact	
	29	Compact	
	30	Compact	
	33	Pellet	
	34	Pellet	
	31	Pellet	122.0
	32	Pellet	
	35	Pellet	
	36	Pellet	
VC02 Non vented part of the capsule	15	Compact	
	16	Compact	
	17	Compact	
	18	Compact	
	19	Compact	174.6
	20	Compact	
	21	Compact	
	23	Compact	
	24	Compact	
	22	Compact (optional)	19.6
	Bottom of reactor		

Table 4: Loading plan of the fuel bodies

Type	N°	µCi Cs137	Meas CO 10^{-3} cc	Theor CO 10^{-3} cc	%	Meas Xe 10^{-3} cc	Theor Xe 10^{-3} cc	%	Meas Kr 10^{-3} cc	Theor Kr 10^{-3} cc	%
VC01 TI/3/3/3F0	1	542	0.632	32.8	1.93	3.29	4.63	71.0	0.301	0.524	57.4
	2	657	0.475	39.7	1.19	4.15	5.62	73.9	0.384	0.635	60.4
	3	482	0.371	29.2	1.27	2.67	4.12	64.8	0.249	0.466	53.4
	4	504	1.170	30.4	3.85	3.00	4.31	89.6	0.278	0.487	57.0
	5	572	1.22	34.6	3.53	3.93	4.89	80.4	0.378	0.553	68.3
	6	554	1.20	33.5	3.58	3.62	4.74	76.4	0.330	0.536	61.6
	7	476	1.10	28.8	3.82	3.30	4.07	81.1	0.270	0.460	58.7
	8	376	0.97	22.7	4.27	3.24	3.21	100.8	0.271	0.364	74.6
	9	372	0.75	22.5	3.33	3.57	3.18	112.2	0.338	0.356	93.9
	10	324	1.03	19.6	5.26	3.00	2.77	108.3	0.290	0.313	92.6
	11	335	1.20	20.3	5.91	3.34	2.86	116.6	0.297	0.324	91.7
Mean value	1-7	541	0.88	32.7	2.69	3.42	4.63	73.9	0.313	0.523	59.8
VC02 TI/3/3/3F0	1	418	0.716	25.29	2.83	3.40	3.57	95.1	0.340	0.401	84.6
	2	413	0.545	24.98	2.18	3.07	3.53	86.9	0.273	0.397	68.8
	3	432	0.735	26.13	2.81	2.94	3.69	79.6	0.321	0.415	77.3
	4	446	0.734	26.98	2.72	2.91	3.81	76.3	0.285	0.429	66.5
	5	416	0.663	24.17	2.63	2.83	3.56	79.6	0.296	0.400	74.0
Mean value	1-5	425	0.679	25.71	2.64	3.03	3.63	83.4	0.303	0.408	74.2
3VC02 SSS/3/2/14F0	1	298	0.233	17.88	1.30	1.80	2.57	70.2	0.181	0.254	71.3
	2	288	0.290	17.28	1.67	1.80	2.48	72.6	0.155	0.245	63.2
	3	258	0.310	15.48	2.00	1.88	2.22	84.6	0.172	0.220	70.2
	4	297	0.308	17.82	1.73	1.45	2.56	56.7	0.131	0.253	51.8
	5	290	0.230	17.40	1.32	1.28	2.50	51.3	0.131	0.247	53.0
Mean value	1-3	281	0.278	16.88	1.66	1.86	2.42	76.9	0.169	0.239	70.6
Mean value	4-5	286	0.270	17.61	1.53	1.37	2.46	55.6	0.131	0.244	53.8

Table 5: Individual results of gas determination and fractional gas release (Analysis conditions: T= 1250°C, t= 20 min except particle n°7 VC01 t=1 min)

Experiment		VC01	VC02	VC02	VC02
Fuel		UO2	UO2	UO2	UO2
Kernel diameter (µm)	(µm)	762	762	760	760
Kernel type*		pow. agglo	pow. agglo.	sol-gel	sol-gel
Enrichment	(%U5)	9	9	4.7	4.7
Burn-up (Cs137)	(%FIMA)	8.7	7.0	4.5	4.5
EFP days		142	247	247	247
Buffer thickness	(µm)	36	36	32	32
Buffer porosity	(%)	50	50	50	50
Free volume	($x10^{-5}$ cm^3)	3.6	3.6	3.15	3.15
Gas determ. Temp	(°C)	1250	1250	1250	1250
Xe release	(%)	73.9	83.4	76.9	55.6
Xe amount	($x10^{-3}$ cm^3)	3.42	3.03	1.86	1.37
Xe pressure	(atm)	615	536	364	263
Kr release	(%)	59.8	74.2	70.6	53.8
Kr amount	($x10^{-3}$ cm^3)	0.313	0.303	0.169	0.131
Kr pressure	(atm)	51	49	31	24
CO release	(%)	2.69	2.64	1.66	1.53
CO amount	($x10^{-3}$ cm^3)	0.88	0.679	0.278	0.270
CO pressure	(atm)	145.8	111.0	51.0	50.0
Total pressure	(atm)	811	696	446	337

Table 6: Gas pressure and fractional gas release – average values

Irradiated particle n°	Coating thickness (µm) / Anisotropy (BAF_{opt})
1	33 / 1.53
2	33 / 1.52
3	28 / 1.83
4	33 / 1.71
5	40 / 1.39
6	30 / 1.67
7	30 / 1.86
8	31 / 1.79
9	38 / 1.55
10	38 / 1.55

Table 7: Anisotropy factor of irradiated particles of the compact 31 (VC01) (measure at a position of mean coating thickness of the outer PyC, BAF: Bacon's Anisotropy Factor))

	Particle radial location (cm)	Temperature (°C)	Thermal gradient (°C/cm)	Migration length (µm)	Remark
Compact 30	0.24	1328	-55	40.0	*
	0.26	1327	-84	27.5	
	0.27	1326	-96	30.0	*
	0.44	1294	-280	60.0	
	0.46	1288	-300	55.0	
	0.48	1282	-320	70.0	**
	0.60	1237	-425	55.0	
	0.60	1237	-425	50.0	
	0.62	1228	-445	60.0	
	0.62	1228	-445	55.0	
	0.63	1223	-455	45.0	
Compact 32	0.17	1360	-135	25.0	
	0.29	1338	-203	40.0	
	0.37	1317	-290	80.0	
	0.37	1317	-290	75.0	**
	0.42	1300	-330	65.0	**

*: inaccurate value

**: SiC attack

Table 8: VC1 Measured length migrations and thermal characteristics of the CPs

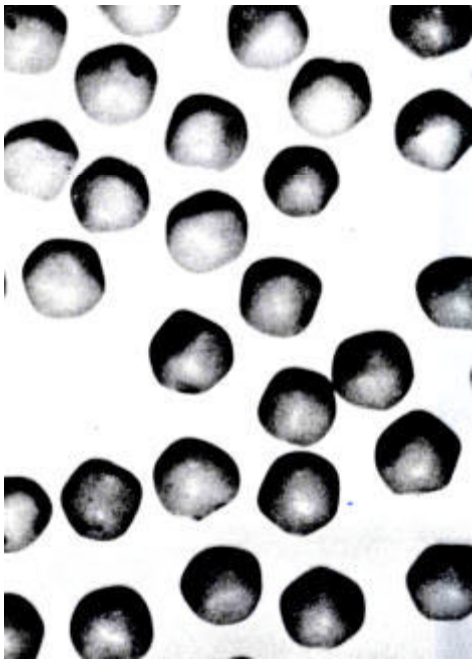

X9

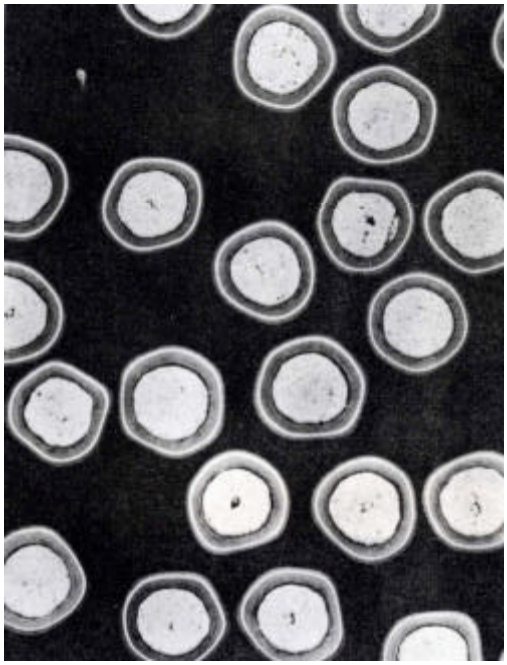

X12

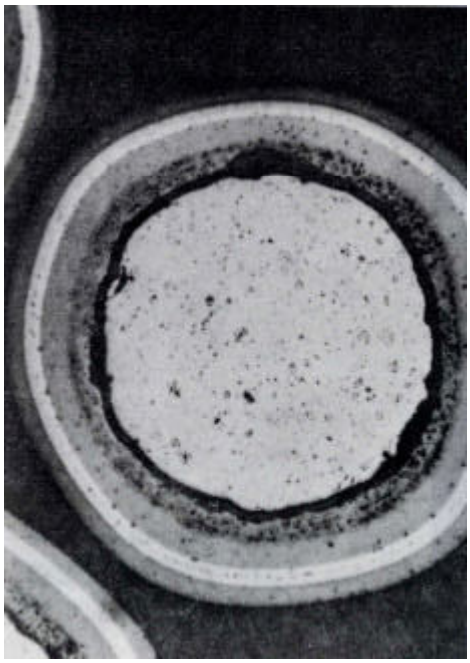

X60

X410

Figure 1: VC01- As fabricated UO_2 Coated particles (Batch TI 3/3/3F)

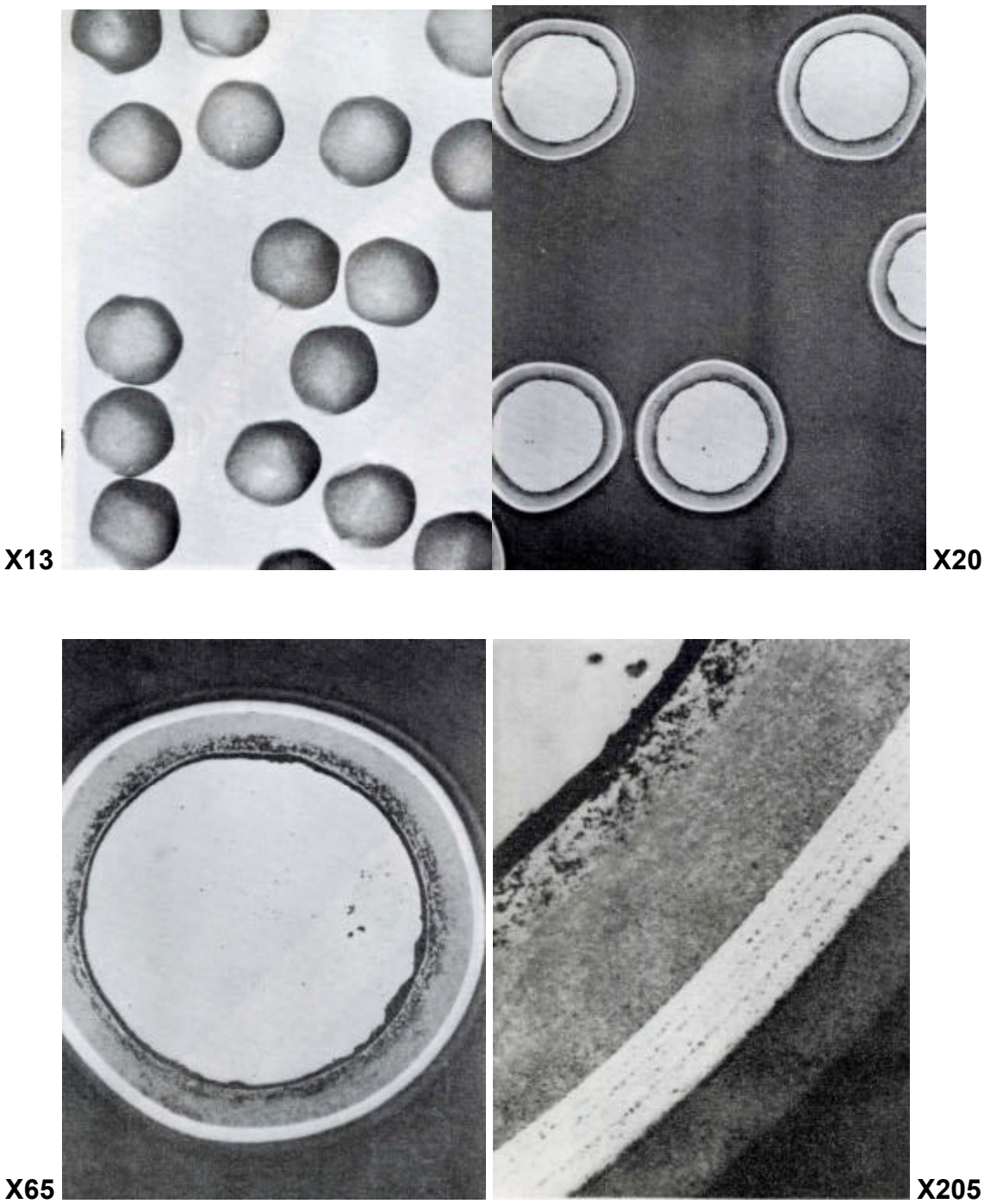

Figure 2: VC02 As-fabricated UO_2 coated particles obtained by sol-gel process (Batch SSS 3/2/2F)

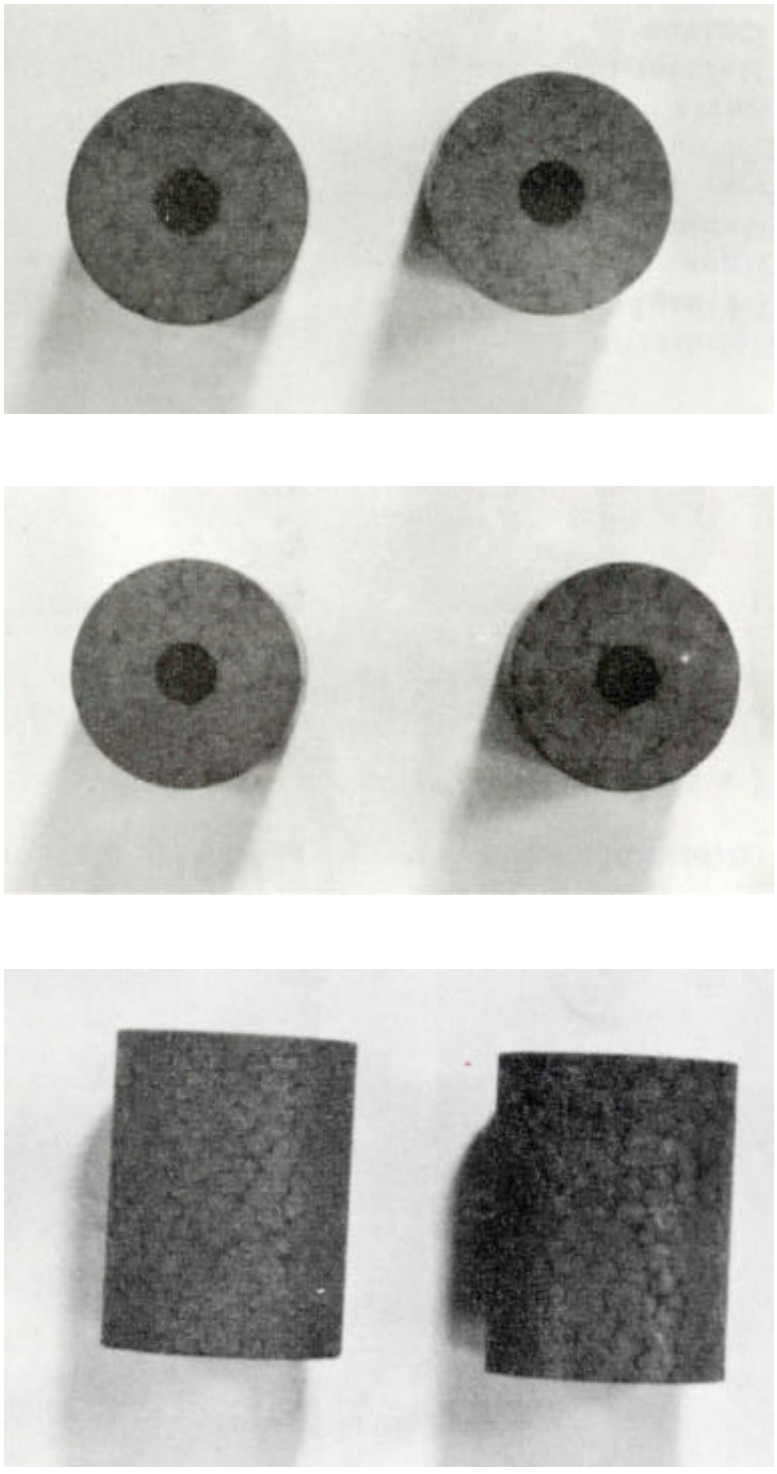

Figure 3: VC01 As fabricated Fuel compacts (Gilsonite structure)

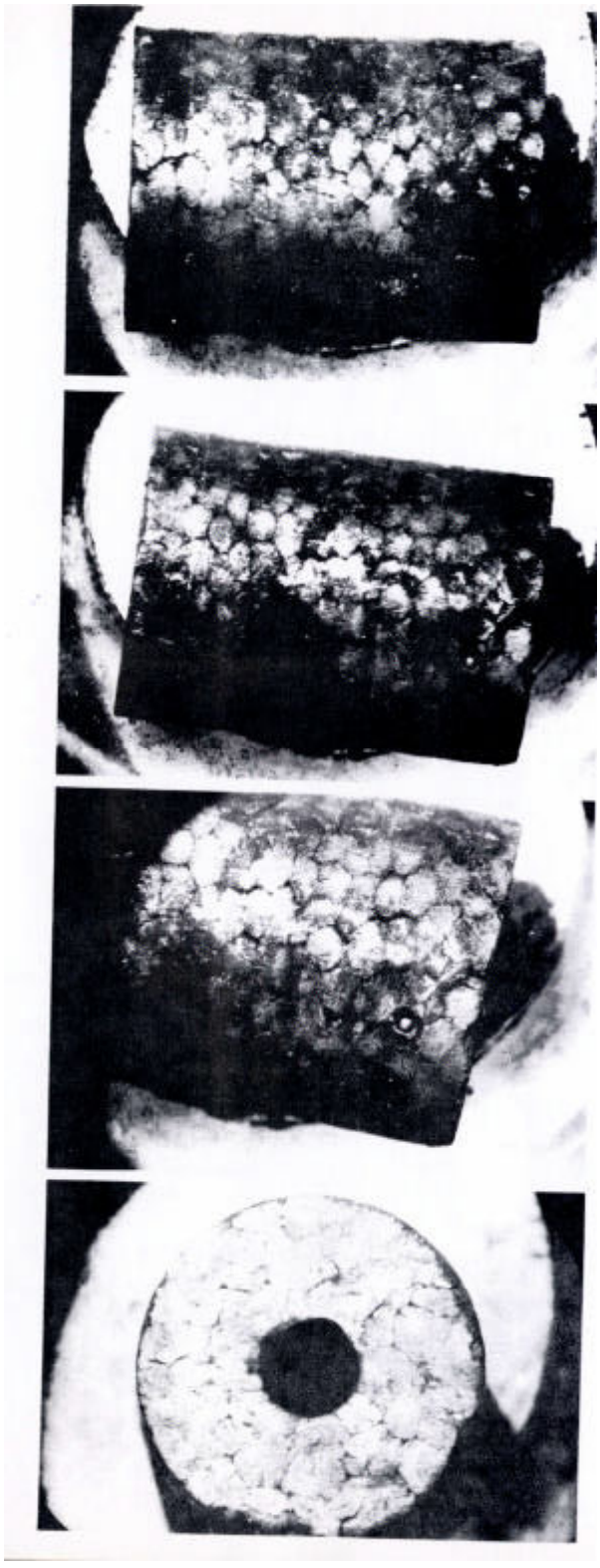

Figure 4: VC01 compact n°26

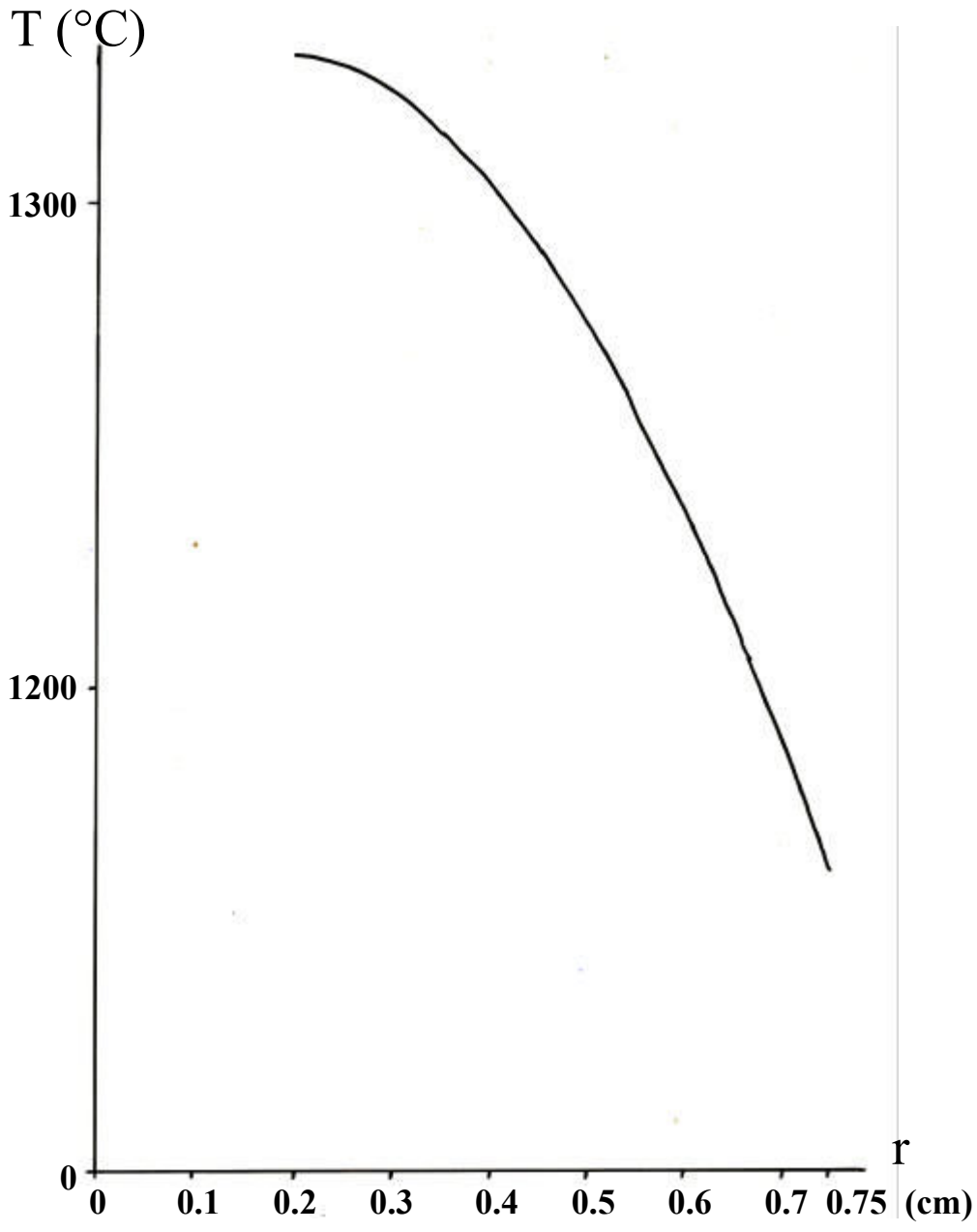

Figure 5: Temperature radial distribution in the compact n°30 (VC01)

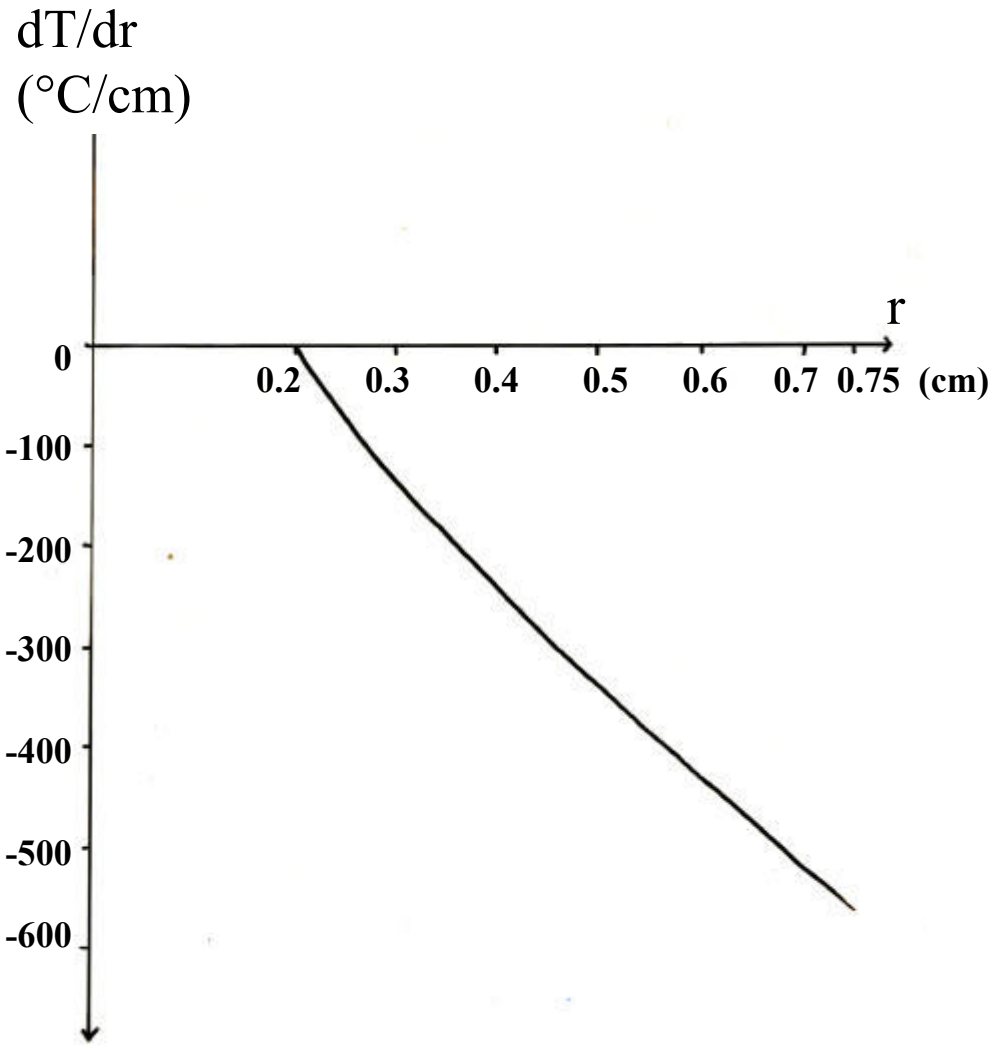

Figure 6: Thermal gradient radial distribution in the compact n°30 (VC01)

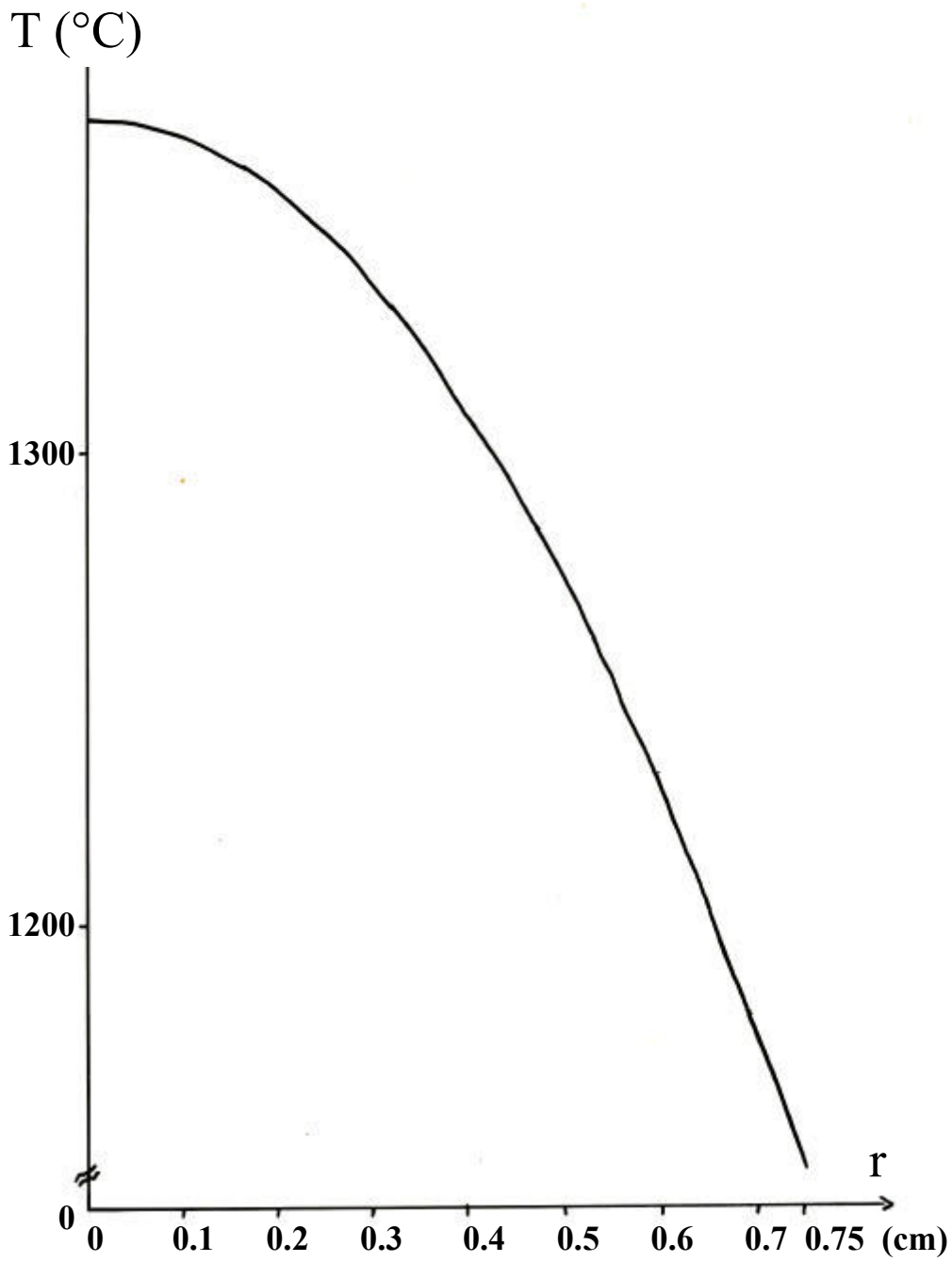

Figure 7: Temperature radial distribution in the compact n°32 (VC01)

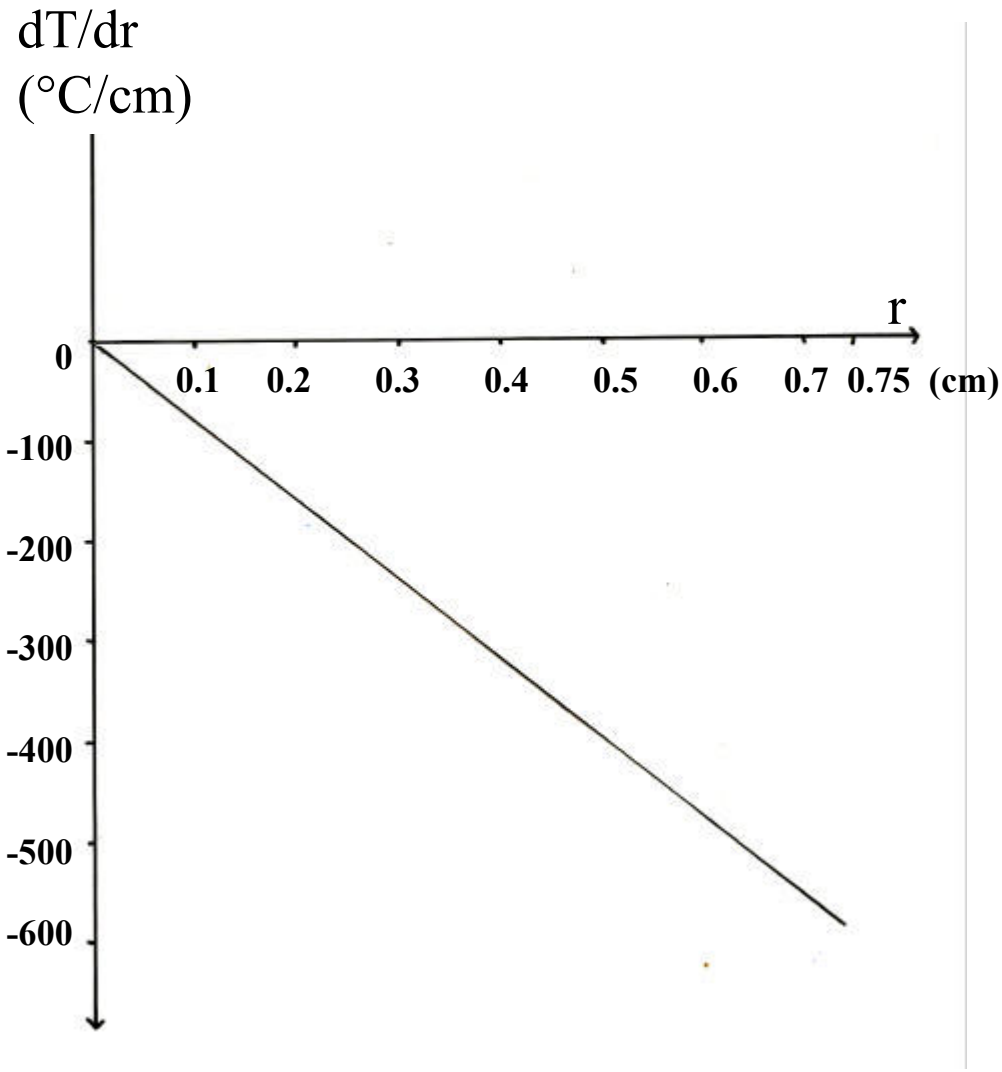

Figure 8: Thermal gradient radial distribution in the compact n°30 (VC01)

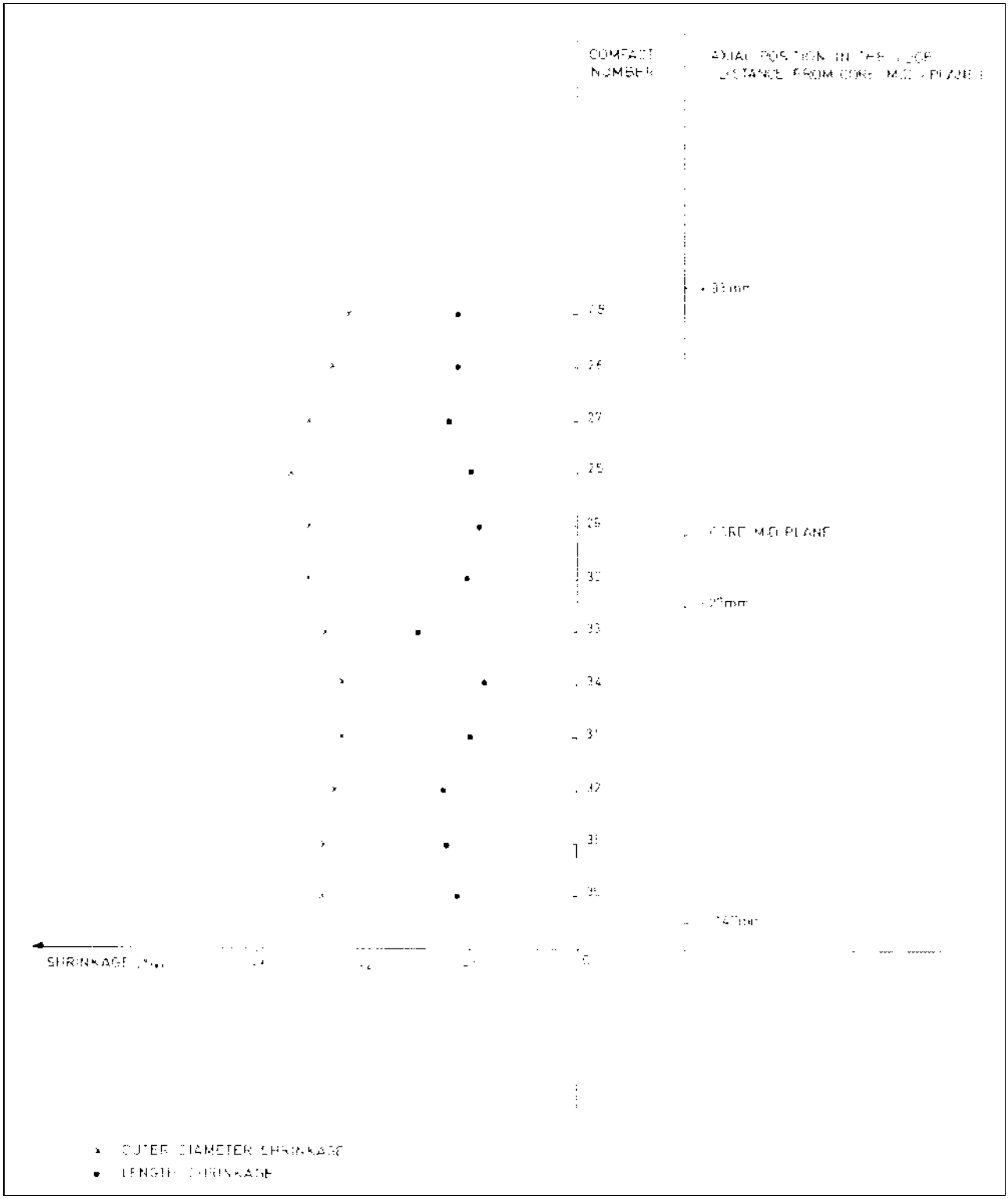

Figure 9: VC01 Compacts outer diameter and length irradiation induced shrinkage

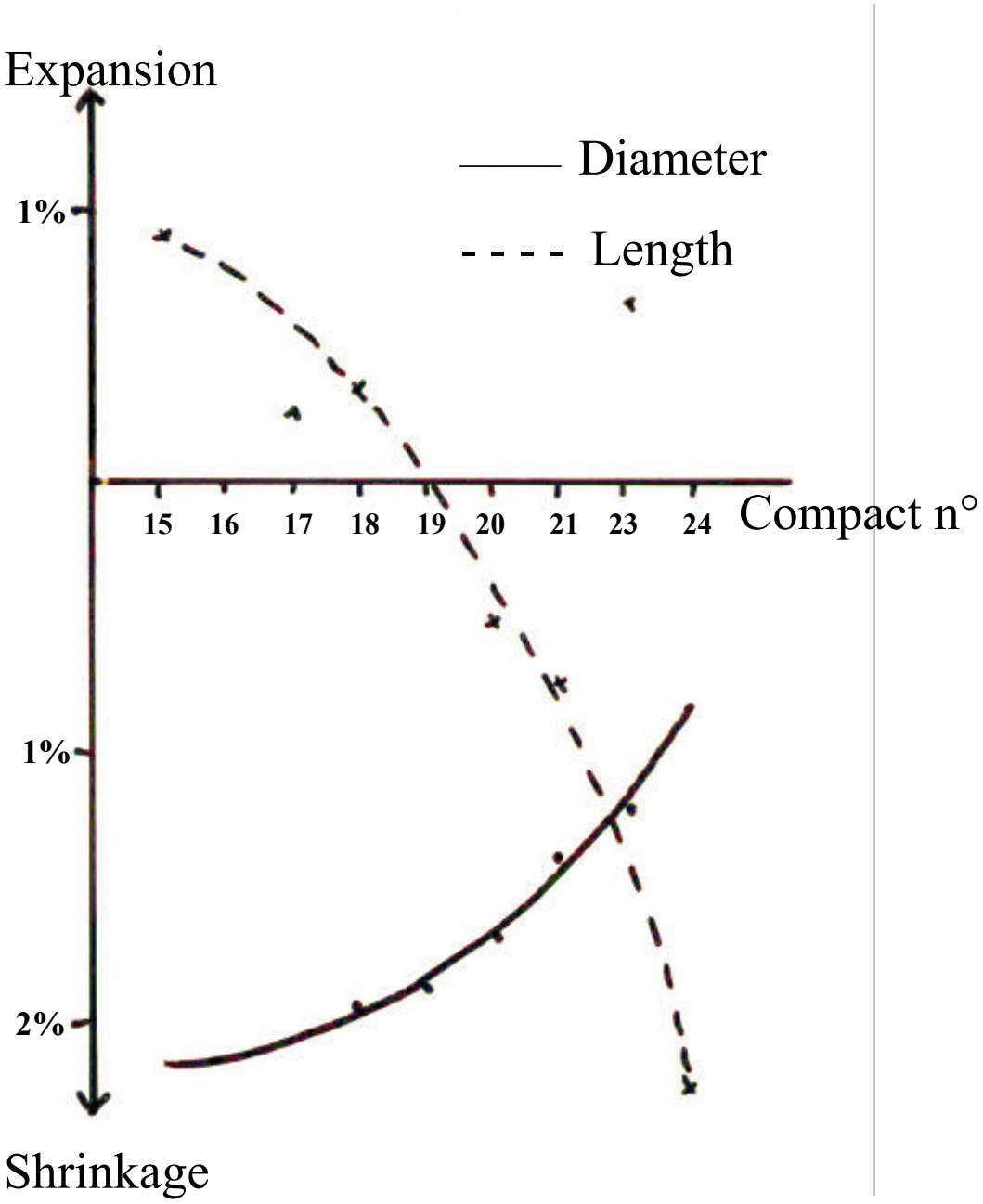

Figure 10: VC02 Compacts outer diameter and length irradiation induced shrinkage

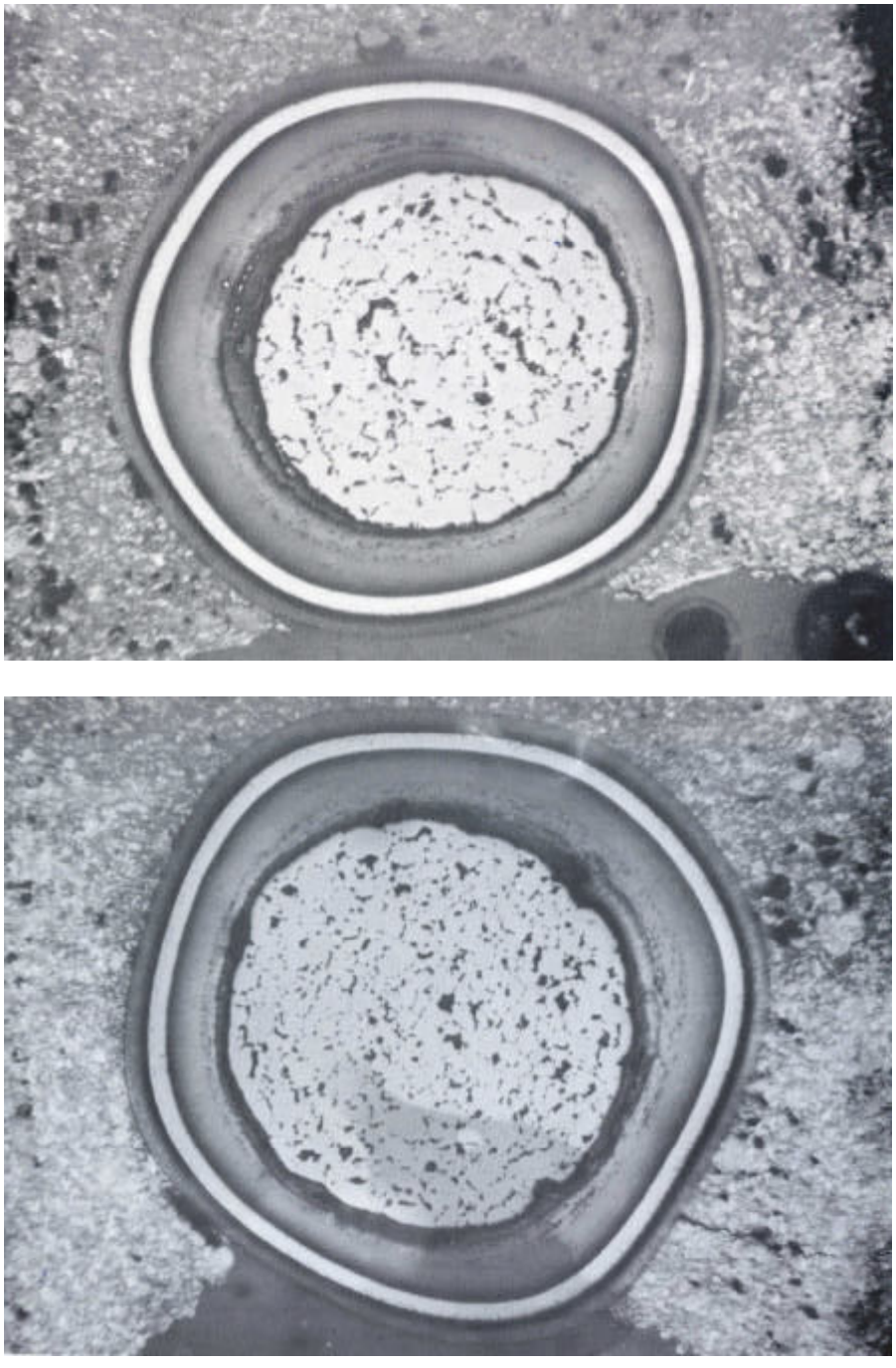

Figure 11: VC01 irradiated compact n°30
Amoeba effect

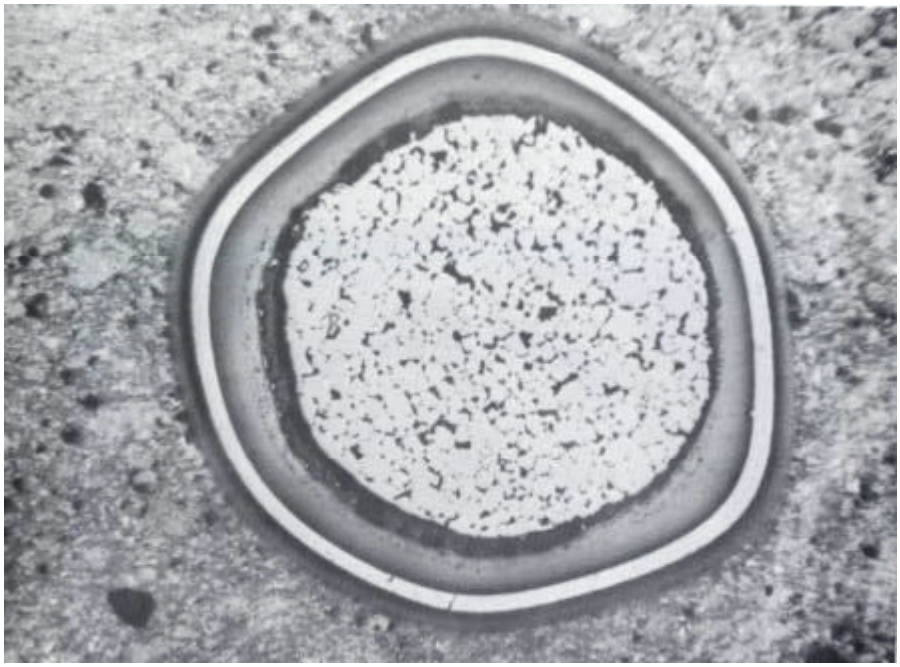

Figure 12: VC01 irradiated compact n°32
Particle showing fissile material segregation

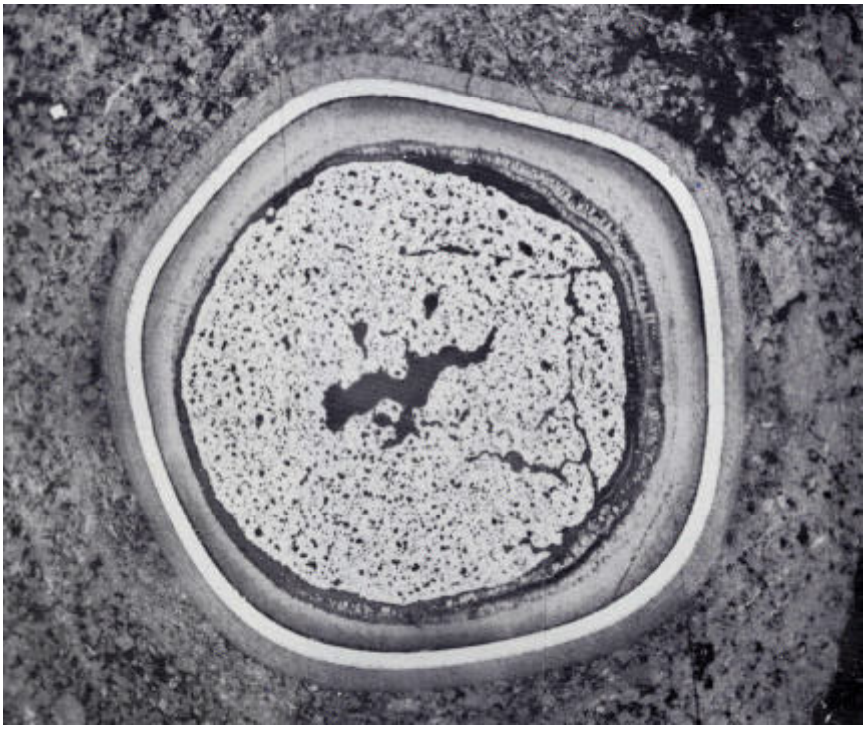

Figure 13: VC02 irradiated compact n°15 - Powder agglomeration coated particle

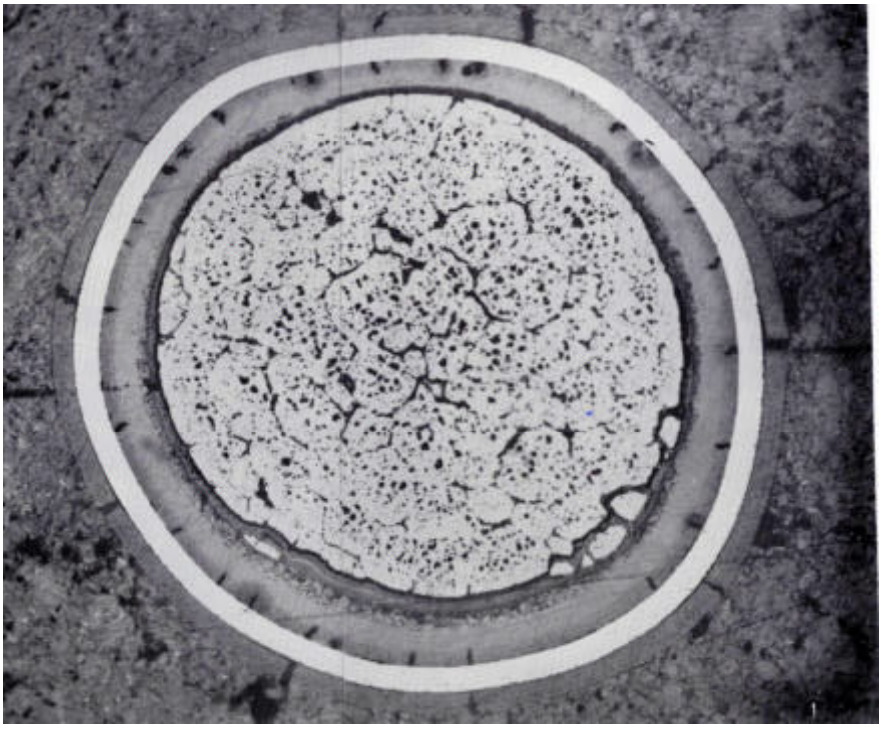

Figure 14: VC02 irradiated compact n°15 - Sol-gel coated particle

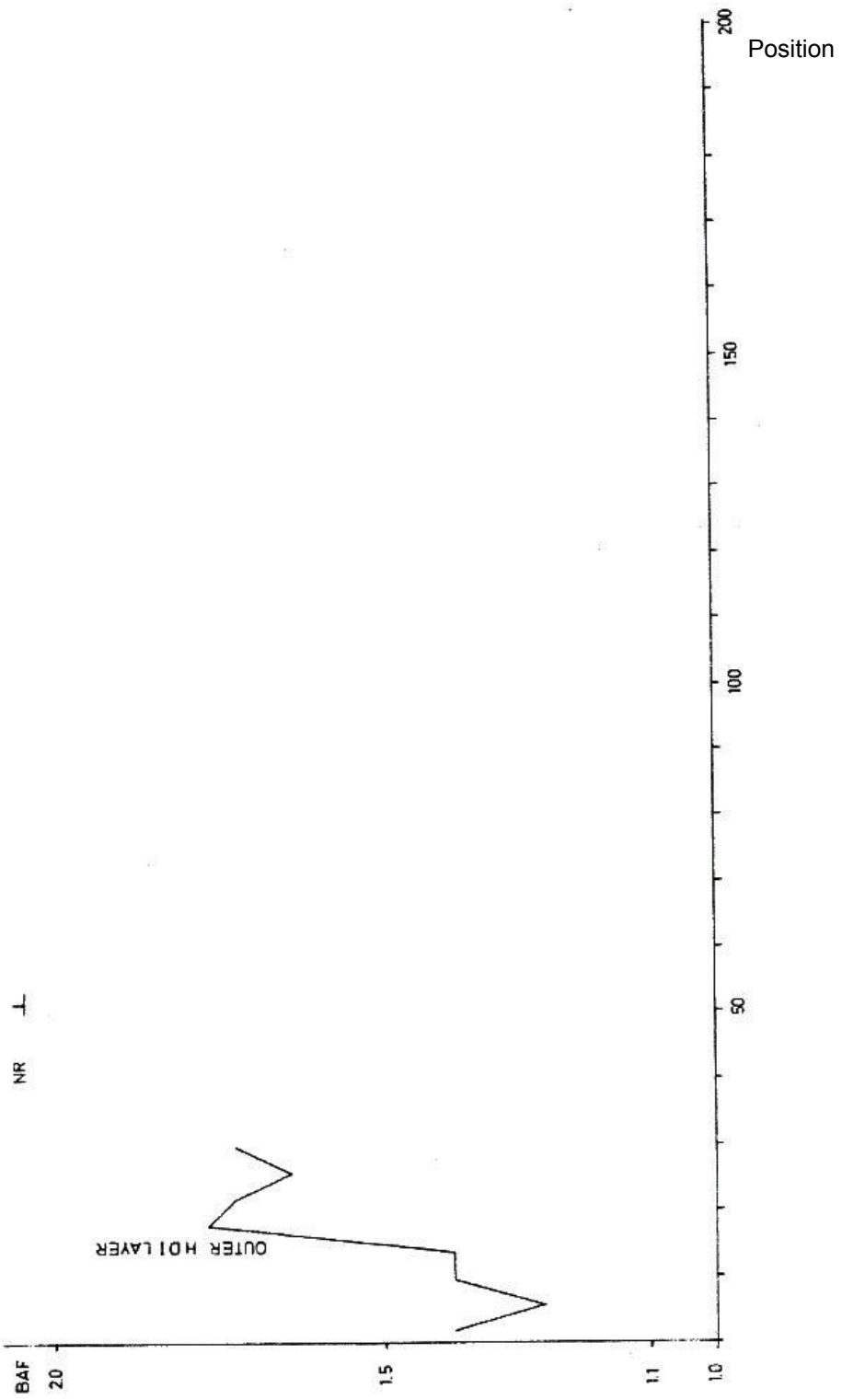

Figure 15: VC01 Anisotropy profile of the outer PyC of an irradiated particle (Particle n°6, compact 31)

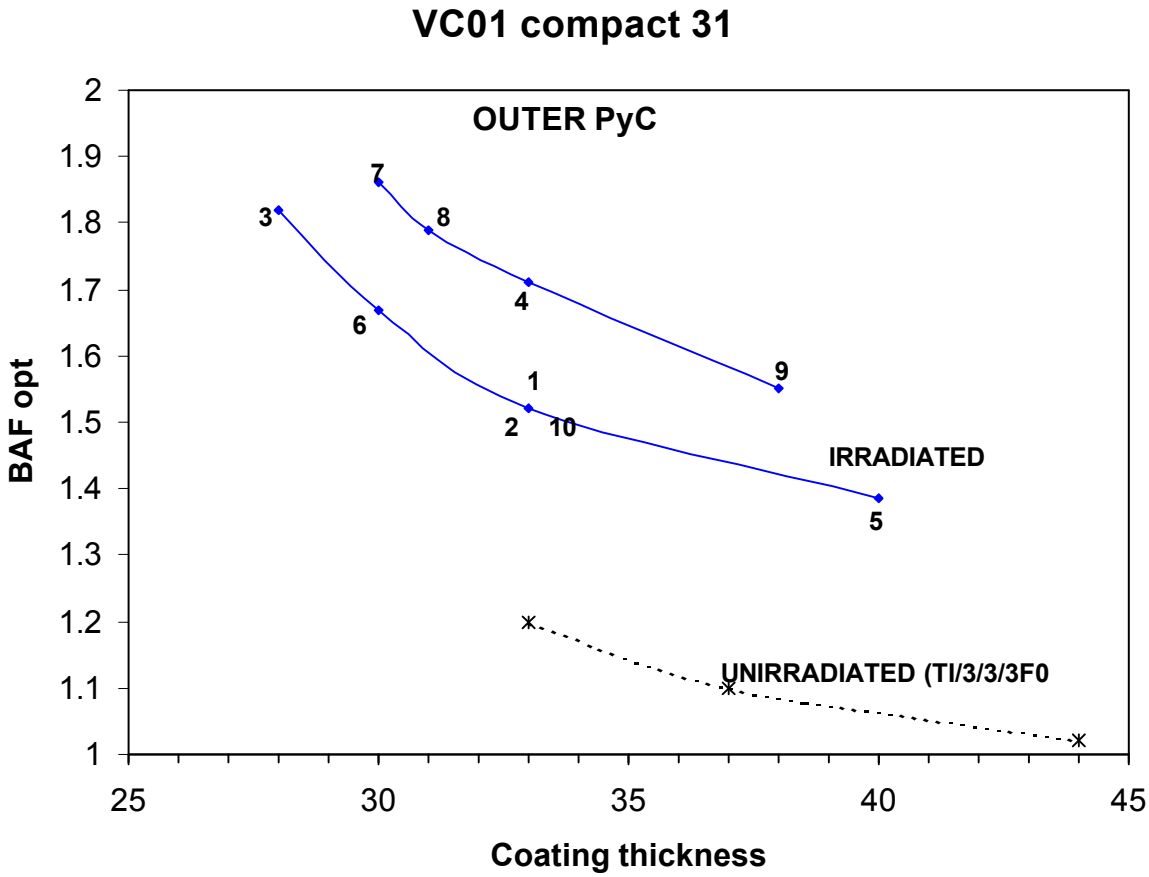

Figure 16: Correlation between anisotropy and coating thickness

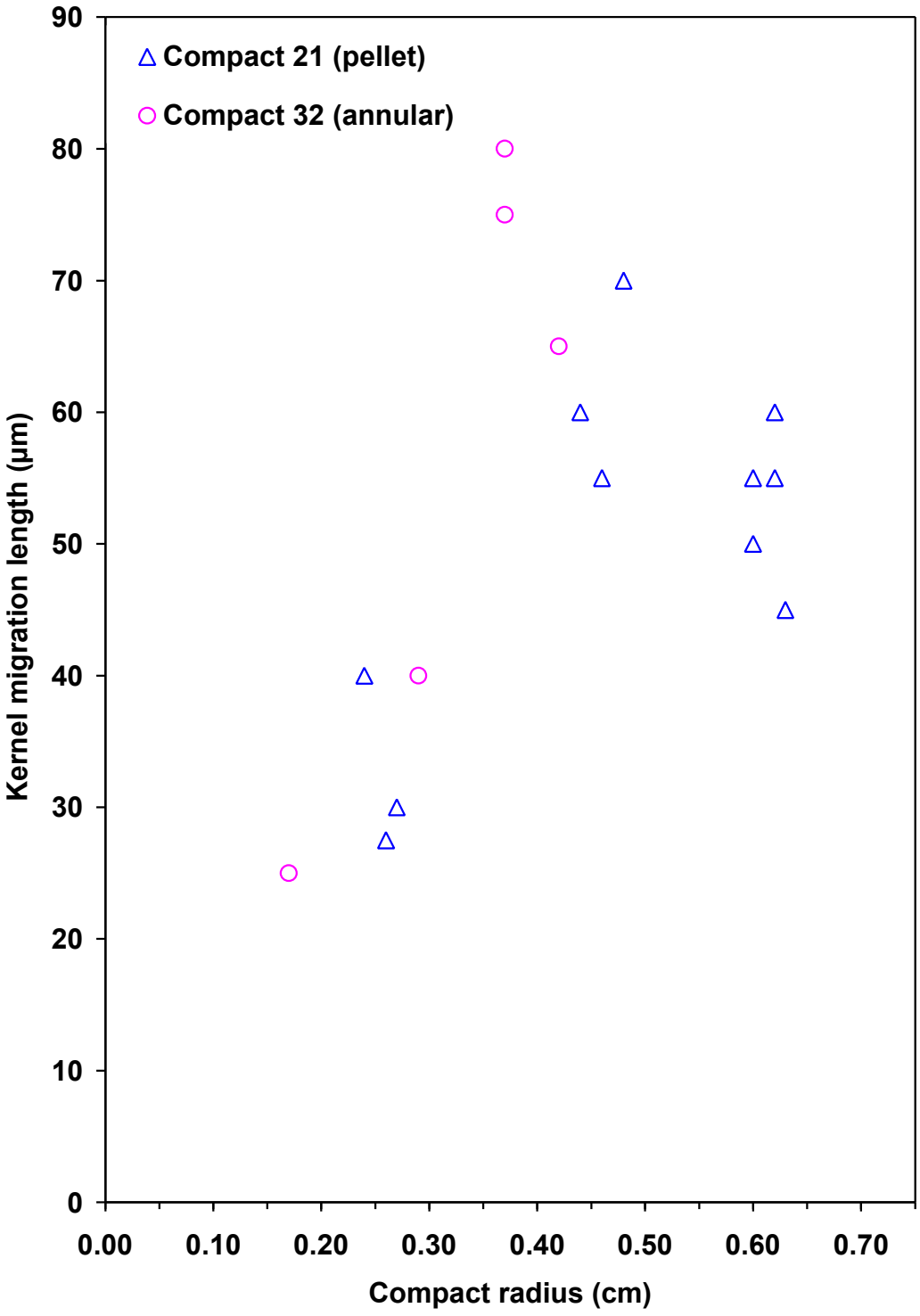

Figure 17: VC01 Kernel migration length versus coated particle radial position